UNIVERSITY OF THESSALY
DEPARTMENT OF COMPUTER AND COMMUNICATIONS ENGINEERING

CHRISTOS V. PAPATHANASIOU

RADIO RESOURCE MANAGEMENT WITH CROSS-LAYER DESIGNS IN BROADBAND WIRELESS ACCESS NETWORKS

A dissertation submitted to the faculty of Computer and Communications engineering of University of Thessaly in partial fulfillment of the requirement for the degree of

Doctor of Philosophy

UNIVERSITY OF THESSALY, DECEMBER 2010

Supervised by
Professor Leandros Tassiulas

Reviewed by

Professor Andreas Polydoros
Professor Leonidas Georgiadis

Volos 2010

Abstract

RADIO RESOURCE MANAGEMENT WITH CROSS-LAYER DESIGNS IN BROADBAND WIRELESS ACCESS NETWORKS

Christos V. Papathanasiou

Department of Computer and Communications Engineering

Doctor of Philosophy

This dissertation is addressed to novel and high innovative technical solutions for broadband wireless access (BWA) networks. The proposed networks are compatible with the existing IEEE 802.11n wireless local area networks (WLANs), wireless metropolitan area networks (MANs) IEEE 802.16e and WiMAX systems(Worldwide Interoperability for Microwave Access). The proposed designs are linked to the specific requirements which will be incorporated into emerging IEEE 802.16m and LTE advanced (Long Term Evolution) standards. These standards aim at defining an air interface that can ensure high mobility, transmit high data rates and offer higher performance compared to the current standards.

The dissertation focuses on advanced radio resource allocation schemes involving cross-layer optimization and hopes to influence these future standards. Radio Resource Management (RRM) algorithms optimize the radio resources especially spectral efficiency and reduce the power consumptions. This work studies mechanisms for downlink (DL) RRM in an environment which suffers from interference created by neighboring transmitters. Beamforming, scheduling and admission control are evaluated. After the description of state-of the-art techniques, advanced algorithms - strategies are developed and simulated. These algorithms take information coming from the radio site (RSSI, CSI, SNR, etc) or from the application layer side (QoS).

Dedicated to my grandfathers

Preface

This thesis represents a culmination of research work that has taken place over a period of four years (2006-2010) at the Department of computer and communications engineering, University of Thessaly, Greece. My deepest gratitude goes to my advisor, Professor Leandros Tassiula for giving me an opportunity to work in such a joyful and inspiring research unit.

Most of the work presented in the thesis was conducted in the Worldwide Interoperability Microwave broadband Access system for the next Generation wireless Communications (WiMAGIC) European project. I thank Professor Andreas Polydoros for my participation at the Institute of Accelerating Systems and Applications (IASA) and WiMAGIC project. I wish to express my gratitude to Dr. Nikos Dimitriou, whose cooperation and instructions have proven to be very efficient and fruitful.

I thank all past and present colleagues at the Laboratory for the joyful working atmosphere and the scientific discussions. In particular, I would like to express my thanks to Dr. Georgos Athanasiou for his friendship and help. The financial support provided by Greek Ministry of National Education and Religious Affairs which I highly acknowledge.

Volos, December 2010 Christos Papathanasiou

Abbreviations

AAS	Adaptive antenna systems
ACK	Acknowledgement
AES	Advanced encryption standard
AMC	Adaptive modulation and coding
A-MPDU	Agregate MPDU
AoA	Angle of arrival
AoD	Angle of departure
AP	Access point
ARQ	Automatic retransmission request
AS	Azimuth spread
AS	Antenna selection
ATM	Asynchronous transfer mode
AWGN	Addituve white Gaussian noise
BE	Best effort
BER	Bit error rate
BPSK	Binary phase shift keying
BRH	Bandwith request header
BS	Base station
BWA	Broadband wireless access
BW/RNG	Bandwidth/ranging
CDF	Cummulative distributed function
CDL	Clustered delay line
CGG	Channel gain grade
CI	CRC indicator
CID	Contention identifier
CL	Cross-layer
CP	Cyclic prefix
CPE	Customer premises equipment
CQI	Channel quality indicator
CRC	Cyclic redundancy check
CS	Controlling station
CSI	Channel state information
CSMA/CA	Carrier sense multiple access/collision avoidance

CW	Contention window
DA	Distributed antenna
D/A	Digital to analog converter
DAC	Digital to analog converter
DCD	Downlink channel description
DCF	Distributed coordination function
DFS	Dynamic frequency selection
DFT	Discrete Fourier transformation
DIFS	Distributed interference space
DL	Downlink
DLFP	Downlink frame prefix
DLFP	DL frame prefix
DoA	Direction of arrival
DoD	Direction of departure
DPC	Dirty paper coding
DSL	Digital subscriber line
DSP	Digital signal processing
DSSS	Digital sequence spread spectrum
DwPTS	Downlink pilot time slot
EC	Encryption control
EKS	Encryption key sequence
E/O	Electronical to optical
ES	Eigen steering
E-UMTS	Evolved UMTS terrestrial radio access
E-UTRAN	Evolved UMTS terrestrial radio access network
EVM	Error vector magnitude
FCH	Frame control header
FCS	Frame check sequence
FDD	Frequency division duplexing
FEC	Forward error correction
FFR	Fractional frequency reuse
FFR	Full frequency reuse
FFT	Fast Fourier transformation
FHSS	Frequency hopping spread spectrum

FRF	Frequency reuse factor
FTP	File transmission protocol
FUSC	Full usage sub-channelization
GMH	Generic MAC header
GP	Guard period
GPP	Generation partnership project
GSM	Global system for mobile communications
HARQ	Hybride ARQ
HO	Hand-over
HPA	High power amplifier
HT	Header type
ICS	Interchange sub-carriers
ID	Identifier
IF	Intermediate frequency
IFFT	Inverse FFT
IMDD	Intensity-modulation direct-detection
IP	Internet protocol
ISI	Intersymbol interference
ISM	Industrial scientific and medical band
ISO	International organization for standardization
ITU	International telecommunications union
LD	Laser diode
LoS	Line of sight
LMI	Linear matrix inequality
LP	Linear program
LPF	Low pass filter
LSP	Large scale parameters
LTE	Long term evolution
MAC	Medium access
MAC CPS	MAC common part sub-layer
MAC CS	MAC convergence sub-layer
MAI	Multiple access interference
MEC	Minimum effective SNR covariance metric
METRA	Multi-element transmit and receive antennas

MIMO	Multiple input multiple output
MMIC	Monolithic-microwave intergrated-circuit
MMSE	Minimum mean square error
MPDU	MAC protocol data unit
MRC	Maximum ratio combiner
MSC	Mean over sub-carrier covariance metric
MSE	Mean square error
MSDU	MAC service data unit
NLoS	Non LoS
nrtPS	non-real –time polling service
OC	Optimum combiner
OFDMA	Orthogonal frequency division multiple access
OSI	Open systems interconnection
PAS	Power azimuth spectrum
PD	Photodiode
pdf	Power distributed function
PER	Packet error rate
PHY	Physical
PPDU	PHY protocol data unit
PRB	PHY resource blocks
PSD	Positive semidefinite
PUSC	Partial usage sub-channelization
QAM	Quadrature amplitude modulation
QCQP	Quadratically constrained quadratic programming
QoS	Quality of service
QPSK	Quadrature phase shift keying
RA	Resource allocation
RAN	Radio access network
RF	Radio frequency
RoF	Radio over fiber
RRM	Radio resource management
RSSI	Received signal strength indicator
RTG	Receive /transmit gap
rtPS	Real-time polling service

RTS/CTS	Request –to-send/clear-to-send
SC-FDMA	Single- carrier frequency division multiple access
SCM	Spatial channel model
SDMA	Space division multiple access
SDP	Semidefinite programming
SDU	Service data unit
SFBC	Space-frequency block coding
SFID	Service flow ID
SIFS	Sort interframe space
SIMO	Single input multiple output
SINR	Signal to interference plus noise ratio
SM	Spatial multiplexing
SNR	Signal to noise ratio
SOFDMA	Scalable OFDMA
SS	Subcarrier station
STC	Space- time coding
SVD	Singular value decomposition
SS	Spatial spreading
TCP	Transport connection protocol
TDM	Time division multiplexing
TDMA	Time division multiple access
TPC	Transmit power control
TTG	Transmit/receive gap
TXOP	Transmission opportunity
UCD	Uplink description
UE	User equipment
UGS	Unsolicited grant service
UL	Uplink
ULA	Uniform linear array
UMTS	Universal mobile telecommunication systems
U-NII	Unlicensed national information infrastructure
UpTS	Uplink pilot time slot
VBR	Variable bit-rate
VRB	Virtual resource block

VQ	Vector quantization
WDM	Wavelength division multiplexing
WiFi	Wireless fidelity
WiMAX	Worldwide interoperability for microwave access
WINNER	Wireless world initiative new radio
WLAN	Wireless local area network
WMAN	Wireless metropolitan area network
XPD	Cross polarization power ratio
ZF	Zero forcing

Contents

List of Figures

Chapter 1

Introduction

1.1 Designing a broadband wireless access network

Existing technologies such as Wireless Fidelity (WiFi), Digital Subscriber Line (DSL), Global System for Mobile Communications (GSM) and the new 3G technologies have not been able to provide a total solution in the communication field. Broadband Wireless Access (BWA) technology has been considered as the complement or even the replacement of 3G applications. From the technology point of view, IEEE specifications select Orthogonal Frequency Division Multiple Access (OFDMA) and Multiple Input Multiple Output (MIMO) antenna technologies to increase robustness to signal fading on the one hand and enhance cell capacity on the other hand. When a broadband wireless network is designed, it is important to keep in mind the following key requirements:

- *High bandwidth:* The network should provide a high bandwidth reliable link that can be shared by multiple users.
- *Low latency:* Latencies of the link should be low. The users should be able to sustain high bit rates with minimum delay.
- *Quality of Service (QoS):* Wireless communication is typically resource constrained. QoS provides means for effectively partitioning the limited resources. Users can be provided different level of services and service provider can use this to derive revenues.
- *Spectral efficiency:* Wireless spectrum is scarce. Wireless communications make achieving high spectral efficiency a challenge.
- *Power saving:* The user should be capable of achieving power savings.

1.2 Adaptive Radio Resource Management

In a communication network, Radio Resource Management (RRM) is the system level control of individual signal transmission parameters. It’s of paramount importance in point to multi point networks. Radio signal suffers typically from noise and interference. While noise is intrinsic to the transmitter-receiver point to point link, interferences can be various and can come from different sources, i.e. from inside or from outside the network. The main benefit of a good RRM algorithm is the optimization of the radio resources of the network and the reduction of power consumptions of the wireless terminals. The maximization of the spectral efficiency should obviously be done by providing the QoS required from the application. RRM shall be studied based on frames of OFDMA

symbols. Allocation unit is small enough and therefore allows addressing up to a number of terminals simultaneously (i.e. during the same OFDM symbol time slot). One OFDM symbol is mapped on a set of subcarriers, the subcarriers being shuffled (by a permutation factor). This shuffling is aimed for interference mitigation between neighboring transmitters. In this dissertation, downlink (DL) RRM for a number of associated or not neighboring cells is studied. Different entities typically form the RRM: power control, radio measurement, scheduling (allocation and permutation factor included), handover, load measurement, admission control, etc. The proposed algorithms should be based on metrics coming either from radio side (power level, Signal to Noise Ratio-SNR, Packet Error Rate-PER,…) or from the application layer (QoS, packet type, packet size, packet arrival time, …).

Radio Resource Allocation techniques may affect network reliability, availability, performance and deployment characteristics [1].

- *Reliability and Availability*: The radio propagation environment changes in the time and frequency domains, affecting connection speeds, error rates and Quality of Service. In an indoor environment, due to multipath propagation as the receiver is moving, it is possible for a link to fail completely. Also, the number of users being served may vary considerably. In this case, an overload may occur resulting to congestion that degrades the services provided by the network.
- *Performance*: A BWA network should be capable of providing high throughput with low latency. Congestion reduces user throughput. Users share the same bandwidth resource, and congestion is likely to happen in areas of high user density.
- *Deployment characteristics*: In a BWA deployment, the cell locations and the radio channels assignment must be selected carefully. In a coverage-oriented design, the cells are placed as far apart as possible in order to minimize installation costs and to avoid overlapping between the coverage areas of cells operating at the same radio channel. Additionally, proper channel assignment minimizes co-channel overlap.

1.3 Cross-Layer design

In order to prevent the deployment of multiple and incompatible network architectures by different vendors, the International Organization for Standardization (ISO) developed the Open Systems Interconnection (OSI) reference model [2]. The OSI reference model provides an abstract framework for network design that enables the interconnection of heterogeneous networks. It can be visualized as a vertical stack of seven independent layers, with the upper layers dedicated to application-related issues and the lower layers to data transmission. Each layer is an entity that addresses a specific functionality, even though the actual protocols that implement the layer

functions may vary depending on the system. Communication is possible only between adjacent layers and is limited to the exchange of a set of primitives through well-defined interfaces. In other words, a layer provides services to the adjacent higher layer and, in turn, receives services from the layer below.

The OSI layered approach enables compatibility among vendors and different devices and makes possible to optimize each layer operation independently of the others, thus facilitating the development of technology. However, the proliferation of wireless and mobile networking and the increased demand for higher performance requirements, especially in terms of Quality of Service (QoS) guarantees for multimedia applications, have posed challenges and opened new possibilities that could not be addressed with the traditional layered approach. Unlike wired links that are considerably stable and predictable along time, the wireless channel changes over time and space with small and large scale variations that are often difficult to predict. This inconvenience can be turned into an advantage with the use of sophisticated communication policies, such as the opportunistic transmission of packets when the channel conditions are favorable. In addition, the randomness in wireless propagation and the broadcast nature of the radio channel create new modalities of communication, such as multipacket reception or user cooperation that are not feasible in wired networks [3]. All these factors have leveraged the need for more flexibility in network design, aiming to adapt the system operation to a dynamically changing channel as well as to the network characteristics and, finally, to enhance the overall communications performance.

This need has led to the concept of Cross-Layer (CL) design, which encompasses all schemes that violate the rigid architecture of the OSI reference model. It is a very wide term that spans from an interlayer dialog and exchange of information to the joint layer design and optimization. The number of participating layers may vary and communication may take place between any layers of the protocol stack. In less conservative approaches, it is also possible to merge layers or even define new external entities to control and coordinate CL interactions.

The authors in [4] introduced the concept of interlayer coordination planes that span vertically across the protocol stack and focus on the resolution of a specific set of problems encountered in wireless mobile systems. More specifically, they have defined four planes devoted to wireless security and encryption, QoS provisioning, mobility issues and link adaptation, as illustrated in Figure 1.1. Each plane is an objective that can be achieved through CL design and thus CL algorithms can be classified in the coordinating planes depending on their targeted goal. Another method of classification focuses on the different layers that are involved in the CL exchange of information. An example of the interactions that can take place between the layers of the OSI stack

(adjacent or non-adjacent) can be seen in Figure 1.2 [5]. A detailed description of all the possible interactions between layers and the exact parameters that can be exchanged is given in [6].

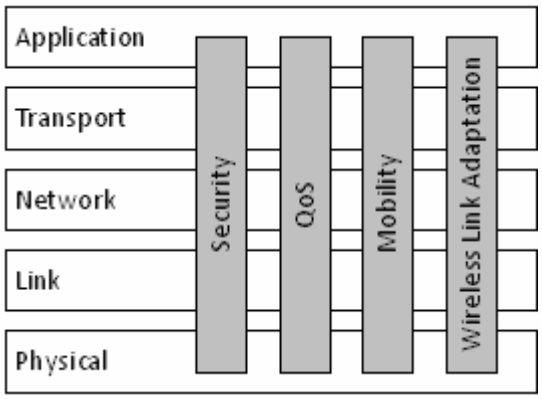

Figure 1.1 – Cross-Layer coordination planes

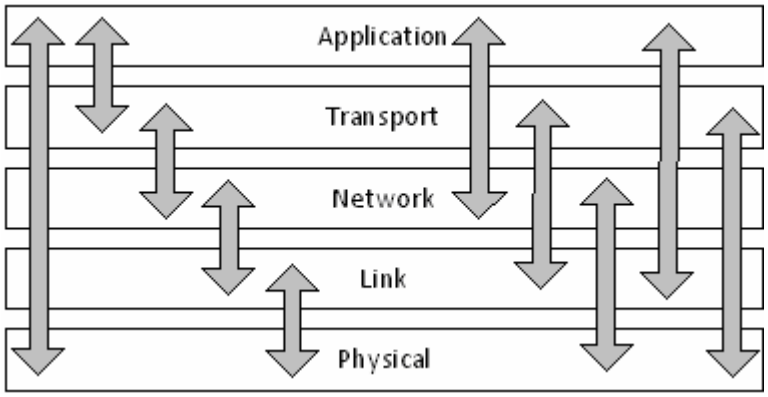

Figure 1.2 – Possible interactions between layers

We consider the gains that can be achieved by a CL approach for a wireless network design, where the knowledge of the wireless medium in the PHY layer is shared with MAC and higher layers in order to provide efficient methods of allocating network resources [7]. Figure 1.3 illustrates the most common tunable parameters of each OSI layer. Channel-state-depend techniques can lead to improved network throughput. The radio propagation environment changes, so one cannot be sure about the reliability of the channel estimated and the sub-channel assignments that are based on those estimates. With cross layer radio resource management, the BWA 'senses' the propagation conditions from time to time and then dynamically adjusts the allocations in the frequency and time domains. The optimal channel allocation minimizes the overlap between the coverage areas of co-channel cells. There are also other factors that influence the selection of the optimal set of frequency assignments. These other factors include the noise and interference (co-channel and adjacent channel) from other networks. Finally, a cell may transmit only occasionally and cause less interference to other cells using the same channel. Additionally, adaptive beamforming techniques can improve the

results of the frequency assignment process by taking into account the changes in the propagation environment and the generated interference from neighboring BWA networks.

Layers	Tunable Parameters
Application	*QoS Constraints* *Source Coding and Application Rate*
Transport	*Flow Control and Congestion Avoidance* *Error Recovery*
Network	*Routing* *Admission Control*
Link	*Medium Access* *Scheduling and Resource Allocation* *Fragmentation and Framing* *FEC and ARQ*
Physical	*Power Control* *Modulation and Coding Schemes* *Channel Estimation*

Figure 1.3– Cross-Layer design tunable parameters

FEC: Forward Error Correction ARQ: Automatic Retransmission reQuest

By allocating sub-channels in a dynamic manner among various data users with smart scheduling mechanisms, we improve the resource utilization efficiently based on the instantaneous user demand and the instantaneous channel states for each user. The achieved gain due to channel-state-dependent scheduling algorithms is called multi-user diversity gain. Various real-time algorithms have been designed that achieve this gain and also support diverse Quality of Service requirements. Since a cell and its associated users share a limited bandwidth resource, networks can become overloaded, leading to congestion and poor performance in terms of provided throughput per user. A user may be able to communicate with two or more networks. Network resources might be allocated using methods that rely on information received from a set of cells. The network can accept the request from a user or can deny the request and advise the user to which cell it should handover its connection.

1.4 Aims and problem definitions

The ever growing demand for high speed data connectivity makes BWA networks for local and metropolitan area one of the hottest topics in the field of telecommunications. The purpose of this dissertation is to address the technical challenges of the advanced air interface for BWA networks. Among the main topics to be addressed are new MIMO schemes offering higher diversity and

multiplexing gains as well as interference cancellation capabilities, advanced OFDMA allocation schemes involving cross-layer optimization, as well as cooperation between neighboring cells. Despite the attractive features and capabilities of the current generation BWA systems, the ever increasing demand for higher data rates and QoS will require further evolutions in the next years. Research results developed within the thesis studies may influence future standards. The developed concepts and algorithms were simulated for testing and validation. This thesis studies two main network types and the prevalent technologies associated with each: Wireless Local Area Networks (WLANs) and Wireless Metropolitan Area Networks (WMANs).

In a WLAN, an Access Point (AP) coordinates the communication between the user terminals. WLANs use width bandwidths (typically 20 MHz) that are available in unlicensed bands and therefore uncoordinated techniques was been developed. Also, the low mobility and limited range requirement as well as the need to combat smaller delay spread simplify some aspects of system design. The knowledge of channel response **H** is available at the transmitter side- full Channel State Information (CSI). WLANs use the robust Carrier Sense Multiple Access with Collision Avoidance (CSMA/CA) for medium access. However, this simple access mechanism is an asynchronous Time Division Duplexing scheme, which imposes a considerable penalty on efficiency. We focus on the recently approved 802.11n standard supports MIMO technologies with rates exceeding 100 Mbps [8,9]. Firstly, we examine performance which efficiently provides coverage and capacity for a single cell. In continuous, we extend our study taking into account interference from other WLANs in unlicensed bands, which impact network performance and QoS. Finally, a multicast transmission strategy using minimum network resources for an 802.11n is proposed.

The objective of the research for WMAN networks is to develop novel and highly innovative technical solutions which be backward compatible with the existing global standards (IEEE 802.16e and WiMAX [10,11]) and linked to the specific end-user requirements which will be incorporated into the emerging IEEE 802.16m standard [12]. IEEE 802.16m aims at defining an air interface that can ensure high mobility (up to 250 Km/h), transmit a data rate of over 100 Mbps and offer higher performance compared to the current IEEE 802.16e standard. We consider the point to multipoint operation mode with one or more Base Stations (BSs). Each BS serves a set of mobile users, with all users receiving the same transmission from the BS. Therefore, suitable techniques with partial CSI were developed to support fast moving users in a metropolitan area. IEEE802.16e standard is based on OFDMA with a burst Time Division Multiplexed (TDM). MAC layer synchronization between BS and mobiles is required. Both downlink (DL) and uplink (UL) directions use a common set of bandwidth scalable radio parameters and support bandwidth from 1.25 MHz to 20 MHz. In this infrastructure deployment, inter-cell coordination by exploiting multi cell information should be

supported in a licensed environment. We propose signal processing algorithms for single cell and multi cell deployment. In latter case, co-channel interference from neighboring cells is presented. Finally, network dimensioning and design for the deployment of mobile WiMAX was studied in order to avoid the build-up of a large number of new BSs.

1.5 Outline of the thesis

Parts of the original contributions in Chapter 5-10 have been published earlier [92-103] or submitted for publication [104-105]. The remainder of the thesis is organized as follows:

Chapter 2 collects description of three systems which are interest for our research:

- The recently approved 802.11n standard adopted in WLANs,
- 3GPP LTE (Long Term Evolution), which is the main competitor of WiMAX and
- IEEE 802.16e which is the standard of our studies for a metropolitan area.

Chapter 3 investigates MIMO channels models and their implementation considering steering channel matrix **H,** spatial correlation coefficients, power delay profiles, fading characteristics and Doppler power spectrum. IEEE 802.11n and WINNER II channel models are described in order to be applicable for the generation of **H** parameters compatible with the emerging IEEE 802.11n and IEEE 802.16m standards.

Chapter 4 introduces the convex optimization methods which will be used in the design of our signal processing algorithms and proposed communication systems. A basic concept is given with emphasis in semi-definite programming. We note that semi-definite relaxation problems are used for calculating downlink beam vectors.

Chapter 5 describes a downlink beamforming method that increases spectrum efficiency and significantly reduces implementation complexity and power consumption compare to beamforming technique at each sub-carrier, proposed in the ongoing IEEE 802.11n standardization. Common transmission weight vectors are used at a set of users in all sub-carriers. We propose a new distributed algorithm that permits interfering APs to select appropriately their operating frequency and suppress interference in a densely deployed WLAN environment where APs could be so close to cause significant channel interference.

Chapter 6 focus on the next-generation WLAN 802.11n and physical layer multicast transmission for delivering multimedia contents which require high throughput and near-real time for quality viewing. We formulate the problem of transmit beamforming to a multicast group and minimize total emitted power adopting a QoS criterion in an unmanaged environment where wireless devices operate in unlicensed frequency bands.

Chapter 7 deals with the problem of applying beamforming to IEEE 802.16 networks that include in their coverage areas fast moving mobiles. The system scenario is assumed to include BSs that can form multiple beams which can steer (rotate) their respective coverage areas. Additionally, the user downlink transmissions are supposed to be dynamically scheduled based on Signal to Noise plus Interference Ratio (SINR) reports for sub-groups of the available OFDMA sub-carriers.

In Chapter 8, a multi-user multi-cell system is studied, in which the BS has only knowledge of the statistics of the channel. A combination of MIMO, OFDMA and Frequency Division Duplexing (FDD) could increase the spectral efficiency in a high speed network. We investigate methods with scalable channel feedback and we analyze the trade off between the amount of CSI to the transmitter and the system performance. The new dynamic radio resource management methods are extended to a reuse-one sectorized cell in order to reduce the cross-sector interference. Finally, the proposed schemes with limited feedback are combined with other cell interference reduction strategies based on cooperation for improving the performance of a coordinated multi-cell system under very dynamic conditions like high velocity and fast fading.

Chapter 9 proposes a novel cell architecture based on a Distributed Antenna (DA) system to provide high data rate transmission. We combine Spatial Multiplexing (SM), beamforming and Radio over Fiber (RoF) technologies taking advantage of the partial CSI of a downlink multi-user system, obtained through correlation channel matrix feedback that is averaged in the frequency domain. In order to improve further the SINR and reduce co-channel interference from neighboring cells, the proposed architecture coordinates the resource allocation among the cells. Under this structure, several BS multi-antenna arrays are geographically distributed in the cell to spatially multiplex separate data streams to each user over each OFDM subchannel with high reliability.

Chapter 10 proposes a new methodology with which a provider will be able to assess the investment cost associated to the vendor’s WiMAX offered solutions. Hypothetical model networks are examined with the purpose to illuminate our methodology in a given environment.

Chapter 11 concludes the thesis. The results and conclusions are summarized and discussed.

Chapter 2

Broadband Access System Architectures

In this chapter, we describe four systems which are potentially active on convergent markets. We focus in particular Physical (PHY) and MAC layer structure of the four systems, in order to understand their operation they use or propose. This chapter helps to understand the innovation features of our proposed cross-layer PHY/MAC algorithms and system design strategies.

2.1 IEEE802.11n WLANs

The most notable advantages that will be offered by the IEEE 802.11n standard compared to previous WLAN technologies are substantial improvement in reliability and greater application data throughput. The IEEE 802.11n standard is expected to deliver data rates of up to 300 Mbps per radio link [13]. The IEEE 802.11a/g solutions can achieve a maximum data rate of 54 Mbps, while the IEEE 802.11b delivers a maximum data rate of 11 Mbps. The operating frequencies of IEEE 802.11n are within the 2.4 GHz and 5 GHz radio bands, thus it is backward compatible to all IEEE 802.11a/b/g variants. The introduced solutions in IEEE 802.11n employ several techniques to improve throughput and reliability. The most representative innovations are:

- Multiple Input Multiple Output (MIMO)
- Packet aggregation
- Channel bonding (40 MHz channel band)

Also, the PHY layer design is based on orthogonal frequency-division multiplexing (OFDM) with MAC layer support, closed loop control of the PHY data rates and QoS handling.

A. OFDM modulation

The IEEE 802.11 standard defines three transmission schemes at the PHY layer: Frequency Hopping Spread Spectrum (FHSS), Digital Sequence Spread Spectrum (DSSS) and Orthogonal Frequency Division Multiplexing (OFDM). The IEEE 802.11a uses OFDM that supports high bit rates (52 Mbits/s maximum physical rate) while IEEE 802.11b allows only DSSS with bit rate too low (11Mbits/s). IEEE 802.11g is compatible with IEEE 802.11b
and supports transmission with both OFDM and DSSS.

OFDM is well suited for wideband transmission when the propagation channel effects include frequency selective fading. In IEEE 802.11n the OFDM modulation is used in the 20 MHz band as in

IEEE 802.11 a/g. It's composed of 64 sub-carriers out of which a total of 48 sub-carriers are used for data and 4 as pilot. The DC sub-band is used to estimate the noise power and the remaining sub-bands are used as guard sub-bands. The 40 MHz band contains 128 sub-carriers (108 data tones and 6 pilot tones) [9]. Fig. 2.1 illustrates the tone design for 20 and 40 MHz channelization. The employed technique that combines two adjacent 20 MHz into a single 40 MHz channel is called bonding and is most effective in the 5GHz frequency band where there are much more available sub-channels. A Cyclic Prefix (CP) with duration 800ns is used to maintain the orthogonality among the sub-bands against the delay spread of the channel. Taking into account that the OFDM symbol is 3.2 μs long, the CP overhead is 20%. For indoor applications with lower delay spreads, the CP can be reduced down to 400ns.

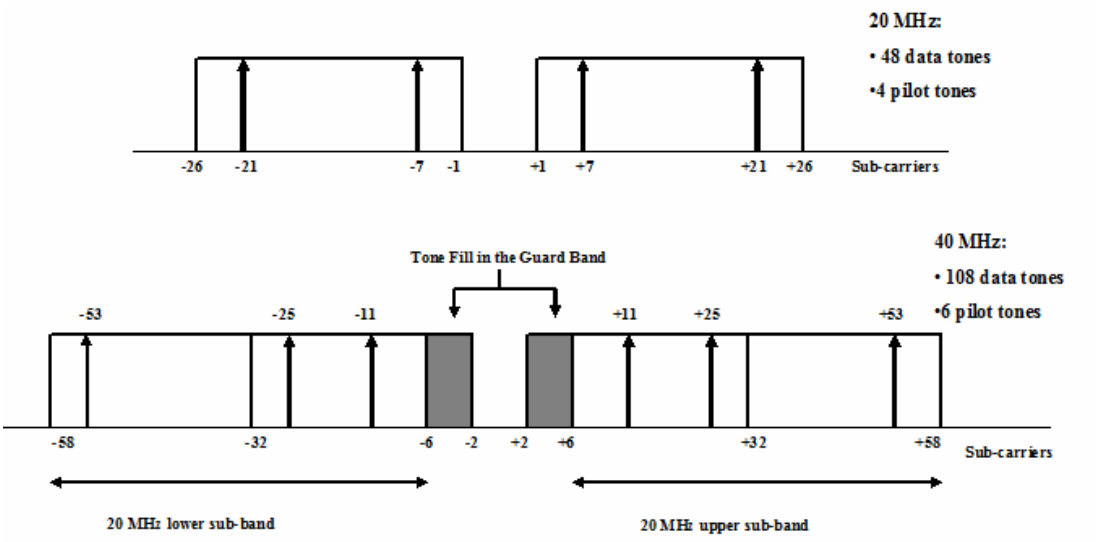

Figure 2.1 Tone design in IEEE 802.11n

B. MIMO

In IEEE 802.11 a/b/g a point-to-point communication through a single spatial stream over a single antenna is established between APs and users. In IEEE 802.11n, APs transmit up to four spatial streams and the mobile terminals employ multiple antennas (two or four) to recover the multiple transmitted data streams. MIMO technology enables the transmission of different bits of a message over separate antennas providing much greater throughput and reliability. In contrast to the previous WLANs technologies, IEEE 802.11n with MIMO exploits multiple transmitted paths and their reflections to increase the range of an AP and reduce "dead spots" in the wireless coverage area.

The MIMO channel response can be represented in matrix form as

$$\mathbf{H}_n = \begin{bmatrix} h_{11}^n & h_{12}^n & h_{13}^n & h_{14}^n \\ h_{21}^n & h_{22}^n & h_{23}^n & h_{24}^n \\ h_{31}^n & h_{32}^n & h_{33}^n & h_{34}^n \\ h_{41}^n & h_{42}^n & h_{43}^n & h_{44}^n \end{bmatrix} \quad (2.1)$$

where h_{ij}^{n} is the channel response between receiver antenna element i and transmitter antenna element j, n is the OFDM sub-band index which characterizes the wideband channel at the discrete frequency n belonging to a set of $\{1, 2, \cdots, N\}$ sub-channels. For 20 MHz channelization, N=52. $\mathbf{H_n}$ has dimensions of N_r x N_t, where N_r is the number of receiver antenna elements and N_t is the number of transmitter antenna elements. When sufficient scattering exists, the maximum number of available spatial transmission channels is limited by the rank of $\mathbf{H_n}$. A trade off between diversity gain and the number of spatial streams on a MIMO channel is selected. Additionally, beamforming was proposed for exploiting the full capacity benefits of MIMO [14,15]. Two categories of design may be used:

- Eigen vector steering (ES) when full Channel State Information (CSI) or complete knowledge of channel $\mathbf{H_n}$ is available at the transmitter.
- Spatial Spreading (SS) when partial CSI or statistical knowledge of channel matrix $\mathbf{H_n}$ is available at the transmitter.

The two modes of operation are referred to as Eigenvector Steering (ES) and Spatial Spreading (SS).

I. Eigenvector steering

When full CSI is available at the AP, the optimum transmit and receive steering vectors may be obtained from the Singular Value Decomposition (SVD) of the channel. The MIMO channel can be decomposed into orthogonal spatial channels commonly referred as eigenmodes.

$$\mathbf{H_n} = \mathbf{U_n D_n (V_n)^H} \quad (2.2)$$

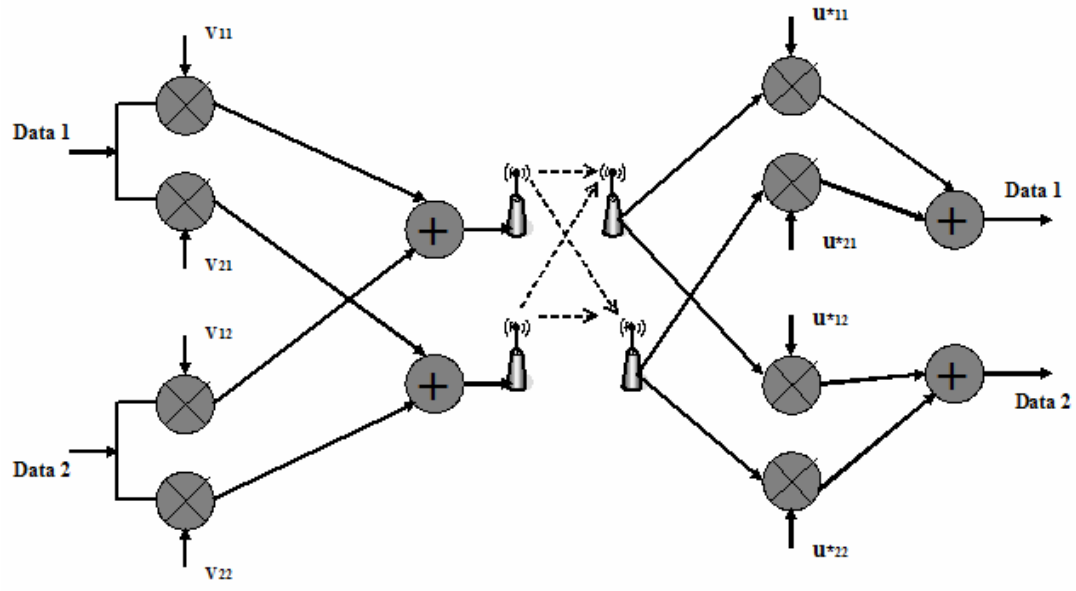

Figure 2.2 ES mode for a single OFDM sub-carrier with 2 antennas at the transmitter and the receiver

$\mathbf{U_n}$ and $\mathbf{V_n}$ are unitary matrices representing the left and right eigenvector of $\mathbf{H_n}$ respectively. $\mathbf{D_n}$ is a diagonal matrix, representing the transmit power at each eigenmode. The columns $\mathbf{v_{ni}}$ of $\mathbf{V_n}$ with

$i = \{1, 2, \cdots, N_t\}$ are used as transmit steering vectors and the rows $\mathbf{u_{nj}}$ of $\mathbf{U_n}$ with $j = \{1, 2, \cdots, N_r\}$ as received steering vectors. $\mathbf{D_n}$ is a diagonal matrix so that there is no cross talk between the estimated symbols at the receiver. Finally, up to min(N_t,N_r) parallel channels can be transmitted. Fig. 2.2 depicts the ES transmission and reception scheme for a 2x2 MIMO channel.
The larger eigenmodes have substantially less frequency selectivity than the smaller ones.

II. Spatial Speading

When full CSI is not available at the transmitter, it is desirable to achieve maximum diversity while transmitting on some or all spatial channels. The receiver spatial processing is responsible for isolating the independent transmitted data streams. The receiver can spatially filter the received signal by using a linear processing based on Zero Forcing (ZF) or Minimum Mean Squared Error (MMSE) algorithms. SS is a generalized space - frequency code over the OFDM sub-carriers. The transmitted signal is multiplied by an orthonormal spatial spreading matrix $\mathbf{W_n}$ that varies among sub-carriers in order to maximize transmit diversity. We could construct matrix $\mathbf{W}$ by using a fixed unitary spreading matrix $\hat{\mathbf{W}}$ in combination with a linear phase shift across the OFDM sub-carriers per transmitted stream.

$$\mathbf{W_n} = \mathbf{C_n}\hat{\mathbf{W}} \quad (2.3)$$

The transmitter spreads the data streams across the min(N_t,N_r) spatial channels by using $\hat{\mathbf{W}}$, which can be a Hadamard matrix or Fourier matrix. The number of data streams is determined from statistical feedback. $\mathbf{C_n}$ is a N_t x N_t matrix which represents the linear phase shift in the frequency domain and may be implemented by fixed cyclic time shift per transmit antenna.

C. MAC Operation

In the IEEE 802.11 MAC protocol operation, the fundamental mechanism to access the medium is called Distributed Coordination Function (DCF). This random access mechanism is based on the Carrier Sense Multiple Access with Collision Avoidance (CSMA/CA) protocol. Binary exponential backoff rules manage the retransmission of collided packets. The default mechanism is a two – way handshaking technique. After the successful reception, the user immediately sends an Acknowledgement (ACK) back to the AP. An optional four way hand-shaking mechanism, known as Request – To –Send / Clear – To – Send (RTS/CTS) could be used along with the default CSMA/CA scheme. In the commercial WLAN deployments, the default setting for RTS/CTS operation is ‘off’. When a station operates in the RTS/CTS mode it has to send a special Request-To-Send short frame before transmitting a packet. The destination station acknowledges the receipt of the RTS frame by sending back a Clear-To-Send frame. Thereafter, the data packets can be transmitted with the ACK

mechanism previously described. This scheme increases system performance by reducing the duration of a collision when long messages are transmitted. The RTS/CTS scheme can effectively resolve the ‘hidden terminals’ issue, according to which two terminals cannot hear each other. In [16] a simple analytical model computes the performance of the 802.11 DCF. For the default mechanism, the performance strongly depends on the system parameters, as the number of users in the wireless network. Fig. 2.3 illustrates the operation of the legacy IEEE 802.11 schemes.

The MAC layer receives a MAC Service Data Unit (MSDU) to transmit. It adds MAC headers and forms the MAC Protocol Data Unit (MPDU). The PHY layer adds PHY headers and forms a PHY Protocol Data Unit (PPDU). A station waits for a fixed time interval before transmitting a PPDU. First, it monitors the channel and if the channel is idle for a period of time equal to a Distributed Interframe Space (DIFS) the station transmits. If the channel is sensed as busy, the station continues to monitor the channel until it is determined as idle for a DIFS. At this point, the MAC layer enters a random backoff procedure which is determined by a Contention Window (CW). If the channel is still idle after the backoff procedure the station can transmit. In this way, the problem of collision with packets by other stations is minimized. DCF adopts an exponential backoff scheme and the backoff time is uniformly selected from 0 to CW-1. The CW depends on the number of transmissions failed for the packet. At the first transmission, CW takes a minimum value CWmin. After each unsuccessful transmission CW is doubled up to a maximum value CWmax. The values CWmin and CWmax are PHY layer specific. After successful packet reception the ACK is immediately transmitted after a period of time called Sort Interframe Space (SIFS). We observe that DCF is inefficient. The overheads (DIFS, CW, SIFS, ACK, PHY and MAC headers) limit the data throughput.

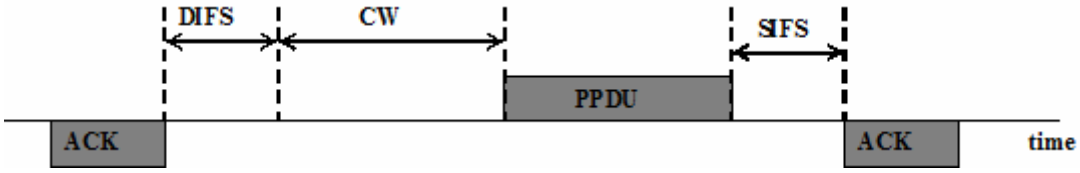

Figure 2.3 Basic access mechanism

In IEEE 802.11e, QoS and Enhanced Distributed Channel Access (EDCA) was introduced [17]. The support of QoS is provided with four access categories. Each access category sets an independent backoff mechanism and different CW parameters as CWmin, CWmax, SIFS in order to provide differentiated QoS priorities. The IEEE 802.11e MAC scheme introduces the Transmission Opportunity (TXOP) mode. TXOP mechanism defines a period of time that a station transmits multiple data frames without entering backoff. The station waits for a SIFS to transmit the next PPDU. A ‘block ACK’ mechanism can be used to further enhance the medium efficiency. A station

transmits multiple PPDU frames in TXOP mode and accepts only one block ACK to all of these PPDU instead of using a legacy ACK for each PPDU.

The IEEE 802.11n technologies improve the MAC layer efficiency by aggregating multiple data packets from the upper layers into one larger aggregated data frame for transmission. Aggregation is more beneficial for File Transmission Protocol (FTP) than real time applications because the packet aggregation scheme may introduce unnecessary latency. For the case of real-time applications (voice, multimedia, etc) the IEEE 802.11n benefits come mainly from the PHY layer enhancements. The block ACK mechanism in 802.11n is modified to support multiple MPDUs. When some aggregate MPDU (A-MPDU) are received with errors, a block ACK is sent that only acknowledges the specific MPDUs that have been correctly received. Thus, the non-acknowledged MPDUs only need to be retransmitted. Finally, in IEEE 802.11n the reverse direction mechanism enhances the efficiency of TXOP for bi-directional traffic applications like VoIP and on line gaming. The reverse direction mechanism allows for the unused TXPO time to be allocated at the reverse direction. The major gain with the reverse direction mechanism is the latency reduction in the reverse link traffic.

2.2 IST-WINNER Project

The WINNER (Wireless World Initiative New Radio) project is an ambitious European research program divided in two phases: Phase I (2004-2005) and Phase II (2006-2007). WINNER aim was the identification and assessment of key technologies for Beyond 3G mobile systems, and the definition of a system concept as well as suitable reference designs for a wide range of scenarios (Wide Area, Metropolitan Area and Local Area are the three basic scenarios covered by WINNER). The goal of the WINNER mobile access network is a system that is highly flexible and efficient and can provide a wide range of services to a multitude of users in many different environments [18].

Here we list a number of key concepts which WINNER used to achieve its promises. WINNER's key concepts at network and Radio Resource Management (RRM) level are:

- Flexible Radio Access Network (RAN) logical nodes, minimizing the number of interfaces.
- Flexible protocol architecture: MAC and PHY layer are present at BS, relay nodes, and MS and are optimized through cross-layer design.
- Relay-enhanced cells.
- Support for shared spectrum operation and inter-system coordination.

WINNER's key concepts at MAC level are:

- Minimization of MAC overhead though intelligent use of cross-layer design.
- Minimization of MAC delay: minimal over-the-air delay of 1 ms in DL and 2 ms in UL (one hop) thanks to short frame duration and tight feedback control loops.

- Advanced interference control: interference averaging, avoidance, and rejection.
- Channel-aware scheduling which jointly takes into account MAC and PHY layers.
- Two types of allocations principles: frequency adaptive transmission (taking advantage of good channel state information at the scheduler) or frequency non-adaptive transmission (taking advantage of channel diversity).
- Advanced link adaptation multi-antenna algorithms.

Capability	**Description**
Spectrum	
Carrier Frequency	From 400 MHz to 5 GHz
System Bandwidth	From 1.25 to 100 MHz
Duplexing	FDD and TDD
Spectrum type	Licensed (optimal) and unlicensed
Spectrum flexibility	Flexible spectrum sharing with other WRANs or secondary systems
Link Adaptation	
Modulation	BPSK, QPSK, 16/64/256-QAM
Channel coding	Convolutional codes, LDPC (Duo-binary Turbo Codes not completely optimized)
Multiple antennas	2 at MS and up to 32 at BS
HARQ	Incremental Redundancy (LDPC, mother code rate 1/3)
Multiple Access	
Multiple access	TDMA/OFDMA + SDMA
Subcarrier spacing	FDD: ~39 kHz; TDD: ~49 kHz
Superframe/frame duration	5.69 ms / 0.6912 ms
Scenarios	
Type	Wide, Metropolitan, and Local Area
Cell radius	~ 1km (cyclic prefix optimal for this value)
Mobility	Fixed, vehicle speed (optimal), high speeds, and up to high train speeds (350 km/h)
Relay	Decode-and-forward, collaborative relaying (optional)
Handover	Inter-system
Peak Rates	100 Mb/s at vehicular speed and 1 GHz at low speed

TABLE 2.1 : WINNER SYSTEM CAPABILITIES.

WINNER's key concepts at PHY level are:

- Optimized design of PHY layer: the PHY layer is based on generalized multi-carrier modulations. Between the selected single-carrier and multi-carrier schemes there is cyclic prefix OFDMA without or with DFT (Discrete Fourier Transform) precoding. This is a shared point both with 3GPP LTE and 802.16m.
- Generic and versatile multi-antenna schemes, which can be configured into a various diversity, multiplexing and/or multi-user MIMO configurations.
- Reduced-size control signaling.

- A variety of pilot schemes for various types of multi-antenna and frequency allocation transmissions, with acceptable overhead.

In WINNER transmission is organized around the so-called super-frame: it contains UL and DL pilots for synchronization and RRM allocation algorithms cannot change the resource allocation inside a given super-frame. WINNER specifies super-frames for FDD and TDD modes: in both cases the super-frame has the same duration: 5.53 ms. In figure 2.4 the representation of WINNER super-frame in TDD mode is given. The super-frame is divided in 8 frames (this value has not been optimized in WINNER and it can be changed). A frame is divided into two slots, which are the temporal allocation unit for the scheduler. In case of TDD, the DL slot always precedes the UL one. At each direction change (DL to UL and UL to DL) a guard interval is introduced.

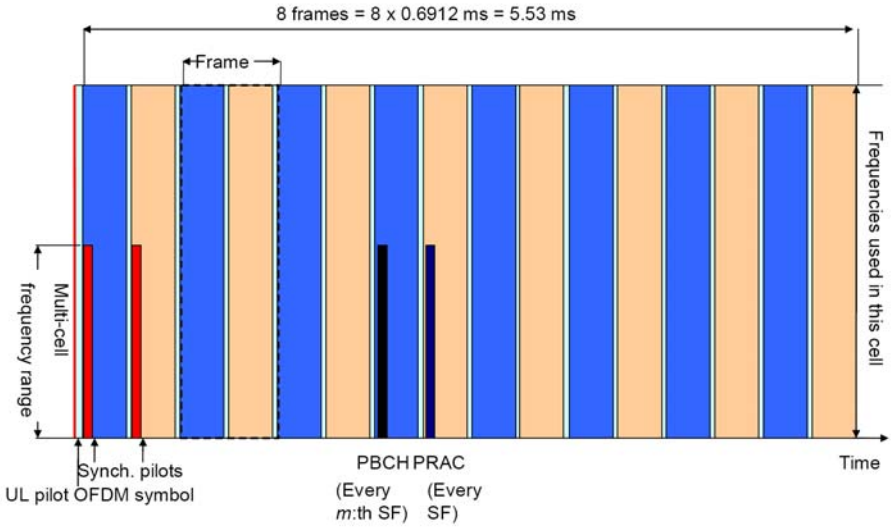

Figure 2.4 : WINNER super-frame for symmetric TDD transmission.

The quantum for resource allocation is called chunk and its dimension are 8 subcarriers (in the frequency domain) and a time slot (in the temporal domain), please see figure 2.5 for a pictorial representation with absolute values. Chunks are mapped to contiguous subcarriers in case of frequency adaptive scheduling, but they are mapped onto dispersed subcarriers when non-frequency adaptive scheduling is used.

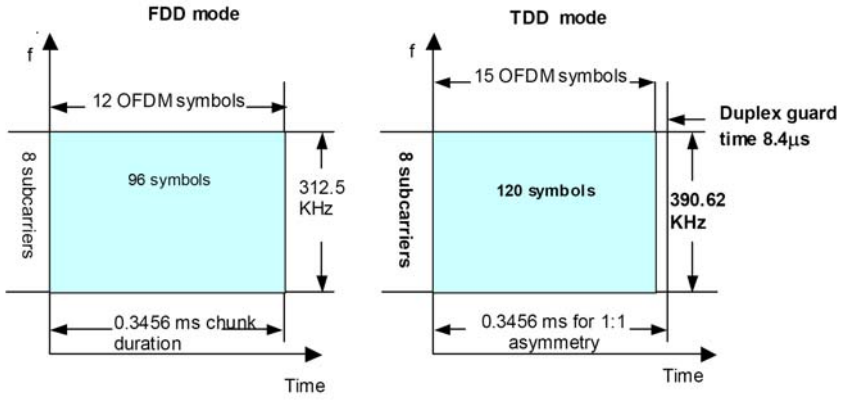

Figure 2.5 : WINNER resource allocation unit (called chunk) in FDD and TDD mode.

2.3 3GPP Long Term Evolution

The competitiveness of UMTS (Universal Mobile Telecommunication Systems) for the next years introduced the concepts for UMTS Long Term Evolution (LTE) in 3GPP (Generation Partnership Project) Release 8. The focus is a high throughput, low latency and packet-optimized radio access technology. LTE is referred to as E-UTRA(Evolved UMTS Terrestrial Radio Access) or E-UTRAN (Evolved UMTS Terrestrial Radio Access Network). The multiple access scheme for the LTE physical layer is based on OFDMA with a cyclic prefix (CP) in the downlink, and on Single-Carrier Frequency Division Multiple Access (SC-FDMA) with a cyclic prefix in the uplink. Downlink modulation schemes QPSK, 16QAM and 64QAM are available. The data channels are shared channels, i.e. for each transmission time interval of 1ms, a new scheduling decision is taken regarding which users are assigned to which time/frequency resources during this transmission time interval. To support transmission in paired and unpaired spectrum, two duplex modes are supported: Frequency Division Duplex (FDD), supporting full duplex and half duplex operation, and Time Division Duplex (TDD). The main system parameters for both FDD and TDD modes are summarized by the following tables [19,20]. Note that each sub-frame is composed of two timeslots.
Different downlink MIMO modes can be adjusted according to channel condition and traffic requirements. The possible transmission modes in LTE are the following:

- Single-Antenna transmission (no MIMO)
- Transmit diversity
- Open-loop spatial multiplexing (no feedback)
- Closed-loop spatial multiplexing (feedback required)
- Multi-user MIMO
- Closed-loop precoding
- Beamforming

Downlink and uplink transmissions are organized into radio frames with $T_f = 307200 \times T_s = 10\,\text{ms}$ duration, where time units $T_s = 1/(15000 \times 2048)$ seconds. Two radio frame structures are supported respectively for FDD and TDD.

The first frame structure is applicable to both full duplex and half duplex FDD. Each radio frame is $T_f = 307200 \cdot T_s = 10\,\text{ms}$ long and consists of 20 slots of equal length $T_{slot} = 15360 \cdot T_s = 0.5\,\text{ms}$, numbered from 0 to 19. A subframe is defined as two consecutive slots where subframe *i* consists of slots $2i$ and $2i+1$.

Transmission BW		1.25 MHz	2.5 MHz	5 MHz	10 MHz	15 MHz	20 MHz
Slot duration		0.5 ms					
Sub-carrier spacing		15 kHz					
Sampling frequency		1.92 MHz (1/2 × 3.84 MHz)	3.84 MHz	7.68 MHz (2 × 3.84 MHz)	15.36 MHz (4 × 3.84 MHz)	23.04 MHz (6 × 3.84 MHz)	30.72 MHz (8 × 3.84 MHz)
FFT size		128	256	512	1024	1536	2048
Number of occupied sub-carriers†, ††		76	151	301	601	901	1201
Number of OFDM symbols per slot (Short/Long CP)		7/6					
CP length (μs/samples)	Short	(4.69/9) × 6, (5.21/10) × 1*	(4.69/18) × 6, (5.21/20) × 1	(4.69/36) × 6, (5.21/40) × 1	(4.69/72) × 6, (5.21/80) × 1	(4.69/108) × 6, (5.21/120) × 1	(4.69/144) × 6, (5.21/160) ×1
	Long	(16.67/32)	(16.67/64)	(16.67/128)	(16.67/256)	(16.67/384)	(16.67/512)

TABLE 1.2 : PARAMETERS FOR DOWNLINK TRANSMISSION SCHEME (FDD).

Transmission BW		1.25 MHz	2.5 MHz	5 MHz	10 MHz	15 MHz	20 MHz
Timeslot duration		0.675 ms					
Sub-carrier spacing		15 kHz					
Sampling frequency		1.92 MHz (1/2 × 3.84 MHz)	3.84 MHz	7.68 MHz (2 × 3.84 MHz)	15.36 MHz (4 × 3.84 MHz)	23.04 MHz (6 × 3.84 MHz)	30.72 MHz (8 × 3.84 MHz)
FFT size		128	256	512	1024	1536	2048
Number of occupied sub-carriers†, ††		76	151	301	601	901	1201
Number of OFDM symbols per Timeslot (Short/Long CP)		9/8					
CP length (μs/samples)	Short	7.29/14	7.29/28	7.29/56	7.29/112	7.29/168	7.29/224
	Long	16.67/32	16.67/64	16.67/128	16.67/256	16.67/384	16.67/512
Timeslot Interval (samples)	Short	18	36	72	144	216	288
	Long	16	32	64	128	192	256

TABLE 2.3- PARAMETERS FOR DOWNLINK TRANSMISSION SCHEME (ALTERNATIVE TDD FRAME STRUCTURE)

For FDD, 10 subframes are available for downlink transmission and 10 subframes are available for uplink transmissions in each 10 ms interval. Uplink and downlink transmissions are separated in the frequency domain. In half-duplex FDD operation, the UE cannot transmit and receive at the same time while there are no such restrictions in full-duplex FDD.

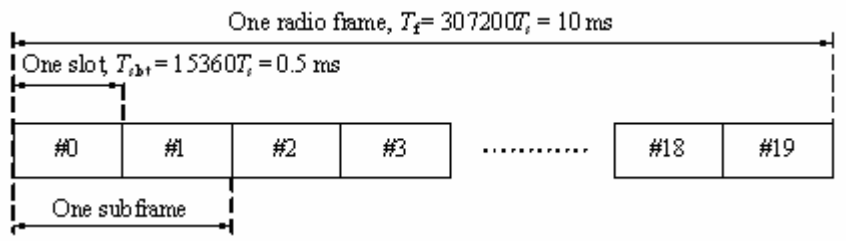

Figure 2.6 Frame structure (FDD).

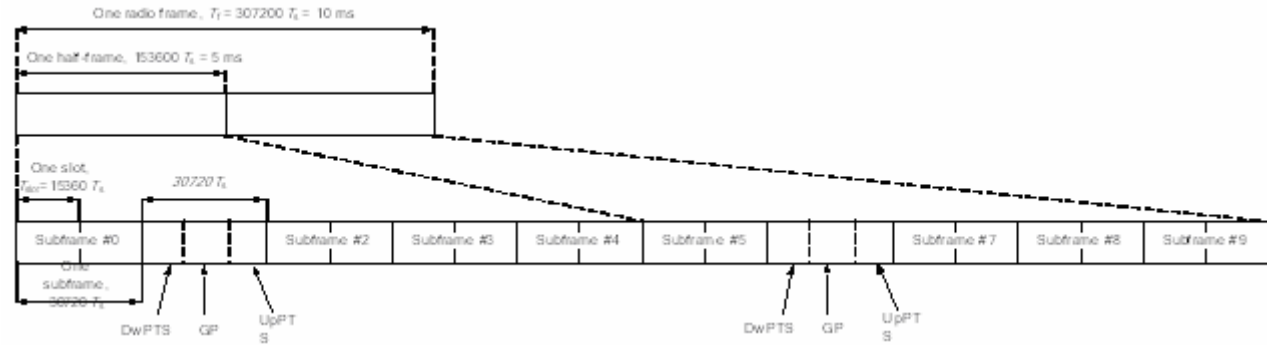

Figure 2.7 Frame structure (for TDD with 5 ms switch-point periodicity).

The second frame structure is applicable to TDD. Each radio frame of length $T_{\mathrm{f}} = 307200 \cdot T_{\mathrm{s}} = 10\,\mathrm{ms}$ consists of two half-frames of length $T_{\mathrm{f}} = 153600 \cdot T_{\mathrm{s}} = 5\,\mathrm{ms}$ each. Each half-frame consists of eight slots of length $T_{\mathrm{slot}} = 15360 \cdot T_{\mathrm{s}} = 0.5\,\mathrm{ms}$ and three special fields, DwPTS(Downlink Pilot Timeslot), GP (Guard Period), and UpPTS (Uplink Pilot Timeslot). The length of DwPTS and UpPTS is given by Table 2.4 subject to the total length of DwPTS, GP and UpPTSbeing equal to $30720 \cdot T_{\mathrm{s}} = 1\,\mathrm{ms}$. Subframe 1 in all configurations and subframe 6 in configurations 0, 1, 2 and 6 in Table 2.4 consists of DwPTS, GP and UpPTS. All other subframes are defined as two slots where subframe i consists of slots $2i$ and $2i+1$. Subframes 0 and 5 and DwPTS are always reserved for downlink transmission. The channel-coded, interleaved, and data-modulated information is mapped onto OFDM time/frequency symbols. The OFDM symbols can be organized into a number of *physical* resource blocks (PRB) consisting of a number (M) of consecutive sub-carriers for a number (N) of consecutive OFDM symbols. The granularity of the resource allocation should be able to be matched to the expected minimum payload. It also needs to take channel adaptation in the frequency domain into account. The size of the baseline physical resource block, S_{PRB}, is equal to MxN, where M=25 and N is equal to the number of OFDM symbols in a subframe. This results in the segmentation of

the transmit bandwidth shown in the Table 2.5. The frequency and time allocations to map information for a certain User Equipment (UE) to resource blocks is determined by the scheduler and may e.g. depend on the frequency-selective CQI (channel-quality indicator) reported by the UE. The channel-coding rate and the modulation scheme (possibly different for different resource blocks) are

Configuration	Normal cyclic prefix			Extended cyclic prefix		
	DwPTS	GP	UpPTS	DwPTS	GP	UpPTS
0	$6592 \cdot T_s$	$21936 \cdot T_s$	$2192 \cdot T_s$	$7680 \cdot T_s$	$20480 \cdot T_s$	$2560 \cdot T_s$
1	$19760 \cdot T_s$	$8768 \cdot T_s$		$20480 \cdot T_s$	$7680 \cdot T_s$	
2	$21952 \cdot T_s$	$6576 \cdot T_s$		$23040 \cdot T_s$	$5120 \cdot T_s$	
3	$24144 \cdot T_s$	$4384 \cdot T_s$		$25600 \cdot T_s$	$2560 \cdot T_s$	
4	$26336 \cdot T_s$	$2192 \cdot T_s$		$7680 \cdot T_s$	$17920 \cdot T_s$	$5120 \cdot T_s$
5	$6592 \cdot T_s$	$19744 \cdot T_s$	$4384 \cdot T_s$	$20480 \cdot T_s$	$5120 \cdot T_s$	
6	$19760 \cdot T_s$	$6576 \cdot T_s$		$23040 \cdot T_s$	$2560 \cdot T_s$	
7	$21952 \cdot T_s$	$4384 \cdot T_s$		-	-	-
8	$24144 \cdot T_s$	$2192 \cdot T_s$		-	-	-

TABLE 2.4 : LENGTHS OF DWPTS/GP/UPPTS.

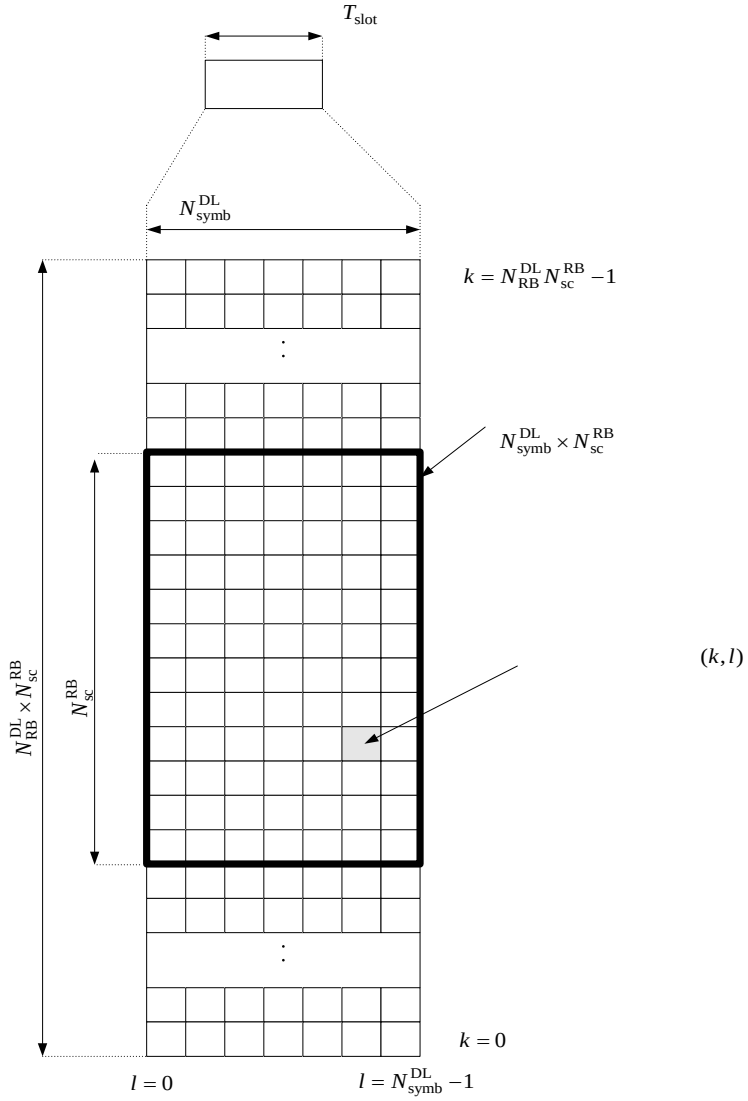

Figure 2.8 : Downlink resource grid.

also determined by the scheduler and may also depend on the reported CQI. Both block-wise transmission (localized) and transmission on non-consecutive (scattered, distributed) sub-carriers are also to be supported as a means to maximize frequency diversity. To describe this, the notion of a *virtual* resource block (VRB) is introduced. A virtual resource block has the following attributes: Size, measured in terms of time-frequency resource. Type, which can be either 'localized' or 'distributed'.All localized VRBs are of the same size, which is denoted as S_{VL}. The size S_{VD} of a distributed VRB may be different from S_{VL}. Distributed VRBs are mapped onto the PRBs in a distributed manner. Localized VRBs are mapped onto the PRBs in a localized manner. The multiplexing of localized and distributed transmissions within one subframe is accomplished by FDM.As a result of mapping VRBs to PRBs, the transmit bandwidth is structured into a combination of localized and distributed transmissions. The UE can be assigned multiple VRBs by the scheduler. Each element in the resource grid for antenna port p is called a resource element and is uniquely identified by the index pair (k,l) in a slot where k,l are the indices in the frequency and time domains, respectively.

Bandwidth (MHz)	1.25	2.5	5.0	10.0	15.0	20.0
Physical resource block bandwidth (kHz)	375	375	375	375	375	375
Number of available physical resource blocks	3	6	12	24	36	48

TABLE 2.5 PHYSICAL RESOURCE BLOCK IN THE DOWNLINK

2.4 Mobile WiMAX

Mobile WiMAX is a broadband wireless access technology based on IEEE 802.16e standard. The WiMAX forum defines mandatory and optional features of the IEEE standard that are necessary to built a mobile WiMAX compliant air interface. The air interface utilizes OFDMA as the radio access method for improved performance in a reach scattering environment. Scalable OFDMA (SOFDMA) is employed by allowing variable channel bandwidth allocation from 1.25 MHz to 20 MHz. as shown in Table 2.6. IEEE 802.16e supports both TDD and FDD modes: However the mobile WiMAX profiles are based only on TDD mode of operation to efficiently support asymmetric DL/UL traffic (adaptation of DL:UL ratio to traffic). The OFDMA symbol; structure is made of three types of subcarriers:

- Data subcarriers
- Pilot subcarriers for estimation and synchronization
- Null subcarriers –guard bands and DC subcarriers

Data and pilot subcarriers are grouped into subsets called subchannels. Subchannelization in both DL and UL direction is supported. Subchannelization schemes divide the frequency/time resources between users and define slots/subchannels. Slot is logical n x m rectangle in the time-frequency grid where n is a number of subcarriers and m is a number of contiguous symbols. Pseudo-random permutation scheme is specified for supporting frequency diversity (full usage subchannelization (FUSC) and partial usage subchannelization (PUSC)) or contiguous assignment (AMC) to support beamforming. Each slot contains 48 data subcarriers for all subchannelization schemes but their arrangement is different in different schemes. With DL PUSC, subcarriers are grouped into clusters containing 14 contiguous subcarriers per symbol with pilot and data allocations in each cluster in the even and odd symbols as shown in Figure 2.9.

System bandwidth (MHz)	1.25	2.5	5	10	20
Sampling frequency(MHz)	1.4	2.8	5.6	11.2	22.4
FFT size	128	256	512	1024	2048
Subcarrier spacing(KHz)	10.94				
OFDM symbol duration (μs)	102.86				
Useful symbol time(μs)	91.43				
Guard time(μs)	11.43- guard time =1/8 useful time				
Subcarrier frequency spacing (KHz)	10.94				
Number of OFDMA symbols(5ms frame)	48				

TABLE 2.6 IEEE 802.16E SCALABLE OFDMA PARAMETERS

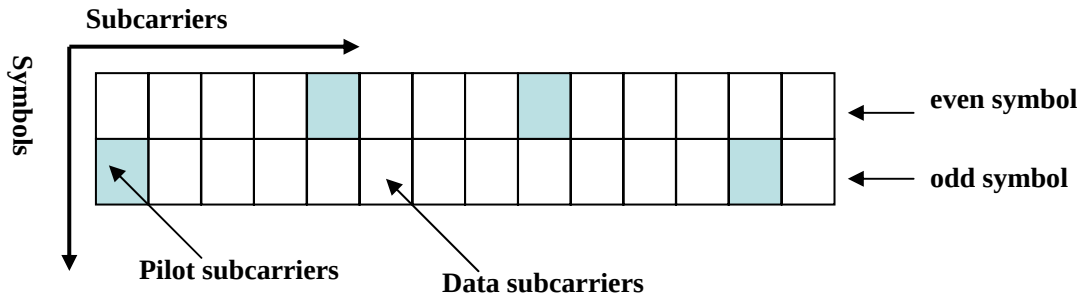

Figure 2.9 : Downlink PUSC cluster structure.

Except SOFDMA, the technologies employed by mobile WiMAX include the following:

- MIMO
- IP (Internet Protocol)
- Adaptive Antenna Systems (AAS) e.g. beamforming, Space Time Code (STC) and Spatial Mulltiplexing(SM)
- Adaptive Modulation Schemes
- Advanced Encryption Standard (AES) encryption

In TDD, the portion allocated for the downlink and portion allocated to the uplink may vary. The Uplink is time division multiple access (TDMA) where bandwidth is split into time slots. Each time slot is allocated to an individual Subcarrier Station (SS) being served by the BS. A downlink sub frame contains two parts. One part is for control information, which holds preamble for frame synchronization and maps and the other contains data. A Downlink map states the starting position and transmission attributes of the data bursts. An Uplink map states the allocation of the bandwidth to mobile station SS for their communication. In contrast to 802.11 CSMA/CA method, 802.16 uses Uplink and Downlink maps to confirm collision free access. We consider an OFDMA frame for TDD. The frame, shown in Figure 2.10, consists of DL and UL subframes, separated by Transmit/Receive and Receive/Transmit gaps (TTG and RTG), respectively.

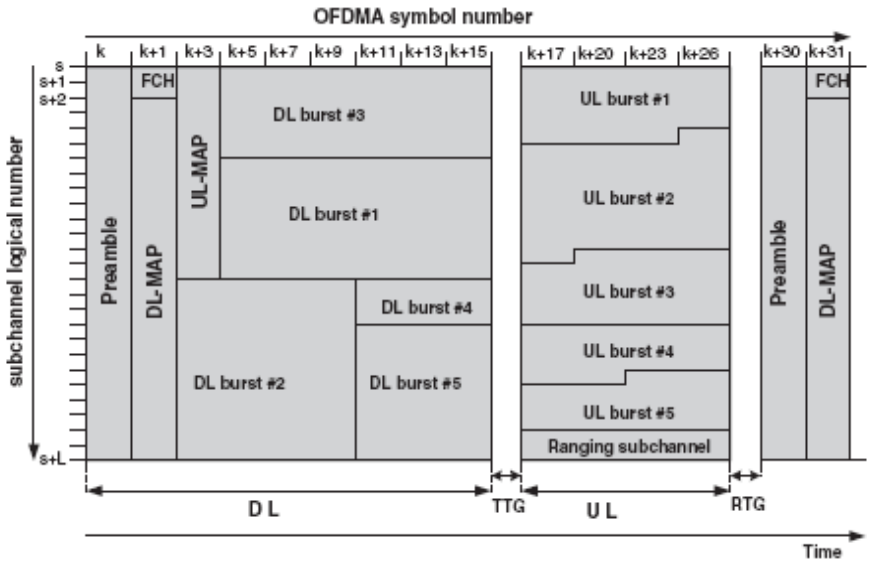

Figure 2.10 One TDD time frame

The DL subframe starts with a preamble which occupies one OFDM symbol. Frame control header (FCH) imm ediately follows the preamble. FCH contains DL frame prefix (DLFP) that specifies the burst profile and the length of the DL-MAP. DL-MAP message always follows FCH, while UL-MAP message always follows a DL-MAP message. Downlink channel descriptor (DCD) and uplink channel descriptor (UCD), if transmitted, follow the DL-MAP and UL-MAP messages. The rest of the frame contains DL bursts, which could be unicast, multicast, or broadcast data.The UL subframe, on the other hand, consists of UL bursts coming from single or multiple stations, as well as bandwidth/ranging (BW/RNG) request allocation portion of the subframe. The MAC layer consists of three sub layers. Service Specific Convergence Sublayer (MAC CS), the MAC Common Part Sublayer (MAC CPS) and the privacy sublayer.The MAC CS sublayer communicates with higher layers and transforms upper level data services to MAC layer flows and associations. The MAC CS has two types of sublayers: one is ATM convergence sublayer for ATM networks & services and the

other one is Packet Convergence sublayer for packet data services for example, Ethernet, PPP, IP and . The basic function of CS Layer is that it receives data from higher layers, classifies data as ATM cells or packets and forwards frames to CPS layer. The Packet Convergence Sub-Layer maps the higher layer PDUs (Protocol Data Units) into appropriate MAC connections and provides also Payload header suppression (optional).

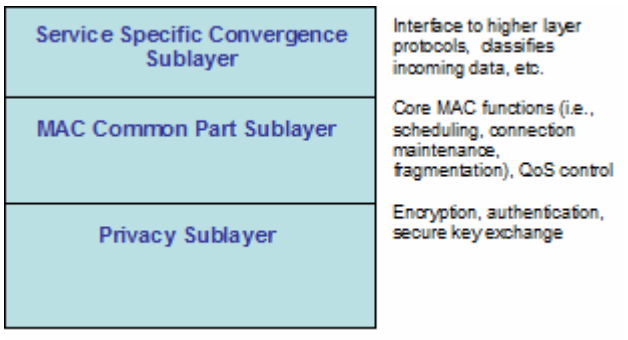

Figure 2.11 MAC layer

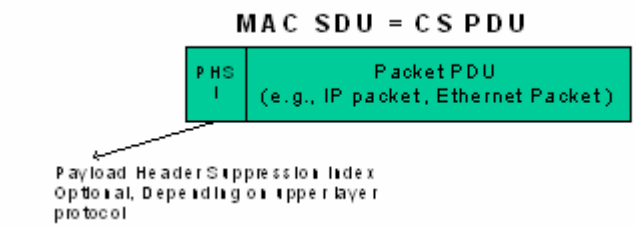

Figure 2.12 MAC SDU (Service Data Unit), i.e, CS PDU, formatting

The core part of the IEEE 802.16 MAC is the MAC CPS, which defines all methods for connection management, bandwidth distribution, request & grant, system access procedure, uplink scheduling, connection control, and automatic repeat request (ARQ). Communication between the CS (Convergence Sublayer) and the MAC CPS are

maintained by MAC Service Access Point (MAC SAP). Creation, modification, deletion of connection and transportation of data over the channel are four the basic functions occuring in this communication process. The Privacy Sublayer is accountable for the encryption and decryption of data that is coming and leaving the Physical layer. It is also used for authentication and secure key exchange. It carries 56bit DES encryption for traffic and 3DES encryption for key exchanges. In IEEE 802.16 network, the Base Station(BS) has 48bit base station ID, which is not a MAC address and Service Station (SS) has 48bit 802.3 MAC address . The 16 bit connection identifier (CID) used in MAC PDU (Protocol Data Units), functions as a reference for all connections and is constantly granted bandwidth on demand . There are two types of MAC connection: one is Management

connection and the other is Transport connection. MAC layer connections are like TCP connections. For example the SS can have several connections to a BS for different services, like for network management or for data transport. In MAC, all associations use different parameters for priority, bandwidth and security. BS always assigns CID for SS. As soon as a SS joins a network, three different CIDs are allocated to it. Moreover, each CID has separate QoS requirements, which are used by different management connection levels: Primary (authentication and connection setup), Basic (used to transfer brief, time critical MAC and Radio Link control messages) and Secondary Management connections (transfer standards based management messages i.e. DHCP, TFTP, and SNMP). Both basic and primary management connections are created when a MS (Mobile station)/SS is joined to a BS network. Transport connections can be established on demand. They are used for user traffic flows, unicast or multicast transmission. Additional channels are also reserved by the MAC to send out uplink and downlink schedule. A single CID can carry traffic for many different higher layer sessions. The IEEE 802.16 MAC Layer is a stateful machine. It has series of state machines to determine the operation of individual process within the MAC structure.

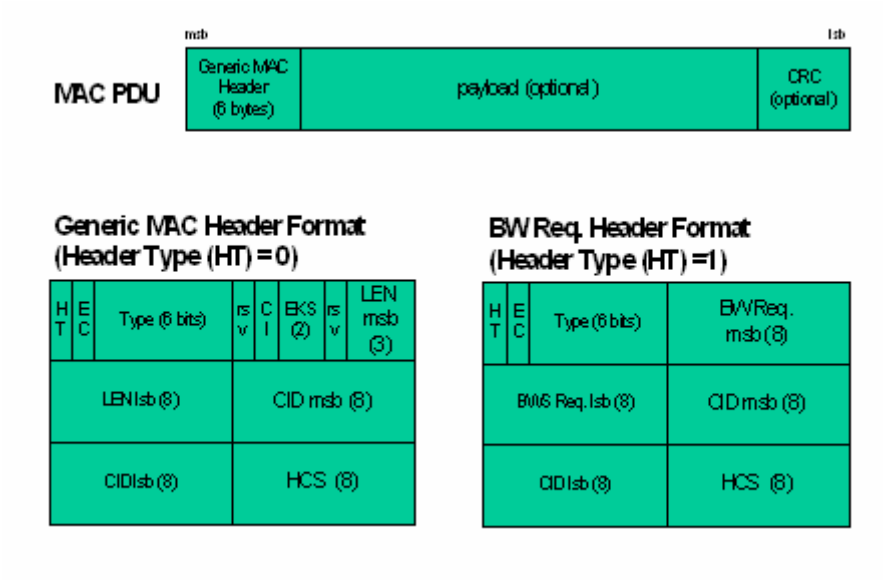

Figure 2.13 MAC PDU format

MAC Protocol Data Units (MPDUs) contains exchange messages of BS MAC and SS MAC. It has three parts: a fixed length MAC header, which contains frame control information; a variable length Payload (frame body) and a frame check sequence (FCS), which holds IEEE 32bit CRC . The maximum length of the MAC PDU is 2048 bytes, including header, payload, and cyclic redundancy check (CRC).A MAC Service Data Unit (SDU) can be divided into one or more MAC SDUs (Fragmentation) or multiple MAC SDUs can be packed into a single MAC PDU payload (Packing).

Again, MAC header types are: MAC Service Data Unit (MSPU), where payloads are MAC SDUs/segments, i.e., data from the upper layer (CS PDUs). Second one is, Generic MAC header (GMH) where the payloads are MAC Management messages or IP packets encapsulated in MAC CS PDUs. Both are transmitted on management connections. The third one is Bandwidth Request Header (BRH) which is sent out without payload. Except the Bandwidth Request PDUs, MAC PDUs may hold either MAC management messages or convergence Sublayer data MSDU.

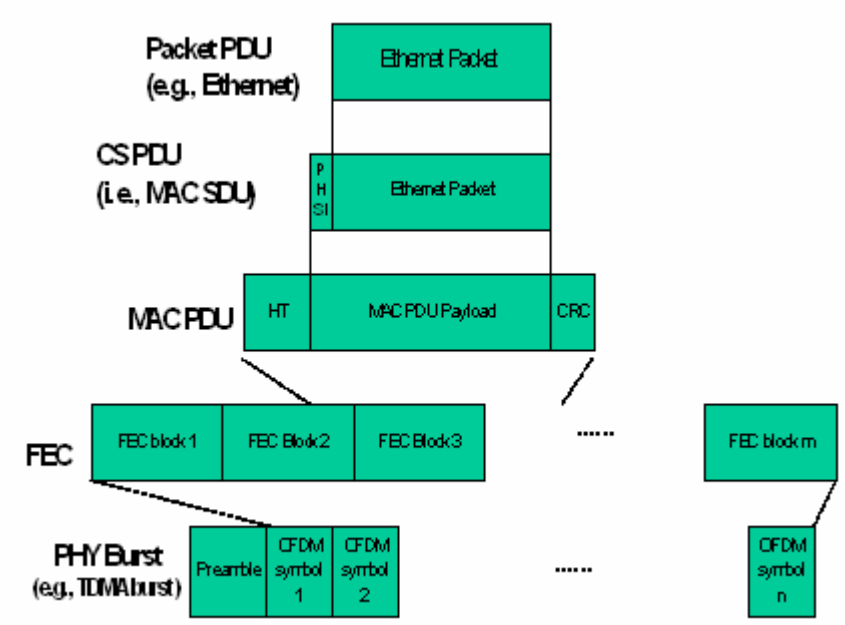

Figure 2.14 Data Packet Encapsulations

For both GMH and MSDU, Header Type (HT bit) is always set to 0 (zero) while Bandwidth Request Header is set to 1 (one). The MAC header contains a flag, which indicates whether the payload of the PDU is encrypted or not (EC: Data Encryption Control). According to IEEE Standard 802.16, MAC header and all MAC management messages are not encrypted. This decision was made to “facilitate registration, ranging and normal operation of the MAC sublayer” as it allows generation of false management messages. In Figure 2.14 , EKS is the Encryption Key Sequence (index of traffic encryption key), CI is CRC indicator.

A fundamental premise of the MAC architecture is quality of service (QoS). QoS provided via service flows. A unidirectional MAC-layer transport service characterized by a set of QoS parameters, e.g., latency, jitter, and throughput assurances and identified by a 32-bit SFID (Service Flow ID). QoS is depending on type of service. The AP sets certain parameters for QoS. Unidirectional flow of packets is provided with a set of QoS parameters. QoS is applied to both downlink (DL) and uplink (UL).

802.16e is an amendment to 802.16d (fixed or nomadic wireless broadband) to support mobility. Mobility adds several new challenges: a) fast Handover b) Adaptive modulation and c) Power efficiency.

A. Power Management

Due to the promising mobility capability in IEEE 802.16e, the mechanism in efficiently managing the limited energy is becoming very significant since SS is generally powered by battery. For this, sleep mode operation is recently specified in the MAC protocol.

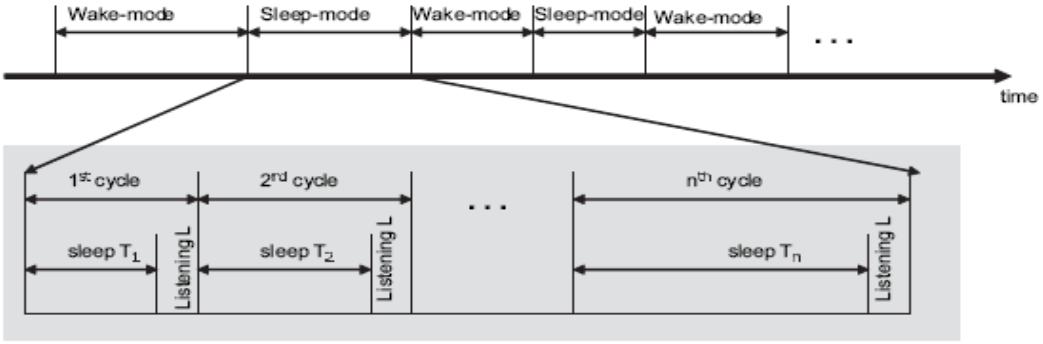

Figure 2.15 Wake mode and sleep mode in IEEE 802.16e

Figure 2.15 shows the wake mode and sleep mode of an SS. Before entering the sleep mode, the SS sends a request message to BS for the permission to transit into sleep mode. Upon receiving the response message from the BS with parameters initial-sleep window (T_{min}), final-sleep window (T_{max}) and listening window (L), the SS enters into sleep mode. After a sleep mode, the SS transits back to the wake mode again. As a consequence, the SS alternatively stays in wake mode and sleep mode during its lifetime. The duration of the first sleep interval T_1 is equal to the initial sleep window T_{min}. After the first sleep interval, the SS transits into listening state and listens to the traffic indication message MOB-TRF-IND broadcasting from BS. The message indicates whether there has been traffic addressed to the SS during its sleep interval. If MOB-TRF-IND indicates a negative indication, then the SS continues its sleep mode after the listening interval L. Otherwise, the SS will return to wake mode. We term the sleep interval and its subsequent listening interval as a cycle. If the SS continues sleep mode, the next sleep-window starts from the end of the previous listening-window; and it shall double the preceding sleep interval. This process is repeated as long as the sleep interval does not exceed the final-sleep window $T_{max.}$ When the SS has reached T_{max}, it shall keep the sleep interval as fixed T_{max}. Idle mode allows SS to become periodically available for broadcast messages without registering at a BS (Paging by DL broadcasting messages).

B. Handover (HO)

Because mobile SS moves to another place, signal strength changes due to Signal fading, interference levels, etc , SS need higher QoS. The change of the BS provides a higher signal quality. The goal of handover is to allow mobile SS to move efficiently between BSs, to provide smooth BSs transitions with minimal loss of PDUs or to provide fast BSs transitions to guarantee QoS. Terminal assisted HO will be implemented. It means that SS collects information related to potential HO and transfers it to the network; network collects relevant information (e.g. PHY measurements from BSs), makes decision and executes the handover.

Types of HO:

• Inter-channel HO: between channels (sectors) at the same BS. In this case BS makes HO decision and executes the handover

• Inter-cell soft HO: between two BSs. In this case serving BS makes HO decision and executes the HO.

• Inter-cell Hard HO in the case MS fails to communicate to the serving BS, it performs complete NW Entry procedure with the best possible BS; new BS informs old BS on theHO.

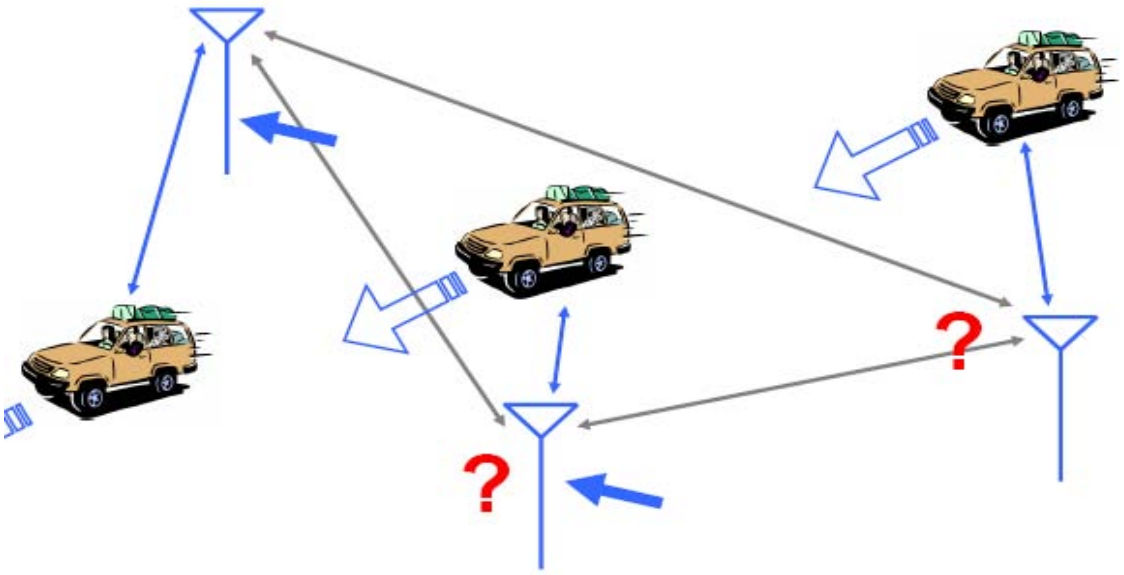

Figure 2.16 High speed handover

In network topology acquisition stage, there is only one BS can be selected as target BS for handover actually. The results gained from scan may be invalid because of the changes of neighbor BSs' channel quality. The throughput will decrease if the scan/association process occupies too many resources. In HO execution stage interruption of data transmission only happens during the network

re-entering process. The time of interruption is called handover delay. Service will be terminated if the handover delay is too long for applications. Using fast ranging and pre-registration schemes can reduce the handover delay, hence increase the successful probability of handovers.

C. Scheduling

The Mobile WiMAX MAC scheduling service is designed to efficiently deliver broadband data services including voice, data, and video over time varying broadband wireless channel. The MAC scheduling service has the following properties that enable the broadband data service:

Fast Data Scheduler: The MAC scheduler must efficiently allocate available resources in response to bursty data traffic and time-varying channel conditions. The scheduler is located at each base station to enable rapid response to traffic requirements and channel conditions. The data packets are associated to service flows with well defined QoS parameters in the MAC layer so that the scheduler can correctly determine the packet transmission ordering over the air interface. The CQICH channel provides fast channel information feedback to enable the scheduler to choose the appropriate coding and modulation for each allocation. The adaptive modulation/coding combined with HARQ provide robust transmission over the time-varying channel.

Scheduling for both DL and UL: The scheduling service is provided for both DL and UL traffic. In order for the MAC scheduler to make an efficient resource allocation and provide the desired QoS in the UL, the UL must feedback accurate and timely information as to the traffic conditions and QoS requirements. Multiple uplink bandwidth request mechanisms, such as bandwidth request through ranging channel, piggyback request and polling are designed to support UL bandwidth requests. The UL service flow defines the feedback mechanism for each uplink connection to ensure predictable UL scheduler behavior. Furthermore, with orthogonal UL sub-channels, there is no intra-cell interference. UL scheduling can allocate resource more efficiently and better enforce QoS.

Dynamic Resource Allocation: The MAC supports frequency-time resource allocation in both DL and UL on a per-frame basis. The resource allocation is delivered in MAP messages at the beginning of each frame. Therefore, the resource allocation can be changed on frame-by-frame in response to traffic and channel conditions. Additionally, the amount of resource in each allocation can range from one slot to the entire frame. The fast and fine granular resource allocation allows superior QoS for data traffic. QoS Oriented: The MAC scheduler handles data transport on a connection-by connection basis. Each connection is associated with a single data service with a set of QoS parameters that quantify the aspects of its behavior. With the ability to dynamically allocate resources in both DL and UL, the scheduler can provide superior QoS for both DL and UL traffic.

Frequency Selective Scheduling: The scheduler can operate on different types of sub-channels. For frequency-diverse sub-channels such as PUSC permutation, where sub-carriers in the sub-channels are pseudo-randomly distributed across the bandwidth, sub-channels are of similar quality.

Frequency-diversity scheduling can support a QoS with fine granularity and flexible time-frequency resource scheduling. With contiguous permutation such as AMC permutation, the sub-channels may experience different attenuation. The frequency-selective scheduling can allocate mobile users to their corresponding strongest sub-channels. The frequency-selective scheduling can enhance system capacity with a moderate increase in CQI overhead in the UL.

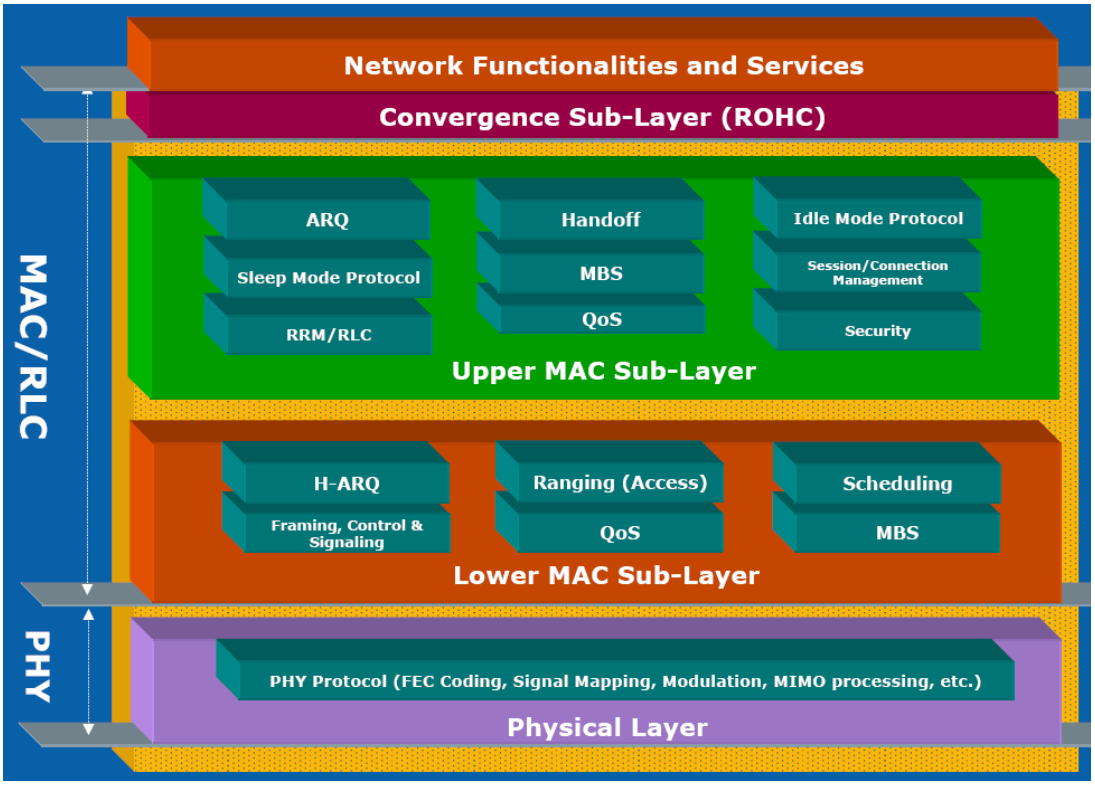

Figure 2.17 PHY-MAC layers in wimax

Scheduling services have represented the data handling mechanisms supported by the MAC scheduler for the data transport on a connection. To provide the service parameters respectively, the traffic management is necessary. The WiMAX standard divides all services in four different classes. Each group corresponds to a single service class, which is associated with a set of QoS parameters for quantifying the aspects of its behavior. These service classes are listed below:

2) Real-time polling service (rtPS): This service represents real time data streams comprising variable bit-rate (VBR) data packets which are issued at periodic intervals, such as MPEG video. This application requires a guaranteed minimum reserved rate and latency, which are same as those of UGS. But the rtPS has to request transmission resources by polling (contention-free).

3) Non-real-time polling service (nrtPS): This service is a delay-tolerant data stream consisting of variable-sized data packets, such as the file transfer protocol (FTP). A minimum data rate is required and the bandwidth request by polling is needed.

4) Best effort (BE): It does not provide any QoS guarantee, like the email or the short length FTP. There is no minimum resources allocation granted, where the occurrence of dedicated opportunities is subject to the network load. The channel access mechanism of this service is based on contention.

QoS Category	Applications	QoS Specifications
UGS Unsolicited Grant Service	VoIP	• Maximum Sustained Rate • Maximum Latency Tolerance • Jitter Tolerance
rtPS Real-Time Polling Service	Streaming Audio or Video	• Minimum Reserved Rate • Maximum Sustained Rate • Maximum Latency Tolerance • Traffic Priority
ErtPS Extended Real-Time Polling Service	Voice with Activity Detection (VoIP)	• Minimum Reserved Rate • Maximum Sustained Rate • Maximum Latency Tolerance • Jitter Tolerance • Traffic Priority
nrtPS Non-Real-Time Polling Service	File Transfer Protocol (FTP)	• Minimum Reserved Rate • Maximum Sustained Rate • Traffic Priority
BE Best-Effort Service	Data Transfer, Web Browsing, etc.	• Maximum Sustained Rate • Traffic Priority

TABLE 2.7 QUALITY OF SERVICE

Chapter 3

MIMO Radio Channel Models

This chapter introduces radio channel models that are used in the thesis to generate channel gain parameters. We select the most promising extisting MIMO channel models for more deep analysis. Based on this analysis, we should understand the reason that the selected channel models are the most suitable models for immediate use. Technical selection criteria may be frequency range, bandwidth, antenna configurations, mobility, correlation characteristics, path loss, sort-term fading, long term fading, etc. In this work, IEEE 802.11n channel models will be used for WLAN applications (short range scenarios) while WINNER II, a more advanced channel model, for WMAN applications (wide-area scanario).

3.1 Mobile Radio Propagation

The main components of radio propagation are the following:

- Propagation path loss
- Large scale propagation models
- Small scale propagation models

Large-scale propagation models predict the mean signal strength over a large transmitter- receiver separation distance (several or thousands of meters). Small-scale propagation models describe multi-path fading, the rapid fluctuation ot the amplitude of the received signal over a short period of time or short travel distance proportional to wavelength λ. Two or more versions of the transmitted signals are combined at the receiver at slightly different time to give a resulting signal which varies widely in amplitude and phase (multi-path fading). The received signal power may vary 30 or 40 dB when the receiver is moved only a fraction of a wavelength λ. We compute the received power by averaging over several (5 to 40) wavelength. The free space propagation model predicts the received signal strength for a Line of Sight (LoS) path without obstacle between transmitter and receiver. The following free space models are widely used:

Friis Free Space Equation

$$P_r(d) = \frac{P_t G_t G_r \lambda^2}{(4\pi)^2 d^2 L} \quad (3.1)$$

where P_t is the transmitted power, $P_r(d)$ the received power which is a function of the separation distance d between transmitter and receiver (~ $1/d^2$), G_t the transmitter anntenna gain, G_r the receiver antenna gain and L the system loss factor not related to propagation (due to transmission line attenuation, filter losses, antenna losses, etc).

Hata Model

This model is an empirical formulation of the graphical path loss data provided by Okumura and it's valid for operation frequency f_c from 150 MHz to 1500 MHz, BS antenna height h_{te} from 30m to 200m and mobile antenna height h_{re} from 1m to 10m.

$$L(urban)(db) = 69.55+26.16\log f_c-13.82\log h_{te}-a(h_{re})+(44.9-6.55\log h_{te})\log d \quad (3.2)$$

where $a(h_{re})$ is the correction factor of effective mobile antenna height and is calculated for different areas (urban, suburban, rural) while the separation distance is referred in Km.

Large scale propagation model (long-term fading)

received signal presents a random variation due to blockage from objects in signal path, changes in reflecting surfaces and scattering objects. This effect is named shadowing and is modeled as a log-normal distribution with parameters $(\epsilon, \sigma^2_{\psi db})$ meaning that the ratio of transmit to receive power is

$$\psi = \frac{P_t}{P_r} = 10^{\frac{\epsilon_{\psi dB}+\sigma_{\psi dB}\ X}{10}} \quad (3.3)$$

where X is a standard normal random variable with $\epsilon_{\psi dB} = 0$ and variance $\sigma^2_{\psi dB}$ expressed in dB. For deviation $\sigma_{\psi dB}$ typical range is 3 db $\leq \sigma_{\psi dB} \leq$ 14db.

$$\psi_{dB} = \sigma_{\psi dB}\ X \qquad \text{and} \qquad L_{\text{tot}}(dB) = L(db) + \psi_{dB} \qquad (3.4)$$

Small scale propagation model (short-term fading)

Two types of small –scale fading may be considered: The first based on multipath time delay spread and the second based on Doppler spread. Multi-path induces inter-symbol interference (ISI) and delay spread. A mobile radio channel should be modeled as a linear filter with a impulse response h(d,t) varying with time. The time variation is due to receiver motion in space. The filtering nature of the channel is caused by the summation of amplitudes and delays of the multiple arriving waves at any instant of time. Delay spread is used to describe the dispersive nature of the channel. Delay spread στ is defined as the standard deviation of Ti, for all $i \in \{1, 2, \cdots N\}$ where Ti is the delay of i-th multi-path component and N the total number of paths. Excess delay is the relative delay of the i-th multipath component as compared to the first arriving component (T1=0). While time dmain focus on excess delay, frequency domain focus on coherence bandwidth Bc which is inverse proportional to rms (root mean square) delay spread σrms (~1 / σrms) . Coherence bandwidth is a statistical measure of the range of frequencies over which the channel can be considered flat, i.e. a channel which passes all spectral components with approximately equal gain and linear phase. Therefore, based on multi-path time delay spread we assume flat fading or narrowband systems where delay spread is smaller than symbol period or the bandwidth of the signal is smaller than coherence bandwith of the channel. Otherwise, we assume frequency selective fading or wideband

systems. Rayleigh distribution is usually used to describe amplitude distribution of the flat fading while M-ray Rayleigh fading model is used for analyzing frequency selective fading. When except scattered waves a LoS or direct signal component is presented at the receiver, the small-scale fading distribution is Ricean.

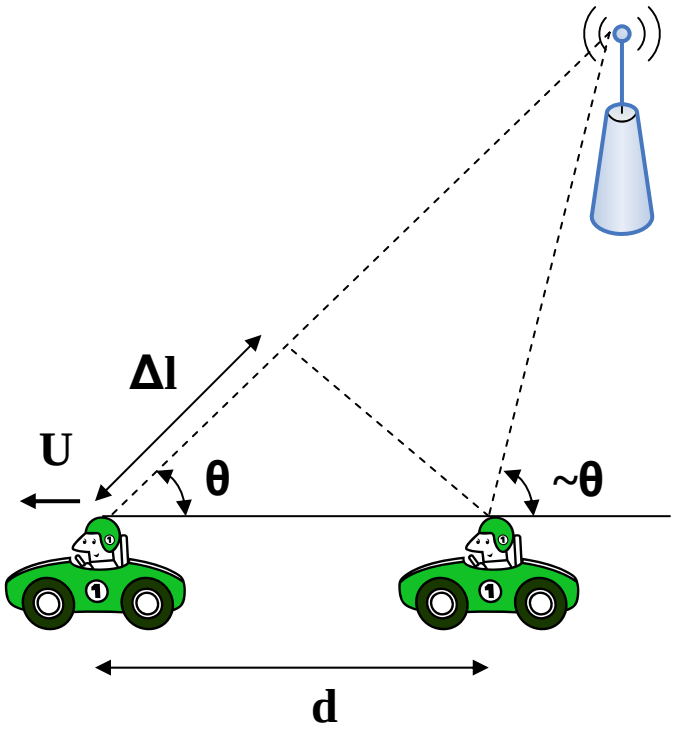

Figure 3.1 Doppler effect

The second type of small-scale fading is based on Doppler frequency shift due to the movement of the mobile relative to BS. In figure 3.1 the difference in travelling distance Δl

$$\Delta l = d\cos\theta = U\,\Delta t\cos\theta \quad (3.5)$$

introduces a phase change

$$\Delta\varphi = 2\pi\Delta l/\lambda \quad (3.6)$$

and therefore a Doppler shift

$$f_d = \frac{1}{2\pi}\frac{\Delta\varphi}{\Delta t} = \frac{U}{\lambda}\cos\theta \quad (3.7)$$

where U is the speed of the mobile. The Doppler spectrum (the received signal spectrum) will be in the range f_c-f_d to f_c+f_d. Doppler spread B_D is defined as the range of frequencies over which the received Doppler spectrum is essentially non-zero. Except Doppler spread, coherence time describe the time varying nature of the channel. Coherence time T_c is a statistical measure of the time duration over which the channel response is invariant. If coherence time is smaller than symbol period of the baseband signal, the channel variations are faster than these of baseband signal fast fading is considering. Otherwise, slow fading with low Doppler spread is assumed.

3.2 MI MO Line of Sight Channel Model

Let us now compute $\mathbf{H_{LOS}}$ channel matrix between transmit and receive Uniform Linear Array (ULA) with distance between elements equal to $d = \frac{\lambda}{2}$. BS is considering far enough from the users so that angle difference between received angles is small. Also, we assume a MIMO channel with only direct line-of-sight path.

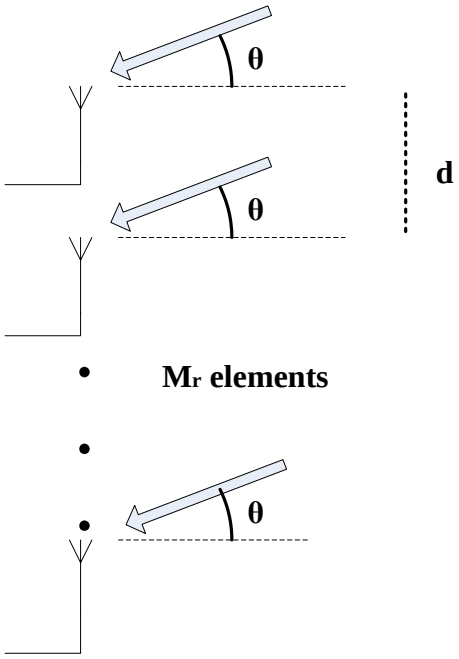

Figure 3.2 Uniform Linear Array at the receiver

Channel gain between k[th] transmit antenna and i[th] receive antenna is

$$h_{ik} = \sqrt{\alpha(u)}\exp(\frac{-j2\pi d_{ik}}{\lambda}) \qquad (3.8)$$

d_{ik} is the distance between the antennas and $\alpha(u)$ the power attenuation from Base Station to User u.

$$\alpha(u) = 10^{-\frac{L_{tot}(dB)}{10}} \qquad (3.9)$$

with $L_{tot}(dB)$ defined in (3.4).

Assuming that antenna array sizes are much smaller than the distance between BS and User,

$$d_{ik} = D + (i-1)d\sin\theta - (k-1)d\sin\theta \qquad (3.10)$$

D is the distance between transmit antenna 1 and receive antenna 1 and θ is the angle of incidence equal to the angle of departure at the line of sight path.

$$h_{ik} = \sqrt{\alpha(u)}\exp(-\frac{j2\pi d}{\lambda})\exp(j2\pi(k-1)d\sin\theta)\exp(-j2\pi(i-1)d\sin\theta) \qquad (3.11)$$

So, we could write the channel matrix $\mathbf{H_{LOS}}$ as

$$\mathbf{H_{LOS}} = \sqrt{\alpha(u)}\exp(-\frac{2\pi D}{\lambda})\ \vec{e_r}\ \vec{e_t}^{*} \qquad (3.12)$$

$$\overrightarrow{e_r} = \begin{bmatrix} 1 \\ \exp(-j2\pi D \sin\theta) \\ \exp(-j2\pi 2D \sin\theta \\ \vdots \\ \exp(-j2\pi(M_r - 1)D \sin\theta \end{bmatrix} \qquad (3.13)$$

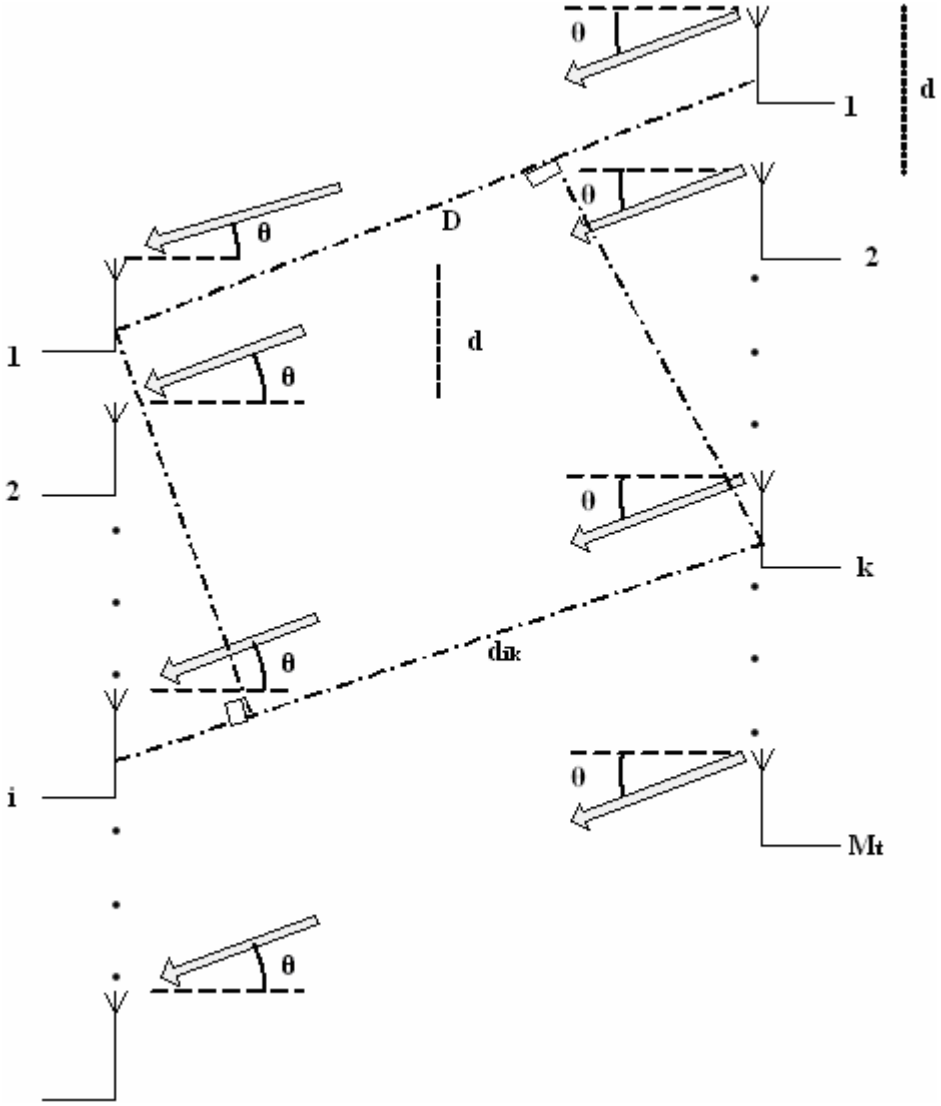

Figure 3.3 LOS channel with multiple transmitted and received antennas.The signals from BS arrive almost in parallel at antenna of user

$$\overrightarrow{e_t} = \begin{bmatrix} 1 \\ \exp(-j2\pi D \sin\theta) \\ \exp(-j2\pi 2D \sin\theta \\ \vdots \\ \exp(-j2\pi(M_t - 1)D \sin\theta \end{bmatrix} \qquad (3.14)$$

3.3 MI MO Stochastic models

Stochastic modelling should be based on physical propagation environment (large measurement campaign. Three types of channel models should be distiguished:

a) Geometrically-based

b) Parametric

c) Correlation-based

The parameters of a 2D (Dimensional) spatial modelling radio channel are:

a) The number of antenna elements at the transmiter and the receiver

b) The spacing and geometry of the antennas

c) The number of scatters and therefore of multipath components

d) Azimuth directions of scatters

e) Power of scatters

f) Delay of scatters

g) Fading characteristics

Geometrically-based models assume a stochastic distribution of scatters around the two ends of the connection. The shape of scattering area depends on the scenario. These models consider only a single bounce of the wave at the scattering surface. The parametric models describe the received signal as sum of multi-path waves and take the form of a tapped delay line where each tap reflects the propagation pah. Each multipath component is characterized from a complex gain, a delay and a pair of Direction of Departure (DoD) Direction of arrive (DoA) regardless of the number of bounces.

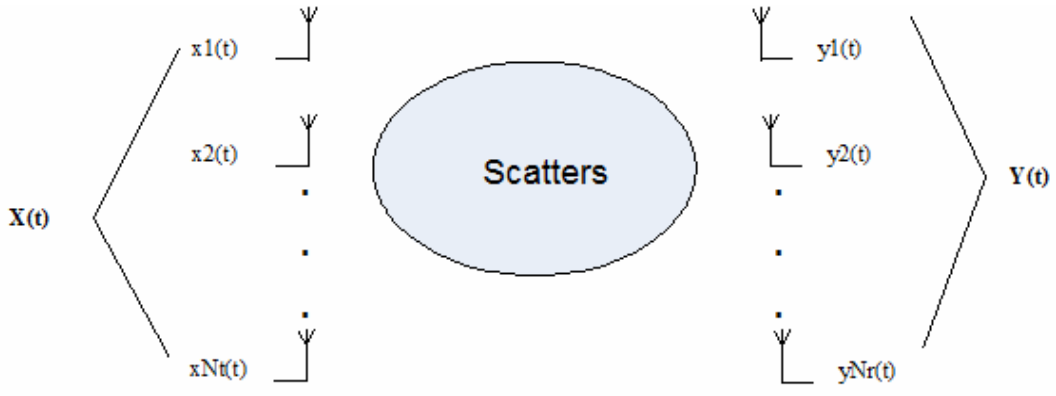

Figure 3.4 MIMO channel modeling

A. METRA channel model

The METRA (Multi – Element Transmit and Receive Antennas) embed the full correlation information of the channel [21]. The main strength of METRA model is that it relies the correlation between the transmitter and receiver arrays in two correlation matrices namely RMS and RBS which characterize the correlation of the link ends.

This model assume that BS and mobile are not spatially correlated and the joint correlation matrix is approximated as the Kronecker product of the R_{MS} and the R_{BS}. The R_{MS} and R_{BS} matrices are calculated from the Power-Azimuth spectrum (PAS) and Azimuth Spread (AS). According to the scenario the power distributed function (pdf) of PAS should be Laplacian, Truncated Gaussian or Uniform. The AS is the standard deviation of angles of arrival weighted with path power. The model is a tapped delay line where each of the tap is a matrix. The size of matrix depends on the number of antenna elements at the transmitter and the receiver. The parameters can be extracted from measurement results. Figure 3.4 illustrates the system model of a MIMO channel. If the channel response $\mathbf{H}$ is represented with the matrix as in (2.1), the relationship between received signal Y(t) and transmitted signal is

$$\mathbf{Y(t)} = \mathbf{H(t)X(t)} \quad (3.15)$$

The spatial complex correlation coefficient at the BS between antenna element m_1 and m_2 is given by

$$\rho_{m1m2}^{BS} =< h_{jm1}h_{jm2} > \quad (3.16)$$

We assume that the spatial correlation coefficient at the mobile is independent of j. The spatial complex correlation at the mobile between n1 and n2 antenna elements is given by

$$\rho_{n1n2}^{BS} =< h_{n1i}h_{n2i} > \quad (3.17)$$

We assume that the spatial correlation coefficient at the BS is independent of i. Correlation matrices R_{BS} and R_{MS} are defined as following:

$$\mathbf{R_{BS}} = \begin{bmatrix} \rho_{11}^{BS} & \rho_{12}^{BS} & \cdots & \rho_{1M_r}^{BS} \\ \rho_{21}^{BS} & \rho_{22}^{BS} & \rho_{23}^{BS} & \rho_{2Mr}^{BS} \\ \vdots & \vdots & \ddots & \vdots \\ \rho_{M_r1}^{BS} & \rho_{M_r2}^{BS} & \cdots & \rho_{M_rM_r}^{BS} \end{bmatrix} \quad (3.18)$$

$$\mathbf{R_{MS}} = \begin{bmatrix} \rho_{11}^{MS} & \rho_{12}^{MS} & \cdots & \rho_{1M_t}^{MS} \\ \rho_{21}^{MS} & \rho_{22}^{MS} & \rho_{23}^{BS} & \rho_{2M_t}^{MS} \\ \vdots & \vdots & \ddots & \vdots \\ \rho_{M_t1}^{MS} & \rho_{M_t2}^{MS} & \cdots & \rho_{M_tM_t}^{BS} \end{bmatrix} \quad (3.19)$$

The spatial correlation matrix is the Kronecker product of the spatial correlation matrices $\mathbf{R_{BS}}$ and $\mathbf{R_{MS}}$

$$\mathbf{R_{MIMO}}=\mathbf{R_{MS}} \otimes \mathbf{R_{BS}} \quad (3.20)$$

METRA model has a behaviour similar to pinhole realization. Reflections around the BS and mobiles are uncorrelated. However the channel rank is low because the scatter rings are too small compare the distance between BS and mobile. Therefore, the model in certain conditions, doesn't deliver the expected capacity improvement.

B. SCM of 3GPP channel model

3GPP-3GPP2 Spatial Channel Model (SCM) is a joint work between 3GPP and 3GPP/2 organizations to develop and specify parameters and methods associated with SCM [22]. The model is a ray-based model where a subset of parameters is stochastic. The center frequency is 2GHz and the bandwidth 5 MHz respectively. It consists of two sub-models: a) link level channel model which is defined only for calibration purposes and b) system level channel model to compare the performance of candidate MIMO schemes. The system level part is based on modeling correlated parameters of different domains and modeling directional information with randomly generated cluster positions. The correlation in space, time and frequency domain is treated implicitly. Different distributions in different domains imply the correlation between different domains. Transmitter and receiver are treated separately. Angle of Departure (AoD) and Angle of Arrival (AoA) are generated separately and the pairing between different rays takes place randomly. This way avoids Kronecker product. The simulations are carried out as a sequence of "drops". Fast fading is implied according to the speed of the mobiles. At each drop, the parameters are generated randomly and stay constant. The principle of SCM geometrical model is illustrated in figure 3.5.

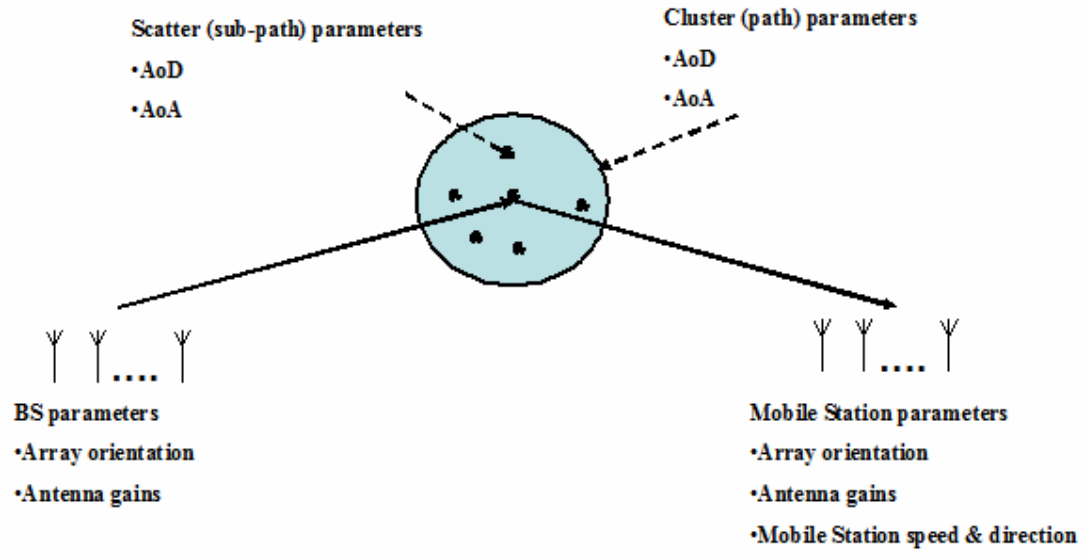

Figure 3.5 SCM channel modeling with one cluster

Each path is formed by adding a number of rays (sub-paths) with spatial, amplitude and temporal properties. The parameters of sub-paths or sub-rays have been predefined to produce the desire AS. Six paths each with 20 sub-rays are used. The cluster is defined as the last interaction with 20 scatters. Rms delay spread, AS and shadowing parameters are generated from distribution functions with predefined parameters. The positions of the clusters are determined randomly based on the above parameters. While the cluster positions are randomly, the positions of scatters within the cluster is fixed in order to produce the fixed per path AS. Each sub-ray of a cluster has the delay and power but different AoA and AoD predefined as a relative offset to the corresponding AoA and AoD of the corresponding ray. The statistical properties of the model are the following:

- Power Delay spectrum
- Power Azimuth spectrum
- The ratio between AS and standard deviation in angular domain
- The ratio between delay spread and standard deviations in delay domain.

3.4 IEEE 802.11n channel models

Channel model of IEEE 802.11n was designed to indoor environments in 2GHz and 5 GHz spectrum for MIMO WLAN applications. Only path loss model depends on frequency band. Modeled environments are small and large offices, residential homes and open spaces in LOS and NLOS conditions. IEEE 802.11 TGn model is a physical model, using a non – geometric stochastic approach.

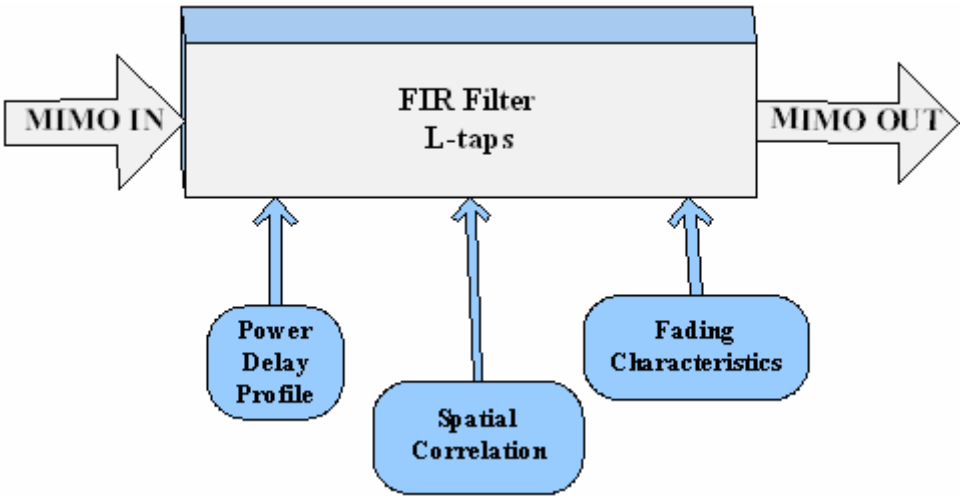

Figure 3.6 Characteristics of channel

Channel matrix **H**, which fully describes propagation channel can be expressed as

$$\mathbf{H}(\tau) = \sum_{l=1}^{L} \mathbf{H_l}\ \delta(\tau - \tau_l) \qquad (3.21)$$

where L is the number of taps. $\mathbf{H_l}$ is channel matrix at each tap and $\mathbf{H}(\tau)$ is $M_r\ x\ M_t$ matrix of the channel impulse response. A multi-cluster model, at which the scatters are divided into groups are considered. Each of the clusters (from 2 to 6) corresponds to one multipath. A Cluster consists of up to 18 delay taps separated by at least 10ns. So, bandwidth of the model is 100 MHz. Channel matrix $\mathbf{H_l}$ for each tap at one instance of time is

$$\mathbf{H_l} = \sqrt{P}\ \left(\sqrt{\frac{K}{K+1}}\ \mathbf{H_F}\ +\ \sqrt{\frac{1}{K+1}}\ \mathbf{H}_\nu\right) \qquad (3.22)$$

where the correlated elements X_{ij} (i=1, …..M_r , j=1,……M_t) of matrix $\mathbf{H}_\nu$ are zero mean, unit variance, complex Gaussian random variables (Rayleigh matrix). $\mathbf{H_F}$ is the fixed LOS matrix. K is Ricean K-factor and P is the power of each tap. For $\mathbf{H}_\nu$ matrix , a Kronecker model is chosen.

$$\mathbf{H}_\tau = [\mathbf{R_{rx}}]^{1/2}\ [\mathbf{H_{iid}}]\ ([\mathbf{R_{tx}}]^{1/2})^T \qquad (3.23)$$

where $\mathbf{R_{tx}} = [\rho_{txij}]\ and\ \mathbf{R_{rx}} = [\rho_{rxij}]$ are transmit and receive correlation matrices and $\mathbf{H_{iid}}$ is a matrix of independent zero mean , unit variance, complex Gaussian random variables. $\mathbf{H_{iid}}$ fading matrix assumes that Tx – Rx antenna pair is independent. At figure 3.2, the correlation between the received signal at antenna elements 1 and 2 is given by $e^{j2\pi\frac{d}{\lambda}\sin(\theta)}$. In indoor environments, the rays reflected from a particular scatter have a mean AoA or AoD and a finite AS. The AoA and AoD also have a particular power angular spectrum (PAS) that gives the distribution of the angles around the mean.

For uniform linear array (ULA), correlation coefficient ρ is expressed as

$$\rho = R_{xx}(D) + jR_{xy}(D) \qquad (3.24)$$

where $D = \frac{2\pi d}{\lambda}$ and

$$R_{xx}(D) = \int_{-\pi}^{\pi} \cos(D\sin(\phi))PAS(\phi)d\phi \qquad (3.25)$$

is cross-correlation functions between real or imaginary parts and

$$R_{xy}(D) = \int_{-\pi}^{\pi} \sin(D\sin(\phi))PAS(\phi)d\phi \qquad (3.26)$$

is cross – correlation function between real and imaginary part. Power Azimuth Spectrum (PAS) follows Laplacian distribution.

$$p(\theta) = \frac{1}{\sqrt{2}\sigma} e^{-\left|\frac{\sqrt{2}\theta}{\sigma}\right|} \qquad (3.27)$$

σ is the standard deviation of the PAS which corresponds to the numerical value of AS (azimuth spread). The range of angular spread is from 20º to 40º. Kronecker approach assumes that Tx and Rx PAS are separable, which is not valid in general.

Channel model of IEEE 802.11 includes tables of parameters for five environments (A-F). The A environment is ideal. Parameter tables contain cluster structure and excess delay, power, Angle of Arrival (AoA), Angle of Departure (AoD), Angular Spread (AS) of departure and incidence angles for each multipath component. Features of the models are path loss, shadow fading, deterministic LOS component and Doppler components. Numerical values of parameters are chosen to satisfy practical measurements. In indoor wireless systems, transmitter and receiver are stationary and people are moving, while in outdoor mobile systems, the user terminal is moving. As a result, Doppler spectrum lies within a $[-f_d , f_d]$ bandwith, where f_d is the maximum Doppler shift/spread

Time variations of the channel are evidenced as a Doppler shift of a spectral line. Dopples power spectrum S(f) (expressed in linear value) is the classical U-shape.

$$S(f) = \frac{1}{1 + A(\frac{f}{f_d})^2} \qquad (3.28)$$

where A is a constant. If A is represented in dB values, S(f) is similar to the “Bell” shape spectrum. This formula is applied to models A-E . For channel F, a Doppler component is included for the 3rd tap that represents a reflection from a moving vehicle. This spectrum shape is called “bell with spike shape”, where an optima additional spike takes place at Doppler frequency that corresponds to vehicles passing. The presence of fluorescent lamps creates fast changes of electromagnetic field. This effect is emulated by introducing artificially an AM modulation at several taps. This effect is included in models D and E. Path loss function has two slopes. Break point distance separates the slopes. Shadow fading is drawn randomly from log normal distribution and is fixed for the single use of the channel model.

TABLE 9.1 CHANNEL MODEL PARAMETERS

Model	Environment	LOS/NLOS	K(dB)	Rms delay spread (ns)	Number of clusters
A	Flat fading	NLOS	-∞	0	1 tap
B	Residential	NLOS	-∞	15	2
C	Residential Small Office	NLOS	-∞	30	2
D	Typical Office	LOS/NLOS	3/-∞	50	3
E	Large Office	LOS/NLOS	6/-∞	100	4
F	Large Space (Indoors and Outdoors)	LOS/NLOS	6/-∞	150	6

TABLE 9.2 PATH LOSS MODEL PARAMETERS

Model	d_{BP}(m)	n	σ_{ψ}(dB) after d_{BP}
A	5	3,5	4
B	5	3,5	4
C	5	3,5	5
D	10	3,5	5
E	20	3,5	6
F	30	3,5	6

Table 3.1 presents channel model parameters and table 3.2 path loss model parameters. K-factor is applied only to the first tap. LOS conditions are assumed up to the break – point distance. MATLAB implementation from L. Schumacher is available [23]. Antenna geometries, distance between Rx and Tx, carrier frequency, correlation coefficient type (complex/real), Doppler spread can be set. Interference from others cells is not included.

3.5 WINNER II channel models

WINNER II channel models can be used in link level and system level simulations for any wireless system operating in 2-6 GHz frequency range with bandwidth up to 100 MHz [24]. The models support multi-antenna technologies, polarization, multi-user, multi-cell and multi-hop networks. The covered propagation scenarios are indoor office, large indoor hall, indoor-to-outdoor, urban micro-cell, bad urban micro-cell, outdoor-to-indoor, stationary feeder, suburban macro-cell, urban macro-cell, rural macro-cell and rural moving networks. Also, propagation scenarios are parameterized for both Line of Sight (LoS) and non-LoS (NLoS) conditions. WINNER II is a geometry-based stochastic model where different antenna configurations and different antenna patterns can be inserted. Statistical distributions for delay spread, delay values, AS, shadow fading and cross-polarization ratio have been extracted from channel measurement. For each channel drop (segment) the channel parameters are calculated stochastically from distributions. Channels are generated geometrically by summing the contributions of rays. Channel matrix **H** of the MIMO channel is given from (3.21) with

$$\mathbf{H}_l(\tau) = \iint \mathbf{F}_{rx}(\theta_{rx})\mathbf{h}_l(\tau, \theta_{tx}, \theta_{rx})\mathbf{F}_{tx}^T(\theta_{tx})d\theta_{tx}d\theta_{rx} \quad (3.29)$$

where $\mathbf{F}_{tx}$ and $\mathbf{F}_{rx}$ are the antenna response matrices for the transmitter and the receiver correspondly and $\mathbf{h}_l$ the propagaqtion channel response matrix , θ_{tx} is the AoD and θ_{rx} the AoA for cluster l as is illustrated in figure 3.6.

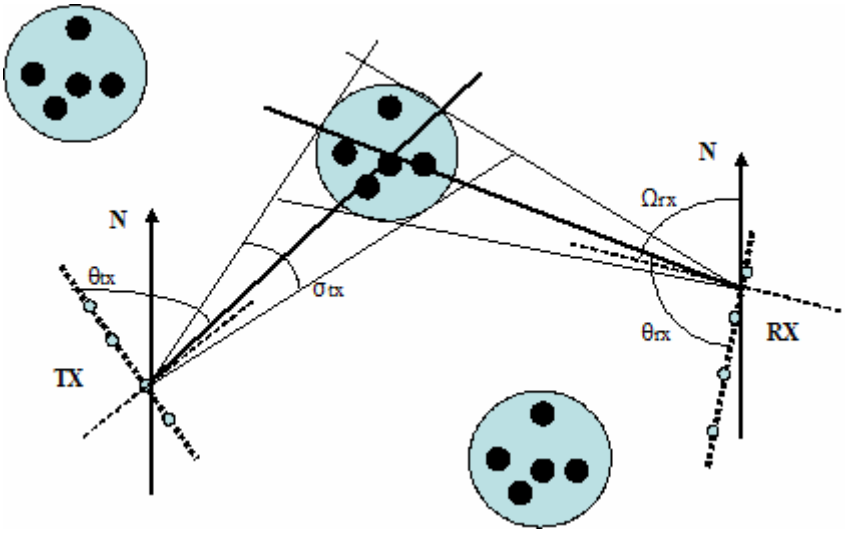

Figure 3.7 Single link approach for WINNER II channel models

Figure 3.7 shows the parameters used in the model. Ω depicts antenna orientation and σ the AS. The north (up) is the zero angle reference. Large Scale parameters (LSP) are used as control parameters when generating the small scale channel parameters. At first LSP like shadow fading, delay and Ass are drawn randomly from tabulated distribution functions. Next the small scale parameters like delays, powers and DoA and DoD are drawn randomly according to tabulated distribution function and LSP. At this stage, geometric setup is fixed and only free variables are the random initial phases of the scatters. Therefore, an unlimited number of different realizations of the model can be generated. When the initial phases are fixed, the model is full deterministic. Correlations of LSPs observed in measured data are not reflected in joint power or probability distributions. Cross-correlation between two LSPs is introduce by the factor ρ

$$\rho_{xy} = \frac{C_{xy}}{\sqrt{C_{xx}C_{yy}}} \quad (3.30)$$

where C_{xy} is the cross-covariance of LSP x and y. Clustered Delay Line (CDL) with fixed large scale and small scale parameters have been created for calibration and comparison of different system level simulations. Figure 3.8 illustrate channel coefficient generation procedure.

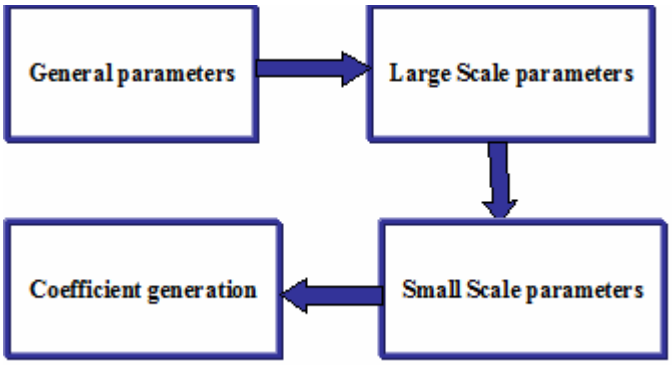

Figure 3.8 Channel coefficient generation procedure in WINNER II

General Parameters

1. Set scenario, number of BS and MS, location of BS and MS, antenna field patterns $\mathbf{F_{rx}}$ and $\mathbf{F_{tx}}$, array geometry, speed and direction of motion of MS and center frequency.

Large scale parameters

2. Assign the propagation condition (LoS/NLoS)

3. Calculate the path loss

4. Generate the correlated delay spread, angular spread Riician K-factor and shadow fading taking account (3.30) which gives the correlations between LSP.

Small scale parameters

5. Generate the delays τ. Delays are drawn randomly from exponential or uniform delay distribution.

6. Generate the cluster powers P. The cluster powers are calculated assuming a single slope exponential delay profile.

7. Generate the azimuth arrival angles and azimuth departure angles (σ_{tx} and σ_{rx} in figure 3.6). If the PAS is modeled as wrapped Gaussian, the AoA and AoD are determined by applying inverse Gaussian with input parameters cluster power P_l and AS (σ_{tx} and σ_{rx} in figure 3.6). The same procedure is applied for elevation angles.

8. Random coupling of rays within clusters. Couple randomly the departure ray angles to the arrival ray angles within a cluster.

9. Generate cross polarization power ratio (XPR) for each ray at each cluster.

Coefficient generation

10. Draw the random initial phase for each ray at each cluster and for four different polarization combinations. Distribution for the initial phases is uniform.

11. Generate the channel coefficients for each cluster and each transmitter and receiver element pair according to (3.29).

12. Apply the path loss and shadowing for the channel coefficients.

Chapter 4
Convex Optimization in Downlink Beamforming

This chapter gives the basic concepts and main techniques used in convex optimization. Emphasis is placed on conic optimization problems, icluding semidefinite programming (SDP) because with this method we will formulate and resolve the downlink beamforming optimization problem. The brief overview here for convex optimization problems is part of [25], which includes several important classes, such as geometric programming.

4.1 Convex Optimization

A generic mathematical optimization problem in minimization form should be formulated as following:

Minimize $f_0(x)$

Subject to $f_i(x) \leq 0$, i=1,2,……,m

$h_j(x)=0$, j=1,2,…….,r

$x \in S$ (4.1)

where $x=(x_1,x_2,……,x_n)$ present the optimization variables, $f_0 : R^n \rightarrow R$ is called the objective or cost fuction, f_i and $h_j : R^n \rightarrow R$ are called the inequality and equality constraint functions respectively and S is called a constraint set. An optimization variables x is feasibles if $x \in S$ and they satisfies all the inequality and equality constraints. A faisible solution **x*** is globally optimal if **x*** has the smallest value of f_0 among all vectors that satisfy the constraints (feasible vectors). In contrast, a feasible vector $\overline{x}$ is locally optimal if there exists some $\varepsilon > 0$ such that $f_0(\overline{x}) \leq f_0(\mathbf{x})$ for all faisible **x** satisfying $\| \mathbf{x}- \overline{x} \| \leq \varepsilon$. The general optimization problem is very difficult to solve. The proposed methods involve some compromise (very long computation time, etc) or not always find the optimum solution. Certain problem classes as convex optimization problems can be solved efficiently and reliably.

Convex Sets

All point $\theta x + (1-\theta) y$ with $0 \leq \theta \leq 1$ are included in a line segment. A set $S \subset R^n$ is said to be convex if it contains the line segment between any two points $x,y \in S$, $\theta x + (1-\theta) y \in S$, with $0 \leq \theta \leq 1$.

A convex set is a solid body, containing no holes and always curve out-wards. Practical methods for establishing convexity of a set are the application of a) definition b) operations that preserve complexity like:

- The intersection of convex sets is convex

- Image and reverse image of a convex set under $\mathcal{F}$ function is convex
- Image and reverse image of convex sets under perspective are convex
- Image and inverse images of convex sets under linear-fractional functions are convex.

A set $\mathcal{K}$ is called a cone, if for every $x \in \mathcal{K}$ and $\theta \geq 0$ we have $\theta x \in \mathcal{K}$. A set $\mathcal{K}$ is a convex cone if it is convex and a cone, e.g. for any $x_1, x_2 \in \mathcal{K}$ and $\theta_1, \theta_2 \geq 0$, we have $\theta_1 x_1 + \theta_2 x_2 \in \mathcal{K}$ (any point of this form is referred as conic combination of x_1 and x_2).

The two-dimensional pie slice with top (0,0) and edges passing through x_1 and x_2 can describe conic combination of points x_1, x_2 as in figure 4.1 .

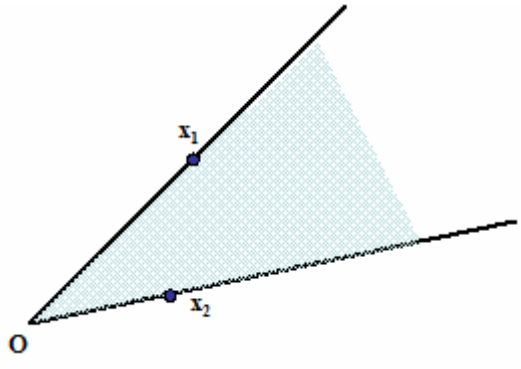

Figure 4.1 Conic combination of points x1, x2 (pie slice)

The most common convex cones are the following:

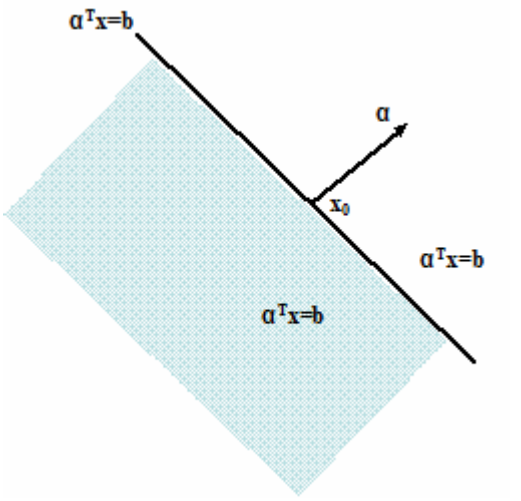

Figure 4.2 The half-space determined by {x | αT (x-x0) ≤ b}

1. No negative orthant R_+^n:
2. A half-space is a convex set of the form $\{x \mid \alpha^T (x-x_0) \leq b\}$ where x_0 lies on the boundary and α is the outward normal vector as is represented in figure 4.2. A half-space is a convex cone if b=0, e.g. $\{x \mid \alpha^T x \leq 0\}$ with $\alpha \neq 0$.

3. Second order cone:

The norm code associate with the norm $\|.\|$ is the set

$\mathcal{K} = \{(x,t) \mid \|x\| \leq t\} \subseteq R^{n+1}$

is a convex cone. The norm cone associated with Euclidean norm is called second-order cone.

$\mathcal{K} = \{(x,t) \mid \sqrt{x^t x} \leq t\}$

4. Positive semidefinite (PSD) cone

We define $\mathbf{S^n}$ the set of symmetric nxn matrices

$\mathbf{S^n}=\{\mathbf{X} \in \mathbf{R^{nxn}} \mid \mathbf{X}=\mathbf{X^T}\}$

We define $\mathbf{S_+^n}$ the set of symmetric positive semidefinite (non negative reals) matrices

$\mathbf{S_+^n}=\{\mathbf{X} \in \mathbf{S^n} \mid \mathbf{X} \succeq 0\}$

The set $\mathbf{S_+^n}$ is a convex cone.

If $\mathcal{K}$ is a cone, dual cone is defined as

$\mathcal{K}^*=\{y \mid x^T y \geq 0 \text{ for all } x \in \mathcal{K}\}$

The dual cone $\mathcal{K}^*$ consists of all vectors which forms a non obtuse angle with all vectors in $\mathcal{K}$. $\mathcal{K}^*$ is a cone and is always convex, even when the original cone is not.We say $\mathcal{K}$ is a self-dual if $\mathcal{K}^*= \mathcal{K}$. The non negative orthant R_+^n is a self dual since $\sum_i x_i y_i \geq 0 \iff y_i \geq 0$.

Also, the second order cone and the symmetric positive semidefinite matrix cone are self-dual

On the set $\mathbf{S_+^n}$ we use the standard inner product tr(**XY**)=**X**• **Y**= $\sum_{ij} \mathbf{X_{ij} Y_{ij}}$. For **X**, **Y** $\in \mathbf{S_+^n}$, tr(**XY**) ≥ 0 for all $\mathbf{X} \geq 0 \iff \mathbf{Y} \geq 0$.

Convex functions

A function f(x): $R^n \rightarrow R$ is convex if the domain of f (*dom* f) is a convex set and for all x,y $\in$ *dom* f with $0 \leq \theta \leq 1$

$f(\theta x+(1-\theta) y) \leq \theta f(x)+(1-\theta) f(y)$

Geometrically, this inequality means that the line segment joining (x,f(x)) and (y,f(y)) always lies above the graph of function f as in figure 4.3. We say that f is concave if -f is a convex.

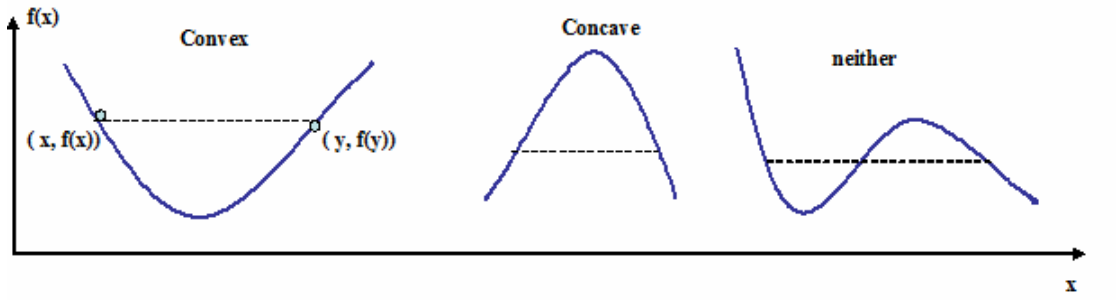

Figure 4.3 Graph of a convex and concave function

The f(x) is differentiable if *dom* f is open (no boundary points) and the gradient $\nabla f(x)$ evaluated at x exists at each x $\in$ *dom* f.

$$\nabla f(x) = \left[\frac{\partial f}{\partial x_1} \; \frac{\partial f}{\partial x_2} \; \cdots \; \frac{\partial f}{\partial x_n}\right]^T$$

The first order Taylor approximation of f(x) at x_0 is

$f(x) \approx f(x_0) + \nabla f(x_0)^T (x-x_0)$

The differentiable function f(x) with convex domain is convex if and only if for all $x, x_0 \in$ *dom* f

$f(x) \geq f(x_0) + \nabla f(x_0)^T (x-x_0)$

This inequality (first order condition) is illustrated in figure 4.4 and shows that from local information about convex function (e.g. its value and derivative at a point x_0) we can derive a global information (i.e. a global under estimation of it).

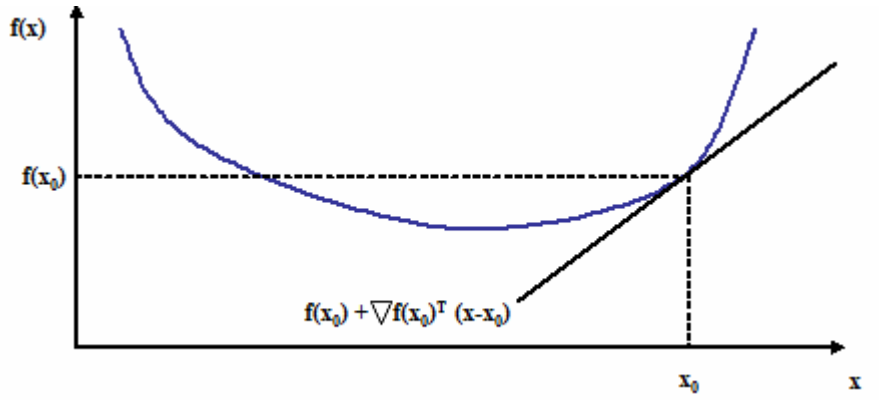

Figure 4.4 First order condition for differentiable convex functions

The Hessian of twice differentiable function f(x) evaluated at x is defined as

$$\nabla^2 f(x) = \begin{bmatrix} \frac{\partial^2 f}{\partial x_1^2} & \frac{\partial^2 f}{\partial x_1 \partial x_2} & \cdots & \frac{\partial^2 f}{\partial x_1 \partial x_n} \\ \frac{\partial^2 f}{\partial x_2 \partial x_1} & \frac{\partial^2 f}{\partial x_2^2} & \cdots & \frac{\partial^2 f}{\partial x_2 \partial x_n} \\ \vdots & \vdots & \ddots & \vdots \\ \frac{\partial^2 f}{\partial x_n \partial x_1} & \frac{\partial^2 f}{\partial x_n \partial x_2} & \cdots & \frac{\partial^2 f}{\partial x_n^2} \end{bmatrix}$$

The second order condition implies that for f(x) twice differentiable, the convexity of f(x) is equivqlent to the positive semidefinitess of its Hessian, e.g. for all x $\in$ *dom* f

$\nabla^2 f(x) \succeq 0$.

Thus, a linear function is always convex while for a quandratic function

$f(x)=(1/2)\, x^T \mathbf{P}\, x + q^T x + r$ with $\mathbf{P} \in S^n$, $q \in R^n$ and $r \in R$

$\nabla f(x)=\mathbf{P}x+q$, $\nabla^2 f(x)=\mathbf{P}$ and therefore f(x) is convex if $P \succeq 0$

The most important properties about convex functions are the following:

- α f is convex if f is convex and $\alpha \geq 0$ (non negative multiple)

- f1 + f2 is convex if f1, f2 are convex (sum). This property should be extended to infinite sums,intergrals
- f is convex if and only if f(x_0 +t h) is convex in t for all x_0,h (composition with affine function)
- if f_1, f_2, …..,f_m are convex then f(x)=max {f_1(x), …….,f_m(x)} is convex (pointwise maximum)
- All norms $\|x\|_p = (\sum_{i=1}^{n} |x_i|^p)^{1/p}$ for p ≥ 1 are convex

Convex optimization problems

The general optimization problem (4.1) is convex if

a) the functions f_i(x), i=1,2,….m are convex
b) the functions h_j(x) are on the form a_j^Tx+b_j, $a_j \in R^n$, $b_j \in R^n$ (affine functions)
c) The set S is convex

If we change “minimize” to “maximize” and change inequiity “f_i(x) ≤ 0” to “f_i(x)≥0”, the problem (4.1) is convex if and only if all f_i(x), i=1,2,….m are concave.

There are high-quality softwares based on interior point method which can achieve accurate solution efficiently. The total number of iterations (in worse case scenario that required a ε-suboptimal solution) is $\log_2(1/\varepsilon)$. For any convex optimization problem, the set of global optimal solutions is always convex. Every local optimal solution is also a global optimal. There is no risk to be at the local solution. In addition, from duality theory for convex optimization problems, it is possible to certificate mathematically the establisment of the infeasibility for the optimization problem. Modern softwares either generate an optimal solution or a certificate showing infesibility. In contrast, softwares for non convex optimization problems cannot detect infeasibility.

Linear Program (LP)

When the objective and constraint functions are all affine, the problem is called a linear program, is a convex optimization problem and has the following form

Minimize c^T x +d

Subject to Gx $\preceq$ h

Ax = b

Where $G \in R^{mxn}$ and $A \in R^{rxn}$. The constant does not affect the optimal set and it is common to omit. Also, we can maximize the affine function c^T x +d by minimize the function -c^T x - d . The geometical interpretation of a LP is given in figure 4.5. The feasible set is the shaded polyhendron. The objective c^T x is linear, so its level curves (dashed lines) are hyperplanes orthogonal to c. The optimum point x* is as far as possible in the direction –c.

In special case, where only inequalities are the constraints x $\succeq$ 0, the LP is given in standard form

Minimize c^T x

Subject to Ax = b

$x \succeq 0$ (4.2)

and its dual becomes

maximize $b^T y$

Subject to $A^T y + s = c$

$s \succeq 0$ (4.3)

s are the "slack" variables to transform the constraints inequilities to equalities.

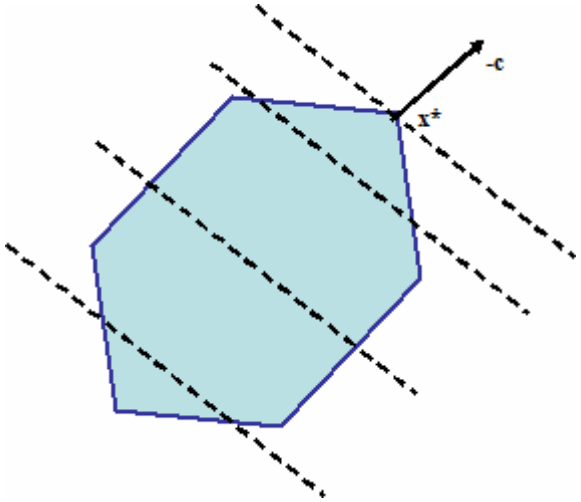

Figure 4.5 Geometric interpretation of a LP

Semidefinite Programming (SDP)

When $\mathbf{S}_+^k$ is the cone of positive semidefinite kxk matrices, semidefinite programming (SDP) problem has the following form:

minimize $c^T x$

Subject to $x_1 \mathbf{F_1} + x_2 \mathbf{F_2} + \ldots\ldots\ldots x_n \mathbf{F_n} + \mathbf{G} \preceq 0$

$Ax = b$ (4.4)

where $\mathbf{G, F_1, F_2, \ldots\ldots\ldots F_n} \in \mathbf{S}_+^k$, and $A \in R^{rxn}$.

Inequality constraint is called linear matrix inequality (LMI). The problem with multiple LMI constraints for example

$x_1 \mathbf{F_{11}} + x_2 \mathbf{F_{12}} + \ldots\ldots\ldots x_n \mathbf{F_{1n}} + \mathbf{G_1} \preceq 0, \quad x_1 \mathbf{F_{21}} + x_2 \mathbf{F_{22}} + \ldots\ldots\ldots x_n \mathbf{F_{2n}} + \mathbf{G_2} \preceq 0$

is equivalent to a single LMI

$$x_1 \begin{bmatrix} \mathbf{F_{11}} & 0 \\ 0 & \mathbf{F_{21}} \end{bmatrix} + x2 \begin{bmatrix} \mathbf{F_{12}} & 0 \\ 0 & \mathbf{F_{22}} \end{bmatrix} + \ldots\ldots\ldots + xn \begin{bmatrix} \mathbf{F_{1n}} & 0 \\ 0 & \mathbf{F_{2n}} \end{bmatrix} + \begin{bmatrix} \mathbf{G_1} & 0 \\ 0 & \mathbf{G_2} \end{bmatrix} \preceq 0$$

The standard form has linear equality constraints and a non negative constraint on the matrix $\mathbf{X} \in R^n$

minimize tr (**CX**)

subject to tr(**Ai X**)=bi i=1,2,….r

$\mathbf{X} \succeq 0$ (4.5)

where $\mathbf{C}$, $\mathbf{A_1}$, …….$\mathbf{A_p} \in \mathbf{S^n}$. The dual problem becomes

maximize $b^T y$

Subject to $\sum_{i=1}^{m} \mathbf{A_i^T} y_i + \mathbf{S} = \mathbf{C}$

$\mathbf{S} \succeq 0$ (4.6)

Chapter 5

Distributed Interference Management for IEEE 802.11n WLANs

Given the unlicensed nature of WLAN technologies and decreasing cost of IEEE 802.11 WLANs, the number of Acccess Points (APs) has multiplied to improve the wireless coverage. Additionally, independent WLANs co-exist in the same region. These Local Wireless Networks are mutually uncoordinated resulting in variable AP densities that are independently managed due to manual setting of AP at the factory. This deployment is characterized in [26] as chaotic and suffers from throughput and latency degradation that seriously affect the Quality of Service (QoS), especially for multimedia applications.

In [27], the effective channel utilization that presents the fraction of time at which the channel can be considered as busy, is minimized for the most loaded (bottleneck) AP. Proper channel assignment minimizes the overlap between coverage areas of co-channel APs. This enhances the performance of the network by reducing interaction between co-channel APs. The problem of assigning channels to APs can be characterized as a graph-coloring problem. The nodes represent APs, the edges correspond to coverage overlaps between APs and the weights associated with the edges give the amount of measured overlapping channels. The goal is to cover APs with the minimum of channels (colors), such that there are no adjacent APs that use the same channel. In [28], the weight indicates the importance of using different colors taking into account co-channel interference as well as the impact of interference between overlapping channels. Distributed algorithms in high node density deployments for channel selection and user association is proposed in [29]. APs are recommended to select channels which minimize the total interference. The proposed algorithms are probabilistic, they require synchronization among the APs and are been long-term efficient. The same optimization philosophy based on the Gibbs sampler is proposed in [30]. In this work, power control and CSMA/CA thresholds are jointly studied to maximize the sum of the long term throughput for all users in the network. In [31], an OFDMA (Orthogonal Frequency Division Multiplexing Access) centralized algorithm is proposed to mitigate co-channel interference for a synchronous system as IEEE 802.16e.

We assume a number of independently managed typical in size wireless co-existing networks with a single AP each. Proper assignment of channels takes full advantage of the total bandwidth offered in each cell. Mechanisms such as automatic frequency selection and CSMA/CA are based on interference avoidance. In a “crowded“ WLAN environment, the above solutions will result in low

throughputs or even in no transmission at all (due to the lack in synchronization). Therefore interference needs to be suppressed. The transmitted power and the channel band are often set without any consideration of the occupancy of the cell and the position of the users to the AP. Such a simple policy is bound to lead to increased interference among the coverage areas of neighboring APs. The goal of this paper is to greatly improve the frequency utilization efficiency and at the same time to keep low implementation complexity, while focusing on the IEEE 802.11n standard. The key idea is to minimize interference and simultaneously keep QoS at an acceptable level even for overlapping networks avoiding the use of CSMA/CA .

We assume an AP a, where the transmitter is equipped with M_t antennas and there are K users. In order to increase throughput, Space Division Multiple Access (SDMA) is used. According to their locations, the users are divided into g groups. The SDMA technique accommodates the g groups using the same frequency within the same cell simultaneously by constructing a spatially independent channel for each group and transmitting signals in parallel. Consequently, frequency utilization can greatly improve. Afterwards, downlink beamformers are designed for the co-channel groups to achieve the minimum required QoS (Signal to Interference plus Noise Ratio at each receiver-SINR). The goal is to minimize total transmission power and thus limit the interference “leakage” to neighboring co-channel groups and cells. We define the operating frequency of AP a as f_a at the center of channel band. From the fixed set of the available channels used by AP a and K users, we select the channel that gives the minimum transmit power after beamforming optimization. This is not a link-by-link optimization problem and therefore doesn’t have a large computation cost. For each group, multi-user diversity can be exploited to find a subset of good sub-carriers to meet QoS requirement. Following the optimal beamformers calculation at the AP, the different sub-carriers of each group can be allocated to different users (OFDMA). By adaptively employing different modulation modes on the sub-carriers according to SINR, the system performance can be enhanced. The drawback in such a group optimization design is that the receivers are located at different points within the cell. The constraint of minimum guaranteed SINR for each receiver must be satisfied. In

order to improve the performance of our system, multiple antennas at the receiver are proposed. The coherent combination of diversity paths increases the SINR in comparison to a single antenna receiver. This growth of SINR is called "array gain". The AP and the users exploit Channel State Information (CSI) to form suitable beamforming weights. In short-rang transmission scenarios like WLAN, CSI is feasible because of low mobility. Our proposed strategy for downlink multi-user MIMO-SDMA-OFDMA systems is characterized by the following:

- The MAC layer takes full advantage of the OFDMA delivery mechanism. Fast retransmission over link and large number of active users is the MAC layer advantages.
- The (low complexity) sub-carrier allocation algorithm achieves complete fairness to the users that is traded off with the total sum rate.
- The users belong to the same group are served by the same beam at different tones.

Therefore, for the users closely locating in the same group, inter-user correlation

is reduced.

- The interference caused by imperfect channel estimation is reduced since the transmit power of co-channel interfering users is minimized.
- The application of SDMA algorithms into WLANs is not straightforward. The acknowledgement (ACK) slots mutually interfere upon arrival to the AP because they almost overlap in time. In our proposed solution, each sub-carrier is allocated only to one user-group. Therefore, there is no mutual interference between the ACKs of terminals is posed.
- Our design offers adaptively to different scenarios-such as propagation conditions (LOS and NLOS) , user density and traffic load.

It will be beneficial for collocated WLANs adapt in a distributed manner their transmission characteristics (beam steering, channel bands, transmitted power) than to selfishly try to use the shared resources each and thus create large amount of interference that will effectively degrade the performance of all APs. Our algorithm works without coordination among neighboring APs. In IEEE 802.11 WLANs, the interference on the same channel can be directly detected through the contention mechanism while adjacent channel interference often contributes to background noise and cannot be handled in an explicit manner. Our design takes into account adjacent channel interference since the used masks involve not ideal band-pass filters. It should be noted that the low efficiency of the High

Power Amplifiers (HPA) for OFDM transmission dictates the operation in the linear region and this along with the use of spectrally efficient modulation leads to smaller adjacent channel interference.

This chapter is organized as follows: in the next section, we describe the unlicensed and uncoordinated environment associated with WLANs and we examine methods for improving the performance of defferent networks in such dense deployment. In section 2 we define the system mode and we describe how it is possible to be implemented our proposed strategy. In section 3, downlink beamforming/SDMA-MIMO algorithms are developed. Section 4 studies the sub-carriers assignment problem. In section 5, the performance of the proposed algorithms is extensively simulated. Section 6 compares implementation complexity and power consumption of our proposed techniques to beamforming at each sub-carrier, proposed in the ongoing IEEE 802.11n standardization.

5.1 Unlicensed and Uncoordinated Wireless Environments

The WLAN market grows exponentially due to low cost and high data rate capabilities. The unlicensed frequency bands offer an attractive alternative to the high cost of the licensed spectrum. The unlicensed 2.4 GHz ISM (Industrial, Scientific and Medical) band covers from 2.4 to 2.4835 GHz with a relatively large available portions of available spectrum (i.e. 75 MHz). The U-NII (Unlicensed National Information Infrastructure) bands that cover the 5.15-5.35 GHz, 5.47-5.725 GHz and 5.725-5.85 GHz bands have been preferred due to higher throughput and greater diversity but these frequencies overlap the C band military radar frequency range of 5.25 to 5.925 GHz. This can lead to degraded performance in the WLAN network and also possibly cause interference problems with military radar systems.

Interference is defined by the International Telecommunications Union (ITU) as the effect of unwanted electromagnetic energy on reception of radio communications, manifested by any performance degradation or loss of information that could otherwise have been extracted in the absence of the unwanted energy. In the ISM band, users can experience significant interference in some locations from ambulances, police cars, citizen’s band radios as well as from other unintentional or intentional electromagnetic radiation such as microwave ovens, cordless phones, Bluetooth systems, etc. These devices are called ‘selfish interferers’ since they run their own protocol for their own benefit without any coordination. WLANs must be robust to interference caused by devices that co-exist with them in the ISM band. The demand for higher bit rates and the requirements for interference avoidance in the ISM band leads 5 GHz band for WLANs. Another RF challenge of U-

NII band operation is the increased isotropic loss for the 5 GHz frequency bands, that is about 7 dB more than that of 2.4 GHz frequency band since the isotropic loss is proportional to the square of the carrier frequency.

WLAN deployment is not planned as in the case of cellular systems. The uncoordinated placement of APs (all sharing the same bands within the ISM region) may result in highly variable density of individually managed APs. This chaotic and uncoordinated nature of WLANs causes unpredictable network performance raises issues related to fairness among users and poses other constraints on the nature of the problem as well as on the possible practical solutions:It's not possible to improve performance in outdoor environments through careful AP placement or site surveys. This approach can be used only in indoor environments. The proposed solutions should not assume any coordination between co-existing WLANs because there is no explicit way of interaction between APs and users of different networks.

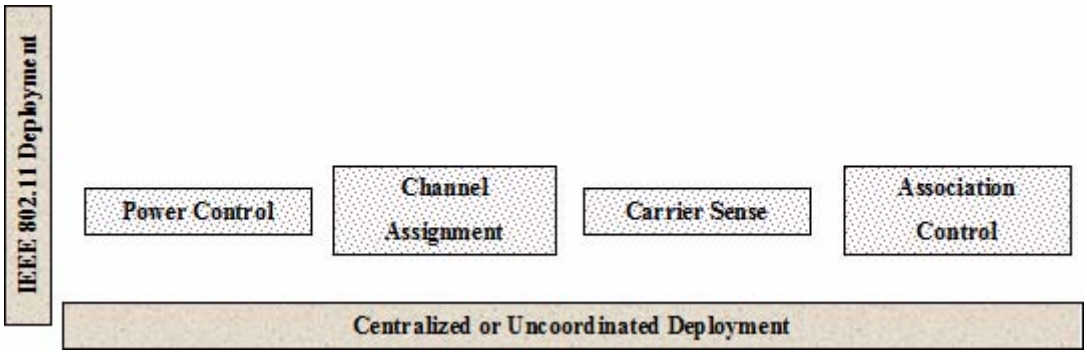

Figure 5.1 Methods of improving 802.11n performance.

In [32] multiple complementary ways of dealing with the aforementioned issues are summarized. Fig. 5.1 illustrates the multiple complementary ways of addressing performance issues in IEEE 802.11 networks. Power control, via the dynamic management of transmit power reduces interference. This technology is referred as Transmit Power Control (TPC) and manages the transmit power of the APs (cell size) while the receiver eliminates interference with CSMA/CA mechanism. Additionally, with careful channel assignment the idea of channel hopping for improving fairness is exploited. APs spend a fixed amount of time in a single channel and switch to a subsequent channel. This technique is of the same nature as Dynamic Frequency Selection (DFS) that is used before an AP transmits on a channel to see if radar is in use nearby. If an active radar is detected, the AP is shut down. The association control, on the other hand, balances the client-load across a set of APs. An AP can become overloaded since the bandwidth resource shared from AP and associated users is limited. An AP that is heavily loaded might not be the best to associate a new user. The WLAN distributes client

associations among APs so that one loaded AP may deny the association request and the client may be associated to a lightly loaded AP. The methodology by which a client decides with which AP to request association is not specified in the standard.

5.2 System Model

A. IEEE 802.11n Parameters

IEEE 802.11n is supposed to operate with 20 MHz bandwidth where the spectrum is limited and 40 MHz with two adjacent spectral channels otherwise (this technique which combines two adjacent channels of 20 MHz into one of 40 MHz is called channel bonding). The transmission of 200Mbits/s in 20 MHz yields a bandwidth efficiency of 10 b/s/Hz.

TABLE 5.1 MODE-DEPENDENT PARAMETERS

Mode	Modulation	Coding rate	Coded bits per sub-carrier	Adjacent channel rejection (dB)	Non adjacent channel rejection (dB)	Minimum sensitivity (dBm)
1	BPSK	1/2	1	16	32	-80
2	QPSK	1/2	2	13	29	-77
3	QPSK	3/4	2	11	27	-75
4	16-QAM	1/2	4	8	24	-72
5	16-QAM	3/4	4	4	20	-68
6	64-QAM	2/3	6	0	16	-64
7	64-QAM	3/4	6	-1	15	-63
8	64-QAM	5/6	6	-2	14	-62

The physical layer (PHY) modes in 20 MHz channel width with different coding and modulation schemes are present in Table 5.1. Minimum receiver sensitivity is the power at the antenna port of the receiver for which the packet error rate (PER) is less than 1% for PHY layer service data unit(PSDU) or payload length equal to 4095 bytes. The total OFDM symbol duration is

$T_{tot}=T_g+T_u=16+64=80$ samples

where T_g is the guard interval duration and T_u is the useful symbol duration. Since the channel bandwidth is 20 MHz, the sampling period is $T_s = \frac{1}{20}\mu\,\mathrm{sec}$ and $T_{tot} = 4\mu\,\mathrm{sec}$. When the guard interval $T_g = 16\mathrm{x}0.05 = 0.8\mu\,\mathrm{sec}$ is longer than the maximum delay spread of radio channel, ISI (InterSymbol Interference) is eliminated. The indoor environment experiences maximum delay spread of a few hundreds of $n\,\mathrm{sec}$. SDMA expands the capacity by allowing up to $M_t = 4$ separate beams. SDMA adds another dimension to the spectrum resource by expanding each packet into M_t space packets, translating into an M_t-fold increase of system throughput. The minimum data rate is given for mode 1.

$$R_{min} = 48 subcarriers x \frac{\frac{1}{2}\ bit}{1 coded\ bit} x \frac{1 coded\ bit}{subcarrier\ symbol} x \frac{1 subcarrier}{4\ 10^{-6}\ sec} x 4 beamvectors = 24 Mbs/s$$

The maximum data rate is achieved for mode 8.

$$R_{max} = 48 subcarriers x \frac{\frac{5}{6}\ bit}{1 coded\ bit} x \frac{6 coded\ bit}{subcarrier\ symbol} x \frac{1 subcarrier}{4\ 10^{-6}\ sec} x 4 beamvectors = 240 Mbs/s$$

The throughput in our design is measured at the top of PHY and it varies between these two extreme values R_{min} and R_{max}.

B. Transeiver Model

Let assume a geographical area where there is a set $\mathcal{A}$ of available APs forming non-cooperative co-existent WLANs compatible with IEEE 802.11n. Consider AP $a \in \mathcal{A}$ with frequency of operation $f_a \in \mathcal{C} = \{1, 2, \ldots F\}$. It was already mentioned in the case of ISM band $F = 3$ while in case of UNII $F = 12$. The generated interference depends on the traffic load; if most APs are involved in occasional transmission, then no degradation in performance occurs. We focus on the downlink, where data is sent by APs to users since this is the dominating wireless traffic link. We assume that the networks are fully saturated, i.e. the APs always have data to send to all the users. We study a cell with a single AP $a \in \mathcal{A}$ and K users. The AP and the user terminals are assumed to be equipped with M_t and M_r array antennas respectively. Consider a total of G sets $\{G_1\ G_2\ \ldots\ G_G\}, 1 \leq G \leq K$, where G_g contains the indices of receivers participating in group g, $g \in \{1\ 2\ \ldots\ G\}$. Each receiver belongs to a single group $G_g \cap G_m = \{\ \}$ with $g \neq m$ and $\sum_{g=1}^{G} |G_g| = K$. Assuming that the channel for user k at the operating frequency f_a is frequency-flat, quasi-static and time-invariant the propagation loss and phase shift are described by the $M_r x M_t$ channel matrix $\mathbf{H_k^{f_a}}$. The operating frequency of our downlink beamforming optimization problem is defined at the center of the band, where according to IEEE 802.11n the sub-carrier is null. Multipath delays cause frequency selective fading and therefore the estimated channel matrices $\mathbf{H_k^{f_a}[1]}$ to $\mathbf{H_k^{f_a}[N]}$ corresponding to the range of sub-carriers 1 to N may exhibit gain variations in the same band. In order to overcome these problems, $\mathbf{H_k^{f_a}}$ is taken as the average channel matrix for all sub-carriers.

$$\mathbf{H_k^{f_a}} = \frac{1}{N} \sum_{i=1}^{N} \mathbf{H_k^{f_a}[i]} \quad (5.1)$$

The received signal at user k belonging to set g is given by

$$\mathbf{y_k^{f_a}} = \mathbf{H_k^{f_a}}\ \mathbf{x_g^{f_a}} + \mathbf{n_k^{f_a}} \quad (5.2)$$

where $\mathbf{x_g^{f_a}}$ is the vector of signal emitted from AP a in set g. If $\mathbf{v_g^{f_a}}\ M_f x 1$ is the beamforming weight vector applied to the transmitter, then the transmit signal is given by

$$\mathbf{x_g^{f_a}} = \mathbf{v_g^{f_a}}\, s_g \quad (5.3)$$

with s_g the information signal directed to receivers in the set g. Assuming that the s_g is zero mean, temporally white with unit variance and the waveforms $\{s_g\}_{g=1}^{G}$ are mutually uncorrelated the transmitted signal is equal to

$$\mathbf{X_{tx}^{f_a}} = \sum_{g=1}^{G} \mathbf{v_g^{f_a}} \quad (5.4)$$

The total radiated power is equal to

$$P_{tx}^{f_a} = \sum_{g=1}^{G} \left\|\mathbf{v_g^{f_a}}\right\|_2^2 \quad (5.5)$$

If $\mathbf{U_k^{f_a}}\, M_r \mathrm{x} M_r$ is the matrix applied at user k, then the estimated signal $\hat{\mathbf{s_k}}(\mathbf{f_a})$ is given from

$$\hat{\mathbf{s_k}}(\mathbf{f_a}) = (\mathbf{U_k^{f_a}})^{\mathbf{H}}\, \mathbf{y_k^{f_a}} \quad (5.6)$$

In this way, the power at the receiver k is

$$P_k^{f_a} = \left|(\mathbf{U_k^{f_a}})^{\mathbf{H}}\, \mathbf{H_k^{f_a}}\, \mathbf{v_g^{f_a}}\right|^2 \quad (5.7)$$

Assuming that the noise at receiver k is zero mean with variance $(\sigma_k^{f_a})^2$ then the noise power is

$$N_k^{f_a} = (\sigma_k^{f_a})^2 \left\|\mathbf{U_k^{f_a}}\right\|^2 \quad (5.8)$$

IEEE 802.11h defines enhancements with the Dynamic Frequency Selection (DFS) procedure [33]. Each user listens to every channel for a specific period of time and performs important channel measurements that reflect the interference level in its

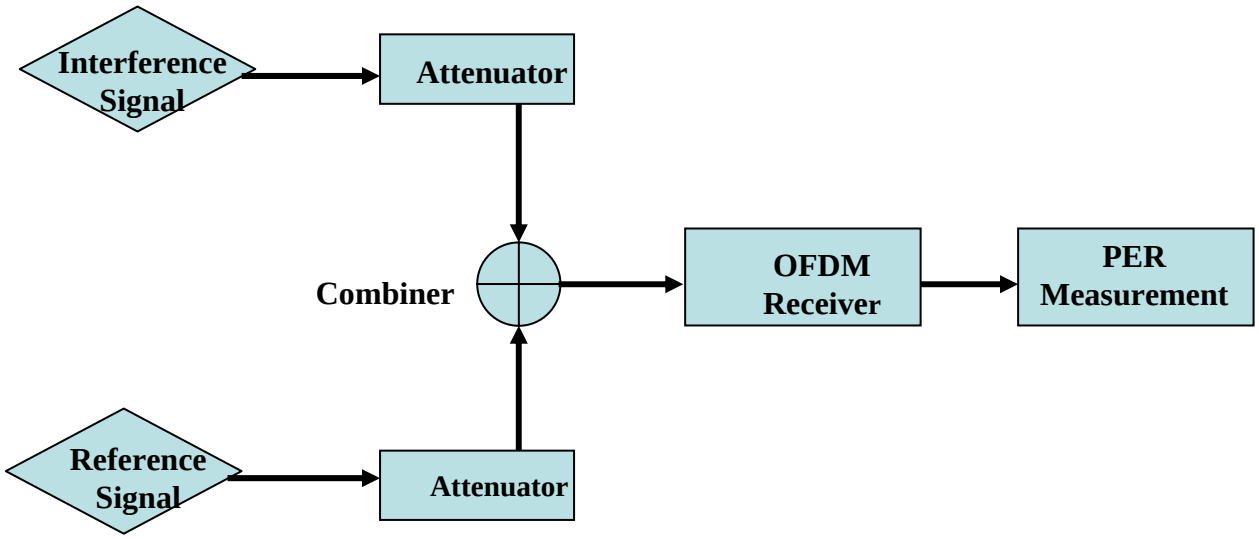

Figure 5.2 Set-up appointed for adjacent channel rejection

vicinity. The wireless card of the user scans the wireless medium, measures and reports the RSSI(Received Signal Strength Indication) values. These measurements are then reported to the AP. We

introduce the notion of Interference Factor or I-factor for short, denoted by $I(f_a, f_b)$, where $f_a, f_b \in \mathcal{C}$ are the frequencies at the center of band for AP $a, b \in \mathcal{A}$. The I-factor presents the normalized fraction of power which is transmitted at frequency f_b and is captured from receiver that works at frequency f_a . In [28], one can see how the I-factor can be calculated. We measure the SINR at the receiver with operating frequency f_a when the transmitted frequency f_{TX} is f_a and f_b. The ratio

$$I(f_a, f_b) = \frac{SINR(f_{TX} = f_b)}{SINR(f_{TX} = f_a)} \quad (5.9)$$

is the interference factor. Figure 5.2 illustrates this measurement of the interference factor in the laboratory. The interfering signal is an OFDM signal, unsynchronized with the reference signal. The main components that remove the interference power on adjacent frequencies are received filters. Assuming $P_k^{f_b}$ to be the average over all sub-carriers power measured from receiver k at frequency f_b, when the AP a is silent, the total interference power at user k is

$$\mathcal{I}_k^{f_a} = \sum_{f_b} P_k^{f_b} I(f_a, f_b) \quad \forall f_b \in \mathcal{C} \quad (5.10)$$

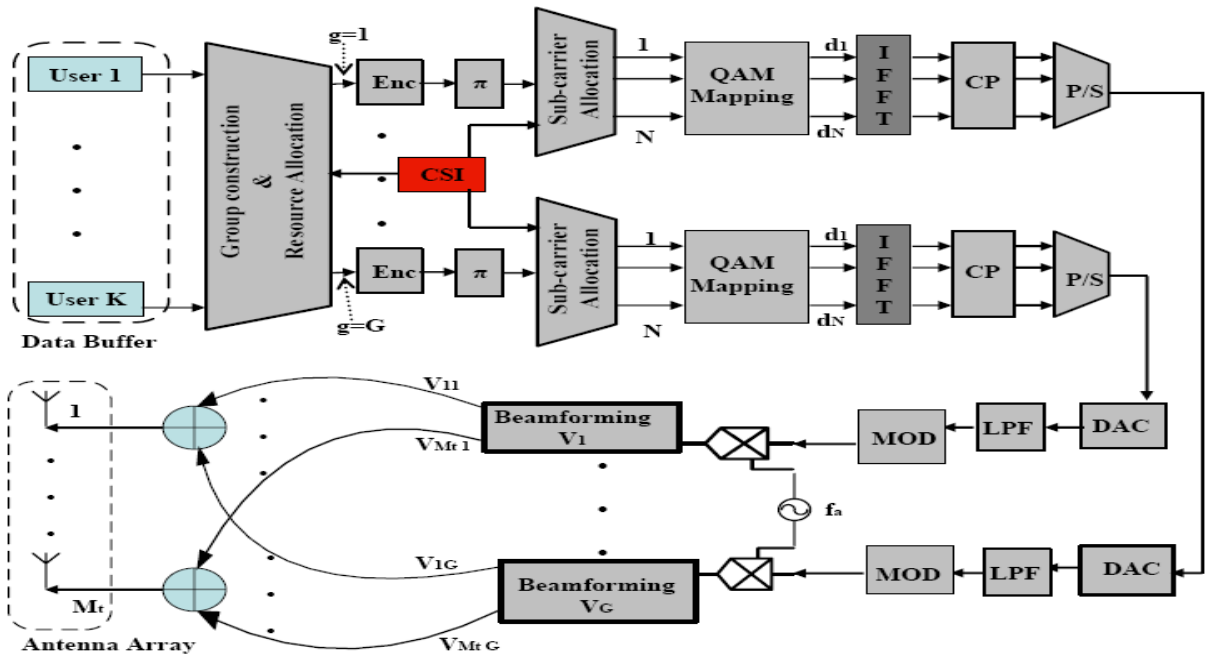

Figure 5.3 The PHY transmitter model for AP

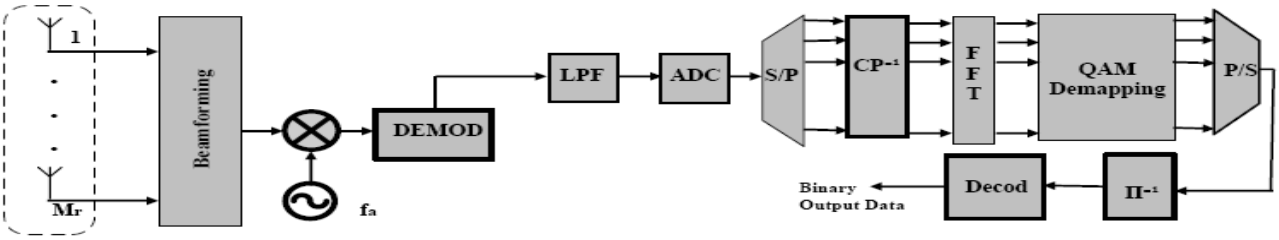

Figure 5.4 The PHY receiver model for user

The schematic model for the AP and the users is depicted in fig. 2 and 3 respectively. At the transmitter, all users' packets are sent to a group construction module. This module processes the data packets with a suitable group and resource allocation algorithm that determines the number of assigned sub-carriers for each user from the total number of data sub-carriers.The binary data are encoded by Forward Error Correction coding (FEC) and appropriate interleaving (π) is added to the transmitted information to avoid the effect of burst errors. The sub-carrier allocation algorithm dynamically assigns the sub-carriers of each group to different users. In the mapper, the binary data is adaptively divided into groups of 2,4 and 6 bits and converted into complex number representing QPSK, 16-QAM and 64-QAM constellation respectively. The OFDM symbol is implemented in discrete time using an Inverse FFT (IFFT) that acts as a modulator. Additionally, a Cyclic Prefix (CP) guard time is added to the OFDM symbol to avoid inter-carrier interference. A Digital to Analog Converter (DAC) with a Low Pass Filter (LPF) transforms the digital data to analog. RF (Radio Frequency) modulation is performed and the signal is up-converted to the transmission frequency f_a, at the center of band. The RF signals of each group are multiplied by complex weights and summed to feed the M_t antenna elements (beamforming). In figure 5.3 , $G \leq M_t$ beamforming modules are used and therefore up to G beams are possible to be constructed. At the receiver, the reverse operation is followed to decode the information bits for every user belonging to group g. To provide high data rate, Adaptive Modulation and Coding (AMC) schemes are adopted on every sub-channel. According to SNR_n^g for the n sub-carrier belonging to group g, different modulation schemes of AMC can be implemented. If the SNR_n^g threshold is guaranteed, no packet errors are assumed. The packet loss only happens when the buffer of the user is overflowed.

The formation of the group need doesn't require any knowledge of the user's position. In a LoS environment, the Angle-of-Arrival (AoA) of the LOS component at the receiving antenna of the AP is estimated. Users whose signals come from the same direction are grouped together. In an environment including many scatters, the LoS component is rarely the dominant one. Up-link waves arrive at the AP predominantly from a few directions. In that case groups with similar power and timing characteristics are constructed according to the AoA of NLoS component with the highest strength assuming there is still a power differentiation among the received components. If however the formulation of co-channel groups in an environment with rich multipath scattering is not possible, broadcasting transmission is chosen. In such a case, the beamforming optimization matches the transmission to more possible eigenmodes of the channel, derived from Singular Value Decomposition (SVD) of the MIMO channel Matrix. In PHY layer, the synchronization, pilot and signal segments are added to the MAC Packet Data Unit (MPDU). Each user estimates the propagation channel from the pilot segments. The CSI is known at the AP by using an up-link channel

to return channel measurements collected during the transmission of the downlink training sequences at 48 data sub-carriers. In IEEE 802.11n explicit feedback is proposed in the TDD mode,ie each user sends to the AP the MIMO channel coefficients.

TABLE 5.2 CSI MATRICES REPORT FOR 20 MHZ

Field	Size
SNR in Rx channel 1	8 bits
……..	
SNR in Rx channel N_r	8 bits
CSI Matrix for Carrier -28	$3+2xN_bxN_cxN_r$ bits
CSI Matrix for Carrier -28+N_g	$3+2xN_bxN_cxN_r$ bits
……..	
CSI Matrix for Carrier -1	$3+2xN_bxN_cxN_r$ bits
CSI Matrix for Carrier 1	$3+2xN_bxN_cxN_r$ bits
CSI Matrix for Carrier 1+ N_g	$3+2xN_bxN_cxN_r$ bits
…….	
CSI Matrix for Carrier 28	$3+2xN_bxN_cxN_r$ bits

The CSI matrix report is depicted in table 5.2, where N_c denotes the number of columns in each CSI matrix and N_r the number of rows. The explicit feedback format field is structured into the Grouping (N_g=1 to 4) and Coefficients Size (N_b=4 to 8 bits) fields. The feedback of a CSI Matrix can be instantaneous or aggregate. The structure of CSI Matrix Report includes all sub-carriers.

In the case where beamforming vector $\mathbf{V}$ is applied at the transmitter and matrix $\mathbf{U_k}$ at user k, the combined channel matrix $(\mathbf{H_{eff}})_{\mathbf{n}}^{\mathbf{k}} = \mathbf{U_k^H H_k^n V}$ is estimated from the receiver. $\mathbf{U_k}$ is known at the receiver side and therefore $\mathbf{H_k^n V}$ is derived by multiplying with $(\mathbf{U_k^H})^{-1}$ the combined channel matrix. The equivalent channel $\mathbf{H_k^n V}$ is still smooth across sub-carriers belonging to the same set of users because these sub-carriers are multiplied by the same vector $\mathbf{V}$. So, we could efficiently estimate the channel by interpolating and smoothing the feedback measurements over the pilot tones.

C. SDMA Transmission Protocol

. The proposed transmission protocol operates as follows:

Step 1: The AP broadcasts an MPDU containing a CSI feedback Request to each of users $1, \ldots K$ sequentially.

Step 2: The users $k = 1, \ldots K$ receive the MPDU using an omni-directional antenna pattern each and perform channel estimation $\hat{\mathbf{H}}_{\mathbf{k}}^{\mathbf{n}}$ with $n = 1, \ldots N$.

Step 3: Upon successful reception of the MPDU, each user quantizes the CSI and sends an ACK containing the CSI feedback.

Step 4: The AP collects the radio channel matrices $\hat{\mathbf{H}}_{\mathbf{k}}^{\mathbf{n}}$ and groups users according the strategy mentioned above.

*Step 5:*The AP transmits the steering MPDU using vector $\mathbf{V}$ after employing the proposed downlink beamforming and frequency allocation algorithms

Step 6: If all K steering ACKs are received from the AP at the allocated frequencies then *step 5* is repeated.

Step 7: If one or more of the ACKs are not received from the AP, then the procedure is interrupted and we begin from *step 1* to estimate the full dimension of the channel matrix $\hat{\mathbf{H}}_{\mathbf{k}}^{\mathbf{n}}$.

5.3 Downlink beamforming design

A.Optimum Receiver Antenna Arrays

The receiver antenna arrays have a properly determined beam pattern. They steer the beams to enhance the total power in all reflected paths at a scattering environment. Array gain is achieved via coherent combining of the signal paths. The proposed strategy is based on ES. $\mathbf{H}_{\mathbf{k}}^{\mathbf{n}}$ can be diagonalized as

$$\mathbf{H}_{\mathbf{k}}^{\mathbf{n}} = \mathbf{U}_{\mathbf{k}}^{\mathbf{n}}\mathbf{D}_{\mathbf{k}}^{\mathbf{n}}(\mathbf{V}_{\mathbf{k}}^{\mathbf{n}})^{\mathbf{H}} = \sum_{i=1}^{q} \sqrt{\lambda_{ki}^{n}}\mathbf{u}_{\mathbf{ki}}^{\mathbf{n}}\mathbf{v}_{\mathbf{ki}}^{\mathbf{n}} \quad (5.11)$$

$\mathbf{D}_{\mathbf{k}}^{\mathbf{n}}$ is a $M_r \mathrm{x} M_t$ matrix where only non zero elements are given by

$$D_k^n[i,i] = \sqrt{\lambda_{ki}^n} \quad (5.12)$$

with $i = 1, \ldots q$. The scalar $q = \min(M_t, M_r)$ denotes the rank of $\mathbf{H}_{\mathbf{k}}^{\mathbf{n}}$ and represents the number of spatial degrees of freedom. The SVD is an appropriate way of diagonalizing the matrix $\mathbf{H}_{\mathbf{k}}^{\mathbf{n}}$ which leads to a number of parallel channels (eigen modes). The power gain of i channel (ith eigen mode) is λ_{ki}^n. The columns $\mathbf{u}_{\mathbf{ki}}^{\mathbf{n}}(\mathbf{v}_{\mathbf{ki}}^{\mathbf{n}})$ of $\mathbf{U}_{\mathbf{k}}^{\mathbf{n}}(\mathbf{V}_{\mathbf{k}}^{\mathbf{n}})$ are orthonormal so that

$$(\mathbf{U}_{\mathbf{k}}^{\mathbf{n}})^{\mathbf{H}}\mathbf{U}_{\mathbf{k}}^{\mathbf{n}} = \mathbf{I}_{\mathbf{M_t}} \quad (5.13)$$

$$(\mathbf{V}_{\mathbf{k}}^{\mathbf{n}})^{\mathbf{H}}\mathbf{V}_{\mathbf{k}}^{\mathbf{n}} = \mathbf{I}_{\mathbf{M_t}} \quad (5.14)$$

The columns $\mathbf{u}_{\mathbf{ki}}^{\mathbf{n}}(\mathbf{v}_{\mathbf{ki}}^{\mathbf{n}})$ are the optimum weights of Rx antenna arrays (Tx antenna arrays) for ith eigen mode [34]. E-SDM forms beams using eigen-vectors and can configure a spatially orthogonal

MIMO channel that is a channel without crosstalk. Therefore, receiver antenna arrays form beams using eigen-vectors and expect to capture all possible orthogonal spatial streams derived from scatters which are found to the neighborhood of transmitter and receiver. SVD must be evaluate at the receiver. The calculation load increases proportionally according to the number of sub-carriers. But the channel in frequency domain is smooth. The adjacent sub-carriers are highly correlated because we multiply all sub-carriers by the same complex weights. This correlation reduces the calculation load. One can estimates $\mathbf{U_k^n}$ matrix in one specific sub-carrier n by interpolation and smoothing over adjacent sub-carriers. In ES technique, the beamformer applied at the transmitter is the matrix $\mathbf{V_k^n}$ at each sub-carrier. The equivalent channel after beamforming is not still remaining smooth leading to higher computation load and high power consumption.

B. Beamforming optimization for AP

The general power minimization problem (subject to SINR constraints) of simultaneously designing beamformers for several co-channels multicast sets of users and frequency flat channel was studied in [35]. This problem can be formulated as a convex optimization problem. However, the optimum solution is considered for a single antenna receiver. We extended this design problem taking account interference from neighboring co-working APs and that the remote users have multiple antennas (MIMO system). Given received vector $\mathbf{U_k^{f_a}}$ for all users of set g, calculating from SVD of the channel matrix, the posed problem is to generate an optimal downlink beamforming at AP a, minimizing at the same time the total transmit power and guaranteeing a prescribed SINR constraints γ_k at each user of set g.

$$\mathcal{Q}5 \quad \min_{\{\mathbf{v_g^{f_a}} \in C^{M_t}\}_{g=1}^{G}} \sum_{g=1}^{G} \left\|\mathbf{v_g^{f_a}}\right\|_2^2$$

$$\frac{\left|(\mathbf{U_k^{f_a}})^{\mathbf{H}}\,\mathbf{H_k^{f_a}}\,\mathbf{v_g^{f_a}}\right|^2}{\sum_{l\neq g}\left|\mathbf{U_k^{f_a}}\mathbf{H_k^{f_a}}\mathbf{v_l^{f_a}}\right|^2+(\sigma_k^{f_a})^2\left\|\mathbf{U_k^{f_a}}\right\|^2+\sum_{f_b}P_k^{f_b}I(f_a,f_b)} \geq \gamma_k$$

$$\|\mathbf{U_k}\|^2 = 1, \qquad \forall k \in \{1,2,\dots K\},$$

$$\forall g \in \{1,2,\dots G\}, \quad \forall f_b \in \{1,2,\dots F\}$$

$\|\mathbf{U_k}\|^2 = 1$ because U ,derived from SVD, is a unitary matrix. This problem was found NP-hard for general channel vector [35,36]. Let's introduce

$$\mathbf{r_k^{f_a}} = (\mathbf{U_k^{f_a}})^{\mathbf{H}}\mathbf{H_k^{f_a}} \quad (5.15)$$

size $M_r \mathrm{x} M_r$ complex matrix, define

$$\mathbf{V_g^{f_a}} = \mathbf{v_g^{f_a}}(\mathbf{v_g^{f_a}})^{\mathbf{H}} \quad (5.16)),$$

$$\mathbf{R_k^{f_a}} = (\mathbf{r_k^{f_a}})^{\mathbf{H}}\,\mathbf{r_k^{f_a}} \quad (5.17)$$

and use

$$\left|\mathbf{r_k^{f_a}}\mathbf{v_g^{f_a}}\right|^2 = (\mathbf{v_g^{f_a}})^{\mathbf{H}}(\mathbf{r_k^{f_a}})^{\mathbf{H}}\mathbf{r_k^{f_a}}\mathbf{v_g^{f_a}} = tr(\mathbf{V_g^{f_a}}\mathbf{R_k^{f_a}}) (5.18)$$

For reason of simplicity, we have the shorthand notation

$\mathbf{R_k}$ for $\mathbf{R_k^{f_a}}$, V_g for $\mathbf{V_g^{f_a}}$, $\mathbf{v_g}$ for $\mathbf{v_g^{f_a}}$ and σ_k for $\sigma_k^{f_a}$. The problem $\mathcal{Q}5$ is transformed as

$\mathcal{Q}'5 \quad \min_{\{\mathbf{V_g}\in C^{M_t \mathrm{x} M_t}\}_{g=1}^{G}} \sum_{g=1}^{G} tr(\mathbf{V_g})$

$$\text{s.t.} \quad \frac{tr(\mathbf{R_k}\mathbf{V_g})}{\sum_{l\neq g} tr(\mathbf{R_k}\mathbf{V_l}) + \sigma_k^2 + \sum_{f_b} P_k^{f_b} I(f_a, f_b)} \geq \gamma_k$$

$$\mathbf{V_g} \geq 0 \qquad \mathbf{V_g} = \mathbf{V_g^H} \qquad rank(\mathbf{V_g}) = 1$$

$$\forall k \in \{1, 2, \ldots K\} \quad \forall g \in \{1, 2, \ldots G\}$$

$$\forall f_b \in \{1, 2, \ldots F\}$$

The constraint $rank(\mathbf{V_g}) = 1$ is applied from the fact that $\mathbf{V_g} = \mathbf{v_g}\mathbf{v_g^H}$. Constrains $\mathbf{V_g} \geq 0$ and $\mathbf{V_g} = \mathbf{V_g^H}$ mean that $\mathbf{V_g}$ is symmetric, positive, semidefinite matrix. In general case, the constraint $\{rank(\mathbf{V_g})\}_{g=1}^{G}$ is not convex [36]. By dropping the associated non convex constraints, the original non-convex Quadratically Constrained Quadratic Programming (QCQP) problem $\mathcal{Q}$ relaxed to a suitable Semi Definite Programming problem (SDP). As shown by Bengtsson and Ottersten, the above relaxation is guaranteed to have at least one optimal solution which is rank one [37]. We introduce K real non-negative "slack" variables $\{s_k\}_{k=1}^{K}$ and we underline the fact that the terms in denominator of linear inequalities are all non-negative; we take the relaxation problem $\mathcal{R}5$.

$\mathcal{R}5 \quad \min_{\{\mathbf{V_g}\in C^{M_t \mathrm{x} M_t}\}_{g=1}^{G}} \sum_{g=1}^{G} tr(\mathbf{V_g})$

$$tr(\mathbf{R_k}\mathbf{V_g}) - \gamma_k \sum_{l\neq g} tr(\mathbf{R_k}\mathbf{V_l}) - s_k = \gamma_k(\sigma_k^2 + \sum_{f_b} P_k^{f_b} I(f_a, f_b))$$

$\mathbf{V_g} \geq 0$, $\mathbf{V_g} = \mathbf{V_g^H}$, $s_k \geq 0$, $\forall k \in \{1, 2, \ldots K\}$

$\forall g \in \{1, 2, \ldots G\}$, $\forall f_b \in \{1, 2, \ldots F\}$

The relaxation technique can be interpreted as the Lagrangian dual of the dual of the original problem because it gives a lower bound for the original problem. The first advantage of using SDP is that problem $\mathcal{R}5$ is a convex optimization problem and hence it has not local minima. The second one is that problem can be efficiently solved by any SDP solver, such as SeDuMi [38], based on interior point methods. Problem $\mathcal{R}5$ can be expressed in the standard prima form used in SeDuMi.

The relaxed problem $\mathcal{R}5$ provides only lower bounds on the optimal solution $\{\mathbf{v_g^{opt}}\}_{g=1}^{G}$ due to the fact that $\mathbf{V_g^{opt}}$ will not be rank – one in general. In [39] randomization is proposed for computing feasible points in a QCQP problem. If $\mathbf{x}$ is the variable matrix of the original problem and $\mathbf{X} = \mathbf{x}\,\mathbf{x^T} \geq 0$ the variable of the relaxed problem then $\mathbf{x}$ is selected as a Gaussian variable with $\mathbf{x} \backsim N(\mathbf{x}, \mathbf{X})$. Afterwards, $\mathbf{x}$ will solve the QCQP "on average". A good feasible point can be obtained by trying enough $\mathbf{x}$. Inspired by the above method, a randomization procedure is employed in [35] to generate candidate beamforming vectors $\mathbf{v_g}$ .This procedure is mentioned as $\mathrm{rand}\,\mathcal{C}$. At the beginning, SVD is used in $\mathbf{V_g^{opt}} = \mathbf{U}\ \mathbf{\Sigma^{\frac{1}{2}}}\ \mathbf{U^H}$ and $\mathbf{v_g} = \mathbf{U}\ \mathbf{\Sigma^{\frac{1}{2}}}\ w_g$ is put, where w_g is a Gaussian variable with $w_g \backsim N(0,1)$ to insure that $E\left[\mathbf{v_g}\ \mathbf{v_g^H}\right] = \mathbf{V_g^{opt}}$. However, the candidate beamforming vectors must satisfy the constraints of original problem $\mathcal{Q}5$. In this way, for each candidate set of beamforming vectors, a multi-group power control $(\mathcal{MGPC})$ problem is solved.

$$\mathcal{MGPC}5 \quad \min_{\{P_g \in \mathcal{R}\}_{g=1}^{G}} \sum_{g=1}^{G} \beta_g\, P_g$$

$$\text{s.t.} \quad \frac{P_g\, \alpha_{g,k}}{\sum_{l \neq g} P_l\, \alpha_{l,k} + \sigma_k^2 + \sum_{f_b} P_k^{f_b} I(f_a, f_b)} \geq \gamma_k$$

$$\forall\, g \in \{1 \ldots G\} \quad P_g \geq 0\, \forall f_b \in \{1, 2, \ldots F\}$$

where

$$\beta_g = \|\mathbf{v_g}\|_2^2 \quad (5.19)$$

$$\alpha_{g,k} = \left|\mathbf{v_g^H R_k v_g}\right| \quad (5.20)$$

and P_g denotes the power boost factor for multicast set of users g. This is a Linear Program (LP) and can be solved by SeDuMi with the computational cost being negligible. Finally, after calculating beamforming weight vectors $\mathbf{v_g^{f_a}}$ applied at the transmitter for all possible operating channels $f_a \in \mathcal{C}$, we select channel $f_c \in \mathcal{C}$ that minimize total transmit power of AP a for all channels. Transmit power $P_{TX}^{f_a}$ is computed from equation (5.7). Therefore,

$$f_c = arg\,\min_{\{f_a \in \mathcal{C}\}} P_{TX}^{f_a} \quad (5.21)$$

5.4 Sub-carrier assignments

The transmission of optimized power at the center frequency follows beamforming; the problem which has to be solved is how to assign N=48 OFDM overlapping data sub-channels to each co-channel set of users. In [40], the posed problem is the allocation of sub-carriers and time slots to sub-carriers so that rate requirements for each user are satisfied. Our application doesn't require

continuous transmission to consider slot allocation. Carrier-Sense Multiple Access (CSMA) is used. Transmitters sense the channel and delay transmission if they detect that another transmitter is currently emitting. A sub-carrier is only allocated to one user. The solution is developed as in [41] in two steps.

a) Resource Allocation: Find the number of sub-carriers that each user will be assigned to,

b) Sub-carrier Allocation: Allocate the sub-channels according to resource allocation and the state of the channel.

Compared to [41], our approach is different due to the fact that the goal is not the minimization of the total transmitted power but fairness with considerable throughput. MAC protocol must support users that demand a mixture of services. The support of these services require a cross-layer design between MAC and PHY with QoS (Bit Error Rate-BER, minimum rate required, etc) that depend on applications. Let's m_k the number of sub-carriers allocated to user k. If set g has K_g users, then

$$\sum_{k=1}^{K_g} m_k = N \quad \forall g \in \{1 \dots G\} \quad (5.22)$$

In this section, we determine the number of sub-carriers taking into account:

a) $SINR_k$ calculated in section 5.3

b) Minimum rate required R_k^{min} in bits per symbol

c) Maximum BER required.

R_k^{min} and maximum BER are related to different classes of services. At each user k, a maximum modulation level with b_k bits per symbol is selected from a set $\mathcal{M}$ of available QAM. For $M-QAM$ modulation, $M = 2^{b_k}$ with $b_k \in \mathcal{M}$ .The throughput of user k for each sub-channel $n \in \{1 \dots N\}$ can be calculated as

$$T_k = W_{subchannel} \log(1 + a\, SINR_k^n) \quad (5.23)$$

where $a = \frac{1.5}{-\ln(5\,BER)}$ for additive White Gaussian noise environment and $a = \frac{1.5}{\frac{0.2}{BER} - 1}$ for Rayleigh fading[42]. In our case, $W_{subchannel} = \frac{312.5}{2}\,KHz$. When $a = 1$, the relationship is similar to Shannon Capacity of user k. Suppose that $SINR_k^n$ is constant and equal to $SINR_k$ for all sub-carriers, the number m_k is

$$m_k = \lceil \frac{R_k^{\min}}{T_k} \rceil \quad (5.24)$$

$\lceil x \rceil$ denotes the smallest integer that exceeds x. For a feasible solution, the minimum value which takes m_k is $\lceil \frac{R_k^{\min}}{T_k} \rceil$ and the maximum is N. We distinguish between two cases:

a) $\sum_{k=1}^{K_g} m_k > N$: The user with maximum calculated m_k is the user who required high bit rate but has small T_k i.e. bad $SINR$. Therefore, fair allocation imposes the removal of one subcarrier.

b) $\sum_{k=1}^{K_g} m_k < N$: in order to achieve maximum throughput, we add one sub carrier to the user with minimum m_k and high $R_k^{\min}$. Under the assumption that the channel is flat for the entire band, we propose the algorithm below:

$\mathcal{R}.\mathcal{A}$ $\quad T_k \leftarrow \log_2\left((1 + a\ SINR_k)\right)$

$m_k \leftarrow \lceil \frac{R_k^{\min}}{T_k} \rceil$

$R_{th} = \text{threshold}$

while $\sum_{k=1}^{K_g} m_k > N$ do

$l \leftarrow \arg \max_{1 \le k \le K_g} m_k$

$m_l \leftarrow m_l - 1$

end while

while $\sum_{k=1}^{K_g} m_k < N$ do

$l \leftarrow \arg \min_{\substack{1 \le k \le K_g \\ R_k^{min} > R_{th}}} m_k$

$m_l \leftarrow m_l + 1$

end while

The hypothesis in that the channel held constant over the whole band is acceptable only for resource allocation. We calculate a list $S_k^{\max}$ with all acceptable sub-carriers for each user k.

for all users

$S_k^{\max} \leftarrow \{\ \}$

end for

for $n = 1$ to N do

calculate $SINR_k^n$

if $SNR_k^n \ge \gamma_k$

then $S_k^{\max} \leftarrow S_k^{\max} \cup \{n\}$

end if ,end for

We normalize $SINR_K^n \quad \forall k \in \{1 \dots K\}$ and $\forall n \in \{1 \dots N\}$ relatively to maximum value $SINR^{\max} = \max SINR_k^n$,

$$w_k^n = \frac{SINR_k^n}{SINR^{\max}} \quad (5.25)$$

If we consider two disjoint sets of vertices, one which represents the K_g users and the other the N sub-carriers then the problem of sub-carriers allocation is transformed into a weighted bi-partite matching. In [43], the authors propose the method of maximum augmenting path to obtain maximal weighted matching. Neverhless, this approach is a modification of alternating path method [44] which is difficult to apply in weighted matching. We propose a heuristic algorithm with fast computation and performance close to the optimal matching. The algorithm is divided in two sub-algorithms. The first, which is referred as Channel Gain Grade $(\mathcal{CGG})$ algorithm, assigns the sub-carriers to users according to highest w_k^n. Let S_k the set of allocated sub-carriers for user k and F the set of available sub-carriers for assignment. Initially, S_k is empty and F contains all sub-carriers with index from 1 to N.

$S_k \leftarrow \{\}$,

$F_1 \leftarrow \{1 \dots N\}$.

The sub-algorithm terminates when the number of elements for set F doesn't change in two consecutive repetitions.

$\mathcal{CGG}$ $i \leftarrow 0$

do

$i \leftarrow i + 1$

$\forall k \in K$ and $n \in F_i$

$(k^*, n^*) \leftarrow \arg\max w_k^n$

$S_{k^*} \leftarrow S_{k^*} \bigcup \{n\}$

$F_{i+1} \leftarrow F_i / \{n^*\}$

$w_k^{n^*} \leftarrow 0 \quad \forall k \in K$

if $(\#S_{k^*} = m_{k^*})$

$(k^*, n) \leftarrow 0 \quad \forall n \in F_{i+1}$

end if

while $\#F_{i+1} < \#F_i$

This sub-algorithm is very efficient when the number of users is small compare to the number of sub-channels as in our case. If there are sub-carriers which are not allocated then we run the below sub-algorithm named InterChange Sub-carriers $(\mathcal{ICS})$ algorithm.

1. The users whose the number of allocated sub-carriers is satisfied $(\#S_k = m_k)$ will be included in set $\mathcal{A}$, otherwise in set $\mathcal{A}'$.

2. Find subset $\mathcal{I}$ of users $k \in \mathcal{A}$ $(\mathcal{I} \subseteq \mathcal{A})$ whose one at least sub-carrier $n \in S_k^{\max}$ could be interchanged with the set of not allocated sub-carriers F $(F \cap S_k^{\max} \neq \{\})$.

3. $(k^*, n^*) \leftarrow \arg\max w_k^n$, $\forall k \in \mathcal{I}$ and $n \in F \cap S_k^{\max}$.

4. $l \leftarrow \arg\min w_{k^*}^n$, $\forall n \in S_{k*}$

5. Swap $n^* \in F$ with $l \in S_{k^*}$

6. Allocate $l \in F$ to one of users $k' \in \mathcal{A}'$ running $\mathcal{CGG}$, $(F_1 \leftarrow F)$

7. Go to step 1 until $F = \{\}$

5.5 Simulation results

The example of simulation scenario is illustrated in figure 5.5. The network consists of 5 cells partially overlapping with $F = 4$ channel reuse in 5GHz spectrum. The cell with an AP at the center is represented by a circle radius $R = 100m$. AP 1 is $D = \sqrt{3}R$ distance from neighboring APs. A possible optimum channel assignment is the following: AP 2 to channel 1, AP 4 to channel 2, AP 3 to channel 3 and AP 5 to channel 4. Our proposed technique enables self-configuration to AP 1, based on the measurement of channel conditions in the wireless environment. Physical layer (PHY) modes compliant to IEEE 802.11n are given in table 5.1 [45]. The received SINR constraints are set $\gamma_k = 15dB$ and the additive noise power at the receiver k is set $\sigma_k^2 = -95dBm$. According to the system description of IEEE 802.11n WG [45], $I(f_a, f_b)$ is equal to

$$\mathrm{I}(f_a, f_b) = \begin{cases} 0\mathrm{dB} & \text{for co-channel} \\ -16\mathrm{dB} & \text{for adjacent channel} \\ -32\mathrm{dB} & \text{in other cases} \end{cases}$$

Maximum transmit power for each AP is P_t =250mW or 24 dBm. The simulation is done with MATLAB environment. Uniform Linear Arrays (ULA) with $M_t = 4$ and $M_r = 4$ antenna elements is considered. The position of users at each cluster follows a Uniform Distribution. 1000 Gaussian randomization samples to solve $randC$ problem are generated. Due to Doppler effect, we have a time varying channel and we collect 104 samples at each user's position. If we take the speed of moving scattering environment to be equal to $v_o = 1.2\frac{Km}{h}$, maximum Doppler shift is

$f_m = \frac{v_o f}{c} = 208Hz$. Coherence time due to Doppler spread is $T_c \approx \frac{1}{f_m} = 40808\mu s$, i.e. 10000 times slower that the transmitted OFDM symbol (~ 4μs) . We model the wireless channel as a sum of two components, a LOS component and a NLOS component

$$H = \sqrt{\frac{K_f}{K_f+1}} H_{LOS} + \sqrt{\frac{1}{K_f+1}} H_{NLOS} \quad (5.26)$$

where K_f is the Ricien K-factor and is defined as the ratio between the power of the LOS component and the mean power of the NLOS component. Channel matrix H_{LOS} is computing with a break point 5m, a path loss exponent 3, a shadowing deviation 4dB and $K_f = 3$. Channel matrix H_{NLOS} is simulated as model B proposed by the IEEE 802.11n channel model [23]. MATLAB implementation of IEEE 802.11n channel model is available from L. Schumacher [46].

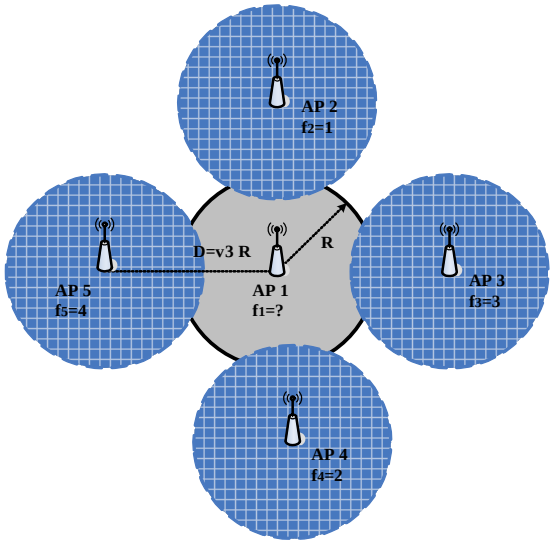

Figure 5.5 Deployment of a configuration with 5 cells partially overlapping

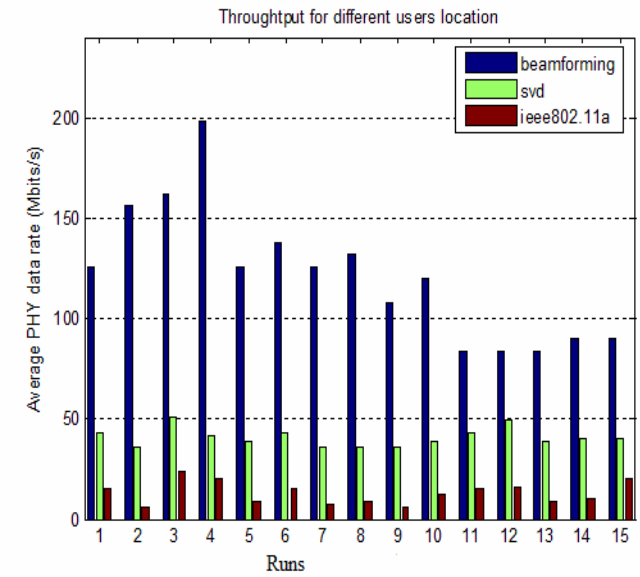

Figure 5.6 Average PHY data rate for different users locations

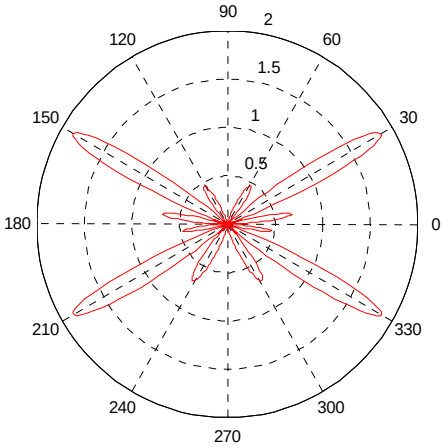

Figure 5.7 Beamforming of neighboring APs - scenario A

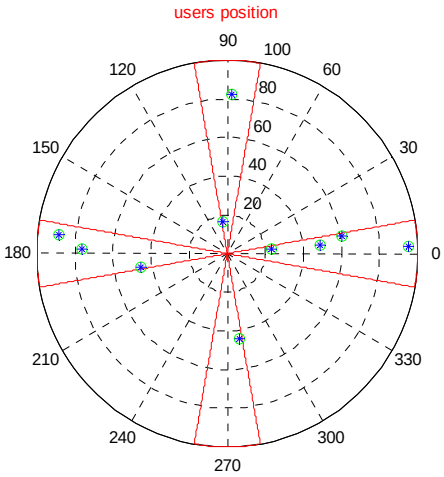

Figure 5.8 Location of 10 users in 4 groups

Figure 5.6 shows the average physical layer data rate of a) our scheme, b) eigen beamforming on every sub-carrier (based on SVD and proposed in the on going IEEE 802.11n standardization) and c) IEEE 802.11a 1×1 standard. The beams of neighboring APs are presented in Figure 5.7.Radiation of interference cells is constant for all runs and it's computing for 4 users placed in 4 sets (each cluster of Figure 5.8 contains one user). At the first five runs, the range of 4 sets is 350-10 degrees, 80-100 degrees, 170-190 degrees and 260-280 degrees. At the next five runs the range of sets is 340-20 degrees, 70-110 degrees, 160-200 degrees and 250-290 degrees. The final five runs correspond to range 330-30 degrees, 60-120 degrees, 150-210 degrees and 240-300 degrees. Improvement of our beamforming technique is noticeable. Throughput from 80Mbits/s to 200Mbits/s in a strong interference environment is achieved for our proposed technique while SVD technique gives data rate not bigger than 50 Mbits/s. We remark that throughput diminish as set of users cover bigger area.

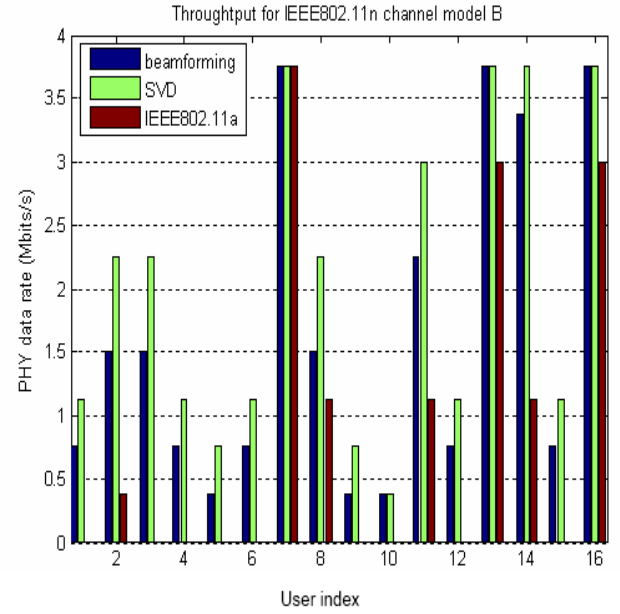

Figure 5.9 Throughput for channel model B

Figure 5.9 shows the average physical data rate when AP broadcast to 16 users in NLOS environment (channel model B) considering that no interference exists from neighoring netwoks. The proposed method and SVD technique (ES) achieve a noticeable improvement over the IEEE 802.11a . ES achieves a total throughput improvement of 0.2286 in comparison to our scheme in NLOS environment. Afterwards, we consider a wireless scenario without interference from vicinity incorporating $K = 4$ users in order to compare the three techniques in LOS/NLOS environment. .

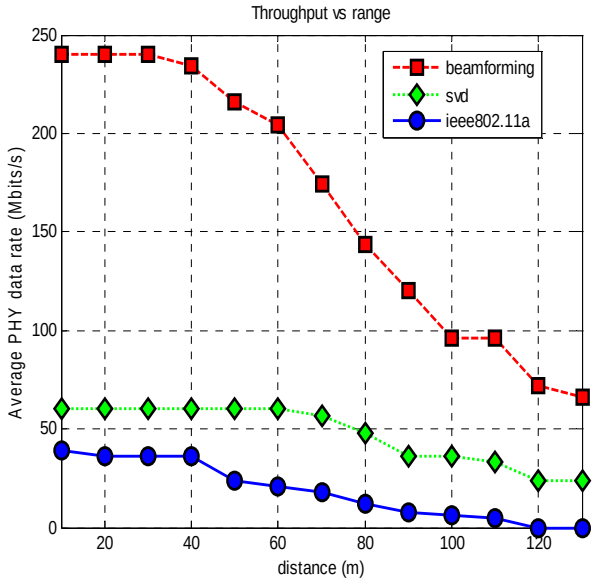

Figure 5.10 Throughput versus range for LOS/NLOS channel

Angular users' direction (θ) is 0º,180º,90º and 270º. We suppose that users are equaled by AP. Knowledge of users' direction permits gathering users in four multicast sets $(G = 4)$. Figure 5.10

shows the average physical layer data rate as function of distance. In continuously, two different simulation scenarios A and B are examined. For simulation scenario A, we make a list of operation frequencies with random order $\mathcal{F} = \{1, 2, 4, 3\}$. Our results are examined for 10 users located at AP 1. The first cluster consists of 4 users, the second of 3 users, the third of 2 users and the fourth contains 1 user as in figure 5.8. Figure 5.7 depicts beams of neighboring APs for scenario A. Figure 5.11 presents radiate power of AP 1 according the list $\mathcal{F}$. Each run corresponds to different locations of users, randomly placed as figure 5.8. The first calculation of each run is for operating frequency 1, the second for 2, the third for 4 and the fourth for 3. The profit of finding optimum frequency is remarkable. In run 1 the difference between maximum power corresponds to frequency 4 and minimum power correspond to frequency 2 is 0.235W.Operating frequencies 1 and 3 which correspond to powers greater than the maximum value of 250 mW are rejected.

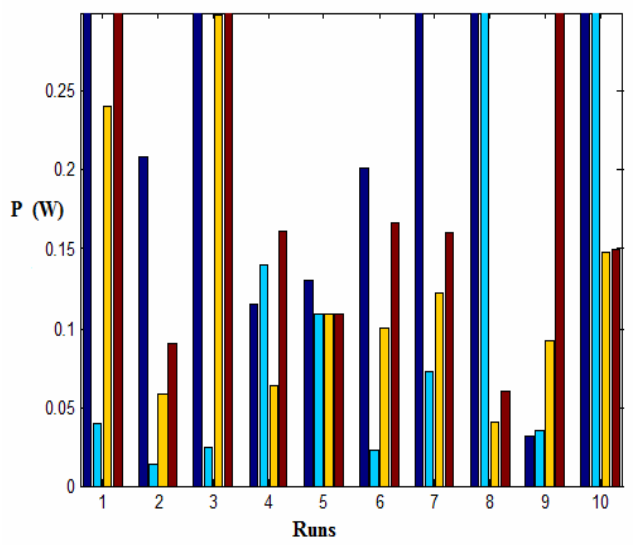

Figure 5.11 Calculated power for 4 operating frequencies-scenario A

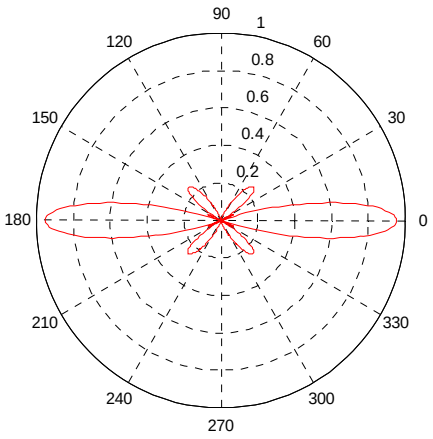

Figure 5.12 Beamforming of AP 3 and 5 scenario B

In run 3 only frequency 2 is acceptable. Finally, a setting in strong interference environment (scenario B) by four users located in four sets (one user at each set) is studied. Five channels are possible for assignment according frequency list $\mathcal{F} = \{5, 1, 4, 2, 3\}$. Figure 5.12 shows beamforming of AP 3 and 5 while figure 5.13 of AP 2 and 4. Figure 5.14 gives the calculated power of scenario B for 15 different runs. We remark that the optimum solution is obtained when channel 5 is assigned to AP 1. The proposed algorithm doesn't give acceptable values of transmit power for run 5,9,10 and 12 in the case where channel 1 to 4 is allowed. If that happens, CSMA mechanism is enable to avoid co-channel interference from neighboring cells and transmitted power is set equal to 250m. For reasons of validating the proposed algorithms in section 5.4, a set of 16 users is used with $SINR$ resulting from section 5.3. Minimum rate required for each user k is equal to

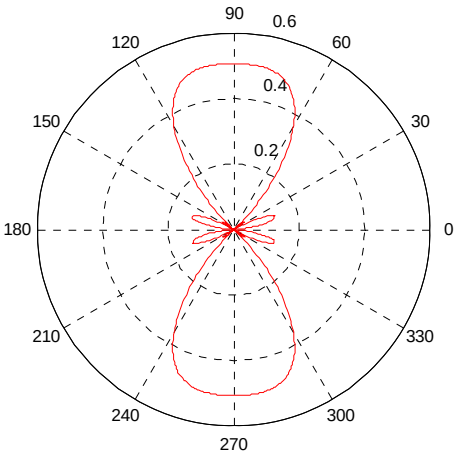

Figure 5.13 Beamforming of AP 2 and 4 scenario B

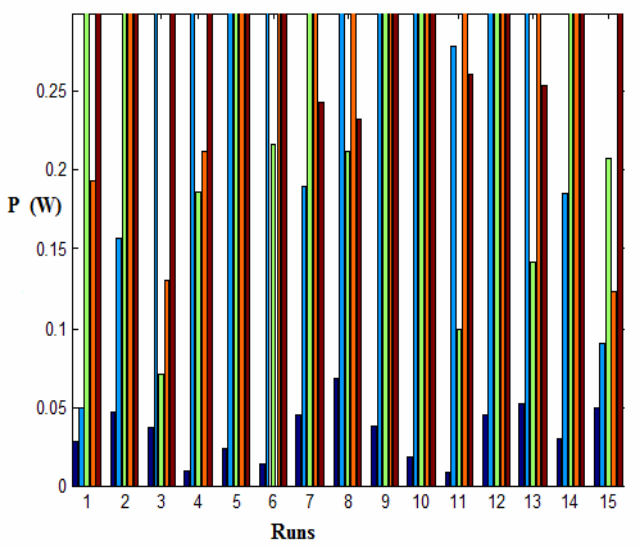

Figure 5.14 Calculated power for 5 operating frequencies-scenario B

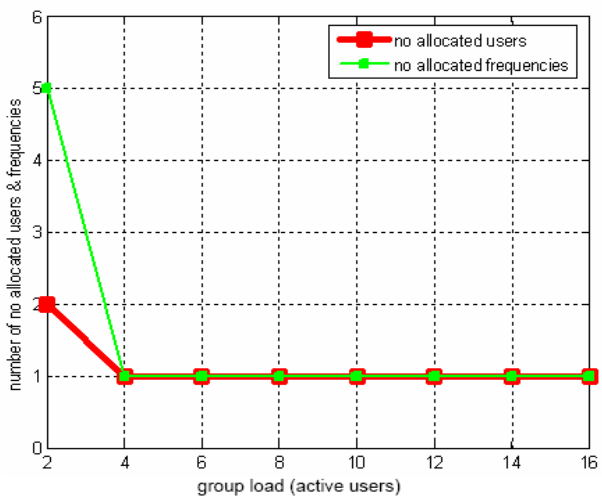

Figure 5.15 No allocated users and frequencies vs active users after running of $\mathcal{CGG}$ sub-algorithm.

$R_k^{min} = 2048\, Kbits/s$. We calculate theoretical throughput T_k considering additive White Gaussian noise with $BER = 10^{-5}$. Normalized elements w_k^n follow a normally distribution with mean value the $SINR_k$ given from section III and deviation $\sigma = 3dB$ as in [40]. We simulate $\mathcal{CGG}$ sub-algorithm for 100 Monte Carlo runs. The results are showed in Figure 5.15. This figure gives the number of no allocated users and frequencies as function of number of active users. It's clear that $\mathcal{CGG}$ sub-algorithm is efficient under our experiment conditions. $\mathcal{ICS}$ sub-algorithm always converges in our network configuration. According to figure 5.16, the number of users $\mathrm{k} \in \mathcal{I}$ which are available to swap their frequencies is large compare to the number of no allocated users $k' \in \mathcal{A}'$. This explain why $\mathcal{ICS}$ algorithm is efficient and always converges.

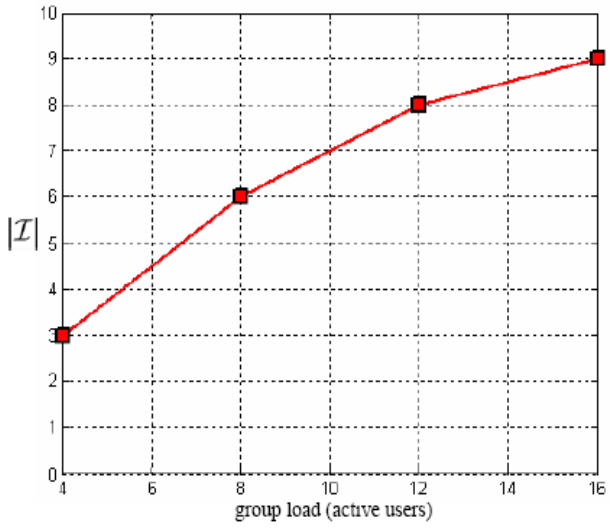

Figure 5.16 Number of allocated users available to swap their frequency vs active users at step 2 of $\mathcal{ICS}$ sub-algorithm.

5.6 Implementation Complexity

OFDM is characterized by its simplicity. OFDM transmitters are low cost due to the ability of replacing the banks of sinusoidal generators by Discrete Fourier Transform (DFT) and as a consequence the implementation complexity of the modem is reduced. The sub-carriers are neither individually filtering nor amplifying. In order to achieve a reasonable complexity, the beamformer must multiply by the same complex weights all sub-carriers. In ES, the AP uses eigenvectors of channel matrix as transmission weight vector and implementation is based on Digital Signal Processing (DSP) at the baseband chip. The precoder of the eigen beamforming is done on every sub-carrier before the information is sent to IFFT module. This implementation suffers from increased complexity and places tough performance criteria on the Digital to Analog (D/A) converter in order to provide accurate delay. Our architecture supports RF-beamforming which offers low cost hardware, more capabilities and particularly higher beam pointing accuracy. Also, our approach has advantages with respect to lower power consumption as signal process is reduced. Additionally, at baseband beamforming scheme, linearity and dynamic range of the Intermediate Frequency (IF) stage and D/A converter will also have to be substantially higher leading to higher power consumption .

Additionally, our beamforming problem can be expressed in the standard prima form used in SeDuMi. It consists of G variables $M_t \mathrm{x} M_t$ and M inequality constraints. SeDuMi is an iterative algorithm. Therefore, the complexity per iteration is $O\left((GM_t^2+K)^3\right)$ and for solution accuracy ω SeDuMi gives $O\left(\sqrt{GM_t^2+K}\,\log(\frac{1}{\omega})\right)$ worst-case iteration bound.

5.7 Conclusions

We studied and developed strategies compliant with IEEE 802.11n standard. Our distributed algorithms suppress interference among vicinities WLANs and allow APs to choose a channel band that will experience minimal interference by enforcing common transmission weight vectors for all sub-carriers allocated to the same set of users. We can efficiently share the wireless resources in an environment with fast and unmanaged deployment of WLANs. We adopt a frequency allocation scheme, which allows channel state driven link adaptation by estimating the state of the channel. Finally, our proposed strategy is a cost-saving and less complex implementation approach.

Chapter 6

Multicast Transmission over IEEE 802.11n WLANs

Multicasting is the ability of a communication network to accept a single message from an application and to deliver copies of the message to multiple recipients at different locations. It allows transmission and routing of packets to multiple destinations using fewer network resources. Multicasting is a more efficient method of supporting group communication than unicasting or broadcasting. Wireless Local Area Network (WLAN) devices are well established due to low cost. PDAs, laptops and cell phones include a WLAN modem as standard. Service Providers have great interest in supporting services with a large number of clients attempting the same content from a single Access Point (AP). Wireless multicast support many important multimedia applications as digital video libraries, distance learning, company training, electronic commerce, on line games, redistribution of TV, etc.

Video streaming is very different from data communication due to inherent delay constraints; as late arriving data are not useful to the video decoder. In this chpter, we focus on IEEE802.11n which transmit higher physical layer data rate and improve MAC efficiency. MAC layer use the simple and robust carrier sense multiple access with collision avoidance (CSMA/CA) technique for medium access which has contributed to the success of 802.11. However, this scheme imposes a considerable penalty on efficiency. Good performance is only obtained when a few users compete for access to the wireless media. Multicast overcomes this inefficiency by reducing the contention. IEEE 802.11n improves preamble overheads at data and controls frame transmission as well as interframe spacing. However, IEEE 802.11n does not provide a reliable multicast service. In the multicast scenario, we have the problem of heterogeneity among receivers since each user have different channel conditions. In order to increase data rate and range without any increase in transmit power, multiple antennas at the receivers is proposed. A WLAN span a small geographic area, typically a single building or a cluster. A transmission from one AP is receiving by all the users of the network. Therefore, in a rich scattering environment, a single multicast group is implemented. Different schemes are introduced for multicast, which make use of the request to send (RTS) and clear to send (CTS) hand shaking to eliminate hidden-station problem [47-48]. In [49] the maximum theoretical throughput in MAC layer would be increased up to 85 per cent for any number of stations when not using RTS/CTS. Clearly, the channel busy status in CSMA protocol can be caused by neighbouring APs transmitting simultaneously. In order to eliminate contention periods and collisions, frequency allocation method is proposed. We analyse a new frequency allocation technique for keeping interference to an

acceptable level, taking into account that there is no coordination among APs. In unicast schemes, the destination station will send back an Acknowledgment (ACK) if the packet has been received without error. For multicasting, IEEE 802.11 does not support a reliable handshaking. If we guarantee a minimum SINR for all receivers, we achieve reliable data exchange. With these ideas in mind, we design a downlink multicast transmit beamforming minimizing the total transmit power and thus leakage in vicinity, subject to providing at least a prescribed received SINR to each intended receiver. From the set of fixed number of available channels using by APs and users, we select the channel that gives the minimum transmit power after beamforming optimization. The key feature of the proposed algorithm is that allows multiple interfering multicast IEEE 802.11n WLANs to select their operating frequency and forming their beams in a way that interference is minimized. APs are able to assess the radio environment and adjust their configuration appropriately. In addition, the low efficiency of Power Amplifier(PA) for OFDM system results high linearity and par consequence spectrally efficient modulation which lead to even less adjacent channel interference.

The chapter is organized as follows. The next section analyzes multicast optimization without interference. In section 6.2, we present our self-configure algorithm. In section 6.3, we evaluate simulation results.

6.1 Optimization without co-channel interference

On purpose to keep cost down and ease backward compatibility, it is proposed the reusage of legacy technologies such as Orthogonal Frequency Division Multiplexing (OFDM) and Quadrature Amplitude Modulation (M-QAM). PHY layer multicasting has been study from prior works for a frequency flat channel [35-36]. Our design is developed for an OFDM system, using multiple antennas at the receiver as in IEEE 802.11n.

When high-speed data is transmitted, OFDM is used to combat frequency selective fading channel. It is a multi-carrier transmission technique, which divides the available spectrum into many sub-carriers, each one being modulated by a low data rate. The transmit signal propagates via different paths caused by reflections of the radio waves from the surround. This is called multipath propagation. Each of the multipath components has different relative propagation delays and attenuations which, when summing up in the receiver, results in filtering type of effect on the received signal where different frequencies of the modulated waveform are experiencing different attenuations and phase changes. This is termed frequency –selective fading. Coherence bandwidth is the range of frequencies over which the channel considered flat, meaning that all frequency components experience similar behavior. When bandwidth of transmit signal is smaller than coherence bandwidth the channel possesses a constant gain and linear phase response. Frequency

selective fading channel is usually modeled as the sum of several flat fading channels with different delays. Antenna arrays form beams to detect or emit signals at directions of interesting paths (spatial filter). Adaptive beamforming to different sub-channels, only the gain of the antennas weights are changed according to attenuation factor. Beamforming acts in spatial domain, where spatial beams are formed . Par consequence, we minimize total transmit power subject to providing at least a prescribed SINR at each receiver, for the sub-channel with minimum gain. Simultaneously this power guarantees the above constraints for all others sub-carriers with greater gain.

Let's study a system with a single AP and K receivers. We indicate with I_{SC} the set of indexes corresponding to the subcarriers. Consider a MIMO system with M_t Tx antennas and M_r Rx antennas. Denoting $\mathbf{H_k^n}$ an M_rxM_t matrix whose entry (i, j) is the complex flat-fading coefficient at subcarrier $n \in I_{SC}$ between the jth transmit antenna and ith receive antenna for user k. From basic properties of linear algebra, every matrix $\mathbf{H_k^n}$ can be factorized by its singular value decomposition (SVD)

$$\mathbf{H_k^n} = \mathbf{U_k^n D_k^n (V_k^n)^H} \quad (6.1)$$

The subcarrier $n_{min}(k)$, which corresponds to weakest gain at each user k, is taken from

$$n_{min}(k) = \arg \min_{n \in I_{SC}} \sum_{i=1}^{q_k(n)} D_k^2(n)\,[i,i] \quad (6.2)$$

$$\forall k \in \{1, 2 \ldots, K\}$$

Therefore, each user is characterized from a subchannel $\nu_k = n_{\min}(k)$ with $\nu_k \in \{1, 2 \ldots, N\}$. Finally, we define the set $I_{\min} = \{\nu_1, \nu_2, \ldots, \nu_k, \ldots, \nu_K\}$.

The separability of the MIMO channel relies on the presence of rich multipath which needs to make the channel spatially selective. Under these conditions, it's possible to transmit min(M_t,M_r) independent data streams simultaneously over the eigenmodes of a matrix channel $\mathbf{H}$. Clearly, the rank of **H** is always both less than the number of Tx antennas and less than the number of Rx antennas. In order to receive scattering energy from all reflected paths and consequently achieve higher reception diversity gain, we apply to our design the rows of $\mathbf{U^H}(\nu_\mathbf{k})$ as weights at each i element of the received array with i=1,2,…,M_r. Reference training sequences are transmitted from AP in 4 pilot tones to estimate the channel matrix $\mathbf{H_k^n}$. The location of pilot carriers is : l=-21,-7,7,21. User k measures subchannel matrice $\mathbf{H}(\nu_\mathbf{k})$ and send it to AP through MIMO channel Mesurement frame defined in 802.11n.

Basic OFDM philosophy is the low cost. Discrete Fourier Transform (DFT) replaces the banks of sinusoidal generators and par consequence the implementation complexity of modem is reduced. The sub-carriers are not individually filtering nor amplifying. Therefore, the beamformer must multiply

by the same complex weights all sub-channels. We treat the problem by transforming the frequency selective channel into a frequency flat channel describing propagation loss and phase shift by $\mathbf{H}(\nu_\mathbf{k})$ with $\nu_k \in I_{\min}$. We have assumed that channel impulse response changes at a rate much slower than the transmitted baseband signal. If Rx matrix is $\mathbf{U}(\nu_\mathbf{k})$, $\mathbf{v}$ N_t x1 is the applying beamforming weight vector to M_t antenna elements then the received power is

$$P(\nu_k) = \left|\mathbf{U^H}(\nu_\mathbf{k})\mathbf{H}(\nu_\mathbf{k})\mathbf{v}\right|^2 \quad (6.3)$$

If the noise is zero mean with variance σ_k^2 then noise power is $\sigma_k^2 \left\|\mathbf{U}(\nu_\mathbf{k})\right\|^2$. Given $\mathbf{U}(\nu_\mathbf{k})$, the pose problem is to generate an optimal downlink beamforming at AP, minimizing at the same time the total transmitted power and guarantying prescribed SNR constraint γ for all users.

$$\begin{aligned} Q6 \qquad & \min \|\mathbf{v}\|_2^2 \\ \text{s.t.} \qquad & \frac{\left|\mathbf{U^H}(\nu_\mathbf{k})\mathbf{H}(\nu_\mathbf{k})\mathbf{v}\right|^2}{\sigma_k^2 \left\|\mathbf{U}(\nu_\mathbf{k})\right\|^2} \geq \gamma \\ & \|\mathbf{U}(\nu_\mathbf{k})\|^2 = 1 \\ & \forall k \in \{1, 2, \ldots, K\} \\ & \forall \nu_k \in I_{\min} \end{aligned}$$

This problem was found NP-hard for general channel vector and should be solve as $\mathcal{Q}5$ in section 5 if noise dominates he terms of interference from the same network and others networks.

Beamforming optimization problem $Q6$ can easily become infeasible. In this situation, scheduler calculates using (6.2) the minimum $n_{min}(k)$ for all $k \in \{1, 2 \ldots, K\}$ and

- Drop the user k (admission control) if scheduler policy is the maximum throughput.
- Remove subchannel n_{min} if scheduler policy is the maximum number of users that can be served (fairness).

6.2 Channel band selection

Consider a geographical area where there is a set A of available APs. AP $a \in$ A has to select an operating frequency channel $f_a \in$ C. If $P_k(f_b)$ is the interfering power at channel f_b, measured from user k when AP a is silent,

$$P_k(f_b) = \left|\mathbf{U^H}(\nu_\mathbf{k})\mathbf{H_k}(\mathbf{f_b})\mathbf{v_b}\right|^2 \quad (6.4)$$

$\mathbf{v_b}$ is the N_tx1 beamforming weight vector applied to AP b. In practice, the power $P_k(f_b)$ is calculated using Dynamic Frequency Selection (DFS) technology. As aforementioned, we estimate the channel

f_b by inserting pilot symbols with known modulation at equal spaced locations in frequency domain. Each user scans for listening every channel at the four pilot tones and measures the Received Signal Strength Index (RSSI). In order to estimate $P_k(f_b)$, we average the RSSI of the four pilot tones. These measurements -channel frequency f_b and interference power $P_k(f_b)$- in the vicinity are reported from user k to AP a. According to what has been described, problem $\mathrm{Q6}$ is reformulated as

$$\begin{aligned} &\mathrm{Int6} && \min \|\mathbf{v_a}\|_2^2 \\ &\text{s.t.} && \frac{\left|\mathbf{U^H}(\nu_\mathbf{k})\mathbf{H}(\nu_\mathbf{k})\mathbf{v_a}\right|^2}{\sigma_k^2 \|\mathbf{U}(\nu_\mathbf{k})\|^2 + \sum_{f_b} \left|\mathbf{U^H}(\nu_\mathbf{k})\mathbf{H_k}(\mathbf{f_b})\mathbf{v_b}\right|^2 \mathrm{I}\,(f_a, fb)} \geq \gamma \end{aligned}$$

$$\|\mathbf{U}(\nu_\mathbf{k})\|^2 = 1 \qquad \forall k \in \{1, 2, \ldots, K\}$$

$$\forall \nu_k \in I_{\min} \forall \nu_k \in \{\nu_1, \nu_2, \ldots, \nu_K\} \qquad \forall f_b \in \{1, 2, \ldots, F\}$$

Equation (6.2), which finds sub-carrier, $\nu_{min}(k)$ is modified as

$$n_{min}(k) = \arg \min_{n \in I_{SC}} \frac{\sum_{i=1}^{q_k(n)} D_k^2(n)[i,i]}{\sigma_k^2 + \sum_{f_b} \left|\mathbf{U^H}(\mathrm{n})\mathbf{H_k}(\mathbf{f_b})\mathbf{u_b}\right|^2 \mathrm{I}\,(f_a, f_b)} \quad (6.5)$$

$$\forall k \in \{1, 2 \ldots, K\} \qquad \forall f_b \in \{1, 2 \ldots, F\}$$

Let's $P_{TX} = \|\mathbf{v_a}\|_2^2$ is the transmitted power of AP a, computing from problem $\mathrm{Int6}$. Our proposed solution focuses on selection a channel f_a that minimize $P_{TX}(f_a)$ for all possible operating channels.

$$f_c = \arg \min_{\{f_a \in \mathrm{C}\}} P_{TX}\,(f_a) \quad (6.6)$$

When the number of users K is too big, received interference for a few users is strong and/or SINR targets are too high, problem Int can easily become infeasible. In this situation, we remove the user k with minimum $\nu_k = n_{\min}(k)$ computing from equation (6.6).

6.3 Performance Evaluation

For validation reasons, we apply the proposed algorithm in a configuration with F=4 channel reuse in 5GHz spectrum. Specifically, the settings correspond to a network that consists of 5 cells non overlapping as in fig. 6.1. Each cell is represented by a circle radius R and served by an AP at the centre of the cell. The distance between two AP is D=2R+d. One possible assignment of four channels to APs is: AP_2 to channel 1, AP_3 to channel 2, AP_4 to channel 3 and AP_5 to channel 4. The channels of neighbouring APs are separated by gaps of 3,2 and 1 intervening channels. Our proposed technique in section 6.3 enables self-configuration of channel assignment to AP1 based on measurement of channel conditions in the wireless environment. The goal is to minimize the impact between neighbouring APs on users' performance of AP1 by choosing one of four channels.

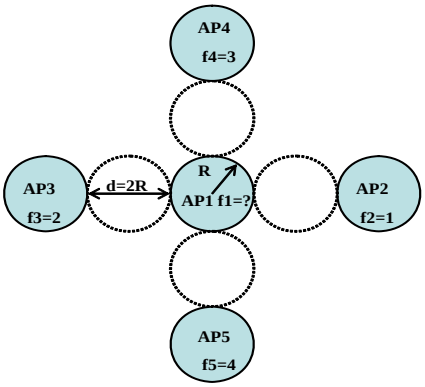

Figure 6.1 Deployment of a configuration

PHY layer modes in 20 MHz channel width with different coding and modulation schemes are present in table 5.1. For bandwidth BW=20 MHz, the noise at the input of receiver is

N(dBm)=10log(KT)+10logBW=-174+73=-101.

K is the Boltzmann's constant and T=290º K is the absolute room temperature. If receiver noise figure is NF=6dB, total noise floor is

N_{floor}=-101+6=-95 dBm.

Minimum sensitivity for each mode requires minimum SINR equal to

SINR(dB)=Sensitivity(dBm)-N_{floor}(dBm)

and is presented in table 6.1. Consequently, the received SINR constraint are set to γ=15dB and the additive power noise σ_k^2=-95dBm.

TABLE 6.1 MINIMUM SNR

Mode	Minimum SNR(dB)
1	15
2	18
3	20
4	23
5	27
6	31
7	32
8	33

At set-up of figure 5.2, the interference signal is an OFDM signal, unsynchronized with regard to reference signal. In table 5.1, adjacent channel rejection is measured by setting the desired signal 3dB above the sensitivity of each mode and raising the power interfering signal until 1% Packet Error Rate (PER)is cause for a payload 4095 bytes. Calculations in section 6.2 are related to minimum SINR equal to 15 dB. Therefore,

$$\mathrm{I}(f_a, f_b) = \begin{cases} 0\mathrm{dB} & \text{for co-channel} \\ -16\mathrm{dB} & \text{for adjacent channel} \\ -32\mathrm{dB} & \text{for other cases} \end{cases}$$

It's important to remark that in IEEE 802.11a, the outer 12 sub-carriers are zeroed in order to reduce adjacent channel interference. Received power and interference power in (6.3) and (6.4) is normalized in relation to transmit power. Therefore, it must be multiply by transmitting power of AP equal in our case to 500 mW. Cell radius is consider equal to R=100m and distance d=2R=200m. The system simulation is implemented within MATLAB environment. APs consist of M_t=4 transmit antenna elements and users of M_r=4. Antenna array is Uniform Linear Array (ULA) with distance between elements equal to λ/2. IEEE 802.11n channel model B in NLOS conditions is used to simulate channel matrices [23]. Multicast beamforming example is consider for AP_1 to AP_5 with K=16 downlink users for each cell. Due to approximation of numerical results, we realize 100 Monte Carlo runs for different locations of users in the cell of AP_1. For the interference cells 2 to 5, a constant location is taken. At each location, 107 interpolated samples are collected for a time varying channel due to Doppler effect. If we take the speed of moving scattering environment equal to v_o=1.2Km/h, maximum Doppler shift is $f_m=v_of/c$ = 208Hz. Coherence time due to Doppler spread is $T_c \approx 1/f_m$=40808 μs, that is, 1000 times slower that the transmitted OFDM symbol. At each run, 1000 Gaussian randomization samples to solve rand C problem are generated.In our analysis, contention periods and collisions within the MAC operation are eliminated.

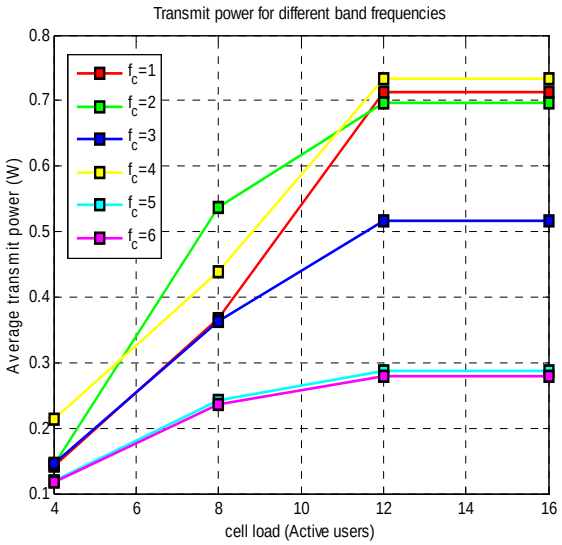

Figure 6.2 Calculated transmitted power for 6 channels vs number of active users

Figure 6.2 shows the average transmitted power in Watt as function of active users for channels 1 to 6. In our network deployment, we remark that the calculated power for channel 1,2 and 4 excess the

maximum value of 500mW and par consequence, these channels does not be accepted from 8 to 16 active users. If our standard supports F=4 channels, our algorithm gives for channel 3 average power approximately equal to 0.5W for 12 and 16 active users. If the number of available channels defined by standard is F=6, then channel 5 or 6 is assigned to AP_1. Figure 6.3 depicts variation in time of transmitted power, calculating for optimum channel 3. In our simulation, we consider that maximum instantaneous power is 2W. The range of emitted power is between 0.4 and 0.7W. Our solution can contribute to reduce non-linearity effect and facilitate the design of RF power amplifier. Let's remember that M-QAM is a linear modulation. Figure 6.4 presents the throughput per user when channel 3 with transmitted power 500mW is selected. In this study, SNR_k^n for user k at sub-carrier n follows Gaussian distribution with mean value computing from simulation for flat frequency channel and standard deviation 3 dB as in [40]. Figure 6.5 shows the number of rejected users, when the optimization algorithm for our configuration can not find a feasible solution.

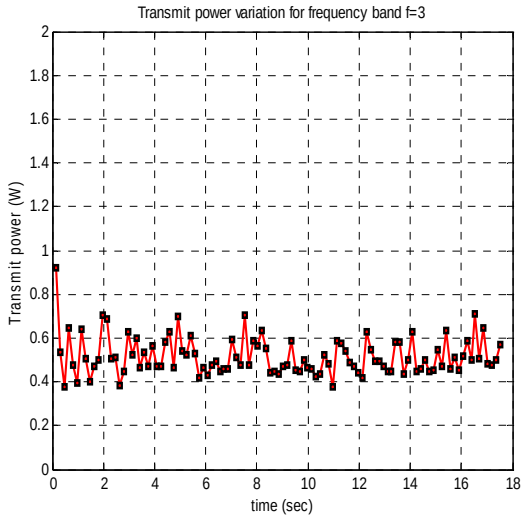

Figure 6.3 Variation of transmitted power in time

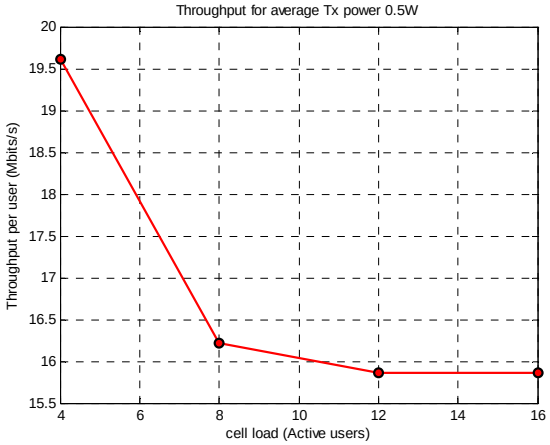

Figure 6.4 Throughput vs cell load

Figure 6.6 shows the average physical layer data rate per user for different users while figure 6.7 presents average PHY data rate versus number of users for a single WLAN. Our propose scheme for beamforming and frequency assignment optimization is compare with a WLAN 802.11n and 802.11a both without cross-layer information. Simulation results in figure 6.6 and figure 6.7 are taken assuming that channel is flat for entire band. We remark that the first technique achieves a noticeable improvement. Figure 6.8 and figure 6.9 compare the two scheduling techniques proposed in section 6.1. The two techniques are equivalent up to K=36 users.

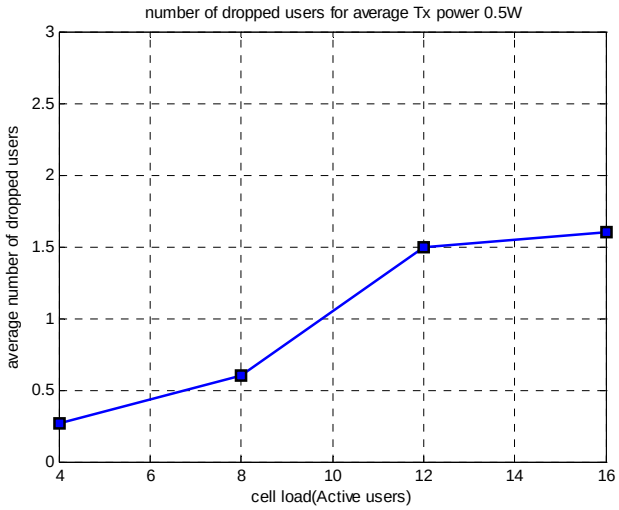

Figure 6.5 Number of dropped users vs cell load

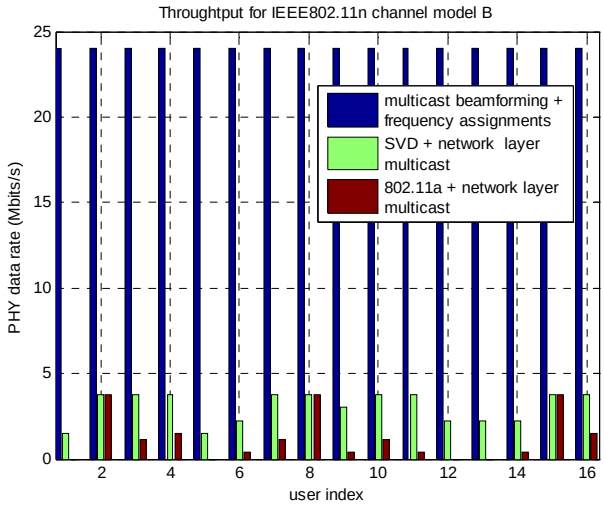

Figure 6.6 Throughput for different users

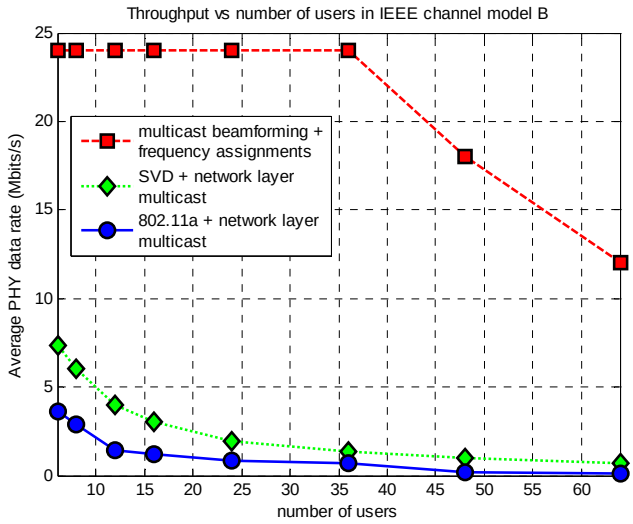

Figure 6.7 Throughput versus number of users

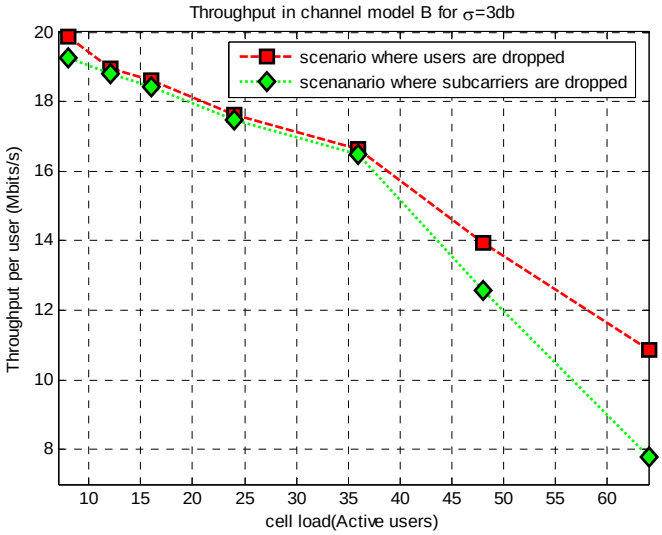

Figure 6.8 Thrroughput per user vs cell load

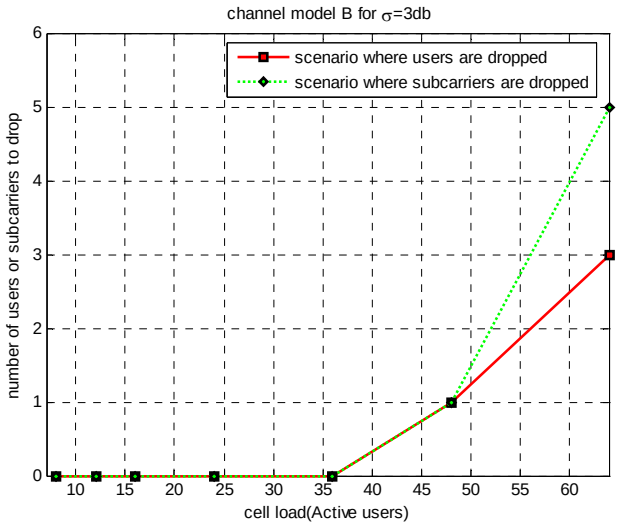

Figure 6.9 Number of removed users or subcarriers

6.4 Conclusions

We have investigated the efficiency of a self-configure algorithm that can be deployed in a multicast IEEE 802.11n AP. The proposed algorithm use local measurement from all interfering WLANs in order to AP selects a channel. We simulate a scenario with strong interference environment. We experience advantages in power efficiency of the power amplifier and bit rate. These advances are related to the use of unlicensed spectrum and multimedia applications.

Chapter 7

On the applicability of steerable Base Station Antenna Beams in IEEE 802.16m Networks with high user mobility

In case of high user speeds, limited (and probably unreliable) channel knowledge is available at the Base Station (BS). Distributed sub-carrier allocation is the default radio resource allocation configuration of IEEE 802.16e networks. It may have the form of either Full Usage of Sub-Channels (FUSC) or Partial Usage of Sub-Channels (PUSC). In FUSC, all sub-carriers are allocated in one cell or sector, while in PUSC only a set of sub-carriers is allocated to reduce interference between neighbouring cells. These schemes provide frequency diversity and perform well in mobile environments. The Adaptive Modulation and Coding (AMC) permutation scheme enables beamforming design and require the knowledge of Channel State Information (CSI) at the BS. AMC is based on grouping of adjacent sub-carriers and provides better protection against fading and interference but is expected to support low speed mobility classes (from stationary to pedestrian).

TABLE 7.1 EXAMPLE OF USERS DISTRIBUTION

Pedestrian	3 Km/h – 60%
Vehicular	30 Km/h – 30%
High speed Vehicular	120 Km/h – 10%

Table 7.1 gives a distribution of users in any given cell of a network in a metropolitan area [50]. From this it is apparent that moderate to high-speed users are a substantial part of the whole cell population, therefore suitable techniques are required to support fast moving users. For this reason, the emerging IEEE 802.16m [51] aims at defining an air interface that can support higher speeds with reasonable degradation to achieve higher spectral efficiency and significantly improve the coverage compared to the current 802.16e system, maintaining backward compatibility.

The objective is to develop a novel technical solution for IEEE 802.16m networks that consists of joint beamforming, feedback design and scheduling in order to improve the system performance. These three mechanisms are closely coupled. The performance of the system depends on the CSI accuracy that is provided through feedback as well as the on the fading rate of each user. In a multi-user Time Division Duplexing (TDD) system, beamforming design could increase the capacity, assuming that the knowledge of CSI is available at the transmitter side. For higher mobility cases, the existence of a feedback delay from the user to the BS degrades the performance rapidly due to outdated and thus mismatched channel quality information. If the radio channel is varying fast, it can be easily understood that any kind of scheme that requires a small amount of channel feedback

information will outperform a coherent beamforming scheme that requires the knowledge of the full instantaneous channel vector.

Multi-user diversity is a form of diversity provided by independent channels across different users. The overall system throughput is maximized by allocating the common channel resource to the user who can optimally exploit it. In [52], opportunistic beamforming artificially induces time fluctuations in the channel to increase the multi-user diversity. In this case, only a single user is scheduled at each time and thus one of the spatial degrees of freedom is being used. Each user k feeds back the overall received Signal to Noise Ratio (SNR) of its own channel to the BS. The gain from multi-user diversity is related to power because the SNR of the user being scheduled is "boosted" accordingly. In reality, the statistics for the channels experienced by different mobiles are not similar due to different distances from the BS, shadowing effects and scattering. It's possible that some mobiles have always better channel conditions than others. The scheduler may not schedule a particular user until its channel conditions are favorable. This causes increased scheduling latency or jitter for the user and leads to unfair resource allocation. One salient feature of the IEEE 802.16e standard is the definition of Quality of Service (QoS) classes, which imposes stringent latency constraints. The scheduler may be forced to schedule the user even when the channel conditions of the user are not favorable, which leads to limited multi-user diversity gain. In [53] an opportunistic Space Division Multiple Access (SDMA) - based scheduling scheme employing multiple orthogonal beams to serve multiple users simultaneously in each slot is proposed. Different low complexity combining techniques are proposed for improving the effective Signal to Interference plus Noise Ratio SINR. The beams are formed without any knowledge about the position of the users. Therefore, channel quality feedback is not necessary for constructing beams (compared to the completely adaptive systems). Following this logic, steerable beams provide a significant range extension and considerable multipath and interference rejection. The BS schedules data transmission by exploiting partial feedback on the minimum SNR per user per sub-carrier. Predicting the downlink SNR at the BS appears to be a challenging task. The necessary number of predictor coefficients is relatively high.

The communications literature has significantly discussed the capacity increase that can be achieved by using scanning beams not linearly but randomly, a technique also named as opportunistic beamforming. Previous such works have been mainly focused on stationary users. The main contribution of this chapter is to propose a MIMO-SDMA-OFDMA downlink system supporting high speed users with stringent QoS requirements. Also, the combination of steerable beams with next generation WiMAX technology is proposed. In order to support higher user throughputs in each BS, the coverage area within each cell is assumed to consist of multiple beams, orthogonal to each other at the same time (SDMA technique). Transmissions are scheduled to far more users as there are more

beams at each time slot at the penalty of increased system complexity (required to support these beams). In the IEEE 802.16e standard, a large number of sub-carriers (e.g. 2048 or 1024) are usually assumed. In order to reduce the amount of feedback, the feedback scheme proposed in [54] is assumed. N sub-carriers are divided into Q clusters of R sub-carriers each so that N=Q R. For low speed users, the channel varies slowly. Therefore a large number of clusters is selected to achieve optimum performance. At high user speeds, only a representative SNR of a small number of clusters or for one cluster (representing all sub-carriers) is sent back because the fast variations of the channel make the large amount of feedback scheme unreliable and yield a mismatch between estimated and instantaneous channel gains. The efficiency of the proposed solution is studied by simulations employing the WINNER II channel model [24]. Figure 1 presents an overview of our proposed technique for evaluation

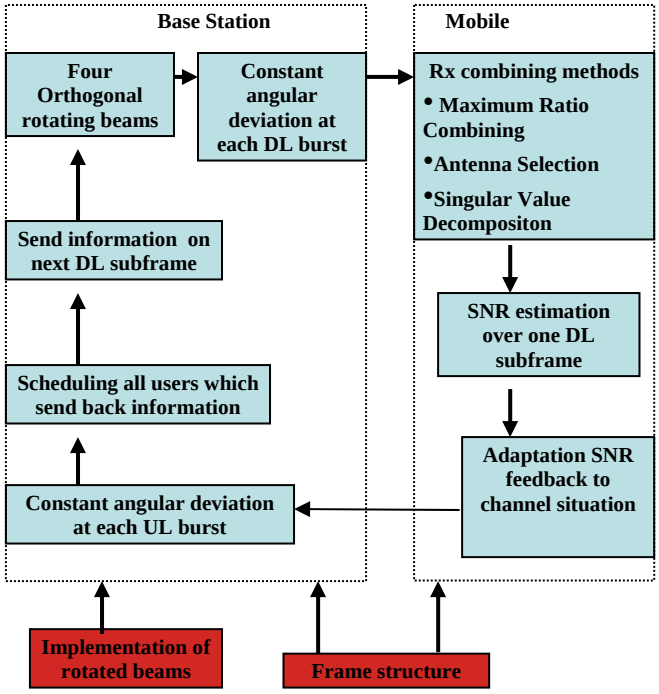

Figure 7.1 Our proposed cross-layer (physical layer-MAC) design

This chapter is structured in the following way: The beamforming pattern is presented in section 7.1. The combining techniques at the receiver are explained in section 7.2. Section 7.3 introduces the feedback schemes. Section 7.4 discusses the required frame adaptation to accommodate the rotated beams. In Section 7.5 the scheduling strategy is described. Section 7.6 gives an overview of the simulation model and section 7.7 presents the performance results .

7.1 Beamforming pattern

A downlink multi-user MIMO-SDMA system with M_t=4 transmit antenna elements at the Base Station (BS) and M_r=4 received antenna elements at each user terminal is considered. Therefore, the maximum number of orthogonal beams is equal to M_t=4, i.e., M_t=4 users can be simultaneously scheduled in each sub-carrier. The hexagonal cell is divided into four service areas S_i, i ∈ {1,2,3,4} as shown in figure 7.2. The BS constructs M_t orthogonal rotating beams $\mathbf{W_i} \in C^{Nt\ x1}$ for i = 1,…..,M_t in order to scan all the cell area. Employing limited feedback requires cooperation between the BS and the users .A general overview for a narrowband system is illustrated in figure 7.3

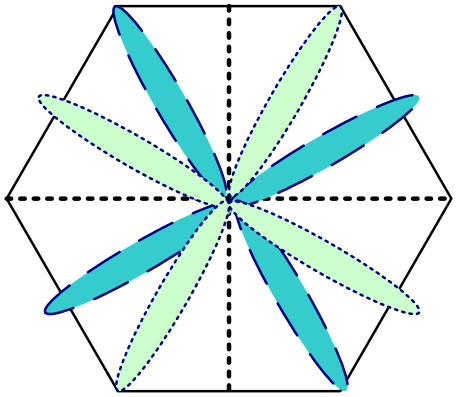

Figure 7.2 A hexagon cell can be scanned from four orthogonal and narrow beams

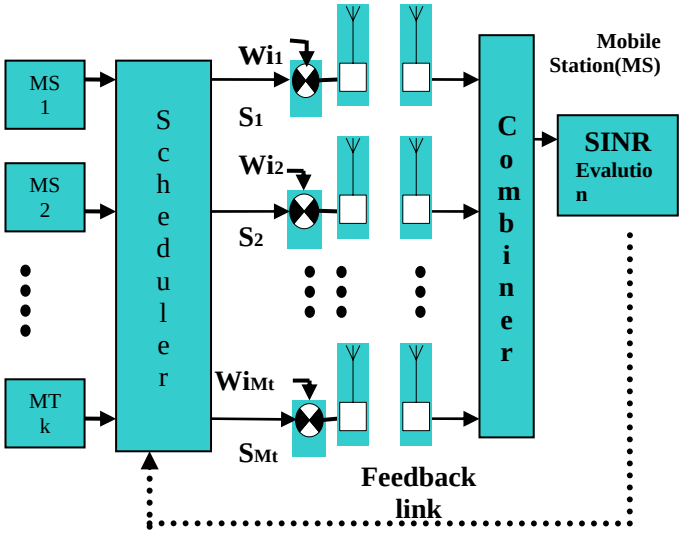

Figure 7.3 MIMO system model with limited feedback

OFDM divides a large band into small narrowband channels using an orthogonal transformation. Therefore, the block diagram of figure 7.3 which is specified for a flat-fading channel could be easily extended to a frequency –selective channel by assuming OFDM. For reasons of simplicity we will evaluate the beamforming technique for a narrowband channel which experiences flat fading because

it can be used successfully for a MIMO-OFDM system. The minimum time-frequency resource that can be allocated is a slot that consists of a group of subcarriers over one or several OFDM symbols. Let $\mathbf{W_i}=[w_{i1},w_{i2},\ldots.w_{iMt}]$ the orthogonal beamforming vector M_t x 1 applied at the BS with M_t antenna elements. During the m-th slot, the beamforming vector applied at the BS $\mathbf{W_i(m)}$ with i={1,2,3,…..M_t} is constant. In the case where the BS antennas have fixed broad-beam coverage, interference within the wide beamwidth cannot be discriminated. Co-channel interference from neighboring beams is a fundamental limiting factor on the capacity that is also affected by channel dynamics linked to high mobility. Excessive transmit power does not improve system performance but only adds to the unnecessary co-channel interference. The magnitude of the composite channel response $|\mathbf{h_{ik}}|$ -$\mathbf{h_{ik}}=\mathbf{H_k}\ \mathbf{W_i}$ is the projection of beam $\mathbf{W_i}$ on the channel $\mathbf{H_k}$ - is maximized when the receiver antenna gain is aligned to the optimum value

$$\mathbf{U_k^{opt}} = \frac{\mathbf{h_{ik}}}{\|\mathbf{h_{ik}}\|} \quad (7.1)$$

the SNR computed at the receiver $k \in S_i$ is

$$SNR_{ik} = \frac{\left|\mathbf{U_k^H h_{ik}}\right|^2}{\|\mathbf{U_k}\|^2 \sigma_k^2} \quad (7.2)$$

It's difficult for the mobile to feedback the optimal gain at each sub-carrier due to the large amount of feedback information that this entails. In opportunistic beamforming the BS simply varies the antenna gain and the mobile report their resulting time-varying SNRs. A mobile will experience a relatively high SNR when the randomly varying antenna gain happens to align closely to the optimal beamforming gain of the user. In order to solve the problem of scheduling latency, we align as much as possible the optimal beamforming gain for all users by scanning narrow wide beams not randomly but linearly from direction 0° to φ_{max} to cover all the area of interest.

Consider that the BWA system contains a sectorized cell grid. Each cell consists of four sector areas S_i, i ∈ {1,2,3,4} . All the available bandwidth is allocated to each sector. The sector area S_i is divided into N_B sub-areas of equal size ΔS (a grid of N_B beams). A narrow width beam is rotated to scan the whole area S_i=360°/4=90°. A conventional beamformer is a simple beamformer with all its weights having equal magnitudes. The phases are selected to steer the antenna array in a particular direction φ_0 , known as the "look direction". Beamforming is assumed to remain constant during each slot which is the scheduling time interval. The array weights for the direction of the main lobe φ_{0i} in the area S_i are given by

$$\mathbf{w}_{\phi_{0i}} = \frac{1}{\sqrt{M_t}}\left[1, e^{i2\pi d/\lambda \sin\phi_{0i}}, \cdots, e^{i2\pi(M_t-1)d/\lambda \sin\phi_{0i}}\right] \quad (7.3)$$

where d is the distance between adjacent antenna elements in a Uniform Linear Array (ULA) and λ is the carrier wavelength. The angle of the steering beam φ_{0i} increases linearly in time

$$\varphi_{0i}(t)=\varphi_{init,i} + \Delta\varphi\ t \quad t=1,2,\ldots\ldots N_T \qquad (7.4)$$

$\varphi_{init,i} \in \{0°,90°,180°,270°\}$ is the initial value of φ_{0i} and depends on the sector area S_i that will be scanned, $\Delta\varphi$ is the angle increment and N_T the period of the beamforming process.

In a metropolitan area, no complete Line of Sight (LoS) propagation exists between the BS and the vehicle. The BS is mounted above rooftops to reduce the near field scattering. The LoS path is attenuated due to the appearance of diffraction at the first obstacle. The reflected signals, originated from local scatters near to the mobile, are received at a comparable power level to the attenuated direct path signal. If transmission occurs at one desired direction, multi-path power can be collected by users which are located at different directions. Therefore, the period of scanning N_T can significantly be reduced if the users in other directions receive the multi-path power. Multi-path power is not considered as interference. Furthermore, one user can be allocated to more than one steering beams during one period of scanning (a user may receive two different beams that have different directions). Consequently, data latency could be reduced. Scanning methods use electronically steerable array antennas in order to cover the surrounding area. Each sector with 90° or 120° angular width can be served by 4 to 8 narrow beams. If the signal phases in a linear array vary, the constructed beam can be steered. In an electronically steered array, programmable electronic phase shifters are used at each antenna element.

By programming the required phase shift value for each element, the antenna is steered. Different approaches can be used. The Butler matrix is one of the most popular switched beam methods [55]. An N x N Butler matrix produces N beams looking at different directions with an N- element array. A number of $N/2\log_2 N$ 90° hybrids are interconnected by rows of $N/2(\log_2 N-1)$ fixed phase shifters (the passive components required). A 4x4 Butler matrix array is shown in figure 7.4. For example, if the 1L input port is excited by an RF (Radio Frequency) signal, all the output ports feeding the four array elements are equally excited but output A1 presents a phase shift of 45°, A2 of 90°, A3 of 135° and A4 of 180°. This results in the radiation of the beam at a certain angle. Therefore, it's easy to implement with a few components a beam switch at a BS with four antenna elements. Four different beams at different times are produced by applying four different delays at the RF (Radio Frequency) signal. The insertion loss involved in hybrids, phase shifters and transmission lines is very small. An additional advantage is the easy integration with the existing architectures in the BS, since only the replacement of the RF front-end is needed. The proper input port is chosen using digitally controlled MMIC switches. In the WiMAX market, baseband architecture using Digital Signal Processing

(DSP) for implementing beamforming can be chosen. This configuration increases the flexibility but this advantage is offset by the high power consumption since N transmitters (RF/IF/baseband stages) operate in parallel. Additionally, the cost and the size of the BS are increased.

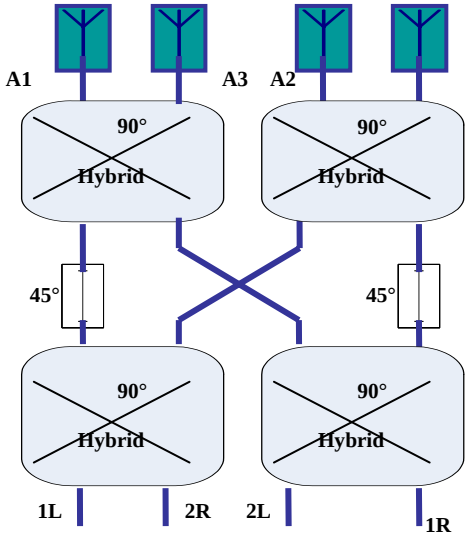

Figure 7.4 4x4 Butler matrix

7.2 Combining techiques at the receiver

In general, the requirement for compact mobile terminals severely limits the number of antennas that can be implemented in them. In IEEE 802.16e standard, $M_r = 2$ or $M_r = 4$ with $d = \lambda/2$. In this work, signals received from two or four antenna elements of each mobile are linearly combined to improve SNR because BS schedules simultaneous data transmission in multiple beams by exploiting limited feedback on the effective SNR.

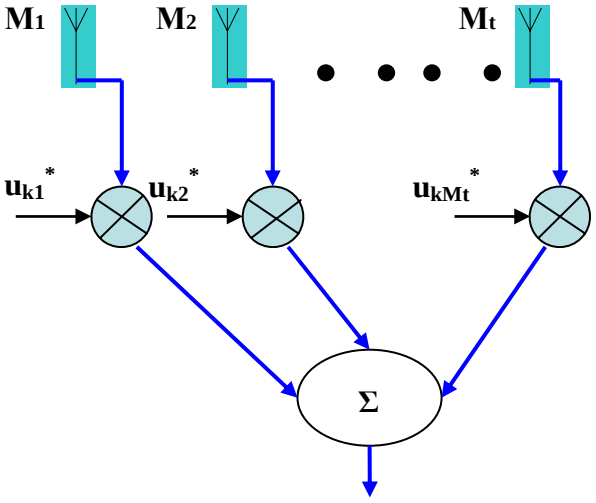

Figure 7. 5 Combining strategy

A linear combiner $\mathbf{U_k} = [u_{k,1}, u_{k,2}, ...u_{k,M_t}]^T$is degnined at the receiver in order to estimate the transmitted symbols as is illustrated in figure 7.5. In [56] the mobile station adopts Minimum Mean Squared Error (MMSE) receiver to exploit spatial multiplexing gain. The common channel is allocated to more than one users simultaneously.

Due to separate layers, this scheme requires additional amount of feedback. In [57], the BS generates the precoding matrix ($\mathbf{V_0}$) in a controlled but pseudorandom fashion. The mobile k multiplies the received signal by the left singular matrix ($\mathbf{U_k^H}$) of the channel matrix

$$\mathbf{H_k} = \mathbf{U_k}\mathbf{\Sigma_k}\mathbf{V_k^H} \qquad (7.5)$$

This scheme results in unwanted self – interference when the channel is not near its peak conditions ($\mathbf{V_k} \neq \mathbf{V_0}$) . In our case, the vector $\mathbf{u_{1k}^H}$ - i.e. the first column of matrix $\mathbf{U_k^H}$- corresponds to the strongest propagation mode and the users must not deviate from their respective peak conditions in order to achieve good SNR. It has been shown that Optimum Combiner (OC) and Maximum Ratio Combiner (MRC) strategies outperform the Antenna Selection (AS) technique, when a limited number of users are served in opportunistic schemes with multiple beams [58]. The asymptotic approach is studied in [59] with asymptotically large number of users ($K \to \infty$). The optimal properties are obtained by scheduling the antenna with the largest SINR (AS).

In MRC method, the antenna is aligned to the direction of h_{ik} defined in (7.1). By combining (7.1) and (7.2), the SNR over the beam i at the user k is

$$SNR_{ik}^{MRC} = \frac{\|\mathbf{h_{ik}}\|^4}{\|\mathbf{h_{ik}}\|^2 \sigma_k^2} \qquad (7.6)$$

According to the OC technique, the optimum value $\mathbf{\Delta X_i} = \mathbf{X_i} - \hat{\mathbf{X}}_\mathbf{i} = \mathbf{X_i} - \mathbf{H_k}\hat{\mathbf{S}}_\mathbf{i}$ of the squared estimation error is found, taking account that the system is domonated by interference, e.g. $\sigma_k^2 \to 0$. In our study, four orthogonal beams are presented at each time instant and therefore intracell interference is negligible compared to additive noise. The system is interference free and the OC method cannot be applied. In the AS technique, for each beam i, the receiver measures separately the SNR at each single antenna. Then the antenna branch with largest SNR is selected. Let‘s assume that the first antenna gives the maximum SNR. The linear combiner vector is $\mathbf{e_1} = [1, 0, ...0]$ and the SINR is equal to

$$SNR_{ik}^{AS} = \frac{|\mathbf{e_1}\mathbf{h_{ik}}|^2}{\sigma_k^2} \qquad (7.7)$$

7.3 SNR feedback

OFDMA exploits the fact that different users experience different amount of fading at a particular instant of time and schedules efficiently the data subcarriers to the users. The most important feature of OFDMA is its capability of exploiting the Multi-user Diversity in order to increase system throughput. An important practical issue is the feedback load. Since a large number of sub-carriers (e.g. 2048 for IEEE 802.16m) is used, feeding back full CSI at the transmitter is prohibitive. For a channel with frequency selective fading, the frequency dimension can also be used to schedule the users. Additionally, multiple antennas increase the number of channel state parameters. The feedback load in a MIMO system generally grows with the product of the transmitter and receiver antenna elements, the number of users while throughput increases almost linearly. In our case, we have four transmit and four receive antennas and therefore the complex channel matrix $\mathbf{H_k}$ is described by 32 parameters (4x4 coefficients for gain and 4x4 for the delay).

To reduce the amount of feedback from the users to the BS, we divide the N sub-carriers into Q clusters of R sub-carriers each. Each user feeds back information only about the weakest subcarrier of each cluster. The mobile estimates the SNR of the subcarriers in each cluster and sends back to the BS only the index and the respective SNR of the weakest subcarrier for the whole cluster. We consider that the feedback channel is error free and delay free. For cluster c, the minimum SNR per cluster at the receiver $k \in S_i$ for all sub-carrier l is fed back,

$$SNR_{ikc}^{min} = \min_{\{l \in \{m, m+1, \cdots, n\}\}} \{SNR_{ikl}\} \qquad (7.8)$$

We suppose that the first sub-carrier of cluster c is m and the last is n. Having small number of sub-carriers per cluster (Q becomes large), we achieve better feedback accuracy for the R sub-carriers in the cluster but we have large amount of feedback information. Having large number of sub-carriers per cluster (Q becomes small) we reduce the required feedback load, but we increase the risk of users feeding back unreliable information for some clusters and sub-carriers. In practice, we must find an optimum cluster size Q. Intuitively, if the R sub-carriers have a cummulative bandwidth of the same order of the channel coherence bandwidth, the degradation on throughput should be very small. The channel variations over sub-carriers within the same clusters are small and thus we achieve the optimum rate. For each cluster in the downlink direction, the BS schedules all the users that feedback that cluster index.

A possible limited feedback scheme is one where the representative rate at each cluster c is computed and is sent to the BS from all users $k \in \{1, 2..., K\}$.

$$r_{ikc} = \frac{1}{m-n}\sum_{l=n}^{m}\log_2(1+SINR_{ikl}) \quad (7.9)$$

If beam i is assigned to user k allocating subcarriers of cluster c, then the BS will transmit at a rate r_{ikc} in all subcarriers for which the achievable rate is greater than the effective value r_ikc. No transmission will be scheduled on the subcarriers of the cluster where the representive rate is less than the effective value. This may lead to zero subcarrier allocation in the case where a small number of users are served by beam i, due to deep fading and there high mobility. Additionally, when the user feeds back the representive rate, it must also inform the BS about the sub-carriers that can support this rate. Therefore, this information increases the feedback load. The representive rate feedback scheme achieves the same system performance with that of the minimum SNR scheme when the number of clusters Q is appropriately chosen so that there is small variation between the subcarriers in each cluster. A simple configuration includes only the maximum representive rate r_{ikc} of all clusters $c \in \{1, 2, ..., Q\}$.

$$SNR_{ik}^{max} = \max_{\forall c} SNR_{ikc}^{min} \quad (7.10)$$

The user feeds back only the value of the best cluster. It's clear that a number of clusters are not chosen by the users, especially when the number of clusters Q is large. This results a system performance degradation. In terms of total throughput, this scheme is asymptotically optimal as the number of users increase. ($K \to \infty$).

In [56] one bit feedback per user is applied with one antenna element at the BS. Our scheme could be adapted to one bit feedback. The BS sets a threshold SNR_{th} for all users and for all clusters. Each user evaluates a representive SNR_{ikc}^{min} during one slot where the channel is approximatly invariant. User k sends "1" to BS if

$$SNR_{ikc}^{min} \geq SNR_{th} \quad (7.11)$$

for each cluster c when the pilot symbol is received at beam i. Otherwise, a "0" is sent. In case where Q=1, the feedback information is consists of only one bit but the degradation of the total sum rate is remarkable. In [56] the BS selects randomly among users for data transmission. It was shown that the 1-bit algorithm achieves the same capacity as full CSI feedback subject to a judicious choice of the threshold. However, the determination of the optimum threshold is a challenging task. Thus, we propose and evaluate a limited feedback scheme defined in (7.8) that adapts the feedback load according to channel conditions at the least possible expense of system throughput.

7.4 MAC frame description

Several options of mapping OFDM subcarriers to each user are specified in order to support two types of subcarrier permutation: The scattered (FUSC, PUSC, etc) and contiguous (AMC) sub-carrier allocation. Our proposed design exploits multiuser diversity and allocates subcarriers to users based on their frequency response. It purports to provide at each user a group of contiguous subcarriers that maximize the received SNR. Thus, we adopt the contiguous permutation to allocate adjacent subcarriers for transmission based on limited channel feedback information. DL and UL directions have the same mapping.

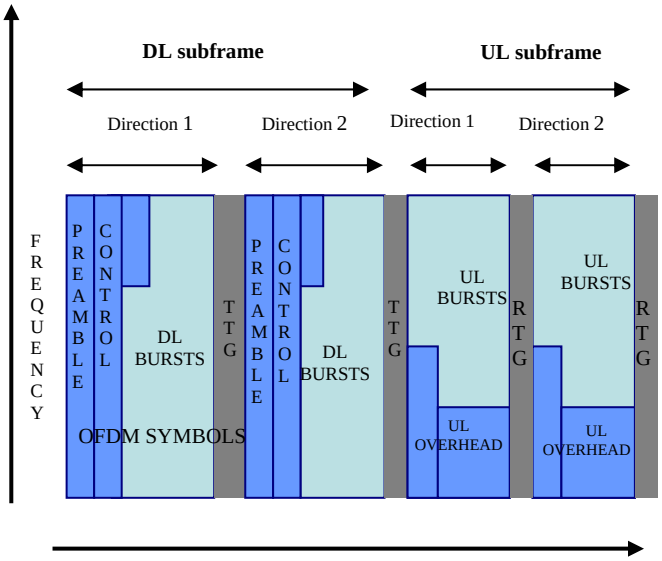

Figure 7.6 MAC frame structure with steerable beams

The DL bursts may be of varying size and type. Although a 5ms frame duration is supported from WiMAX vendors, the frame size can be variable on a frame-by frame basis from 2ms to 20ms. Figure 7.6 shows MAC frame structure when the BS in each cell is enchanced by two steerable beams in directions 1 and 2. The frame has a duration of 5ms and it is divided into N_B=2 DL subframes (DL subframe 1 and DL subframe 2) and N_B=2 UL subframes (UL subframe 1 and UL subframe 2). The DL subframe 1 schedules transmission on the first direction. It's weighted by the linear rotated vector given from (7.3) and (7.4) for t=1. The steered vector remains constant throughout the DL subframe 1. The DL subframe 1 starts with a preamble for synchronization and identification purposes. The control message (FCH, DL MAP,UL MAP) indicates the DL and UL transmission format and resource allocation for the group of downlink/uplink users which are found in the direction 1. Then the mobiles calculate a representative $SNR_{j,k,c}^{min}$ for all clusters c. Each user k sends back this channel information at the UL subframe 1 related to fixed beam $\phi_{0j}(t=1)$. A guard interval is introduced when the direction of the beam changes. The BS transmits DL bursts at the next DL subframe 1 only

to users that send $SNR_{j,k,c}^{min}$ feedback information. The BS doesn't make predictions for SNR on all the subcarriers of each cluster but makes the scheduling according to representative minimum value of SNR. Also, overhead channels at the UL subframe 1, which include ACK feedback, channel quality feedback and the ranging /contention based channel, refer only to users that receive information when the DL subframe is transmitted.

OFDMA/TDMA accommodates the mobiles in both the frequency and the time domain while SDMA in the space domain. Figure 7.7 illustrates how this objective is achieved in the SDMA/TDMA dimension. The SDMA expands the capacity by allowing up to M_t=4 mobile users in each slot and within each slot spatial beams are performed to acquire packets from mobile users. In our design, SDMA expands each frame into M_t=4 space frames, translating into an 4-fold increase of system throughput. Our proposed solution assigns "orthogonal" mobiles to the same slot and thus the spatial resource is efficiently exploited.

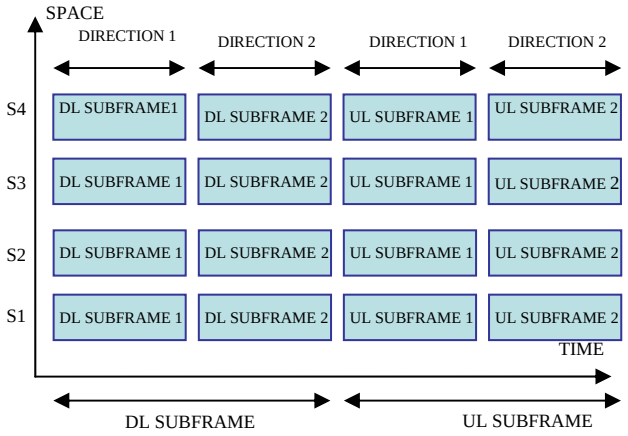

Figure 7.7 MAC frame structure in SDMA scheme

7.5 Scheduling

The cluster allocation scheme subdivides the total bandwidth into Q clusters of R adjacent sub-carriers each. Without loss of generality we suppose that N is a multiple of Q so that each group will have the same number of subcarriers R and $N = QR$. The clusters (instead of sub-carriers) can use one feedback unit each because the subcarriers within a cluster are correlated. The correlation between the subcarriers depends on the cluster bandwidth, channel delay spread, etc. The orthogonality between sub-carriers can be ideally maintained at the receiver in a frequency – selective but time-invariant radio channel. However, in an environment with moving users and therefore time-variant radio channels, the orthogonality between sub-carriers is degraded due to Doppler spread on the different signal paths which results to decreased SNR for the subcarriers. Note that the scheduling in this chapter is related to the mobility of the users and takes fairness into account. A maximum

throughput scheduling would give a greater throughput. In the realistic scenario of table 7.1, only few of the MTs will be highly mobile. Our scheduling strategy is described as the following way:

1. Each user k feeds back information to the BS at each direction of the beam $\phi_{0i}(t)$ with $t = 1, 2, \cdots, N_B$. The mobile users with high velocity send $SNR^{min}_{i,k,c=1}$ as information for channel state, which correspond to the minimum SNR of all sub-carriers ($Q_{highspeed} = 1$). On the other hand, pedestrian or vehicular users send more load information during c frames, e.g SNR^{min}_{ikc} $c = 1, 2, \cdots, Q$.

$$Q_{pedestrian} > Q_{vehicular} > Q_{highspeed} \qquad (7.12)$$

2. The BS constructs a set $\mathcal{C}_k$ of users having feedback information.

3. The number $\#\mathcal{C}_k$ of users which should be allocated is computed.

4. The number of sub-carriers that correspond to each user at each cluster c is

$$n_{c,k} = \lfloor \frac{R_{pedestrian}}{\#C_k} \rfloor \qquad (7.13)$$

If $Q_{pedestrian} = \mu\, Q_{vehicular}$ with μ integer, the information of one vehicular user SNR^{min}_{ikc} is used at μ of $Q_{pedestrian}$ clusters, while the information of high speed users is used at all clusters.

5. Firstly, sub-carriers of mobile users are allocated. For a cluster c, with m mobile users , the allocation of sub-carriers is realized with step

$$\Delta f_c = \frac{R}{n_{c,k} * m} \qquad (7.14)$$

Therefore, the first sub-carrier of cluster c is randomly allocated to one of the mobile users, the $(1 + \Delta f_c)$th sub-carrier to another mobile user, etc. In this way, we achieve maximum frequency diversity for the subcarriers of each mobile user.

6. The order of allocation for the subcarriers of pedestrian and vehicular users is random, because feedback information corresponds to the minimum SNR of each cluster.

7. If $\sum_{k=1}^{\#\mathcal{C}_k} n_{c,k} < R_{pedestrian}$, we add the remaining of sub-carriers to stationary users in order to achieve maximum total system throughput.

8. Let us define as K_i the set of users feed back information over the ith beam. Since $K_i \cap K_l = \{.\}$ for $i \neq l$, the scheduler selects different users over different beams.

Our scheduler can deliver broadband services (voice, data, video, etc) over time varying wireless channel efficiently. The scheduler is located at the BS to enable rapid response to traffic requirements

and channel conditions. The feedback information enables the scheduler to choose the appropriate MCS for each allocation. The resource allocation can be changed on a frame-by-frame basis in response to traffic and channel conditions. Furthermore, with orthogonal DL subchannels, there is no intra-cell interference. DL and UL scheduling can allocate resources more efficiently (total throughput could be quadrupled in the best scenario) and better enforce QoS. Additionaly, the fast and fine granular resource allocation allows superior QoS for data traffic. Consequently, the scheduler can enhance system capacity with moderate increase the overhead of the UL channel.

7.6 Simulation model

This study focuses on the performance for the downlink direction. The system specifications of IEEE 802.16e are considered. The main system parameters are given in table 7.2. Different scenarios are simulated in the following analysis. An overview of the scenarios is given in table 7.3. Simulation scenario I defines a cell with one BS and 30 mobiles randomly positioned on the positive halfspace ($x \geq 0$). All resources are utilised in this area. Uniform Linear Arrays with half wavelength spacing are used at both ends. The type of modulation and coding rate is chosen following the received SNR values of table 7.4 which is compliant to IEEE 802.16e standard 11].

TABLE 7.2 SYSTEM MODEL PARAMETERS

Parameter	Value
Cell Radius (m)	3300
Frequency Band (GHz)	5.25
Number of BS array antenna elements	4
Number of MS array antenna elements	4
Mobile Velocity (Km/h)	110
Channel Bandwidth (MHz)	10
Frame Duration (ms)	5
OFDM Symbol Duration (μs)	102.86
Number of Data Subcarriers	800
BS Transmit Power (mW)	250
Channel Profile	WINNER II C1 Metropolitan
Mobile Station Distribution	Uniform, random positioning, 30 users per cell
Traffic Model	Full Buffer

TABLE 7.3 OVERVIEW OF SIMULATIONS SCENARIOS

Scenario	Description
I	30 users randomly positioned in one cell
II	One user on a circular trajectory with radius 1km
III	One user moves along the horizontal axis (azimuth always 0°)
IV	Two users move along the vertical axis-One with azimuth always 90° and the other with azimuth always 270° and another user along the horizontal axis (azimuth 0°)

TABLE 7.4 MCS ACCORDING SNR

Modulation	Coding	SNR (dB)
BPSK	1/2	3
QPSK	1/2	6
QPSK	3/4	8.5
16 QAM	1/2	11.5
16 QAM	3/4	15
64 QAM	2/3	19
64 QAM	3/4	21

In the mobile WiMAX systems, high modulation orders are seldomly utilized because of their high SNR requirements. This situation is largely improved by the utilization of steering beams which is shown in the following simulation results.

Simulation scenarios II to IV correspond to specific cases with one or three users in order to evaluate SNR versus azimuth and coverage area. As a first step, these specific scenarios are evaluated and in the end results for simulation with more users (scenario I) are given. The transmitted signal is reflected and it arrives at the receiver via different paths with different delays. Consequently, we sum the delayed and attenuated received signals. This assumption is valid only for narrowband systems or for OFDM with transmission over narrow subchannels. Let us first have a look at the special case where one MS moves across a circular path with radius R=1Km (scenario II). We diagonalize the channel matrix H_k as in (15) for the different locations with azimuth φ=270°, 310°, 0°, 50°, 90°. Figure 7.8 illustrates the optimum transmit eigenvector, obtained from the first column of $\mathbf{V_k}$. We remark that the strongest eigenvector V_1 has azimuth range beetwen φ=340° to φ=20°. These results are explained from the CDL channel model , where the AoD of 16 clusters vary from -33 degrees to 35 degrees. In order to cover the halfspace cell area, we form steering beams from direction φ=340°

to φ=20°. We note that all transmit beam patterns are symmetric to the vertical axis due to the inherent radiation symmetry of the ULA (The symmetric part between 90° and 270° is not shown in the figures) The region of interest (covering the AoD of the different scatterers) is scanned by three beams with steering directions as is shown in figure 7.9. In order to obtain also deep fades in the simulated channel profiles, we set in the WINNER II channel model the parameter 'sample Density' equal to 64, which means that 128 channel samples per wavelength are taken. The total number of time samples is 1000. The output of the channel is in the time domain. The frequency domain output is taken by applying the FFT algorithm. The maximum frequency depends on the number of samples. We obtain the bandwidth of 10 MHz by applying zero order hold interpolation with oversampling factor 198. We don't take double-sided spectrum because it is symmetric to the central frequency of operation f_c=5.25 GHz.

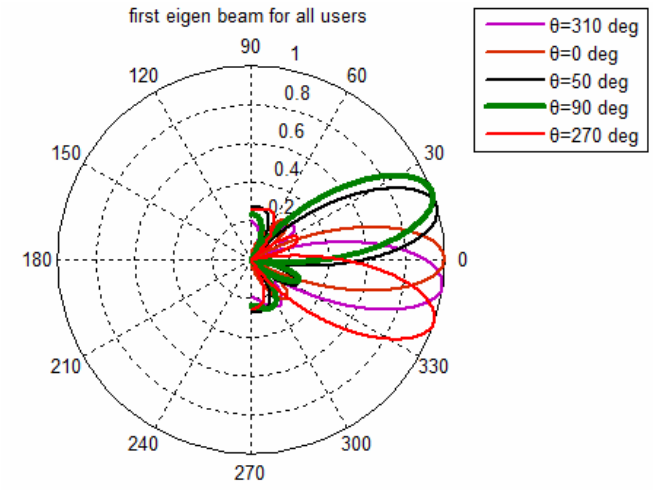

Figure 7.8 First eigen beams for different azimuth

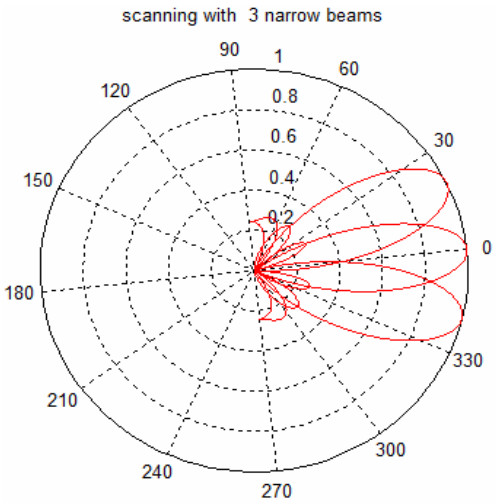

Figure 7.9 Scanning with three narrow beams

Therefore, we double the power of each frequency component. After oversampling, we have 990000 points at the frequency axis.

Remark: It is possible to cover all the cell area for scenario C1 with two beams having opposite directions. These beams are orthogonal and therefore the achieved total throughput is twofold from our simulation region since one beam scans the positive halfspace.

7.7 Simulation results

In the following, the results of the four above mentioned scenarios are presented. The average SNR versus azimuth angle for scenario II is shown in figure 10. The SNR at each user k is calculated for MRC reception. It can be observed that anywhere on the circular trajectory of scenario II, an SNR between 12 to 15 dB is measured.

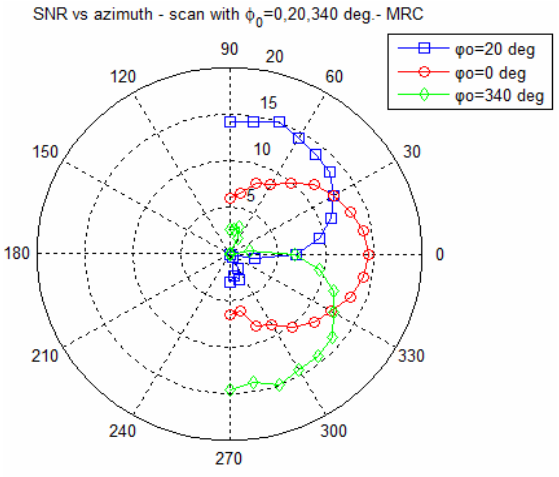

Figure 7.10 SNR versus azimuth

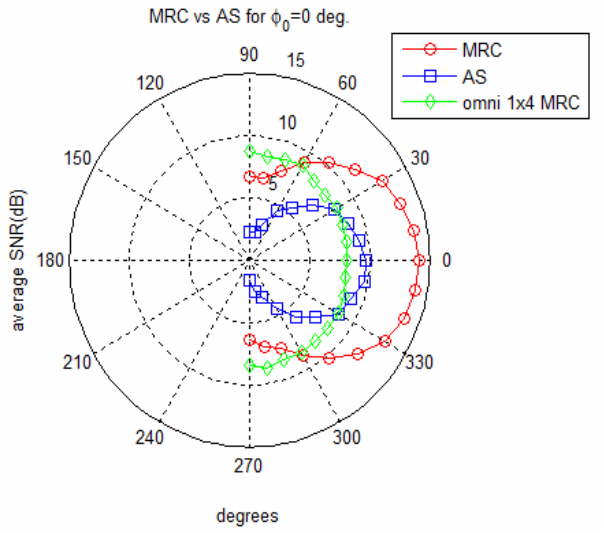

Figure 7.11 SNR for MRC and AS technique

We remark that the service area (positive half space) can be covered by three beams with directions φ=0°, 20° and -20° with 3 dB variation approximately in SNR when the mobile is located 3Km away from the BS.

The reason is that in an NLOS environment, due to the reflections and diffusion of emitted energy in different directions the azimuth angle of the first eigen beam has a range of 40° as we can see in figure 7.8.In order to compare MRC and AS receiver methods, we apply one single beam at the direction of 0° and measure again the SNR along the circular trajectory of scenario II. The polar graph is plotted in figure 7.11. MRC gives approximately 5dB better average SNR than AS. In the case where the mobile is located at φ=0° and performing MRC reception, beam steering shows a gain of 6.5 dB in SNR compared to a 0dBi omni antenna (SIMO 1x4).

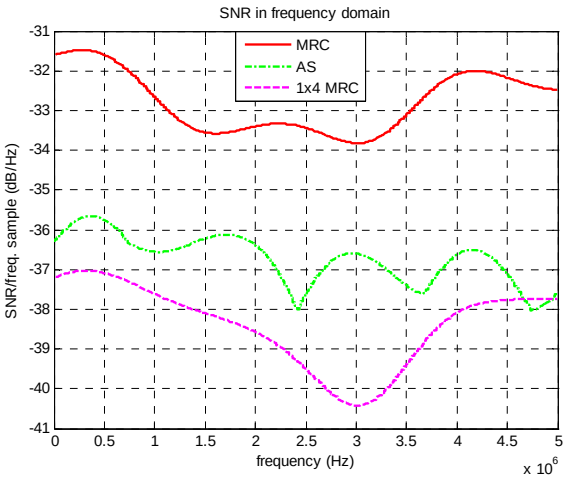

Figure 7.12 SNR for MRC and AS technique in frequency domain

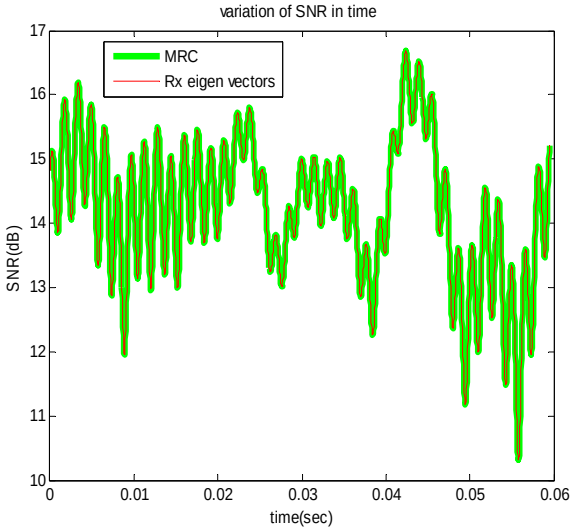

Figure 7.13 MRC and receiver eigen vector technique in time

In this article, the SNR and throughput of the omnidirectional transmit system at BS with four antennas at the receiver – Single Input Multiple Output – is also given to serve as a lower bound. The MIMO A mechanism with four transmit antennas, also known as space time coding (STC) or Alamouti and proposed by IEEE 802.16e, is known to give 2-4 dB diversity gain relative to single antenna transmission. Figure 7.12 compares the SNR in the frequency domain. The variation of SNR is smoother with the MRC method. The MRC scheme gives better performance because it can profit from the combination of the four transmitted paths and not only from the best path as in AS scheme. Figure 7.13 compares the received SNR variation of the MRC and Rx eigenvectors steering techniques over time. According to this technique, the rows of $\mathbf{U}^{\mathbf{H}}$ obtained from the SVD of the channel matrix are used as receive steering vectors.

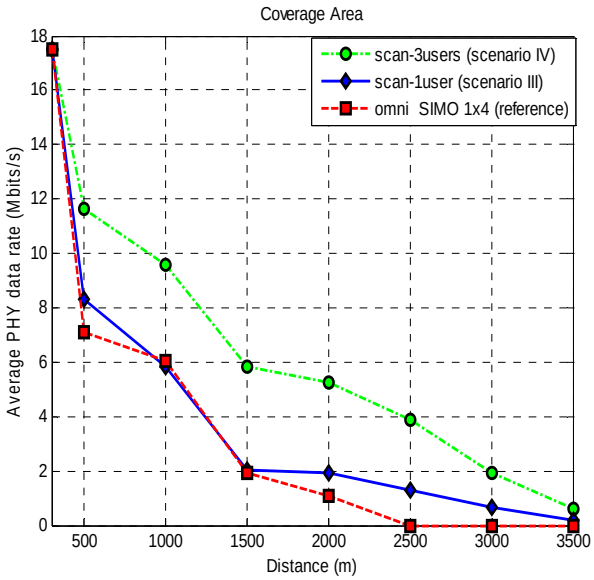

Figure 7.14 PHY data rate versus distance

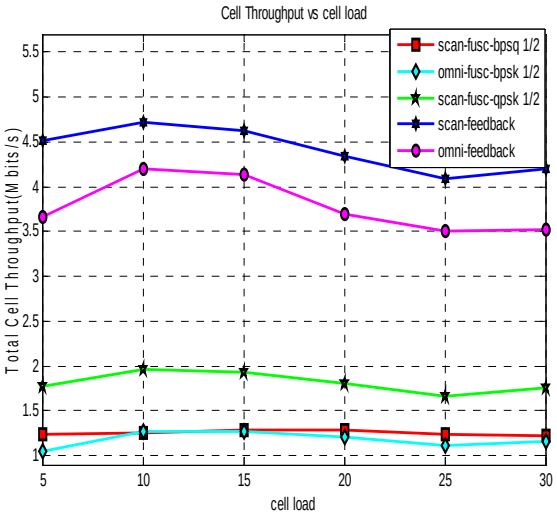

Figure 7.15 Total cell throughput versus cell load

We obtain the same SNR for the two cases because the transmit strategy is associated with the largest eigenmode instead of the optimum transmission with four eigenmodes. In other words, if we scan with narrow beams, we transmit at each eigenmode which corresponds to the optimum scheme. Figure 7.14 shows the average physical layer data rate as a function of the distance for two different scenarios and the omni SIMO case. In the worst case scenario III, one user moves along the horizontal axis. In the best case scenario IV with three users, the first user moves along the horizontal axis and the others along the vertical axis. Our scheme for scenario IV achieves a 55% improvement of range (minimum data rate 1Mbits/s) over SIMO 1x4 configuration with 0dBi omni BS antenna. The reason for the coverage increase when rotated beams are used is given by the fact that the narrow beams concentrate the power in one path which corresponds to strongest eigen mode.To identify the gains from scanning and beamforming in terms of cell throughput and fairness, in the following, scenario I is used for simulation. Figure 7.15 shows the cell throughput for different numbers of users (cell load) using the information from 20 clusters for feedback.

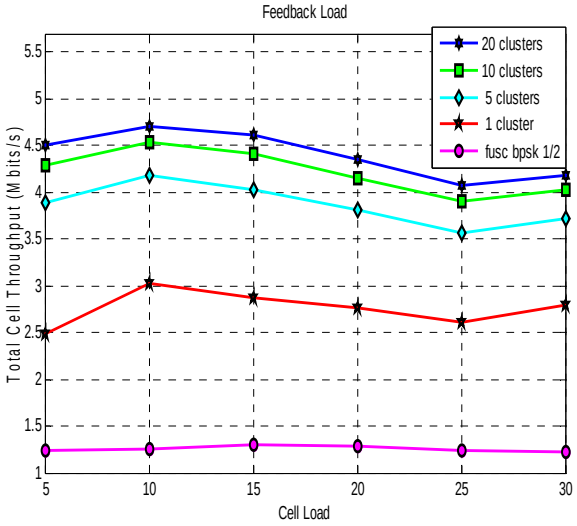

Figure 7.16 Total cell throughput versus feedback load

Our subcarrier allocation strategy is comparable to Full Usage SubChannelization (FUSC). FUSC is described in the IEEE 802.16e standard and provides the frequency diversity required for operating under high-mobility. FUSC does not need feedback information. It can be observed that the cell throughput can be improved by around 350% when using our proposed scheme instead of using omni directional antenna at BS and FUSC with BPSK at coding rate ½ (½ BPSK is taken as baseline performance). Comparing our scheme to omni directional antenna transmission with feedback we still observed a gain of about 20% in total cell throughput. Figure 7.16 shows total cell throughput for different amounts of feedback. The system capacity can be significantly enhanced using feedback, e.g. the cell throughput is improved from 1.25 Mbits/s to more than 2.5 Mbits/s if only the minimum rate

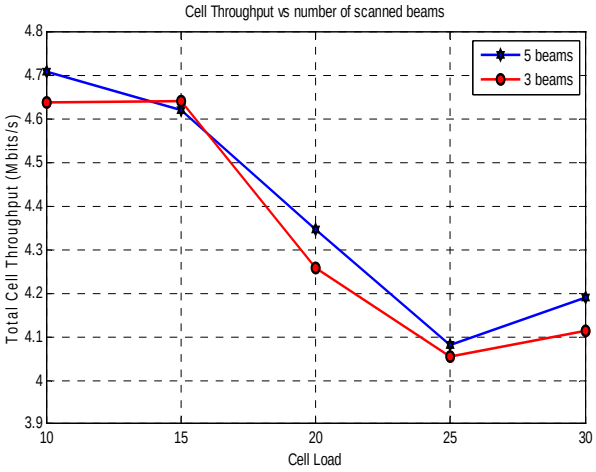

Figure 7.17 Throughput for 3 and 5 scanned beams

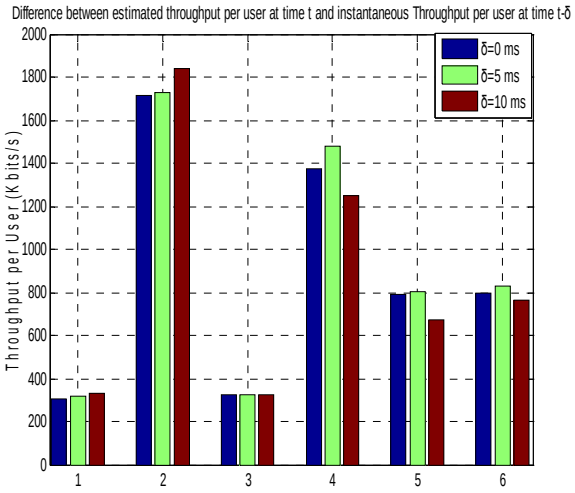

Figure 7.18 Difference between estimed throughput per user and instantaneous throughput user at time t-δ

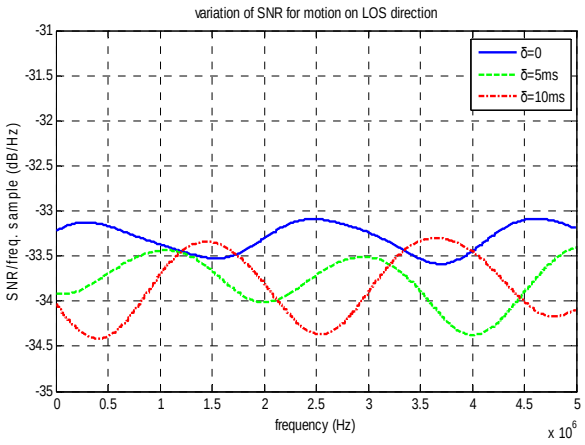

Figure 7.19 Variation of SNR for motion on LOS direction

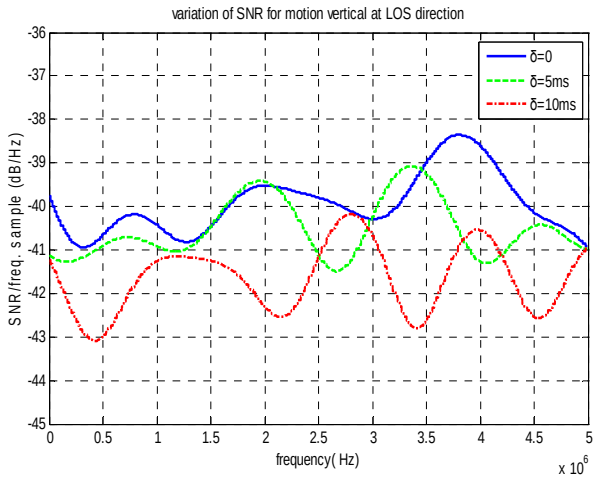

Figure 7.20 Variation of SNR for motion vertical at LOS direction

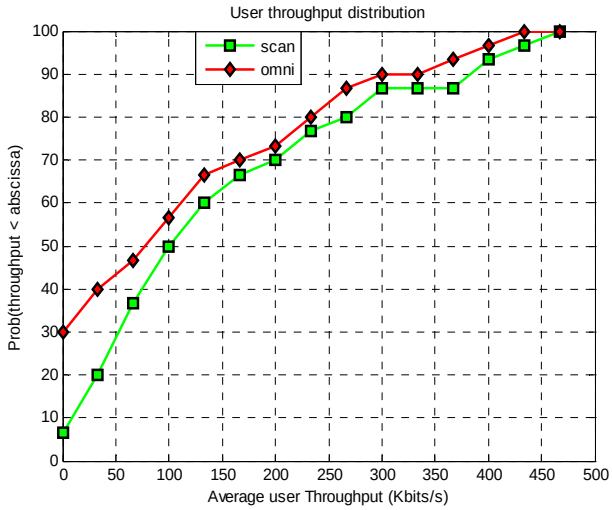

Figure 7.21 Users throughput distribution

from all subcarriers is calculated at the terminal and sent back to the transmitter (BS) and to more than 4 Mbits/s if the 400 single side band subcarriers (the total number of data subcarriers is 800) are divided into 20 clusters. These throughput numbers do not take into account the throughput loss due to signalling but only consider data subcarriers, eg throughput is measured at PHY and not at MAC layer. The results of figure 7.15 and figure 7.16 are explained from the fact that our strategy with steerable beams which increases the received SNR exploits the partial CSI efficiently. In figure 7.16, only 17% is the augmentation of throughput if the signle side band is divided into 20 clusters instead of 5 clusters. This behavior is reflected from the channel variation in spectrum when MRC is used. It can be seen by figure 7.12 that if five clusters are selected, the four clusters can be considered approximately constant. In figure 7.17, simulations have been performed with 3 and 5 scanning beams

with directions of rotated beams 340°, 350°, 0°, 10° and 20°. The performance is similar in the two cases because the width of three steerable beams is enough to cover the area of interest with azimuth angle from 340° to 20°. We studied the effect of feedback delay by calculating the throughput per user for six users in scenario I. Figure 7.18 plots the degradation of throughput per user in case of ideal feedback delay, (δ=0ms), one frame (δ=5ms) and two frames (δ=10ms) delayed feedback information. In the worst case, a 10ms delay causes a throughput loss of 10% per user, while a 5ms delay does not significantly change the user rate. The motion of the user can be analysed in two directions. The first in the direct signal path between BS and mobile eg Line of Sight (LOS) direction and the second in the vertical to LOS direction. Figure 7.19 and 20 present the variation of the channel (and the received SNR) in the frequency domain in the next frame and after two frames when the mobile moves away from the BS on LOS direction and on the vertical direction correspondingly to fully observe the performance degradiation of figure 7.18. The maximum variation of channel gain in the LOS direction is 0.9 dB for one frame delay and 1.4 dB for two frames delay. The change of the channel is more dynamic in the vertical direction. We see a variation of the channel gain about 2 dB for one frame delay and 3.8 dB for two frames delay.

Finally, figure 7.21 shows the CDF of user throughput for our proposed scheme and for the SIMO 1x4 scheme. It can be seen that the fairness is improved among the users for rotated beams compared to the omnidirectional transmission scheme as expected. In the omnidirectional scheme, 30% of the users cannot transmit while in the first scheme only 8% of the users don’t establish connection. For higher user throughput the CDF shift is smaller.

7.8 Conclusions

We have investigated a multi-user downlink transmission strategy that refers to beam-steering method, feedback design and scheduling for improving performance of 802.16e links in the context of communication between high speed vehicles and BS. It was shown that the proposed scheme significantly enhances the coverage area, the overall system throughput and fairness among the users. The simulation results show that the total throughput doesn’t increase proportionally to the number of clusters and is approximately constant if the number of fixed beams that are scanned in each sector is greater than a minimum value. Finally, the system throughput is independent of the cell load.

Chapter 8

Dynamic resource and interference management

In realistic systems, the channel changes over time due to the user mobility and the scattering environment. The influence of user mobility in a multi-path propagation environment can be modeled by an individual Doppler shift on each signal path. Information about the channel quality cannot be instantaneous and is outdated to some degree. Second order statistics describe the fluctuation of channel parameters with time. We define the covariance matrix of channel gain $\mathbf{H}(\mathbf{t})$ as $\mathbf{R} = \mathcal{E}\{\mathbf{H}(\mathbf{t})\mathbf{H}^{\mathbf{H}}(\mathbf{t})\}$. The symbol $\mathcal{E}\{.\}$ denotes the expected value. The channel is fast fading and the feedback information could be only low rate. Therefore, feedback is used for the next transmission process. The mobiles perform channel estimation, averaged over N_D slots and send back the covariance matrix by explicit feedback. This technique has been referred in literature as covariance feedback. In [60], an optimization problem is solved for a MIMO point to point system. The transmitter has partial channel knowledge (mean or covariance of the channel coefficient). It was found that the capacity improvement can be significantly high and that beamforming performs close to the optimal strategy. A similar problem is studied in [61], where it's shown that transmitting to the direction of the eigenvectors of the correlation matrix is the optimal transmission strategy. The statistical model depends on the time scale. In short term, the correlation of channel matrix $\mathbf{H}(\mathbf{t})$ reflects the geometry of a particular propagation environment. Over a longer term, the channel coefficients may be uncorrelated due to the averaging over several propagation environments.

The key idea of our design is based on the short-term CSI at the transmitter by averaging the channel covariance matrix over the duration of one frame (5 msec). We derive coarse channel estimation via closed loop schemes, suitable for Frequency- Division Duplexing (FDD). Also, we assume that the receiver has perfect channel knowledge (full CSI). In a MIMO system, the application of multiple antennas at the transmitter and the receiver increases the number of channel state parameters. The feedback requirements grow with the product of the number of transmitter antennas, receiver antennas, the delay spread and the number of users. Statistical feedback in a channel that varies rapidly reduces the feedback requirements. Given a low–rate feedback channel with FDD, this information may be easily obtained at the BS. An OFDM system divides a large spectrum into small narrow bands using an Orthogonal Transformation in order to have signals at each narrow band experiencing flat fading. The statistical feedback techniques designed for narrowband MIMO systems can be successfully used in MIMO – OFDM systems. But the number of sub-carriers in OFDM may be considerably large, e.g. 1024 or 2048. In [62], the transmitter antenna

with the best subchannel towards the receiver antenna is selected to transmit non-zero information. Aiming to reduce the feedback load in the frequency domain, we utilize the feedback scheme proposed in [63]. N subcarriers are divided into Q clusters of L adjacent subcarriers each, so that $N = Q\ L$. The number of clusters Q is scaled down until it gets the value $Q = 1$ when the channel varies rapidly and is scaled up to exploit strong channel modes associated with a static or slowly varying channel (stationary, pedestrian users). Additionally, in the downlink direction, when the BS transmits over the same channel to multiple users, inter-user Multiple Access Interference (MAI) is present. The BS constructs appropriate beams in order to mitigate MAI, if CSI is available at the transmitter. In our case, where the channel is changing rapidly, accurate CSI is difficult to obtain. Therefore, second order statistical information can be used to form beams at each cluster but not to separate users in the spatial domain. Beamforming seeks to improve the total throughput or minimize the total transmitted power. Our approach is robust and non risky taking into account the coarse estimation of CSI at the transmitter. Statistical information can be used for scheduling the users in a multiuser Time-Division MIMO-OFDM system. We optimize the time sharing of the users at each cluster in order to achieve maximum overall throughput or minimize the emitted power guaranteeing the QoS for all users. The aim of this paper is to combine MIMO, OFDM and FDD research challenges in a highly mobility environment to offer better performance compared to the current 802.16e standard.

Due to the fact that each user is allocated sub-channels of the full OFDMA band, Fractional Frequency Reuse (FFR) is effectively employed. Cell sectoring improves the average signal to interference plus noise ratio (SINR) and the related spectral efficiency, since frequencies can be reused in each sector. Universal FFR (f=1) simplifies cell planning but increases co-channel interference at the edge of the sectors. We present a reuse-1 (f=1) scheme, based on multi-user beamforming MIMO techniques. A four beam adaptive array is proposed, in which each beam module captures a different sector. The capability of resolving multiple time slots at the same time and frequency is referred as space division multiple access (SDMA) and increases system capacity. Additionally, dynamic sub-carrier and slot assignment is integrated into the downlink scheduling. This allows limiting the cross-sector interference without introducing more packet delays for the edge users with great channel fluctuations in the time domain. The problem of finding the minimum length SDMA/TDMA subframe in order to accommodate a set of users, is an NP-complete problem [64].

In a cellular system, we assume B neighboring BSs. Based on the analysis in a single-cell, we extend our study on interference from other cells. MIMO receivers decode the received signal by suppressing the spatial interference between the beams sent from B BSs by using linear signal processing techniques over the signals received by all antennas in order to fully suppress inter-cell

interference. It should be note that the size limitations of the handset impose constraints to the number of received antennas. We consider a network infrastructure based on cooperative processing. Although BS cooperation increases system complexity, it has the potential for significant capacity improvements. The BSs may be connected via radio over fiber (RoF) technology or wireless microwave links. Our approach applies adaptive beamforming and exploits the possibility of neighboring BSs to dynamically schedule their transmissions in a cooperative fashion. Beamforming is used to maximize the signal energy sent to the desired users, while it minimizes the interference sent toward interfering users. We reduce inter-cell interference indirectly, since statistical interference knowledge for the neighboring BSs is not necessary. Universal frequency reuse is used for the central users and cooperative scheduling transmission for edge users to share dynamically the resources in the frequency and time domains. Cooperative scheduling requires minimal information among neighboring BSs. We expect practical BS cooperation techniques to be implemented in the next generation mobile BWA systems.

The organization of this chapter is as follows: Section 8.1 describes the system model. In section 8.2 feedback strategies are presented while in section 8.3 the weights of the beams at the BS for each cluster are designed. In section 8.4 an algorithm which finds a time-sharing solution is proposed. In section 8.5, we examine a cell structure with four adjacent sectors that share the same frequency band. Section 8.6 investigates the scenario where the BSs are interconnected and can share different amount of information while section 8.7 describe how the new techniques can be implemented to the 3GPP Long Term Evolution (LTE) radio interface. Simulation results are presented in section 8.8.

8.1 System model

The downlink scheduler is assumed to select K users. Each user $k \in \{1, 2, \cdots, K\}$ has M_r receiver antennas while the BS has M_t transmitter antennas with a maximum power constraint P_{max}. We assume that a matrix $\mathbf{H_k^n}$ of size M_r x M_t represents the channel between the user k and BS at subcarrrier $n \in \{1, 2 \cdots N\}$. Finally, we suppose that the channel is frequency-flat due to OFDM modulation, $\mathbf{V_n}$ is the beamforming vector (of size M_t x 1) operated to the transmitter antennas at subcarrier n and σ_0 is the variance of the Gaussian noise applied at the input of the receiver. In our design, the signals received from M_r antenna elements are linearly combined to improve SNR. Also, CSI is available at the receiver. The received signals are multiplied by a coefficient vector $\mathbf{U_k^n}$ of size M_r x 1. According to the Maximum Ratio Combining (MRC) technique, the antenna is aligned to the Rx direction of $\mathbf{H_k^n}\ \mathbf{V_n}$ and therefore the MRC weights are given by [65]

$$\mathbf{U_k^n} = \frac{\mathbf{H_k^n}\ \mathbf{V_n}}{\|\mathbf{H_k^n}\ \mathbf{V_n}\|} \quad (8.1)$$

The SNR_k^n calculated at the receiver k is given by

$$SNR_k^n = \frac{\left|(\mathbf{U_k^n})^{\mathbf{H}}\mathbf{H_k^n}\mathbf{V_n}\right|^2}{\left\|\mathbf{U_k^n}\right\|^2\sigma_0^2}$$

$$SNR_k^n = \frac{\left|\mathbf{V_n^H}(\mathbf{H_k^n})^{\mathbf{H}}\mathbf{H_k^n}\mathbf{V_n}\right|^2}{{\sigma_0}^2} \quad (8.2)$$

Statistical feedback contains information $\mathbf{R_{k,c}}$ about the covariance channel gains that correspond to cluster $c \in \{1, 2 \cdots Q\}$.

$$R_{k,c} = \mathcal{E}\{\mathbf{H_{k,c}}(\mathbf{H_{k,c}})^H\} \quad (8.3)$$

Equation (8.2) could be transformed as

$$SNR_{k,c} = \frac{\left|\mathbf{V_c^H}\mathbf{R_{k,c}}\mathbf{V_c}\right|^2}{{\sigma_0}^2} \quad (8.4)$$

Assuming that the transmitted signal $\mathbf{Sc}$, of dimension M_t x 1, that is directed to receivers in cluster c is zero mean, with unit variance ($\mathcal{E}\{|\mathbf{S_c}|^2\} = 1$), the total radiated power at BS is

$$\sum_{c=1}^{Q} \|\mathbf{V_c}\|^2 \leq P_{max} \quad (8.5)$$

A frame structure applicable to the FDD mode is considered. The DL sub-frame has duration $T_f = 5ms$ and consists of $S = 8$ time slots of length $T_{slot} = 0.5ms$. If the number of time slots, allocated to user k, at each subcarrier $l \in \{1, 2 \cdots L\}$ belonging to cluster c is $S_{k,c}^l$, the total number of time slots must be at least S.

$$\sum_{k=1}^{K} S_{k,c}^l \leq S \quad (8.6)$$

If the total OFDM symbol duration is T_{OFDM}, the number of symbols S_{OFDM} transmitted in a slot is equal to

$$S_{OFDM} = \frac{T_{slot}}{T_{OFDM}} \quad (8.7)$$

A modulation level with $b_{k,c}$ bits per symbol is selected from a set $\mathcal{M} = \{1, 2, 4, 6\}$ of available QAM constellations. For M-QAM modulation with M equal to $2^{b_{k,c}}$, $b_{k,c} \in \mathcal{M}$, the minimum required SNR $\gamma(b_{k,c})$ to achieve a BER lower than a pre-specified value ϵ is given in [42]

$$\gamma(b_{k,c}) = -\frac{\ln 5\epsilon}{1.5}(2^{b_{k,c}} - 1) \quad (8.8)$$

Given that $SNR_{k,c} = \gamma(b_{k,c})$, $b_{k,c}$ is computed from equation (8.8). The rate of user k, calculated for one frame duration is

$$R_k = \frac{S_{OFDM} \sum_{c=1}^{Q} \sum_{l=1}^{L} b_{k,c} S_{k,c}^{l}}{T_f} \quad (8.9)$$

The transmitted power at cluster c can be written now as

$$P_c = \sum_{k=1}^{K} \sum_{l=1}^{L} \frac{\|\mathbf{V_c}\|^2 S_{k,c}^{l}}{S} \quad (8.10)$$

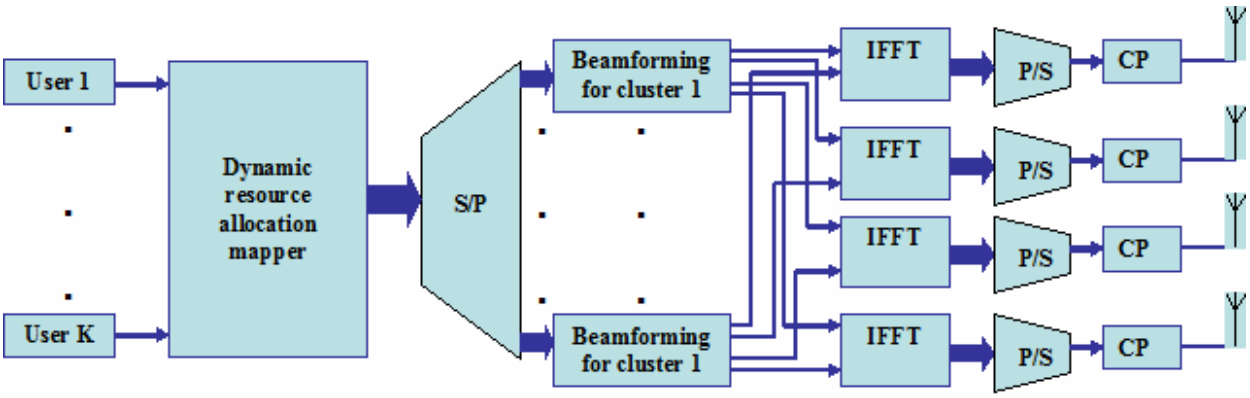

Figure 8.1 The proposed transmitter with adaptive beamforming

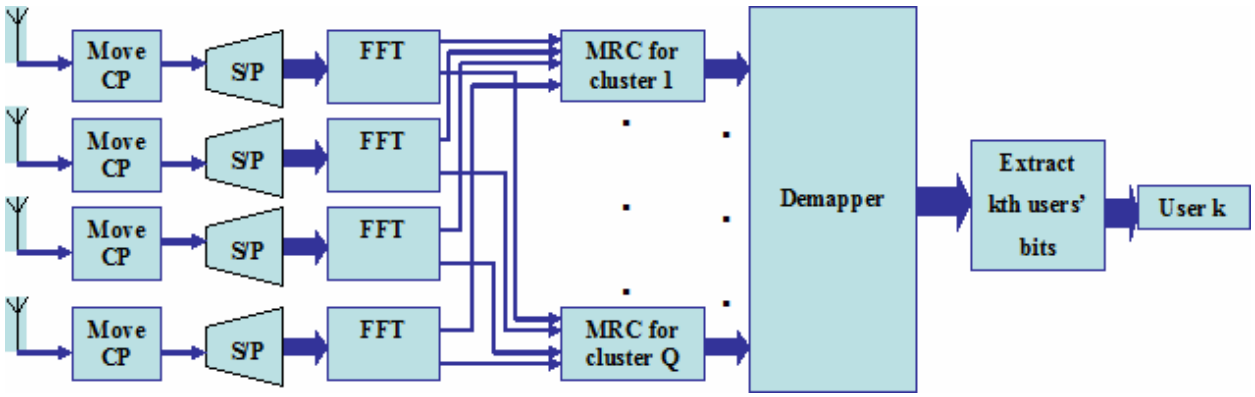

Figure 8.2 The proposed receiver scheme

The downlink transmitter model is presented in figure 8.1. All users' packets are sent to a dynamic resource allocation mapper. The information bits are mapped by converting them into complex numbers representing QPSK, 16 QAM and 64 QAM constellation mapping. Then, the beamforming vector $\mathbf{V_c}$ is applied on every cluster at the frequency domain. All the sub-carriers belonging to the same cluster are multiplied by the same weighting vector $\mathbf{V_c}$ M_tx1. Then the symbols are sent into an IFFT module to perform OFDM modulation for every transmitter antenna and the cyclic prefix (CP) is added to every OFDM symbol for transmission over the air. At the receiver, the reverse operation is done to decode the information bits for every user. The MRC algorithm is applied at the frequency

domain taking account of the channel impulse response of the weakest sub-carrier at each cluster. In case of cell sectoring, M_t=4 transmit antennas with four transmitted modules are employed. In figure 8.3, four beams are formed from the BS in the downlink direction.

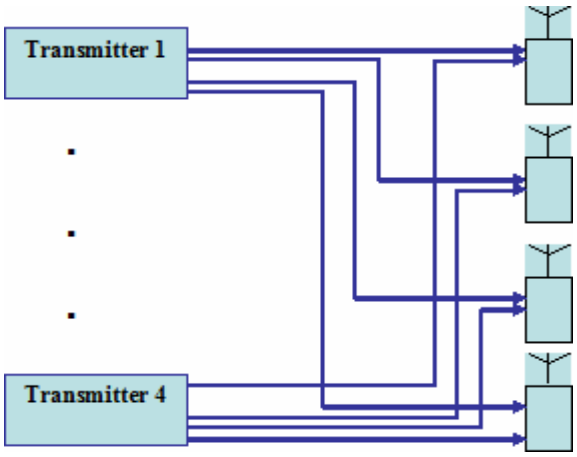

Figure 8.3 The proposed BS for cell sectoring

8.2 Reduced feedback scheme

Closed-loop schemes are suitable for FDD where channel reciprocity cannot be exploited. The solution of operating CSI per carrier is suboptimal since it does not take advantage of the fact that channel vectors at different carriers are correlated. We consider that the feedback channel is error -and delay -free. We propose the simplified feedback design based on clustered OFDM. As it's referred L adjacent OFDM sub-carriers are grouped into Q clusters so that $N = Q\ L$, N being the total number of sub-carriers. Each user feeds back information only about the clusters. This technique greatly reduces the amount of uplink control information. In situations when the channel changes rapidly, the channel information feedback to the transmitter is outdated. Only the statistics of the channel coefficient would be of significant benefit to the system design. We have defined the covariance matrix of the channel gain as

$$\mathbf{R_{k,c}}^{l} = \mathcal{E}\{\mathbf{H^{l}_{k,c}}(\mathbf{H^{l}_{k,c}})^{\mathbf{H}}\} \quad (8.11)$$

that is derived from averaging in the time domain over the duration $T_f = 5ms$ of the DL frame. The idea to feedback the covariance comes from the fact that it changes slower, e.g. second order statistics have a longer coherence time compared to that of fast fading. Also, from (8.4), the channel covariance is the only metric that is representative of the received SNR and is better than feeding back the channel autocorrelation. Additionally, the users inform the BS only about the value of the representative subcarrier in order to achieve feedback reduction. The following two feedback strategies are proposed:

A. Mean over subcarrier covariance metric (MSC)

The estimated covariance matrix from user k $\mathbf{R_{k,c}^{l}}$ is indicative of gain variations in cluster c. The representative value is obtained from averaging the covariance matrix of all subcarriers that belong to cluster c

$$\mathbf{R_{k,c}} = \frac{1}{L}\sum_{l=1}^{L}\mathbf{R_{k,c}^{l}} \quad (8.12)$$

B. Minimum Effective SNR covariance metric(MEC)

Each user calculates the effective SNR at each subcarrier $l \in \{1, 2 \cdots L\}$.

$$ESNR_{k,c}^{l} = \mathcal{E}\{SNR_{k,c}^{l}\} \quad (8.13)$$

$SNR_{k,c}^{l}$ is computed from equation (2) taking into account that each receiver k has perfect knowledge of the channel in all subcarriers and for all antennas. In this scheme, the covariance matrix $\mathbf{R_{k,c}}$ corresponds to subcarrier l^* with the minimum effective SNR.

$$\mathbf{R_{k,c}} = \mathcal{E}\{\mathbf{H_{k,c}^{l^*}}(\mathbf{H_{k,c}^{l^*}})^H\}$$

$$l^* \leftarrow \arg\min_{\forall l \in L}\{ESNR_{k,c}^{l}\} \quad (8.14)$$

Both schemes offer a considerable reduction in the amount of feedback and complexity of the allocation process but also decrease the system throughput. The scheduling isn't done for each subcarrier individually because our scheme proposes the same value of supportable throughput for all subcarriers of the cluster. This considerably reduces the allocation complexity especially for a small number of clusters Q. It's clear that when having small clusters, many users achieve their throughput target but the feedback load isn't much reduced. The choice of large clusters reduces feedback but increases the risk of achieving lower data rates than those required. If the size of clusters is of the order of the channel coherence bandwidth, no degradation in the system throughput occurs. The channel variations over subcarriers are small and thus we achieve the optimum capacity. This cluster size is the optimum in the case that users move with low speeds and large amount of feedback is feasible. In order to reduce the feedback load even more in situations where the channel changes rapidly, each user sends back only the covariance matrix of the strongest cluster c_{max}. c_{max} corresponds to the cluster with the greatest minimum ESNR. Therefore

$$\mathbf{R_{k,c_{max}}} = \mathcal{E}\{\mathbf{H_{k,c_{max}}^{l*}}(\mathbf{H_{k,c_{max}}^{l*}})^H\}$$

$$c_{max} \leftarrow \arg\max_{\forall c} ESNR_{k,c}^{l^*} \quad (8.15)$$

This approach can lead to many users not reaching their target rate. If there are few active users and they feedback information about only one cluster, there is a high probability that the BS receives no information about some clusters. The amount of feedback could be scaled for higher speeds. The users estimate the set $\{ESNR_{k,c}^{l^*}\}_{c=1,\cdots,Q}$ of the effective SNR on the weakest subcarrier at each cluster c. The clusters are sorted in increasing order. Let $C_{\pi(1)}, C_{\pi(2)}, .., C_{\pi(Q)}$ be the sorted clusters. Each user k sends to the BS information only for $\pi(\alpha)$ clusters with $\alpha \in \{1, 2, \cdots, Q\}$. The cluster – size α is scaled according to mobility-speed classes. It takes the maximum value for the stationary users where optimum performance is required and the minimum value equal to one for the high speed users in order to ensure baseline performance.

Remark: No transmission will be scheduled on the cluster that $ESNR_{k,c}^{l^*} \leq \overline{ESNR}$, where $\overline{ESNR}$ is a predefined threshold.

8.3 Beamforming weights among clusters

A downlink beamforming method is proposed that uses a common transmission weighting vector for each cluster. This technique utilizes feedback information and assumes flat-fading or narrowband cluster with a modified covariance channel matrix $\mathbf{R_{k,c}}$ derived from section 8.2. Our proposed scheme consists of simultaneously designing downlink beamformers to multiple clusters in order to maximize the total throughput or minimize the transmit power, under the constraints on providing at least a specified received SNR to each intended receiver keeping also the total BS transmit power (sum power) upper bounded. Given the covariance matrix $\mathbf{R_{k,c}}$ calculated from user k and γ_k the guaranteed specified SNR for user k at each cluster c and also considering that the low rate feedback channel is error and delay free, the optimization problem can be described as

$$\begin{aligned} &\mathcal{C}8 && \min \|\mathbf{V_c}\|_2^2 \\ &s.t. && \frac{\left|\mathbf{V_c^H R_{k,c} V_c}\right|^2}{{\sigma_0}^2} \geq \gamma_k \\ &\forall k \in \{1, 2, \cdots K\} && \forall c \in \{1, 2, \cdots Q\} \end{aligned}$$

The above problem is NP-hard but it can be relaxed into a convex optimization problem and be solved as in section 5.3(problem $\mathcal{Q}5$).

From the calculated beamforming vectors $\mathbf{V_c}$, the vector with minimum $\|\mathbf{V_c}\|^2$ is selected. In case that our goal is to maximize the total throughput under the transmit power constraint P_{max} , we introduce a transmit vector for each cluster $\mathbf{V'_c} = \sqrt{P_c}\mathbf{V_c}$. P_c denotes the power boost factor for cluster c . The boost factor changes only the gain of the antenna weights. If the transmit power is distributed equally at all clusters then

$$\|\mathbf{V_c}\|^2 P_c = \frac{P_{max}}{Q} \Rightarrow P_c = \frac{P_{max}}{\|\mathbf{V_c}\|^2 Q} \quad (8.16)$$

An important issue is how to quantize the information needed at the transmitter. In 3GPP standards, closed-loop feedback is used to enable the diversity mode for two adaptive transmit antennas [66]. Two schemes are proposed for the feedback design:

a) Quantized phase information where a set of bits is used to quantize the phase angles needed to perform equal gain beamforming and

b) Direct channel quantization with a set of bits for the gain and the phase of the channel. In this case, the feedback consists of sending back the unquantized channel coefficients transmitted as real and imaginary parts of a complex modulation symbol.

Our approach is based on feedback of statistical channel information. The computed channel mean or channel covariance at each downlink subframe is quantized using a limited number of bits. Statistical feedback cannot be used when the channel is static or varying slowly. In this case, the goal is not the reconstruction of the channel but the mapping of possible precoding matrices to a codebook [67]. The optimal codeword is based on achieving the spatial diversity by quantization of the beamforming direction. Each single codebook is optimized for one specific user. In IEEE 802.16e systems, a single precoding matrix for one user is applied to the whole band over a long period (e.g. for eight frames). The precoding matrix is computed from the covariance matrix. In [68], a multi-code book is utilized for beamforming and multi-user scheduling in order to exploit both spatial diversity and multi-user diversity. One single codebook is utilized for each resource block (a resource block is a basic unit defined in the frequency and time domains) but it switches for different resource blocks. The design of limited feedback codebooks cannot be applied to our proposed strategy because we construct beams for a set of users. Instead of quantizing properties of the transmitted signal, we can quantize the channel matrix by using intelligent vector quantization (VQ) techniques [69]. The channel matrix at each user k ($\mathbf{H_k}$) is reformulated into a $M_r . M_t$x1 complex vector $\mathbf{h_k^{vec}}$.

$$\mathbf{h_k^{vec}} = vec(\mathbf{H_k}) \quad (8.17)$$

where vec denotes vectorization. The $vec(\mathbf{x})$ creates a long vector by stacking the columns of matrix $\mathbf{x}$ on top of each other to form a vector. The $\mathbf{h_k^{vec}}$ is then quantized to $\widehat{\mathbf{h_k^{vec}}}$ by using a VQ algorithm. These algorithms map complex valued vector realizations by minimizing some functions such as the average mean squared error (MSE) $\mathcal{E}\{\mathbf{h_k^{vec}} - \widehat{\mathbf{h_k^{vec}}}\}$. Feeding back either the precoding matrices or the covariance channel matrix has almost exactly the same performance but the precoding matrix reduces the overhead compared to the covariance matrix over long periods (long term beamforming) [70].

8.4 Optimal time-sharing

OFDMA has emerged as a promising technology for the next generation BWA networks. OFDMA provides scheduling flexibility of resource units in both frequency domain (subcarriers) and time domain (time slots). After the subcarrier allocation and optimal beam construction, we treat the problem of time slot assignment. This problem is especially crucial if the target rates of the users are predetermined. In [71], the authors deal with a joint multiuser time –sharing and power allocation problem assuming that the transmitter knows only the statistical information about the channel. The initial problem is not convex and is modified into a sub-optimal convex optimization problem.

The WiMAX standard divides all services into four classes. Each class is associated with a set of QoS parameters. These service classes support constant bit rate (VoIP), real time data streams (MPEG video), variable-size data packets (FTP) and best effort allocation (e-mail). Thus, the minimum rate required R_{min}^{k} in bits per second and the maximum BER ϵ are related differently in the different classes of services for each user k. The exact order of time slot allocation is not important because only channel statistics are known at the transmitter. Therefore, we are interested in the number of slots assigned to users at each cluster. In addition, each subcarrier of the same cluster supports the same modulation level. Therefore, we could use LS timeslots and not require specific sub-carriers for each cluster. Equations (8.6), (8.9) and (8.10) can be written

$$\sum_{k=1}^{K} S_{k,c} \leq LS \quad \forall c \in \{1,2,\cdots,Q\} \quad (8.18)$$

$$R_k = \frac{S_{OFDM} \sum_{c=1}^{Q} b_{k,c} S_{k,c}}{T_f} \; \forall k \in \{1,2,\cdots K\} \; (8.19)$$

$$P_c = \frac{\sum_{k=1}^{K} \|\mathbf{V_c}\|_2^2 \, S_{k,c}}{LS} \quad \forall c \in \{1,2,\cdots,Q\} \quad (8.20)$$

Our goal is to maximize the total throughput while ensuring the users' individual QoS by optimizing the time-sharing S_k^c for all users. Mathematically, this optimization problem can be presented as

$$\begin{aligned} \mathcal{T}8 \qquad & \max S_{OFDM} T_f \sum_{k=1}^{K} \sum_{c=1}^{Q} b_{k,c} S_{k,c} \\ s.t. \quad & \frac{S_{OFDM}}{T_f} \sum_{c=1}^{Q} b_{k,c} S_{k,c} \geq R_{min}^{k} \\ & \sum_{k=1}^{K} S_{k,c} \leq LS \\ & S_{k,c} > 0 \\ \forall k \in \{1,2,\cdots K\} \quad & \forall c \in \{1,2,\cdots Q\} \end{aligned}$$

A simple approach is to schedule equal time slots at each cluster. If F_c is the number of users which sends back information for cluster c then the number of time slots allocated to each user is

$$S_{k,c} = \lfloor \frac{SL}{F_c} \rfloor \quad (8.21)$$

Finally, we consider the problem of minimizing the overall transmit power guaranteeing a specified QoS by optimizing the time-sharing $S_{k,c}$

$$\begin{aligned} \mathcal{P}8 \qquad & \min \frac{\sum_{c=1}^{Q}\sum_{k=1}^{K} \|\mathbf{V_c}\|_2^2 S_{k,c}}{LS} \\ s.t. \quad & \frac{S_{OFDM}\sum_{c=1}^{Q} b_{k,c} S_{k,c}}{T_f} \geq R_{min}^{k} \\ & \sum_{k=1}^{K} S_{k,c} \leq LS \\ & S_{k,c} > 0 \\ & \forall k \in \{1,2,\cdots K\}\ \forall c \in \{1,2,\cdots Q\} \end{aligned}$$

Problems $\mathcal{T}8$ and $\mathcal{P}8$ are Linear Programming (LP) problems and they could be solved optimally by using SeDuMi [38].

8.5 Adaptive radio resource management in a sectored cell

The IEEE 802.16e reference network (as a 3G cell communication system) uses cell sectoring and frequency reuse techniques [72]. Cell-sectoring replaces an omni-directional BS antenna with several directional antennas collocated at the same site. The hexagonal cell is divided into sectors. Each sector can be viewed as a mini-cell using different sets of radio resources. Frequency reuse planning is denoted by frequency reuse factor (c,s,n) where c represents the number of cells needed to realize the frequency partitioning; s represents the number of sectors per cell and c the number of frequency subsets used. Most of multi-cell network planning schemes use a (1,3,3) configuration: 1 cell,3 sectors and 3 subsets of frequencies. Since each cell is split into three sectors, the cell capacity is multiplied by three but 1/3 of the available channels are available in each sector. Therefore the (1,3,3) scheme does not affect the capacity. However, it minimizes the interference at the cell edge and improves SINR without increasing the transmitted power due to directional antennas. Since the operating spectrum is a scarce resource in network deployment and must be utilized efficiently, there is significant interest to transmit data at every sector using the same frequency band (universal frequency reuse). In this case, the radiated diagrams of adjacent antennas are overlapping. For the users located in the overlapping regions between adjacent sectors even though they are near the BS, their own received power is weak (low transmit antenna gain) and the co-channel interference from

the adjacent sector is strong and therefore the received SINR is low. For the users located in the direction of main beam, the transmit antenna gain is high and the desired received signal strength is high. The interference power is low because the antenna gains from adjacent sectors are low. A simple way to handle the interference is to allocate different sub-carriers to different sectors (static separation) or to avoid using in overlapping regions the sub-carriers already in use in other regions (dynamic separation). Both schemes are particular cases of FFR and therefore the spectral efficiency drops due to a larger reuse factor. Additionally, the cell-edge users suffer from loss of frequency selectivity gain.

The proposed solution uses a BS antenna with four elements and four transceivers. We handle the interference in the overlapping region of the antenna radiation diagrams in two adjacent sectors. The problem of universal frequency reuse pattern with a cell divided into four sectors is illustrated in figure 8.4. The blank regions in this figure are low interference regions. By applying common transmission weight vectors in each cluster for the set of users belonging to sector $s \in \{1, 2, 3, 4\}$, we may suppress interference in neighboring sectors. The users of each sector can be treated indepedently of each other for designing beams with partial CSI. We minimize inter-sector interference and at the same time we keep the Quality of Service (QoS) at an acceptable level (by having a guaranteed minimum attained SINR by each user). By applying space division multiple access techniques (SDMA) and common weighting vectors at each cluster, we can theoretically improve the frequency utilization efficiency for the blank regions.

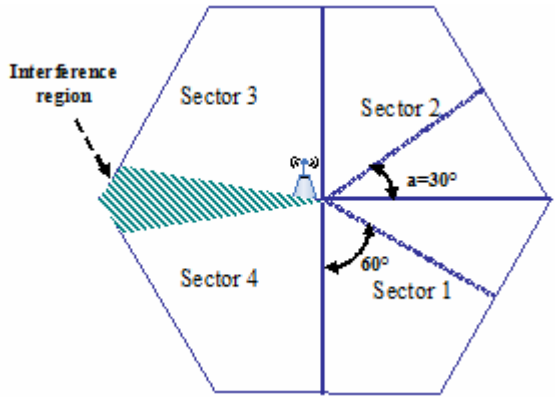

Figure 8.4 Interference regions in a cell with four sectors

The maximum number of beams at each BS is four (equal to the number of antenna elements M_t). If $\mathbf{V_{cs}}$ is the weighting vector applied at the sector s and cluster c and $\mathbf{R^s_{k,c}}$ the covariance matrix calculated from user k belonging to sector s, the problem $\mathcal{C}8$ is transformed as

$$\mathcal{C}''8 \qquad \min \|\mathbf{V_{cs}}\|_2^2$$

$$s.t. \qquad \frac{\left|\mathbf{V_{cs}^H R_{k,c}^s V_{cs}}^2\right|}{{\sigma_0}^2} \geq \gamma_k$$

$$\forall k \in \{1,2,\cdots K\} \quad \forall c \in \{1,2,\cdots Q\} \quad \forall s \in \{1,2,3,4\}$$

We transmit simultaneously $\mathbf{V_{cs}}$ beams and therefore mutual interference among these beams must be taken into account

$$SINR_{k,c} = \frac{\left|(\mathbf{U_{k,c}})^{\mathbf{H}} \mathbf{R_{k,c}^s V_{c,s}}\right|^2}{\sum_{l \neq s} \left|(\mathbf{U_{kc}})^{\mathbf{H}} \mathbf{R_{k,c}^s V_{cl}}\right|^2 + \|\mathbf{U_{kc}}\|^2 \sigma_0^2} \quad (8.22)$$

The main source of interference comes from collisions among the same sub-carriers scheduled over the same time-slots in neighboring sectors. The burst allocation in the downlink subframe impacts the collision rate. In (8.22), full cell loading and so maximum collision rate are considered. SDMA increases the number of time and frequency resources by four. Consequently, lower traffic conditions may occur compared to the available resources and subframes may be expected to be partially occupied in time. We find the remaining time slots which are not assigned at each cluster and sector

$$S_{c,s} = LS - \sum_{k=1}^{K} S_{k,c}^s \quad (8.23)$$

$$\forall k \in \{1,2,\cdots K\} \quad \forall c \in \{1,2,\cdots Q\} \quad \forall s \in \{1,2,3,4\}$$

The minimum number of available time slots for allocation is given by

$$S_c^{min} = \arg\min_{\forall s} S_{c,s} \quad (8.24)$$

Then the optimization problem $\mathcal{C}''8$ is applied for the shared regions $s \in \{5,6,7,8\}$ while the problem $\mathcal{P}8$ is now solved separately for four sectors by replacing the maximum number of time slots LS with S_c^{min}. If θ_s is one of the four fixed angular values that correspond to one of the four sector sites ($\theta_s \in \{45°, 135°, 225°, 315°\}$), $s \in \{1,2,3,4\}$ is chosen such that θ_s is as close as possible to the mobiles' direction of arrival (DoA).

8.6 Network Deployment and adaptive radio resource management

FFR uses orthogonal frequency resources among neighboring cell edge users to mitigate inter-cell co-channel interference. In order to reduce the interference without losing the frequency resources in each cell, cell users may be partitioned into two classes, namely interior and exterior users. Frequency resources are universally used in all interior cell areas whereas users of exterior zones have a frequency reuse factor strictly higher than one. Figure 8.5 illustrates different clusters (f1 to f6) of the OFDMA band. Universal frequency reuse is realized for users close to the center. Static FFR

suffers from loss of frequency selectivity gain and from a corresponding drop in the spectral efficiency due to the large reuse factor. It's widely accepted that cross-layer interactions between the MAC and PHY layers are needed so that the limited wireless resources could be optimally used while satisfying the QoS requirements. By having interactions between both the MAC and PHY layers, the optimum parameters can be obtained.

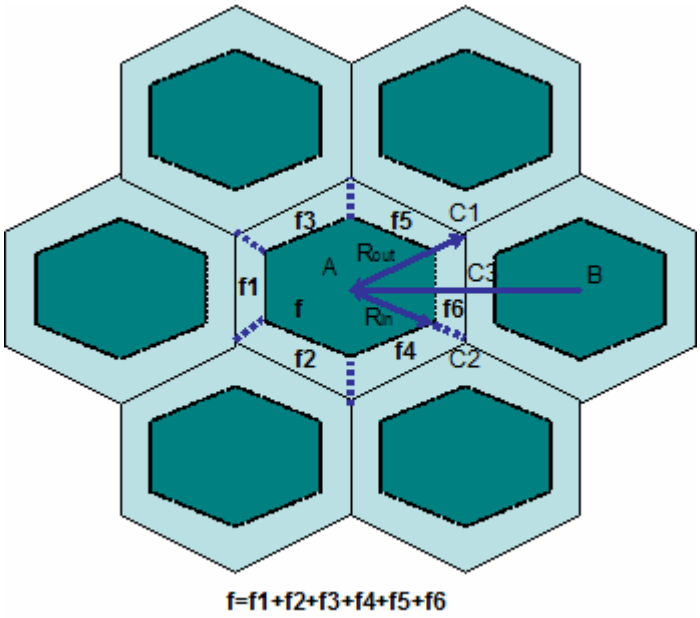

Figure 8.5 Francional Frequency Reuse

This solution presents a limitation of the exchangeable parameters only between PHY and MAC layers without taking account of specific applications provided from other available networks. The BS coordination has been proposed to mitigate interference in a multi-cell environment. In [73], the dirty paper coding (DPC) scheme among neighboring BSs achieves maximum theoretical capacity for a multi-user MIMO downlink channel, if the received interference signals are known to the transmitter. However, this technique gives theoretical upper bounds because it requires exact knowledge of CSI at all the transmitters. In [74] different combinations of precoder and power allocation algorithms are considered. An opportunistic inter-cell scheduling scheme is applied to TDMA systems in order to increase the cardinality of the selection pool [75].

We propose the development of a novel cross-layer technique where the cross-layer scheme is expanded into a cross-layer and cross-system strategy that maintains the flow of parameters between the various layers of various systems. We investigate an alternative to the traditional static FFR scheme where neighboring BSs dynamically schedule their transmissions to reduce inter-cell interference. By adaptively using different weights according to the channel conditions, the SINR may be improved and therefore higher order modulation modes may be employed. Dynamic scheduling and adaptive beamforming for mobile users are based on partial CSI. The combination of

the abovementioned techniques fully exploits the frequency selectivity gain and avoids deep fades for edge users without introducing more packet delays for related delay sensitive services. Suppose that B=7 is the total number of co-channel adjacent BSs as in figure 8.5. If $\mathbf{V_{bs}}$ are the beamforming weights applied at each BS $b \in \{1, 2, \cdots, B\}$, we calculate from problem $\mathcal{C}8$ beam vectors without taking into account inter-cell interference. For each cell and each cluster, we find the number of allocated time slots only for cell edge users by modifying the problem $\mathcal{P}8$ as in the following:

$$\begin{aligned} \mathcal{P}' \qquad & \min \frac{\sum_{k=1}^{K} \|\mathbf{V_{bc}}\|_2^2 S_{k,c,b}}{LS} = P_{c,b} \\ s.t. \qquad & \frac{S_{OFDM} b_{k,c,b} S_{k,c,b}}{T_f} \geq \frac{R_{min}^k}{M} \\ & \sum_{k=1}^{K} S_{k,c} \leq LS \\ & S_{k,c} > 0 \end{aligned}$$

$\forall k \in \{1, 2, \cdots K\}\ \forall c \in \{1, 2, \cdots Q\}\ \forall b \in \{1, 2, \cdots B\}$

M is the number of clusters allocated for edge users and is a function of the number of edge users. For each cell we select the M clusters with minimum $P_{c,b}$

$$C_b^{min} = \{c_{1b}^{min}, c_{2b}^{min}, \cdots, c_{Mb}^{min}\} = \arg\min_{\forall c} \sum_{c=1}^{M} P_{cb} \quad (8.25)$$

We calculate $\mathbf{V_{bc}}$ and $S_{k,c,b}$ for center users with $c \in \{1, 2, \cdots, Q\} - C_b^{min}\ \forall b \in \{1, 2, \cdots, B\}$

For the estimation of $SINR_{k,c,b}$, inter-cell interference must be taken account.

$$SINR_{k,c,b} = \frac{\left|\mathbf{V_{cb}^H H_{k,b,c}^H H_{k,b,c} V_{cb}}\right|^2}{\|\mathbf{H_{k,b,c}}\|^4 \sigma_0^2 + \sum_{d \neq b} \left|\mathbf{V_{cb}^H H_{kbc}^H H_{kdc} V_{cd}}\right|^2} \quad (8.26)$$

The advantages of our strategy are summarized in the following points:

1. The complexity and advanced signal processing is shifted to the BS side that accommodates and processes the received partial CSI.
2. Our design doesn't require channel information for the neighboring BS's ($\mathbf{H_{k,d,c}}$). The monitoring of pilot channels from neighboring BS's is a complex process and requires complicated detectors for the mobile device, increasing the feedback load in order to update this extra information to the BS. Our method (described in section 8.3 and 8.4) is based on the single cell downlink transmission with the goal to minimize the total transmitted power to the neighbouring cells. This means that $\sum_{d \neq b} \left|\mathbf{V_{bc} H_{k,b,c}^H H_{k,d,c} V_{dc}}\right|^2 << \sigma_0^2$ in (8.25) as inter-cell interference is neglected.

In the literature, the BS cooperation scheme assumes that the desired and interfering signals arrive simultaneously at each mobile [76]. This is unrealistic especially for scenarios involving fast fading and highly mobile users. Our scheme doesn't require synchronization among different BSs which leads to complex signal processing based on asynchronous system model. It's important to note that in cooperative transmission, even when the desired signal components arrive synchronously (perfect-timing), multi-user interference is asynchronous by nature and leads to a significant performance degradation of the linear transmission strategies.

8.7 Mobile LTE network

The above analysis for mobile WiMAX networks is applicable to the Long Term Evolution (LTE) radio interface as is defined by the 3rd generation partnership project (3GPP) [77]. OFDMA with data transmission on parallel narrow-band subcarriers is the basis of the LTE downlink radio transmission. In FDD, during each frame duration of 10ms there are 10 downlink subframes, each of 1ms duration. Each subframe is divided into slots, each of 0.5 ms duration. In our system, the mobile terminal averages the channel estimates over 2 (1ms) or more (up to 10ms) slots depending on the variation of the channel. The short subframe duration of 1ms allows relatively faster channel variations to be tracked compared to WiMAX where the subframe duration is 5ms. Our adaptive beamforming and channel-dependent scheduling in time and frequency domains, when it is applied to the LTE radio access, exploits better the variations in the channel quality and makes more efficient use of available resources.

Multi-antenna schemes with up to four antennas at the transmitter and receiver sides are also supported by LTE. Transmit diversity is based on space-frequency block coding (SFBC), complemented with frequency-switched transmit diversity. Spatial multiplexing provides simultaneous transmission of parallel data streams and is based on a precoder matrix of size 4x4 when four antennas and therefore four independent streams are assumed. In the special case, where the precoder vector is 4x1 (rank-1 transmission), beamforming is selected. Codebook-based beamforming is a special case of the spatial multiplexing (SM). LTE also supports non-codebook based beamforming. "LTE-Advanced" aims to further enhances the LTE radio access performance and capabilities [78]. The components being discussed includes:

- Extended multi-antenna transmission by increasing the number of downlink transmission streams to eight
- Coordinated multipoint transmission/reception by joint exploitation of multiple cell information.

Our discussion is applicable to “LTE-Advanced” and may contribute and influence this standard as well.

8.8 Simulation results

A network deployment with one cell of radius R=500m and one BS at the center of the cell is considered. The number of BS and MS antennas is four. Uniform Linear Arrays (ULA) with half wave length spacing are used at both ends. The network is assumed to operate at 5.25 GHz and OFDM with 800 sub-carriers is used within the 10 MHz transmission bandwidth. All simulations, throughput and transmit power calculations were generated in the Matlab system. A summary of the system parameters is provided in Table 7.2 The channel model was related to the C2 Metropolitan area for typical urban macro-cell scenario from WINNER II [24]. The model is applicable for mobiles located in an outdoor environment at street level communicating with fixed BSs installed above rooftops. Non Line Of Sight (NLOS) propagation is the typical case scenario in such cases. Table 7.4 demonstrates the type of modulation and coding rate which was selected in relation to the received SNR (all values were compliant to the IEEE 802.16e standard). In the following, the performance of optimization problem $\mathcal{C}8$ is evaluated. The feedback scenario with 5-clusters is used. All clusters are sent as feedback information from the 15 mobiles to the BS. Furthermore, the total throughput of an omnidirectional transmit system at a BS with four antennas at the receiver – Single Input Multiple Output – is also given to serve as a lower bound. This SIMO 1x4 system could be compliant to an IEEE 802.16e in case of high mobility, where no CSI is available at the BS.

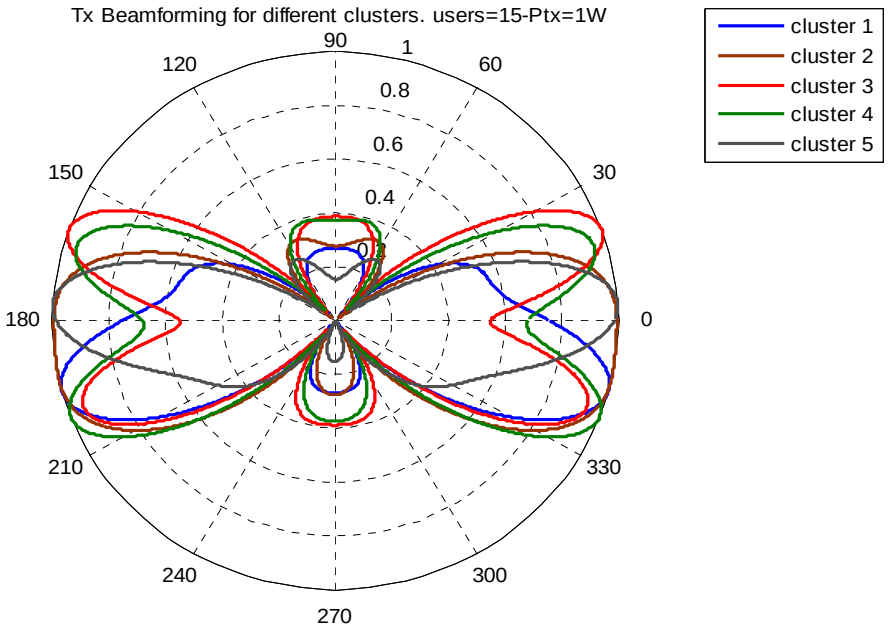

Figure 8.6 Transmit beams for different clusters

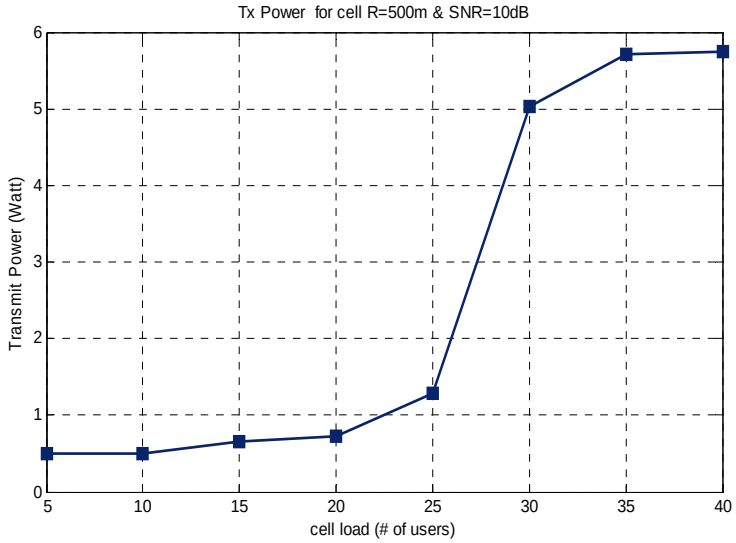

Figure 8.7. Transmit power versus cell load

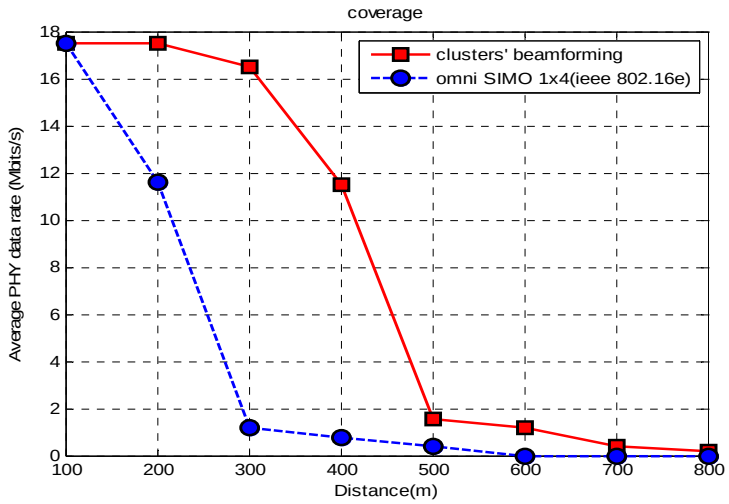

Figure 8.8. PHY data rate versus distance

Transmitted beams for different clusters are highlighted in figure 8.6 to show the effect of our approach. The transmitted power as a function the number of users (cell load) guaranteeing an SNR=10 dB for all mobiles is depicted in figure 8.7. For a number of mobiles, approximately equal to 20 and randomly distributed in the cell, an emitted power level of one Watt (30 dBm) could support the required SNR and a power level of lower than six Watt (38dBm) would be adequate to have the same effect when 40 mobiles are located in the cell. Figur 8.8 presents the average physical layer data rate as a function of distance for a user that moves along the horizontal axis. We remark that our scheme improves the coverage area at about 100% over SIMO 1x4 system, when a minimum data rate of 1Mbits/s is required over the air. Additionally, figure 8.9 shows that fairness is improved among the users with our beamforming design. In this scheme 10% of users achieve an SNR lower than 10 dB while in SIMO 1x4 scheme only 50% of mobiles present SNR greater than 10 dB.

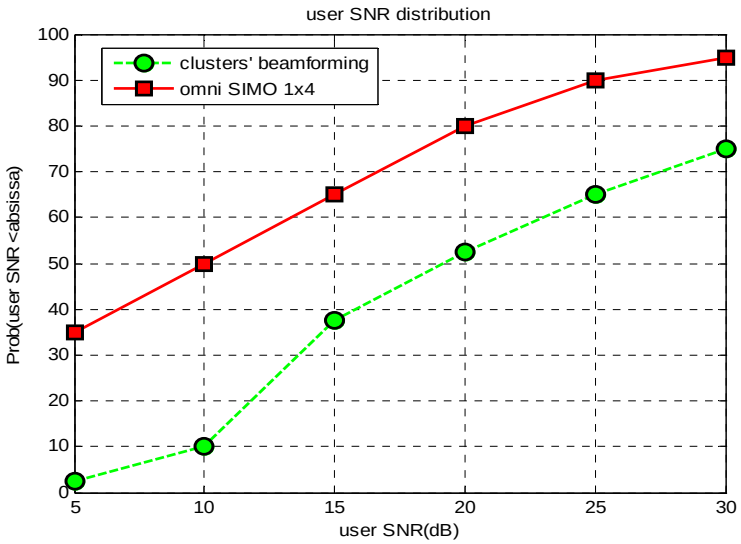

Figure 8. 9. Users' SNR distribution

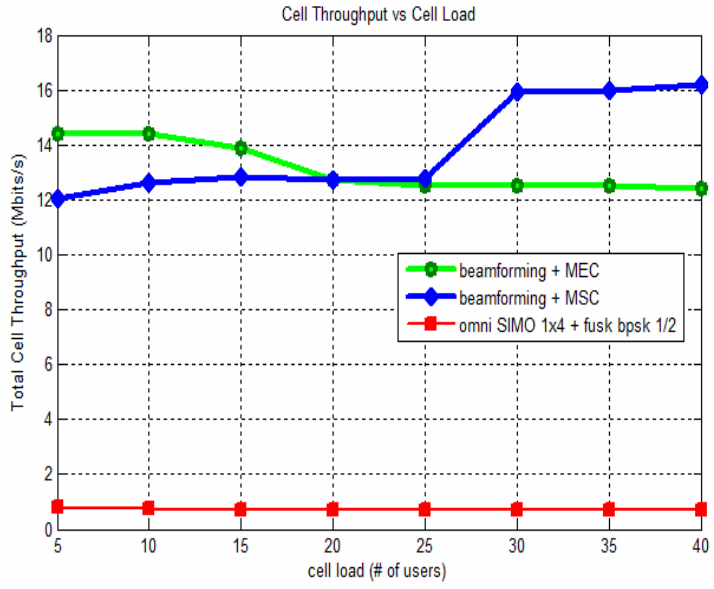

Figure 8.10 . Cell throughput versus cell load

Figure 8.10 compares the Mean over Subcarrier Covariance (MSC) statistical feedback strategy, the Minimum Effective SNR covariance (MEC) feedback scheme and the omnidirectional SIMO 1x4 system, where FUSC scheduling with BPSK modulation type and ½ rate coding are supported in order to provide frequency diversity for high-speed users. FUSC doesn't need feedback information. As figure 8.10 indicates, the performance with feedback may be significantly enhanced, e.g. the total cell throughput is improved from 1 Mbits/s to more than 12 Mbits/s. The performance with MSC feedback is better when the number of mobiles grows than that with the MEC feedback scheme. This can be justified by the fact that a large number of users provide increased multiuser diversity. The large number of users involves large number of independent channels. The MEC scheme takes into consideration more reliable information about the correlated channel based on the weakest sub-

carrier. When a wider variety of different channels is present, the resource management algorithm with MEC has more chances to improve the efficiency of the system. Figure 8.11 depicts the achievable system throughput as a function of feedback load if the 800 OFDMA sub-carriers are divided into 20 clusters for a system with the MEC feedback scheme. The total cell throughput increases from 1Mbits/s, when the strongest cluster is fed back to more than 10 Mbits/s in the case where the five clusters with bigger minimum ESNR are used. A degradation of the system performance of about 15% is observed if 5 clusters instead of 20 are selected to be fed back.

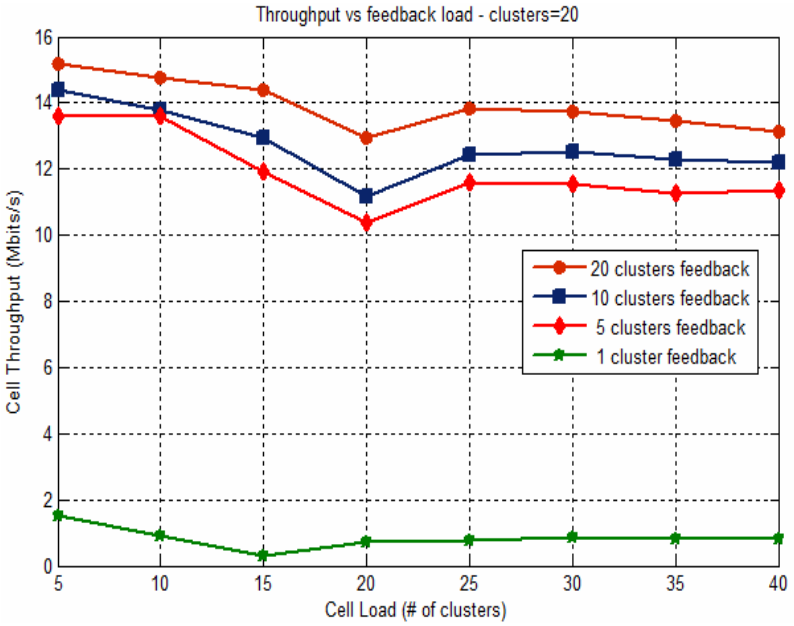

Figure 8. 11 . Total cell throughput versus feedback load

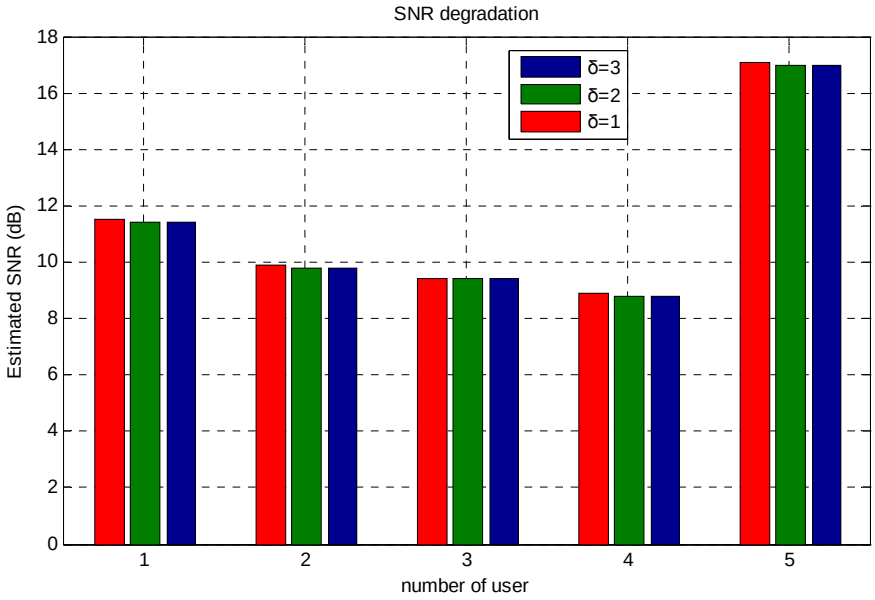

Figure 8. 12. Estimated SNR at time t-δ

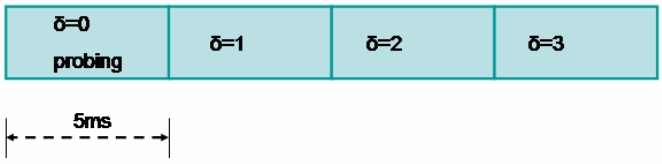

Figure 8.13. Frames' transmission in time domain

In order to assess the impact of the Channel Quality Indicator (CQI) delay, a 5 user system is scheduled with delayed CQI. Figure 8.12 plots the estimated SNR with δ= 1, 2 and 3 frames delayed CQI when frame duration is 5ms. At the FDD frame structure of figure 8.13, during the first frame (δ=0) the covariance matrix is computed for using at the SNR of the next frame (δ=1) or after two or three frames (δ=2,3) . We observe that the SNR is approximately the same for the three cases.

Computer simulations have also been conducted to evaluate the performance of the optimization problem $\mathcal{T}8$ after the beamforming and frequency allocation problem is solved for 5 clusters. Our proposed algorithm for optimal time –sharing is compared to the equal-time method (equal number of slots is allocated to each user) in figure 8.14. Target rates of users are predetermined to 500 Kbits/s. When the number of users is greater than 15, our optimal strategy tends to allocate similar number of slots with the equal-time method. The total throughput versus the target rate for 10 users is plotted in figure 8.15. All the users have the same target rate. Results indicate that the total throughput decreases from 14.5 Mbits/s when the minimum rate required is 10 Kbits/s to 11 Mbits/s when the minimum rate is 1 Mbits/s. In figure 8.16, the total throughput versus the number of time slots allocated at each cluster (S) is illustrated. We assume that the minimum required rate is 1Mbits/s while the number of users is 10.

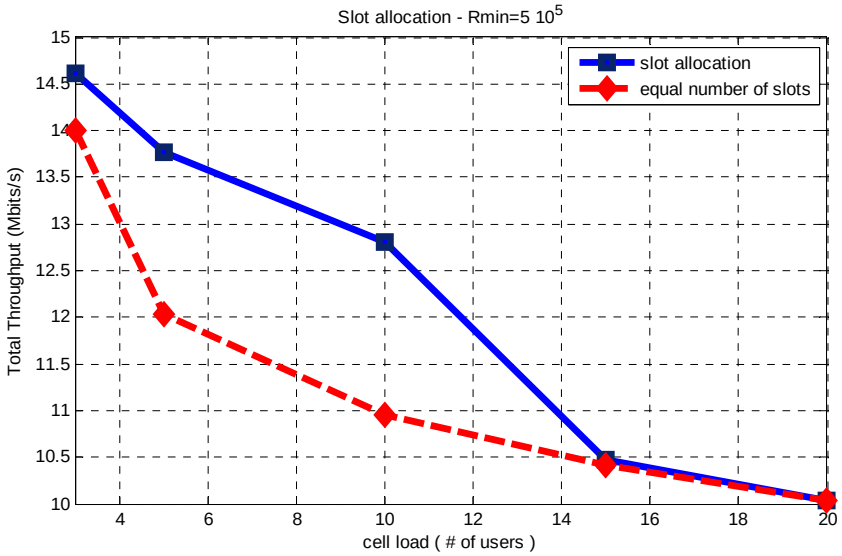

Figure 8.14 Total throughput versus cell load for the sharing-time problem

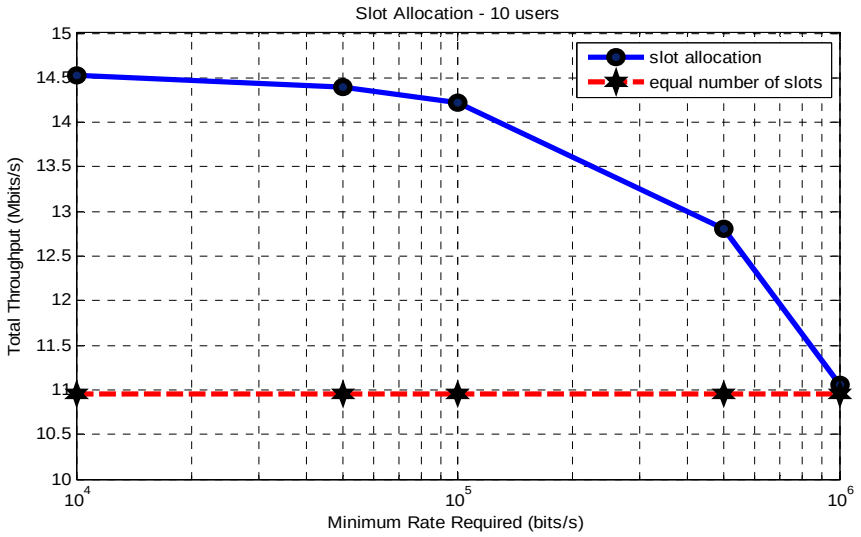

Figure 8.15 Total Throughput against the target rate

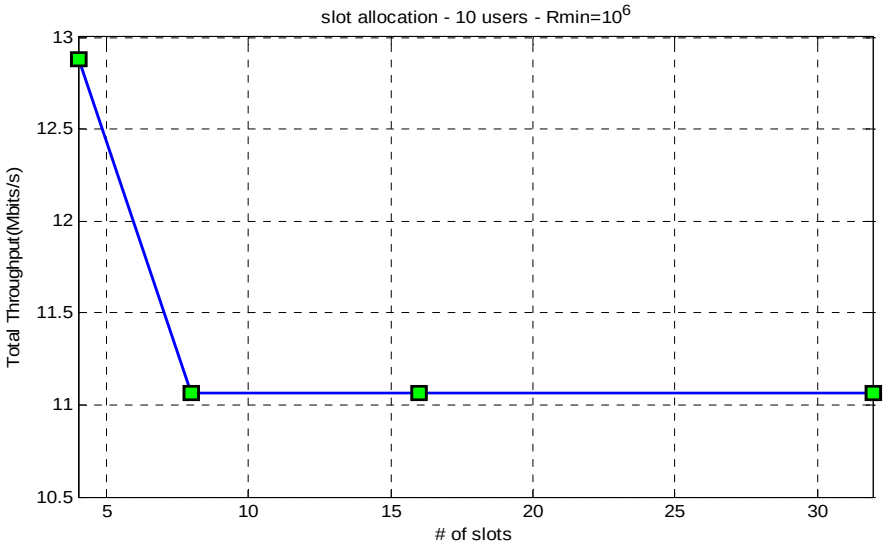

Figure 8.16 Total Throughput versus number of slots

As we can see, from S=8 to S=32, the performance is independent of the number of time slots. The value S=4 gives the maximum throughput, equal to 13 Mbits/s.

In the multi-cell environment, the results of two different scenarios are presented. The MEC feedback scheme with 3 clusters is applied. We assume that the BS's are placed following the pattern depicted in fig. 5 (B=7), transmitting at full power (1Watt). In the first scenario, six mobile users are distributed in the interior-cell edge. Each user moves along a line connecting neighbouring sites, for example along the line connecting A and B in fig. 5. Figure 8.17 shows the PHY data rate of the six interior edge users against the radius of the interior cell R_{in}. We remark that co-channel interference from other cells leads to a performance degradation compared to the "one cell" mode without inter-cell interference. For R_{in}=250m, inter-cell interference causes an average cell throughput loss of 22%

while for R_{in}=150m no degradation in throughput can be observed. The second scenario is refers to the users in the cell exterior. Cell edge users are divided into six regions according to their respective neighboring cells. The dynamic allocation of one cluster to each area is performed so that neighboring areas do not utilize the same cluster. A frequency reuse of 3 is performed. In figure 8.5, f6=f1, f5=f2 and f3=f4. We consider an external area with three users located at one edge with polar coordination (R_{out}, 0°), (R_{out}, 30°) and (R_{out}, -30°). It can be seen by figure 8.18 that throughput for this area can be improved around 49% when R_{out}=400m by fully exploting the frequency selectivity gain.

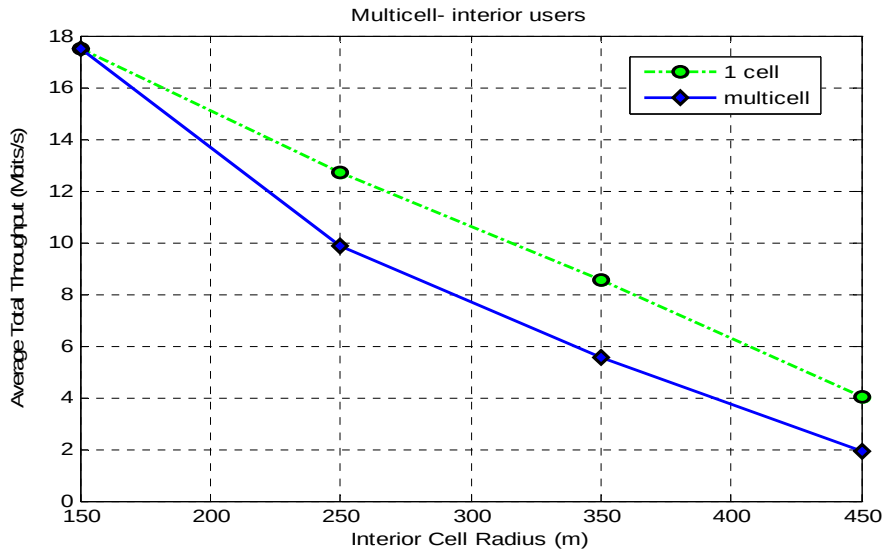

Figure 8.17 Throughput degradation of interior users

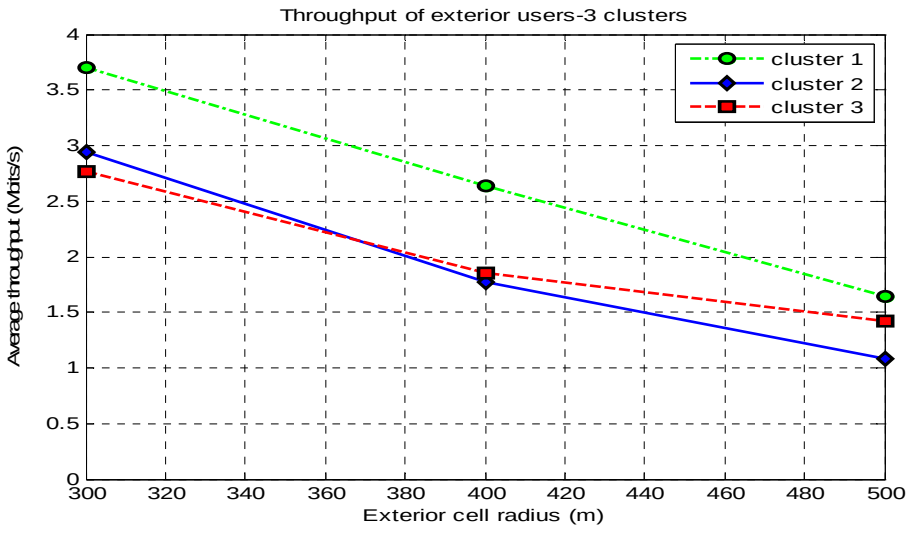

Figure 8.18 Frequency diversity for exterior users

In the sectorized cell study, the most important issue is the cross correlation between the beams of the neighboring sectors, as it tends maximize when the shaded area of figure 8.4 is minimized. Figure

8.19 shows the average PHY layer data rate of two users which are found on the edge of two sectors as a function of the distance from BS. The angle between the two sectors (the angle width of the shaded area) is a=20°. In other words, the direction of the transmitted beam patterns have a difference of a=20° as is illustrated in figure 8.20. An improvement of 2Mbits/s is achieved for R=400m and R=300m when two separate beams are used instead of one. When the users are located near to the BS, the inter-beam correlation problem can heavily degrade the performance of a sectorized cell. The simulation results are taken for the MEC feedback scheme with 3 clusters. The transmitted power of a single beam is 2 Watts for comparison reasons.

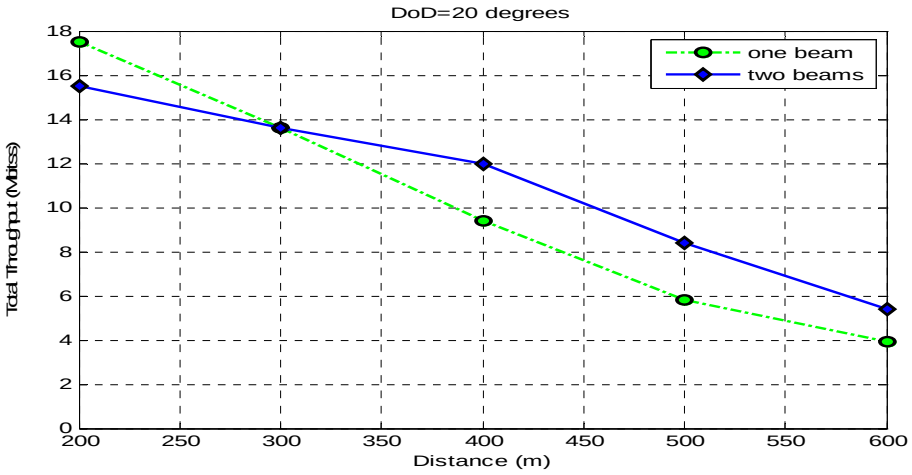

Figure 8.19 Performance of a sectorized cell system

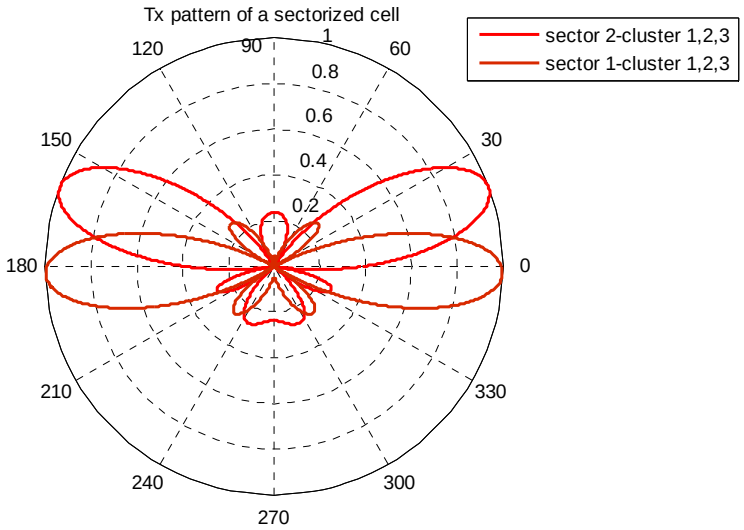

Figure 8.20 Tx patern of a two sectors with a=20°

8.9 Conclusions

This chapter has addressed the multiuser multi-cell MIMO/OFDMA problem of beamforming and scheduling in the frequency and time domains when the transmitter has only the knowledge of channel statistics of the users. We proposed and developed two new, flexible and scalable low rate feedback schemes in a network with rapidly time-varying channels. We have proposed system-level techniques that can be combined with the advanced algorithms already proposed in literature to reduce intra-cell interference and to coordinate the user transmissions aiming at increased throughput and better spectrum exploitation. Our results indicated that the proposed strategies can meet the requirements of the promising the future IEEE 802.16m and LTE advanced standard technologies.

Chapter 9

A remote base station network architecture

IEEE 802.16e networks with full frequency reuse suffer from low SINR for all users at the cell border. Poor SINR conditions due to the high amount of interference from neighboring cells give low throughput. If beamforming and smart antennas are used compared to a scenario without smart antennas the SINR at the cell edge users can be improved [79]. Spatial multiplexing (SM) increases throughput dramatically and is considered as a key technology for improving the capacity of the future BWA systems. But SM loses much of their effectiveness as interference increases (causing low SINR). In fact, as SINR decreases, it's often better in terms of spectral efficiency to send a single stream, because diversity outperforms SM in terms of both data rate and reliability. In [80], it was shown that for a 2x2 MIMO system, for SINRs below 5dB in highly correlated channels and up to 20dB in channels with low correlation, STC achieves higher capacity than SM. In conventional MIMO-OFDM systems, cell sectoring and frequency reuse are commonly used to mitigate intercell interference. Cell sectoring consists of directional antennas which radiate within a specified sector area. In hexagonal cell patterns, three sectors of 120° are used.

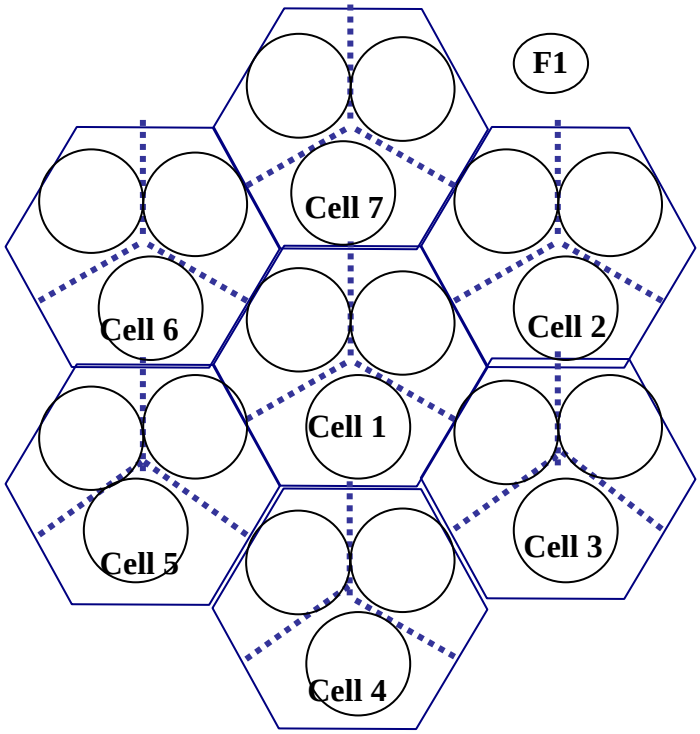

Figure 9.1 (1,3,1) cellular configuration

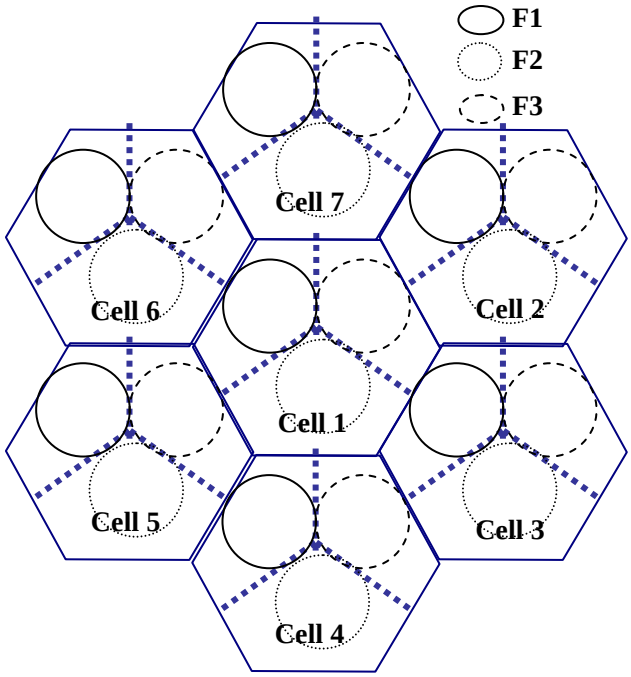

Figure 9.2 (1,3,3) cellular configuration

Frequency reuse consists in dividing the total available bandwidth into subsets and allocating those subsets to different clusters of cells. These techniques can be applied to combat co-channel interference during SM transmission in a OFDMA cellular system. Figure 9.1 and figure 9.2 illustrate a cell configuration with three sectors per cell and Frequency Reuse Factor (FRF) equal to one and three respectively. These schemes are referred as (1,3,1) and (1,3,3)- 1 cell, 3 sectors, 1 or 3 subsets of frequencies. In fig. 1, the SINR of the mobiles that in each sector (either at the edge or near the center) area is low, because the received signal and interference are at the same power due to the antenna gain. The distance from the two neighboring BSs is approximately the same. The user may choose the interfering sector with high probability as the home sector. In figure 9.2, the spectral efficiency is reduced compared to fig. 1 since only 1/3 of the available spectrum is used at each sector. Also, when FRF=3, the mobiles uses 1/3 part of frequency diversity in the whole frequency band and therefore this technique suffers from loss of frequency selectivity gain in an OFDMA system.

Radio over Fibre (RoF) systems may be employed to distribute Radio Frequency (RF) signals from a central location to remote antennas. RoF adds potential advantages to WiMAX technology [81]. No RF signal processing beyond optoelectronic convertion and amplification at the Distributed Antennas (DAs) is required, which leads to a simplification of the required equipment. The DAs architecture has been proposed to reduce inter-cell interference. The antennnas are geographically distributed in the cell forming a “distributed” or “virtual” MIMO configuration. Each user is close to some antennas and therefore the transmitted power is reduced. The user is connected with the DA that has the minimum

propagation path loss. The corresponding diversity gain increases the received SINR especially for users that are found near the DAs. The cellular architecture for seven cells, with one antenna at the original BS and six DAs spread in circular layout throughout cell is studied in [82]. DAs reduce other-cell interference and selection diversity outperforms the blanket transmission where all antennas in the cell broadcast the same data. In [83], an omni-directional DA is employed to enhance the received Carrier to Interference (C/I) ratio at the cell edge users in a multi-cell environment. A sectorized DA system for OFDMA systems is proposed in [84]. In each sector every user may be served by one, two or three distributed antennas. The whole frequency band is available and could be dynamically assigned according to the traffic load and interference measurements. In this chapter, we combine beamforming, MIMO, RoF and OFDMA techniques for the downlink direction of a high speed multi-user multi-cell system. We investigate the advantages in the downlink in terms of PHY data rate improvements by placing DAs in proper locations for two transmission strategies: selection diversity where just one DA array is chosen for transmission and SM where four DA arrays transmit different data streams. The results show that our proposed cellular architecture provides highly spectrally efficient data transmission to high speed users and thereby meet the requirements of IEEE 802.16m standard for future generation of BWA systems.

The rest is organized in the following way: In section 9.1, RoF technology for the deployment of WiMAX networks is provided. Section 9.2 describes transmission strategies and section 9.3 introduces multi-cell DA array architectures. Section 9.4 analyzes MIMO combined with transmit beamforming techniques for interference reduction while section 9.5 describes receiver MIMO techniques. Simulation results are presented and explained in section 9.6.

9.1 Radio over fiber for wimax networks

The DA architecture requires a large number of BSs to cover the service area. Also, low cost BS's are required. The limitations in the infrastructure costs led to the development of centralized systems where signal routing, handover, frequency allocation are carried out at a central Controlling Station (CS) rather than at BSlevel. Since the optical fiber (fibre) has low loss and ultra-wide bandwidth, the RoF network is used to link the CS with BSs. The resources provided by the CS can be shared among many BSs. The remote BSs perform only simple functions, they have small size and low cost. At frequencies used for WiMAX, directly modulated semiconductor lasers (LD-Laser Diode) and single mode fibre are preferred due to low transmission losses, engineering simplicity, low cost and small size [85]. When Direct Intensity modulation is combined with direct detection using Photo-Diode (PD), it is reffered to as Intensity-Modulation Direct-Detection (IMDD). A Semiconductor laser directly converts a small-signal RF modulation into a corresponding small-signal modulation

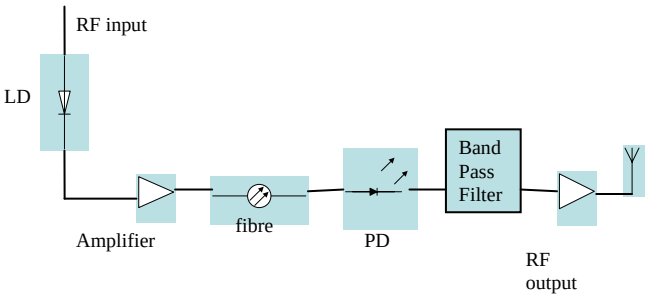

Figure 9.3 Simple IMDD link configuration

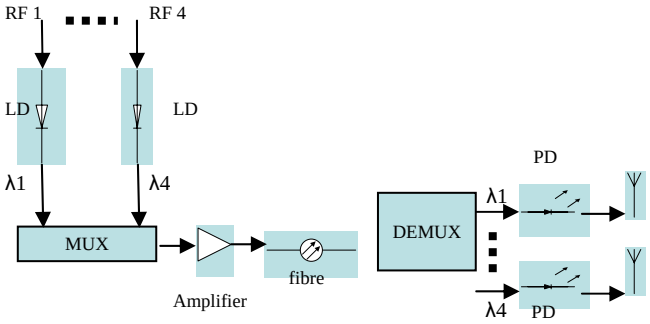

Figure 9.4 Application of WDM in beamforming technique

of the intensity of photons emitted. Thus, a single device serves as both the optical source and the RF/optical modulator. The resulting intensity modulated optical signal is transported over the length of the fiber optic to remote a BS. There, the emitted RF signal is recovered by direct detection in a PIN PD. The signal is then amplified and radiated by the antenna. Figure 9. 3 depicts a classical point to point IMDD analog optical link.

In [81] the development of RoF technology for the transmission of WiMAX signals in the 3.5 GHz band for several single mode fibres up to 5 Km is studied. Measured spectral mask and maximum allowed Error Vector Magnitude (EVM) for ¾-64 QAM modulation and coding are compliant with the limits defined in the IEEE 802.16 standard. In case of a BS forming a four DA array for implementing beamforming techniques, Wavelength Division Multiplexing (WDM) scheme could be developed. Figure 9.4 depicts how we could transfer the four RF signals from the CS to a remote BS in order to feed the four antenna element with minimum cost.. The four optical RF wave signals from four LDs are multiplexed and the composite signal is optically amplified and transported over a single fiber. The remote BS demultiplexes the RF signals which feed the four DAs. The wavelength multiplexing causes chromatic dispersion. In a fibre, the index of refraction n ($n = c/v_g$, c is the light

speed and v_g the group velocity) is function of the wavelength. Therefore, certain wavelengths will propagate faster than others. The delay effects caused by the fibre on the beamforming technique are studied via simulations in [86]. The phase shift differences corresponding to a 2m difference in the fibre lengths give a 10° misadjustment in the beam steering. In high speed user network, the fast radio channel changes introduce greater delays than the delays caused by the fibre.The SM technique is not affected by RoF since the phase shift generated by several RoF links in parallel is included in the CSI, which is fed back to the CS.

9.2 Multiple access transmission strategy

In a BWA system four different channel scenarios can be considered:

a) BS and mobile are in line of sight (LOS). In this case, the channel matrix has rank one and beamforming technique is used to increase SINR.

b) The user is found at the edge of the cell and therefore wireless channel has low SINR. In this cas beamforming is selected to increase the robusteness of the link.

c) Poor scattering environment and medium SINR. Few channel eigen-modes are able to transmit parallel streams. STC scheme is required to increase diversity gain.

d) In the rich scattering environment with high SINR, SM transmission increases spectral efficiency by allowing the transmission of several simultaneous data streams.

In practice, a small percentage from users experience good channel conditions and high SINR to enable SM. By applying beamforming to a SM signal, not only SINR is improved - and so high order modulation can be applied - but much larger percentage of users in that cell area can profit from SM scheme. The result is much higher data throughput since SM and higher order modulations are enabled. Geographically distributing the antennas around the users (virtual MIMO configuration) will increase the rank of the channel matrix (high angular spread) and therefore will ehhance the number of possible spatial subchannels available for the users to transmit. We assume an array of directive antennas, with spacing higher than λ/2 (λ is the wavelength), each having also multiple antenna elements, with respective spacing among them lower than λ/2.

The beamforming technique is based on the assumption that the CSI is available at the transmitter in order to adapt the transmit signal to the channel. Our study is reffered to rapidly time-varying channel and accurate CSI is not easy to be obtained. We assume an OFDMA system with imperfect CSI due to high speed users. Aiming to achieve low rate feedback from the users to BS in frequency domain, we utilize the following feedback scheme. N subcarriers are divided into Q clusters of L adjacent subcarriers each, so that

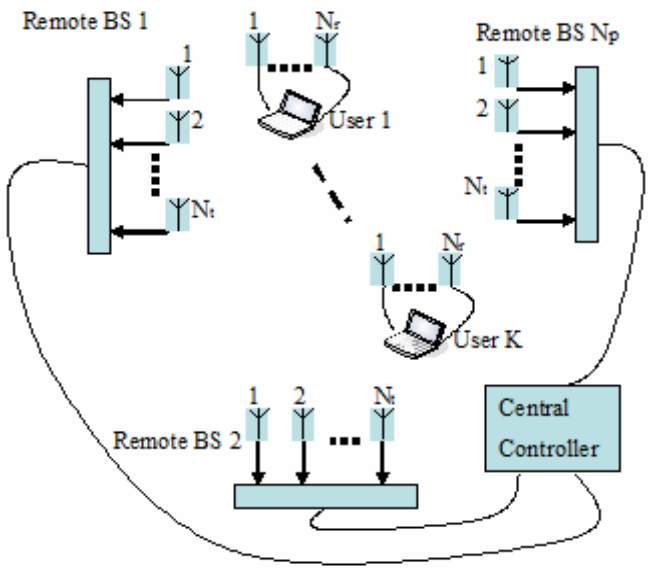

Figure 9.5 Cell deployment with remote BSs

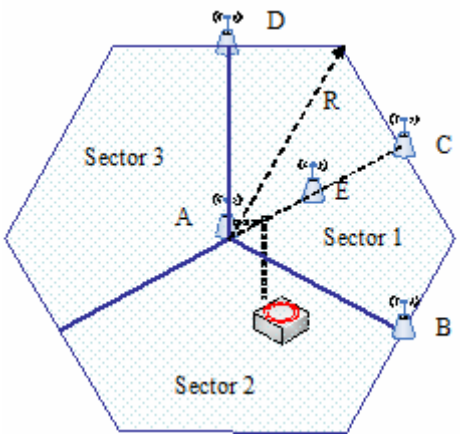

Figure 9.6 Proposed cell architecture with remote BSs

$$N = QL \tag{9.1}$$

In the short term, channel coefficients $h(t)$ may have one set of correlation which reflects the geometry of the propagation environment. Each mobile k estimates the CSI and calculates the correlation function $\mathbf{R_{k,c}}$ for each cluster $c \in \{1, 2, ...Q\}$ during one downlink subframe (5ms).

$$\mathbf{R_{k,c}} = \mathcal{E}\{\mathbf{h_{k,c}(t)h^{*}_{k,c}(t)}\} \tag{9.2}$$

where $\mathcal{E}\{.\}$ denotes expected value. To reduce more the amount of feedback, common transmission weights for all clusters are used. Therefore, the average correlation matrix

$$\mathbf{R_k} = \sum_{c=1}^{Q} \mathbf{R_{k,c}} \tag{9.3}$$

is sent back to the transmitter. Beamforming could support the communication of multiple-users with the same BS simultaneously in the same frequency band through the Spatial Division Multiple-Access (SDMA) technique. In this approach, the transmitter constructs beams in order to spatially separate several users and therefore reduce interference on each-other. In a network with fast moving users and where the channel changes rapidly, it's difficult to enable SDMA since imperfect CSI is known at the BS. Beamforming combined with SM provide parallel spatial channels with high power and thus give multiple high data rate streams. Using more spatial degrees of freedom for each individual link, the interference to neighboring cells increases and spectral efficiency is reduced. The approach of cell sectoring and frequency reuse is proposed due to its simplicity and practicality. The (1,3,3) scheme as in fig. 2 splits each cell into three sectors. The cell capacity is multiplied by three but since a separate subset of frequencies is allocated to each sector, three subsets of frequencies are needed to serve the entire cell. In that case, it appears that increasing the FRF from 1 to 3 combined with sectorization does not affect the capacity. However, it allows limiting the inter-cell interference.

Under the assumption of the knowledge of the correlation function $\mathbf{R_{i,k}}$, $i \in \{1, 2, ..., N_p\}$ and $k \in \{1, 2, ...K\}$, where N_p is the total number of DA arrays and K the total number of users in the sector, our proposed scheme consists of simultaneously designing downlink beamformers for each of three sectors in order to maximize the total throughput under the constraints of achieving a minimum received SINR to each intented receiver and keeping the transmit power smaller than a maximum value. Guaranteeing a minimum SINR=20 dB at each mobile, we can enable SM in an efficient manner. Over a frequency selective channel, different users experience different amount of fading at a particular period of subframe. We take advantage of multiuser diversity by applying the OFDMA technique and scheduling efficiently the data tones to the users. For each group of subcarriers belonging to one of the clusters of the sector, each user sends back a representive rate about the DA array i

$$C_{i,k,c} = log_2(1 + SINR_{i,k,c}) \qquad (9.4)$$

Within one cluster, all subcarriers may not support the representive rate $C_{i,k,c}$. The users inform the CS regarding the subcarriers that could be employed. Additionally, multiuser diversity in an OFDMA system provides another form of diversity in the frequency domain by assigning different clusters to different users according to SINR and may reduce intercell interference. However, the proposed cell architecture has the drawback of the Fractional Frequency Reuse (FFR) sheme. The mobiles belonging to a sector that can only use part of the whole frequency band and suffer from loss of frequency diversity gain.

9.3 Cell architecture

We developed an RoF system in order to reduce the cost of the remote DA arrays. All signal processing (beamforming, scheduling, RF generation and modulation, etc) is made in the CS. The signal to be transmitted by remote BSs is transmitted from the CS to the BS's in the optical band via a fiber optic network. Each remote BS includes only Optical to Electronical (O/E) and Electronic to Optical (E/O) convertes, the antenna array (N_t=4 antenna elements with omnidirectional or 180° sectorized radiation pattern) amplifiers (power at the transmission and low noise at the receiption. The considered system is shown in figure 9.5. Multiple remote BSs are connected to one CS. There are N_p remote BSs distributed around the cell each with N_t antenna elements. At each downlink subframe, the N_p DA arrays construct beams that are allowed to simultaneously transmit streams of OFDM modulated symbols to users. The users separate the respective streams by processing the signal vectors received at each antenna array with N_r antenna elements. The proposed cell architecture is depicted in figure 9.6. Each cell is assumed to have a hexagonal shape with radius R and is partitioned into three 120 degrees sectors. FRF=3 is employed. Two structures of the remote BSsis investigated:

a) One remote BS at each sector positioned at the center of sector (point E) or at the edge of the sector (point C). The deployment could be approached as circular layout with radious $r = \sqrt{3}/4R$ and $r = \sqrt{3}/2R$.

b) Four remote BSs are placed at the edge of each sector (points A,B,C and D). The concept of Virtual Cell (VC) is used [87]. The mobiles belonging to a sector have their own VC and they change as they move from one sector to another. The VC is composed from the remote BSs belong ing to one sector and is mobile-centered. The mobiles communicate only with the antennas within their VC. Each CS dedicates a subset of its remote BSs to a VC according to the received signal power or the more reliable SINR. High data rates can be supported by applying the SM and beamforming techniques into the DA arrays VC.

9.4 Multiuser downlink beamforming

The transmit beamforming with partial CSI available at the transmitter is the optimum scheme for a MIMO point to point system [73]. The beamforming vector $\mathbf{V_{ik}} = [v_{i1}^k \; v_{i2}^k \; v_{i3}^k \; v_{i4}^k]^T$ is applied before the data symbols being transmitted. At each remote BS, the $N_t = 4$ antenna elements form a uniform linear array. The antenna elements are highly correlated due to half wave length spacing between consecutive antennas (e.g. d=λ/2). The number of receive antennas is $N_r = 4$ with spacing λ/2 too.

These values are compliant with [10,11]. Let's assume $\mathbf{H_{ik}}$ the channel matrix between i remote BS and mobile k. This channel matrix can be represented as

$$\mathbf{H_{ik}} = [h_{jl}^{ik}]$$

$$j \in \{1, 2, ..., N_r\}$$

$$l \in \{1, 2, ..., N_t\} \quad (9.4)$$

Let's assume the matrix H_k that is composed of the equal size submatrices $\mathbf{H_{ik}}$

$$\mathbf{H_k} = [\mathbf{H_{1k}}|\mathbf{H_{2k}}|...|\mathbf{H_{N_pk}}] \quad (9.5)$$

Then we define the transmit matrix $\mathbf{V_k}$, which is composed of N_p beamforming vectors $\mathbf{V_{ik}}$

$$\mathbf{V_k} = [\mathbf{V_{1k}}|\mathbf{V_{2k}}|...|\mathbf{V_{N_pk}}] = \quad (9.6)$$

$$\begin{bmatrix} v_{11}^k v_{12}^k v_{13}^k v_{14}^k & 0\ 0\ 0\ 0 & \cdots & 0\ 0\ 0\ 0 \\ 0\ 0\ 0\ 0 & v_{21}^k v_{22}^k v_{23}^k v_{24}^k & \cdots & 0\ 0\ 0\ 0 \\ \vdots & \vdots & \ddots & \vdots \\ 0\ 0\ 0\ 0 & 0\ 0\ 0\ 0 & \cdots & v_{N_p1}^k v_{N_p2}^k v_{N_p3}^k v_{N_p4}^k \end{bmatrix}^T$$

If the transmit signal is presented with vector X_0, of size N_p x 1 (N_p streams are transmitted at the same time slot), where

$$\mathbf{X_0} = [x_0^1\ x_0^2\ ...\ x_0^{N_p}] \quad (9.7)$$

and the received matrix is

$$\mathbf{Y_k} = [\mathbf{Y_1}|\mathbf{Y_2}|\cdots|\mathbf{Y_{N_p}}] \quad (9.8)$$

with

$$\mathbf{Y_i} = [Y_1^{ik}\ Y_2^{ik}\ \cdots\ Y_{N_r}^{ik}] \quad (9.9)$$

of size N_r x 1 is given by the following equation

$$\mathbf{Y_k} = \mathbf{H_k}\ \mathbf{V_k}\ \mathbf{X_0} + \mathcal{N}_\mathbf{k} + \mathcal{I}_\mathbf{k} \quad (9.10)$$

$$\mathcal{N}_\mathbf{k} = [n_k^1|n_k^2|\cdots|n_k^{N_p}] \quad (9.11)$$

n_k^i is the zero mean Additive White Gaussian Noise (AWGN) size N_r x 1 .

$$\mathbf{I_k} = \overbrace{[I_0^k|I_0^k|\cdots I_0^k]}^{N_p} \quad (9.12)$$

is the inter-cell co-channel interference measured from user k in the multicell deployment

$$I_0^k = \sum_{c=2}^{C} \sum_{p=1}^{N_p} |\mathbf{V_{ck}^p H_{ck}}|^2 \quad (9.13)$$

where C is the total number of cells. The $N_p I_0^k$ values in (9.12) are all the same. Note that while the above analysis is specific to a flat fading channel, it can easily be extended to a frequency – selective channel if the system uses OFDM. The OFDM technique effectively divides a large frequency band into small narrowbands so that the transmitted signals on each narrow band experience flat fading. Since we focus on transmit beamforming, we assume that the receiver k only combines the signals from antenna elements and that co-channel interference between the streams is not present. For each remote BS i belonging to a sector $s \in \{1,2,3\}$, we design downlink beamforming by minimizing the total transmit power under the constraint of providing a required received SINR to each mobile k of the sector s. Our assumption is the knowledge of the correlation matrix $\mathbf{R_k}$.

$$\begin{aligned} \mathcal{Q}9 \qquad & \min \|\mathbf{V_i}\|_2^2 \\ \text{s.t.} \quad & \frac{|\mathbf{H_{ik}V_i}|^2}{\sigma_0^k + I_0^k} \geq \gamma_{ik} \\ & \forall k \in \{1,2,\cdots,K\} \\ & \forall i \in \{1,2,\cdots,N_p\} \end{aligned}$$

σ_0^k is the noise power at the receiver and γ_{ik} is the guaranteeing SINR. We remark that $\|\mathbf{H_{ik}V_i}\|^2 = \mathbf{V_i^H H_{ik}^H H_{ik} V_i} = \mathbf{V_i^H R_{ik} V_i}$. The problem $\mathcal{Q}9$ can be written

$$\begin{aligned} \mathcal{Q}'9 \qquad & \min \|\mathbf{V_i}\|_2^2 \\ \text{s.t.} \quad & \frac{\mathbf{V_i^H R_{ik} V_i}}{\sigma_0^k + I_0^k} \geq \gamma_{ik} \\ & \forall k \in \{1,2,\cdots,K\} \\ & \forall i \in \{1,2,\cdots,N_p\} \end{aligned}$$

For general channel vector V_i, the problem $\mathcal{Q}'9$ can be solved as in section 5.3.

9.5 MMSE-SIC receivers

The independent data streams arrive at the multi-user receivers in a cross-coupled fashion. The receivers must separate efficiently the data streams by exploiting the spatial degrees of freedom. Firstly, we assume that instantaneous CSI is available at the receiver side. Maximal likelihood (ML) detection minimizes the bit error rate probability. It's a non linear operation with high implementation complexity and power consumption, which are both very important constraints for a mobile device. We make a trade-off between performance and complexity by considering Minimum Mean Square Error (MMSE) receivers. It's very difficult for a MMSE receiver with M_r =4 antenna elements to suppress intercell interference. If each one of the C-1 neighboring cells is developed with N_p BS , the total number of independent interferes is N_p x(C-1) << M_r .

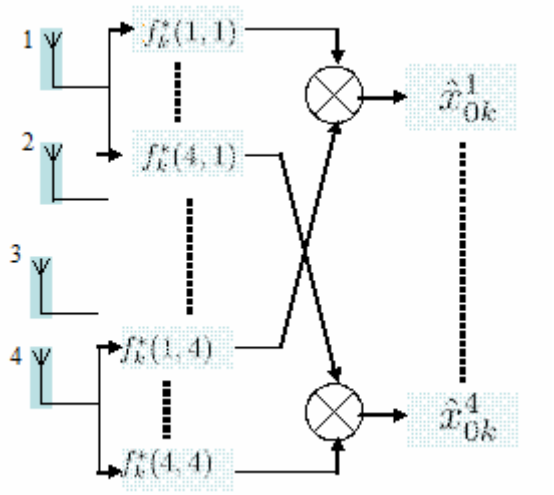

Figure. 9.7 MMSE filter banks with four antenna elements at the receiver

The MMSE algorithm separates the signals of the simultaneous streams by a minimum mean square error linear filter. The estimation vector $\hat{\mathbf{X}}_\mathbf{0}$ is obtained using the theory for linear optimum discete-time Wiener filters[88].

$$\hat{\mathbf{X}}_\mathbf{o}^\mathbf{k} = \mathbf{F}_\mathbf{k}^\mathbf{H}\mathbf{Y}_\mathbf{k} \qquad (9.14)$$

The filter weights are

$$\mathbf{F_k} = [f_k(i,j)] \qquad (9.15)$$

The coefficients $f_k(i,j)$ are designed to minimize the mean square error

$$d_k = \mathcal{E}\{(x_{0k}^i - \hat{x}_{0k}^i)^*(x_{0k}^i - \hat{x}_{0k}^i)\} \qquad (9.16)$$

The computation of the optimum filter coefficients requires the knowledge of the correlation matrix of the received signal $\mathbf{Y_k}$ and the desired response $\mathbf{X_{0k}}$.

$$\mathbf{F_k} = \mathcal{E}\{\mathbf{Y_k}\mathbf{Y_k^H}\}^{-1}\mathcal{E}\{\mathbf{Y_k}\mathbf{X_0^H}\} \qquad (9.17)$$

Assuming $\mathcal{E}\{\mathbf{X_0^H}\mathbf{X_0}\} = \mathbf{I_{N_p x N_p}}$ and that the channel matrix $\mathbf{H_k}\mathbf{V_k}$ is known without any error at the receiver we get

$$\mathbf{F_k} = \mathbf{H_k}\mathbf{V_k}[\mathbf{H_k}\mathbf{V_k}(\mathbf{H_k}\mathbf{V_k})^\mathbf{H} + (\sigma_0^k + \mathbf{I_0^k})\mathbf{I_{N_r x N_r}}]^{-1} \qquad (9.18)$$

A bank of separate MMSE filters, each estimating the parallel data stream i is illustrated in figure 9.7. The inter-stream interference is suppressed if the "spatial signature" $\mathbf{H_{ik}}$ of each stream i is not a linear combination of the spatial signatures of the other streams. Therefore, the number of data streams N_p is chosen to be smaller or equal to the number of receiving antenna elements M_r. The

$SINR_k(i)$ observed at the output of the receiver after equalization (multiplication with filter coefficients) for each user k is

$$SINR_k(i) = \frac{\left|(\mathbf{f}^{\mathbf{i}}_{\mathbf{sdm,k}})^{\mathbf{H}}\mathbf{H_{ik}}\mathbf{V_i}\right|^2}{\sum_{l\neq i}\left|\mathbf{f}^{\mathbf{i}}_{\mathbf{sdm,k}}\mathbf{H_{ik}}\mathbf{V_l}\right|^2 + \left\|\mathbf{f}^{\mathbf{i}}_{\mathbf{sdm,k}}\right\|^2(\sigma_0^2 + I_0^k)} \qquad (9.19)$$

$\mathbf{f}^{\mathbf{i}}_{\mathbf{sdm,k}}$ is the ith row of the matrix $\mathbf{F_k}$. In the selection diversity strategy where just one BS is chosen for transmission, the BS i_k^{max} with the maximum magnitude of subchannel response is selected to carry data symbols.

$$i_k^{max} = \arg\max_{i,\forall q}\sum_{j=1}^{M_r}\sum_{l=1}^{M_t}\left|\tilde{h_{jl}^{ik}}(q)\right|^2 \qquad (9.20)$$

where $\tilde{h_{jl}^{ik}}(q)$ is the average value in the frequency domain for cluster q. Although optimal linear filtering is applied at the receiver along with beamforming at the transmitter and the streams themselves do not have a high degree of correlation in their channel vectors, inter-stream interference may be still present, especially in multipath channels, where the frequency response presents deep attenuation for certain sub-carriers. To deal with this, the Succesive Interference Cancellation (SIC) technique can be used. SIC is nonlinear and ranks the streams at each user k and provides reduction of inter-stream interference for weaker streams. SIC is asymptotically optimal when perfect CSI is assumed but is very sensitive to inaccurate CSI. Additionally, SIC presents high complexity for low power mobile units. In our case, SIC algorithm is implemented in the following way:

1st step: The $SINR_k(i)$ for all streams $i \in \{1, 2, ...N_p\}$ is calculated. The stream with the largest $SINR_k(i)$ is selected as the target stream. Without loss of generality, we assume that streams have decaying SINR from 1 to N_p. The estimate $\hat{x_{0k}^1}$ for the data stream 1 is obtained by applying the vector $\mathbf{f}^{\mathbf{1}}_{\mathbf{sdm,k}}$ as in figure 9.7.

2nd step: The interference that may originate from the stream 1 is reconstructed and subtracted from the initial received signal $\mathbf{Y_k}$. This operation models the SIC and is realized by putting $\mathbf{H_{1k}}$ equal to zero matrix.

3rd step: Step 1 is repeated until all streams are detected.

9.6 Simulation results

A system according to IEEE 802.16e specifications is assumed. Simulations were done in the MATLAB environment. The analysis model contains a hexagonal cell grid consisting of cells with radius R=500m and includes six interfering cells. Sectorization (cell layout with three sectors) and frequency reuse with FRF=3 at each sector to mitigate co-channel interference are assumed. Table 7.2

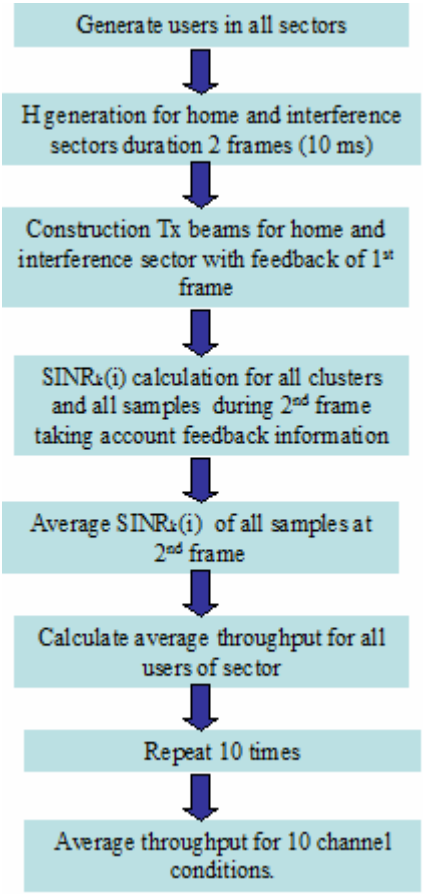

Figure 9.8 Simulation procedure

summarizes our simulation parameters. All cells have the same configuration. The position of the distributed BS is set as in figure 9.6, according the symmetry of the sector. A conventional cell with a BS at the center of the cell is used for comparison. For reasons of fairness, the transmitted power of the conventional cell is assumed to be equal to the sum of the transmitted powers of all distributed BSs in the cell. We assume an (1,3,3) cellular configuration and that the users are uniformly generated in one sector with the same subset of frequencies for reducing the computation load. In other words, we don't take into account adjacent channel interference but only co-channel interference from neighboring cells. Channel matrices for the home sector and interfering sectors users are generated. $SINR_k(i)$ is calculated at the home sector considering pathloss, shadowing, multi-path fading, inter-stream interference and inter-cell interference. The PHY data rate according to the SINR at each stream is calculated from table 7.4, which gives the type of modulation and coding rate that is used to a WiMAX receiver in relation to the received SNR. Simulations are performed at least ten times, for collecting sufficient statistics of the channel. Figure 9.8 presents simulation procedure. The C2 metropolitan area for urban macro-cell from WINNER II channel model is used [24]. The BSs are placed above roof tops and the mobiles move on the streets. The spatial channel model parameters which characterize each channel scenario are based on the WINNER measurement campaigns at a

central frequency within the range 2-6 GHz and at bandwidth of 100 MHz. The model generates the MIMO channel matrices for all links over a specified number of time samples. The channel matrices are produced in the time domain. OFDMA technique is applied in the frequency domain. In this case, the generated channel samples are interpolated and Fast Fourier Transform (FFT) is done to transform the samples in the frequency domain. The WINNER channel is a spatial channel model (SCM) with correlated shadow fading, delay spread and angular spread. Shadow fading is a log-normally distributed random variable with 8dB standard deviation.

The performance gains obtained by placing different numbers of distributed BS's at different positions are investigated. First, only one BS per sector is employed to achieve performance improvement with minimal cost. The different positions of the antenna arrays are set as in figure 9.6. Figure 9.9 presents the average total throughput per sector as a function of the number of users for different schemes:

a) One BS is placed at the point C on the cell edge (4DA-HL scheme)

b) One array is set at the center of sector (point E) (4DA-CL scheme)

c) one antenna element is placed also at point E (1DA-CL scheme)

d) Conventional layout where one BS is located at the center of cell.

Figure 9.10 illustrates the average PHY data rate for different cell radii while figure 9.11 shows the distribution of the achievable throughput per user within the sector. It can be seen that the architecture with antenna arrays has superior performance due to the beamforming technique. The small amount of throughput improvement when the BS is placed at the cell edge instead of the center of the sector is justified by the fact that in the first case, antenna elements with 180 degrees pattern can be used instead of omnidirectional ones. Furthermore, figure 9.11 shows the fairness improvement among the users. Figure 9.12 shows that similar performance is obtained if the BS with four 180° sectoral antenna elements is placed at the cell edge or at the cell center. Finally, we evaluate the performance of SM for the proposed architecture with four BS's at the sector border as in figure 9.6 (points A, B, C and D). The proposed distributed MIMO scheme (SM-4BS) is compared with the "Best BS "selection scheme and with the layout where one BS is placed at the center of the cell. Figure 9.13 and 9.14 present the significant improvements of the SM technique for one and ten users randomly distributed in one sector. The throughput variation in figure 9.14 is smaller due to the user diversity. Figure 9.15 compares the MMSE and SIC technique in case of 15 users randomly distributed in the sector and when SM is applied. We don't observe significant spectrum efficiency improvements due to SIC technique because of beamforming and of the geographical distribution of theBS's that yield additional gains and spatial degrees of freedom for extracting the data streams with MMSE.

Furthermore, the fairness is improved among the users as is illustrated in figure 9.16. Without SM, the maximum average throughput per sector is 10 Mbits/s and in case of SM only 5% of users achieve throughput smaller than 15 Mbits/s.

Figure 9.17 shows the variation of the constructed beamforming at four consecutive frames due to the WINNER II channel changes. The mismatch is negligible between the 1st and 2nd frames. Additionally, no degradation exists between the instantaneous average SINR per user within one frame delay (figure 9.18). Therefore, our proposed feedback scheme doesn't yield a considerale CSI mismatch for one frame delay. The average covariange feedback scheme during one frame cannot be considered as "obsolete" and contains useful information for constructing beams and scheduling at the following frame.

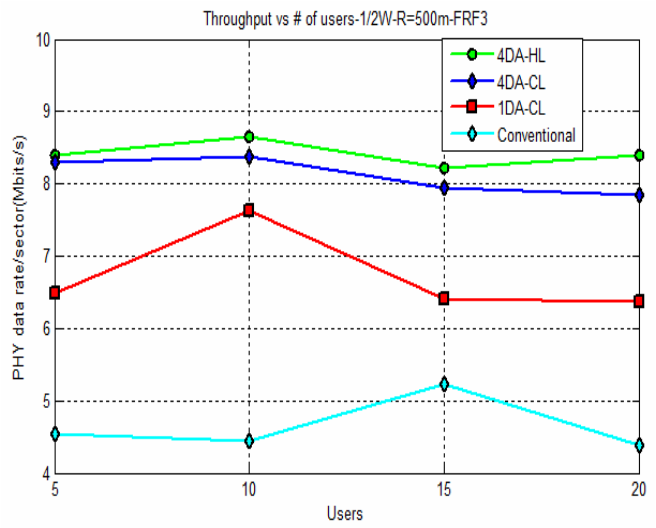

Figure 9.9 Average PHY data rate throughput per sector versus number of users when one BS is placed in different positions of the sector

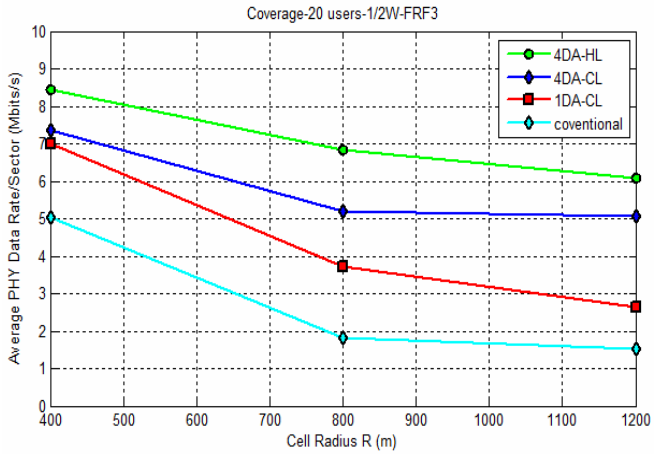

Figure 9.10 Coverage for the different schemes with 20 users randomly disttrbuted in the sector

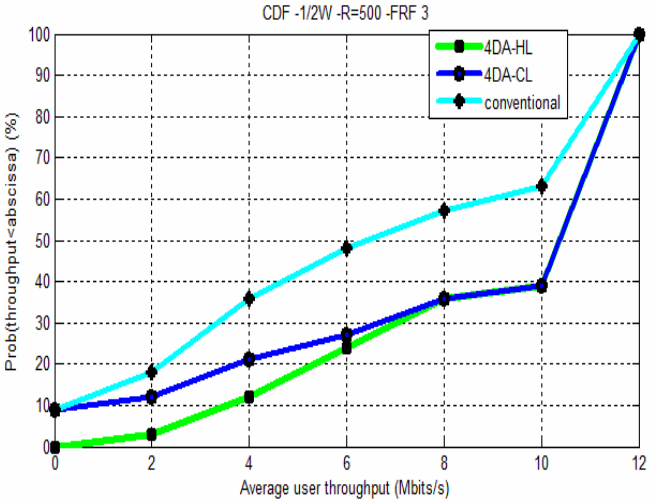

Figure 9.11 Users' throughput distribution

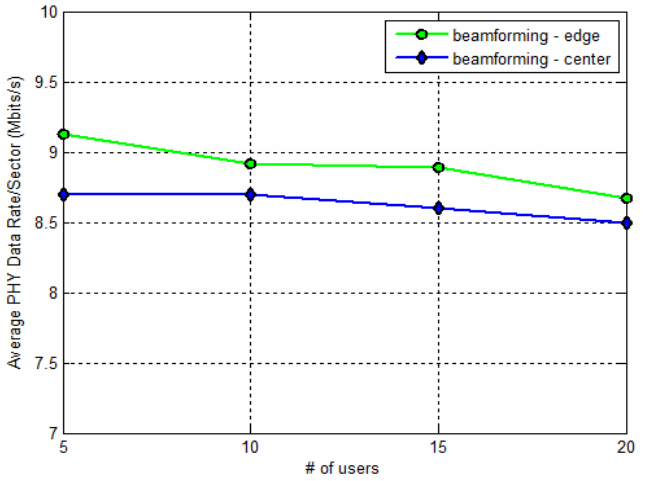

Figure 9.12 Average PHY data rate per sector versus number of users for sector edge - center position of BS

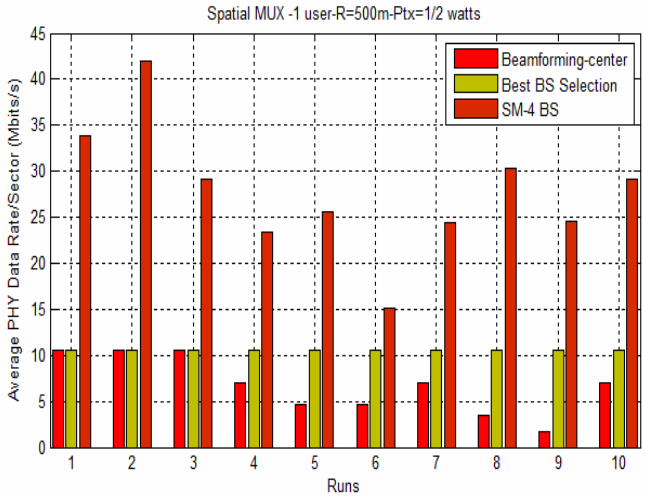

Figure 9.13 Average PHY data rate per sector of SM technique for 10 runs with 1 user randomly distributed

in the sector

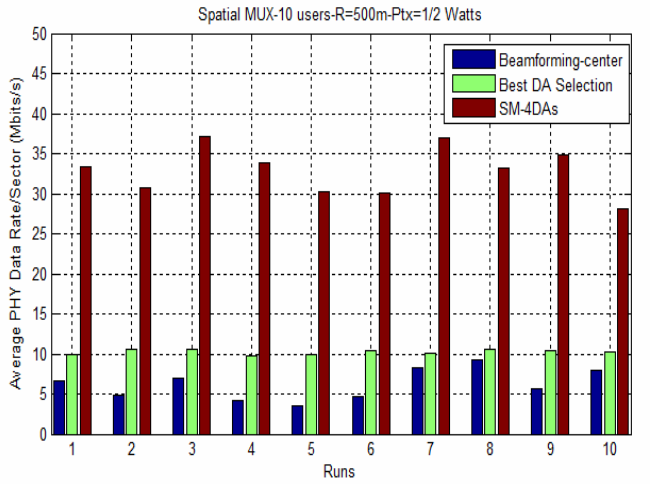

Figure 9.14 Average PHY data rate per sector of SM technique for 10 runs with 10 usersrandomly distributed

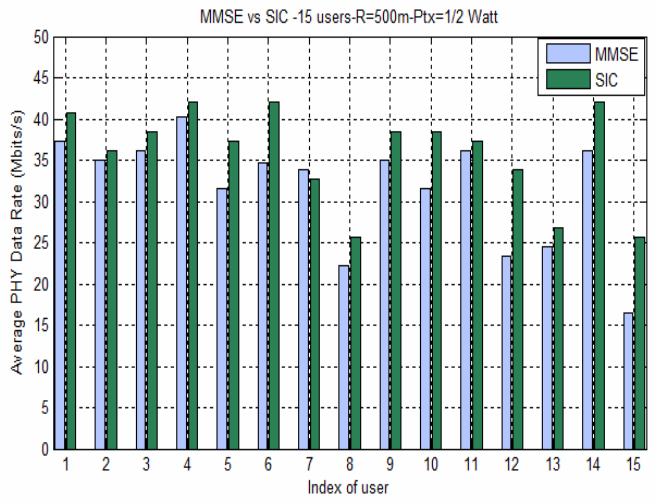

Figure 9.15 MMSE versus SIC

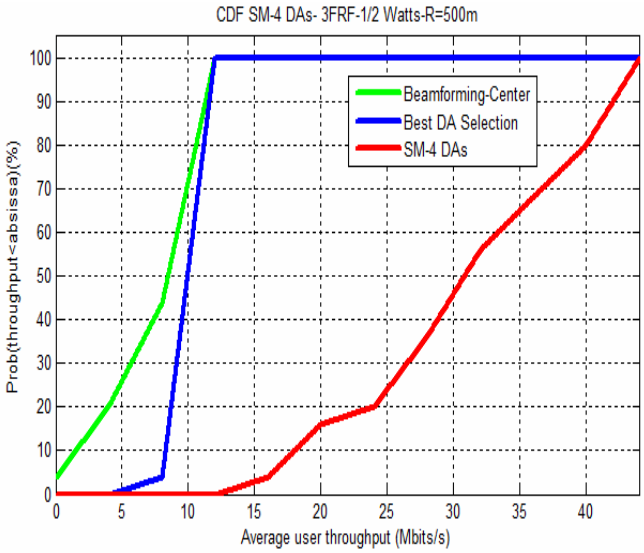

Figure 9.16 Users' throughput distribution when SM is applied

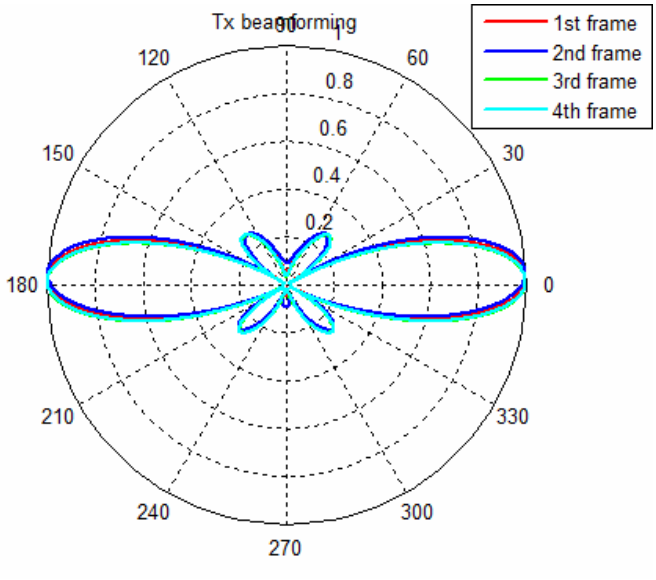

Figure 9.17 Beamforming - mismatch in WINNER II channel model

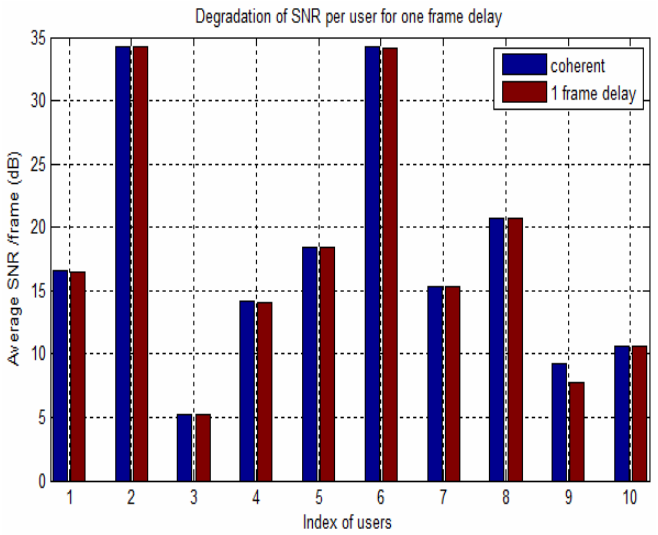

Figure 9.18 Degradation of SNR per user for one frame delay

9.7 Conclusions

Novel cell architecture with distributed antenna arrays for a mobile WiMAX system in a multi-cell interference environment were presented. We have analyzed the advantage of combining SM, beamforming and distributed Antenna Arrays. The computer simulation results suggest that the proposed system efficiently reduces co-channel interference from neighboring cells and improves the SINR leading to a great improvement of highly mobile users in terms of total throughput and fairness.

Chapter 10

Provision for the deployment of a wimax solution

Modern communication systems providers, that have been dynamically present in the market, intend to deploy a Mobile WiMAX system for extending the coverage of their Next Generation Networks. The vendors target flexible solutions in order to deploy an ambitious mobile WiMAX network with appropriate scale economics. The objective of this chapter is to analyze the deployment of a WiMAX network and provide an understanding of the cost structures, taking into account the information and features for the Base Station (BS) and Customer Premises Equipment (CPE) from the vendors.Network planning is the primary stage before any system deployment. It provides the necessary estimates for capacity and coverage with the most cost-effective set of sites. However, network planning is an on-going process during the whole lifecycle of the network for determining the best placement of the BSs and assigning the frequency channels. The number of BSs determines the installation cost. Besides, the planning process for a WiMAX system has more parameters to configure than a traditional system.

The dimensioning of a point to multi-point WiMAX link with relays in order to confirm the existence of Line of Sight (LOS) conditions is presented in [89]. The design of the link had taken into consideration the carrier to noise ratio and the minimum carrier to noise ratio with fading for different types of modulations. The principles of a WiMAX dimensioning tool introduced by Fujitsu are described in [90]. The computation of cell throughput is based on the summation of the capacity that corresponds to each Adaptive Modulation and Coding (AMC) scheme. System capacity is theoretically calculated. The difference with our work is that the calculation of link budget, coverage and capacity takes account the values from data sheets. Additionally, the throughput of the external ring boundary is not defined only from maximum allowable path loss as in[90] but also the coverage area is considered under the assumption of uniform distribution of subscribers. Finally, infrastructure with hexagonal and not circular cells as in [90] is taken into account.

In this work, we define a novel methodology, based on the dynamic nature of the WiMAX network for the estimation of the number of sites. We compare different hypothetical vendor solutions by specifying how many BSs will be covering a given area under the same propagation parameters (propagation model, antenna height, etc), margins (building penetration, interference margin, etc) and cell throughput requirements. The main contribution of this paper is that it proposes a simple method for a WiMAX provider to compare the technical solutions offered by the vendors and

demonstrates how the promised mandatory and optional features affect the cost of infrastructure. Since WiMAX demands a guaranteed Quality of Service (QoS), careful dimensioning ensures that the deployment for coverage does not sacrifice capacity and vice versa. The number of BSs and the data density required form the key elements in a mobile WiMAX network. The case study for selected regions of deployment with three WiMAX technical solutions aims to help understanding the benefits that WiMAX technology brings, its architecture and shows how to dimension the access network.

This chapter is organized in the following way: Section 10.1 presents the novel methodology for the estimation of the number of sites. Simulation results are shown and explained in section 10.2.

10.1 Methodology

Our objective is to estimate the number of sites required to provide coverage and capacity for a service area. Capacity requirements are determined from the following factors:

- marketing parameters such yearly equipment and forecast for a longer term
- demographic region
- QoS to be offered to the subscribers including web browsing, e-mail, Voice over Internet Protocol (VoIP), real time applications like video games, etc
- Data density which imposes the classification of the users according to the load that they demand.

Also, BS and mobile equipment data sheets are required. For the dimensioning process the following assumptions are adopted:

a) The air interface is modeled based on the modified COST 231-Hata propagation path model. This model includes correction factors to accommodate frequencies supported by WiMAX

b) The area of interest is covered uniformly by the estimated cells

c) The cell shape is considered to be hexagonal

d) Each cell is sectorized according to the geographical coverage requirements

e) The subscribers are assumed to be distributed in a uniform manner throughout the area of interest

f) Full Frequency Reuse (FFR) scheme is assumed according to which a mobile uses all the available subchannels when it is close to the center of the cell. At the borders, it uses only part of the subchannel set. This technique avoids the need for interference management planning and optimization. A mobile WiMAX system transmits on subchannels and does not occupy an entire

channel which gives the advantage of the FFR. All hexagons use the same frequency/set of frequencies. This may lead to increased interference but results in high overall spectrum usage. The interference is a function of the transmitted power, DoA (Direction of Arrival) and DoD (Direction of Departure) of interfering signals, directional patterns of Tx and Rx antennas, the path loss of each interfering signal and collision probability. The co-channel interference is not explicitly calculated but taken into account as a certain constant performance degradation value.

g) Fade margins are approximated selected in order to support the worst case scenario. To that aim, a building penetration loss parameter is selected to specify the maximum path loss between BS and mobile.

The AMC scheme leads to a ring structure for capacity calculation. The key feature of AMC is that it dynamically increases the range to which a higher modulation and coding scheme can be used. According to fading conditions, the system can have a flexible AMC allocation instead of having a fixed scheme that is related to the worst case conditions. Strong Reed Solomon FEC, convolutional encoding and interleaving is used to detect and correct errors. HARQ is used to correct errors that cannot be corrected by the FEC. At the beginning, the PHY throughput is calculated for ring boundaries, which are determined from eight MCS combinations as in figure 10.1. The inner ring corresponds to 64 QAM with code rate 5/6 mode while the outer ring to QPSK with ½ code rate . Path loss is estimated for each mode $M \in \{1,2,\cdots 8\}$.

$$PL(M) = EIRP(BS) - RXsensitivity(M) - FM \qquad (10.1)$$

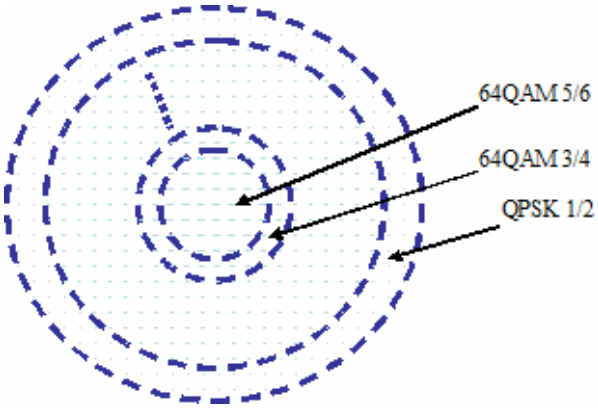

Figure 10.1 Relative cell radius for adaptive modulation and coding scheme

Where the *EIRP(BS)* the effective isotropic radiated power measured at the BS. Tx beamforming gain and diversity gain for MIMO A scheme are added to the *EIRP(BS).* The *RXsensitivity(M)*

consists of the receiver sensitivity for all the AMC schemes obtained from the equipment vendor's datasheet. The extra gain by macro diversity handover, subchannelization gain and receiver diversity gain are included. *FM* is the link margin which is the sum of building penetration loss, repetition coding gain, HARQ gain and interference margin. The COST-231 Hata propagation model uses an expression for the median path loss *PL(M)* as a function of carrier frequency, antenna heights and the distance between the BS and mobile. This extended path loss model is given by the following formula:

$PL=46.3+33.9\log_{10} f-13.82\log_{10} hb + (44.9-6.55\log_{10} hb)\log_{10} d - a(hm)+CF \quad (10.2)$

The mobile antenna-correction factor *a(hm)* is given by

$a(hm)=(1.11\log_{10}-0.7)\,hm-(1.56\log_{10} f-0.8) \quad (10.3)$

where f is the carrier frequency in MHz, *hb* is the BS height in m, *hm* is the mobile antenna height in m and *d* is the distance between the BS and mobile in Km. For an urban area the correction factor *CF* is 3 dB and for suburban and open area is 0 dB. The model is valid for the following range of parameters:

- 150 MHz $\leq$ f $\leq$ 2000 MHz
- 30m $\leq$ *hb* $\leq$ 200m
- 1m $\leq$ *hm* $\leq$ 10m
- 1Km $\leq$ *d* $\leq$ 20Km

If R_M =*d* is the ring radius that corresponds to different AMC modes ($R_9 = 0$) and is calculated from Hata propagation model we introduce

$$Q_M = \frac{\pi R_M^{\,2} - \pi R_{M+1}^{\,2}}{\pi(\max R_M)^2} \qquad (10.4)$$

This factor expresses the percentage of each ring area to cell area. The cell throughput is equal to

Throughput_cell (R_M)=Σ {*Rx_throughput(M)* * Q_M } (10.5)

Rx_throughput(M) is the receiver throughput of the equipment for each MCS mode given from vendor's datasheets. It depends on the type of MIMO scheme (A or B), the specific TDD frame DL-UL ratio, the sub-carrier allocation scheme, the consequent signaling overhead and the available operating bandwidth. An interpolation technique between calculated data points *Throughput_cell* (R_M) is applied for calculating the PHY cell throughput as a function of cell radius R_i. Our method was based on a circular grid pattern. We replace in equation (10.4) the circular area $\pi R_M^{\,2}$ with the

area of hexagon $3\sqrt{3}/2\, R_M^2$ which is inscribed inside the circle radius R_M . So, we transform a circular cell into a hexagonal one. Then we estimate the number of BSs in the following way:

1.We make an effort to fit the service area with hexagon cells, all with maximum radius R_1 (QPSK ½ mode).

2. If the capacity requirements can be handled by that radius then the final number of BS is calculated

3. If the capacity requirements are bigger than the calculated throughput then we reduce the radius by a small quantity ΔR and go back to step 2.

10.2 Simulation results

Simulation results are based on information from three typical and hypothetical vendors I, II and III which support four and three sectors configuration at the operating frequency of 3.5 GHz. The system Gain for the three vendors after analytical calculations, taking account link budget template of [91], has been produced and is presented in Table 10.1. We suppose that the three vendors support MIMO and beamforming technology to reduce the number of cell sites needed to cover an area and increase the cell capacity. Table 10.2 shows the calculation of the Effective Isotropic Radiation Power (EIRP) for the three vendors in Downlink and Uplink directions. Matrix A for vendor I offer an additional link budget 2dB at the transmitter and 3 dB at the receiver (2 antennas). Vendor II supports MIMO A scheme by applying beamforming. Eight antennas are used at the Base Station (power combining gain 9 dB) Beamforming MIMO scheme with 8 antenna elements give an extra gain 9 dB in the link budget. Vendor III supports MIMO A transmitters according to the standard. Tables 10.3, 10.4 and 10.5 present receiver sensitivity and throughput for different MCS modes. These values could be picked from equipment data sheets. Throughput values are taken for channel bandwidth 7MHz, assuming the MIMO A scheme and DL:UL ratios of 60% **:** 40%. Figure 10.3 presents the variation of downlink throughput versus the cell radius of cell. For radius bigger than 250m vendors III and II give identical values of throughput. Vendor I has always smaller throughput. When the cell radius is equal to 2.5 Km the downlink throughput is approximately equal for the three vendors. Figure 10.2 shows the variation of uplink throughput versus the cell radius. For cell radius values from 500m to 1.5 Km vendor II solution presents the greater value of throughput and vendor III the smaller while for cell radius bigger than 1.5 Km vendor I has the greater uplink throughput. Finally, we calculated the number of Base Stations for the three vendors under the same propagation

TABLE 10.1 COMPARISON OF THREE VENDORS RADIO SOLUTION

	VENDOR I	
	Uplink	Downlink
EIRP(dBm)	34	50
Minimum receiver sensitivity(dBm)	-98	-96
System Gain (dB)	**132**	**146**
	VENDOR II	
	Uplink	Downlink
EIRP(dBm)	23	64
Minimum receiver sensitivity(dBm)	-123	-98
System Gain (dB)	**146**	**162**
	VENDOR III	
	Uplink	Downlink
EIRP(dBm)	32	56
Minimum receiver sensitivity(dBm)	-96	-94
System Gain (dB)	**128**	**150**

TABLE 10.2 **EIRP CALCULATION**

	VENDOR I	
	Uplink	Downlink
Tx power [dBm]	27	32,5
Number of Tx antennas	1	2
Tx antenna gain [dBi]	7	14,5
Tx cable loss [dB]	0	0
Power combining gain [dB]	0	3
EIRP [dBm]	**34**	**50**
	VENDOR II	
	Uplink	Downlink
Tx power [dBm]	20	30
Number of Tx antennas	2	8
Tx antenna gain [dBi]	3	25
Tx cable loss [dB]	0	0
Power combining gain [dB]	0	9
EIRP [dBm]	**23**	**64**
	VENDOR III	
	Uplink	Downlink
Tx power [dBm]	26	36,5
Number of Tx antennas	1	2
Tx antenna gain [dBi]	6	17
Tx cable loss [dB]	0	0,5
Power combining gain [dB]	0	3
EIRP [dBm]	**32**	**56**

parameters (propagation model, Antenna height, etc), margins (building penetration, interference margin, etc.), capacity requirements for two service areas I and II. Simulation results are presented in Table 10.9. Our calculations are based on propagation parameters and margins of Table 10.6. Table 10.7 depicts the capacity requirements (Mbps) for subscribers/business in DL and UL direction while

Table 10.8 depicts the required area of service (square Km).We remark that the number of sites is approximately the same for vendor III and II. If 4-sector solution of vendor I is chosen, it needs 33% and 27% more sites than vendor's III solution for the 1st and 2nd year of deployment in the service area I. For service area II, it needs 19% and 20% more number of sites respectively. If a 3-sector solution of vendor I is chosen, 62% and 56% more sites than those for the vendors III solution are required for 1st and 2nd year at service area I. For service area II, the corresponding increase in the number of sites is 44% and 50%.Regarding vendor's I solution, due to the low link budget, the coverage area is smaller and the calculating throughput is substantially bigger than the throughput required. In this case, there is no need for additional Base Station to be deployed if more capacity is demanded.

TABLE 10.3 RECEIVER SENSITIVITY AND THROUGHPUT PER MCS FOR VENDOR I

	Vendor I			
	DL		UL	
Modulation & Coding	Sensitivity (dbm)	Throughput (Mbs/s)	Sensitivity (dbm)	Throughput (Mbs/s)
QPSK 1/2	-96	1,7	-98	1,3
QPSK 3/4	-93	2,5	-95	2
16QAM 1/2	-91	3,4	-92	2,8
16QAM 3/4	-87	5,1	-89	4,2
64QAM 1/2	-86	5,1		
64QAM 2/3	-83	6,9		
64QAM 3/4	-81	7,7		
64QAM 5/6	-79	8,6		

TABLE 10.4 RECEIVER SENSITIVITY AND THROUGHPUT PER MCS FOR VENDOR II

	Vendor II			
	DL		UL	
Modulation & Coding	Sensitivity (dbm)	Throughput (Mbs/s)	Sensitivity (dbm)	Throughput (Mbs/s)
QPSK 1/2	-98	2	-123	0,6
QPSK 3/4	-95	3	-120	0,9
16QAM 1/2	-92	4	-117	1,2
16QAM 3/4	-89	6,1	-114	1,8
64QAM 1/2	-87	6,1		
64QAM 2/3	-84	8,2		
64QAM 3/4	-83	9,2		
64QAM 5/6	-81	10,2		

TABLE 10.5 RECEIVER SENSITIVITY AND THROUGHPUT PER MCS FOR VENDOR III

Modulation & Coding	Vendor III			
	DL		UL	
	Sensitivity (dbm)	Throughput (Mbs/s)	Sensitivity (dbm)	Throughput (Mbs/s)
QPSK 1/2	-94	2	-96	1
QPSK 3/4	-90	3	-93	1,6
16QAM 1/2	-87	7,7	-91	2
16QAM 3/4	-83	11,6	-87	3
64QAM 1/2	-82	11,6		
64QAM 2/3	-79	15		
64QAM 3/4	-78	17		
64QAM 5/6	-76	19		

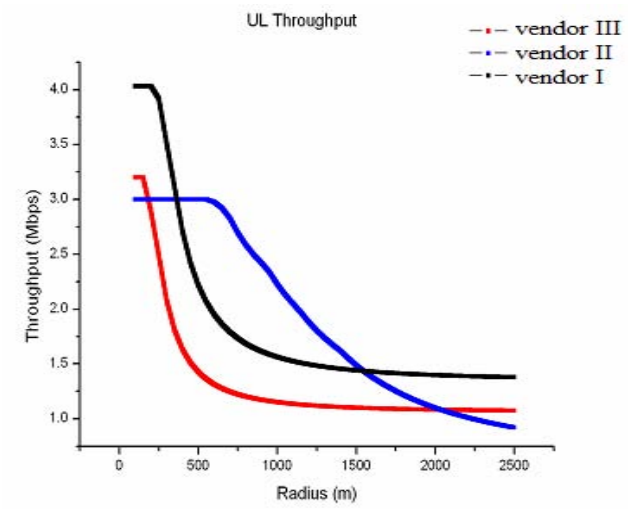

Figure 10.2 Throughput per sector versus radius of the cell for UL direction

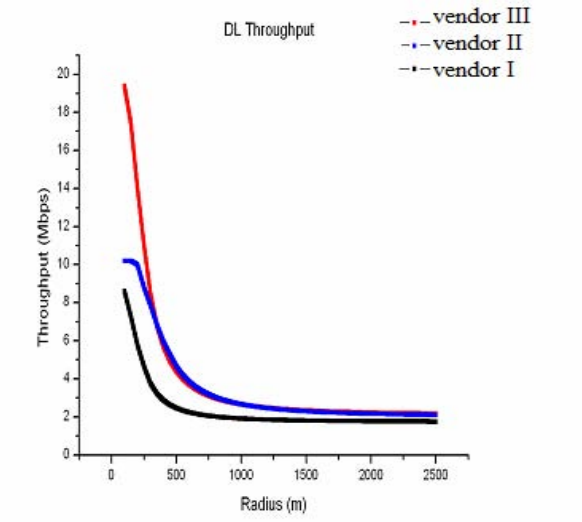

Figure 10.3 Throughput per sector versus radius of cell for DL direction

TABLE 10.6 PROPAGATION PARAMETERS AND MARGINS FOR THREE VENDORS

Propagation Parameters	
BS Height(m)	25
MS height	1,5
Cost-231 Hata Correction factor (dB)	3
Margins	
Fade Margin (dB)	9
Shadow Margin (dB)	10,3
Building penetration loss (dB)	15
Interference margin (dB)	1

TABLE 10.7 CAPACITY REQUIREMENTS FOR THREE VENDORS

Mbps	**Year 1**	**Year 2**
Service Area I	1470	1980
Service Area II	165	220

TABLE 10.8 SERVICE AREA

Sq Km	**Year 1**	**Year 2**
Service Area I	130	350
Service Area II	85	85

TABLE 10.9 SIMULATION RESULTS UNDER COMMON PROPAGATION PARAMETERS AND MARGINS

	Vendor III		
year 1	Sites	Throughput (Mbps)	Area
	100	1775	I
	16	211	II
year 2	Sites	Throughput (Mbps)	Area
	156	2454	I
	20	280	II
	Vendor I		
year 1	Sites	Throughput (Mbps)	Area
	133	2200	I
	19	237	II
year 2	Sites	Throughput (Mbps)	Area
	198	2911	I
	24	318	II
year 1	Sites	Throughput (Mbps)	Area
	162	2108	I
	23	227	II
year 2	Sites	Throughput (Mbps)	Area
	243	2786	I
	30	303	II
	Vendor II		
year 1	Sites	Throughput (Mbps)	Area
	104	1933	I
	17	199	II
year 2	Sites	Throughput (Mbps)	Area
	166	2628	I
	22	274	II

10.3 Conclusions

This chapter explains an approach for understanding the vendors' WiMAX solutions. We introduced a dimensioning method that allows a straightforward estimate of the deployment cost associated with the vendor's offered solutions. In the mobile market, WiMAX and 3G technologies provide the same set of services but since 3G is the evolution of the existing GSM it requires only software upgrades while the WiMAX network has to be built from the beginning. Consequently, our dimensioning method reduces the necessary time and cost for the cell design and assists in the decision of WiMAX vendors for the required network infrastructure investment.

Chapter 11

Conclusions

The technical challenges of the advanced air interface for broadband wireless access systems are addressed. Advanced radio resource allocation schemes involving cross-layer optimization with increased mobility requirement, as well as cooperation between base stations are among the new proposed schemes. The developed concepts and algorithms were simulated for validation. The new technologies that are proposed dramatically improve the performance of the current solutions. Novel cross-layer optimization techniques which support interaction between the application, MAC and PHY layer of BWA systems has been developed in this dissertation.

Each of chapters 5-10 contains significant new contributions. In chapter 5, by applying common transmission weight vectors in all sub-carriers at a set of users, a new distributed algorithm that permits interfering APs to select appropriately their operating frequency and suppress interference in co-working IEEE 802.11n WLANs is proposed. This method increases system performance and significantly reduces implementation complexity and power consumption. Simulation results in a strong interference environment show substantial gain for our proposed strategies. Chapter 6 introduces physical layer multicast transmission and describe a cross-layer approach, enabling techniques as beamforming, MIMO antennas, OFDM and low latency MAC operation.

A dynamic resource allocation algorithm with beam steering is evaluated in chapter 7 for providing broadband wireless access to mobile users of the emerging IEEE 802.16m air interface standard. Coverage area and total throughput be significantly enhanced, compared to the current IEEE 802.16e standard. Our proposed solution supports high mobility, improves fairness among the users and is backward compatible to the mobile networks based on the 802.16e. Chapter 8 studies a multi-user multi-cell MIMO/OFDMA system for next generation BWA networks in which the BS has only knowledge of the statistics of the channel. A combination of MIMO, OFDMA and FDD could increase the spectral efficiency in a high speed network. We investigate methods with scalable channel feedback and we analyze the trade off between the amount of Channel State Information (CSI) to the transmitter and the system performance. The new dynamic radio resource management methods are extended to a reuse-one sectorized cell in order to reduce the cross-sector interference. Finally, the proposed schemes with limited feedback are combined with other cell interference reduction strategies based on cooperation for improving the performance of a coordinated multi-cell system under very dynamic conditions like high velocity and fast fading. Simulation results

demonstrate that substantial gain is obtained by the proposed schemes which take advantage of the statistical information of the highly dynamic channel.

Chapter 9 presents mobile networks based on the IEEE 802.16e standard and provides broadband wireless access to mobile users by applying MIMO and Orthogonal OFDMA techniques. Spatial Multiplexing (SM) increases spectral efficiency but at low SINR) conditions space – time block codes and beamforming achieve higher capacity and throughput. We propose novel cell architecture based on a Distributed Antenna (DA) system to provide high data rate transmission. We combine SM, beamforming and Radio over Fiber (RoF) technologies taking advantage of the partial Channel State Information (CSI) of a downlink multi-user system, obtained through correlation channel matrix feedback that is averaged in the frequency domain. In order to improve further the SINR and reduce co-channel interference from neighboring cells, the proposed architecture coordinates the resource allocation among the cells. Under this structure, several Base Stations (BS) multi-antenna arrays are geographically distributed in the cell to spatially multiplex separate data streams to each user over each OFDM subchannel with high reliability. The proposed architecture enhances the performance of the users and the overall cell throughput. Furthermore, it meets the requirements for the next generation IEEE 802.16m system with high speed users

Chapter 10 proposes a new methodology with which a provider will be able to assess the investment cost associated to the vendor’s WiMAX offered solutions. Hypothetical model networks are examined with the purpose to illuminate our methodology in a given environment.

References

[1] Hills, A., Friday, B. ,“ Radio Resource Management in Wireless LANs”, Communications Magazine, IEEE, Dec. 2004.

[2] International Organization for Standardization and International Electrotechnical Commission, “Information Technology – Open Systems Interconnection – Basic Reference Model,” *International Standard ISO/IEC 7498*, 1984.

[3] V. Srivastava and M. Motani, “Cross-layer design: a survey and the road ahead,” *IEEE Communications Magazine*, vol. 43, pp. 112–119, Dec. 2005.

[4]G. Carneiro, J. Ruela, and M. Ricardo, “Cross-layer design in 4G wireless terminals,” *IEEE Wireless Communications*, vol. 11, pp. 7–13, Apr. 2004.

[5] L. Alonso and R. Agustí, “Optimization of wireless communication systems using cross-layer information,” *Signal Processing*, vol. 86, pp. 1755–1772, Dec. 2006.

[6] V. T. Raisinghani and S. Iyer, “Cross-layer design optimizations in wireless protocol stacks,” *Computer Communications*, vol. 27, pp. 720–724, May 2004.

[7] Shakkottai, S. Rappaport, T.S. Karlsson, P.C., “Cross – Layer Design for Wireless Networks”, Communications Magazine, IEEE, Oct. 2003.

[8] “IEEE Standard for Information technology – Telecommunications and information exchange between systems – Local and metropolitan area networks – Specific requirements – Part 11: Wireless LAN Medium Access Control (MAC) and Physical Layer (PHY) specifications,” *IEEE Std 802.11-2007* (Revision of IEEE Std 802.11-1999), Dec. 2007.

[9] “IEEE Standard for Information Technology – Telecommunications and information exchange between systems – Local and metropolitan area networks – Specific requirements Part 11: Wireless LAN Medium Access Control (MAC) and Physical Layer (PHY) specifications Amendment 5: Enhancements for Higher Throughput,” *IEEE Std 802.11n-2009*, Oct. 2009.

[10] “Mobile WiMAX-Part I: A Technical Overview and Performance Evaluation”, WiMAX Forum, Feb. 2006.

[11] “Air Interface for Fixed and Mobile Broadband Wireless Access Systems”, IEEE STD 802.16e-2005, Feb. 2006.

[12] IEEE 802.16 Broadband Wireless Access Working Group, “IEEE 802.16m System Requirements’, 2007-10-19.

[13] “802.11n Wireless Technology Overview”, White paper, Cisco, 2007.

[14] Nanda, S. Walton, R. Ketchum, J. Wallace, M. Howard, S. , “ A high performance MIMO OFDM Wireless LAN”, Communications Magazine, IEEE, Feb. 2005.

[15] Irina Medvedev, Rod Walton, John Ketchum, Sanjiv Nanda, Bjørn A. Bjerke, Mark Wallace, and Steven Howard “Transmission Strategies for High Throughput MIMO OFDM Communicaton” ICC 2005.

[16] Bianchi, G.,“Performance Analysis of the IEEE 802.11 Distributed Coordination Function”, Selected Areas in Communications, IEEE Journal on**,** Mar. 2000.

[17] Mangold, S. Sunghyun Choi Hiertz, G.R. Klein, O. Walke, B.,“Analysis of IEEE 802.11e for QoS support in wireless LANs”, Wireless Communications, IEEE, Dec. 2003.

[18] IST-4-027756 WINNER II Deliverable 6.13.14, “WINNER II System Concept Description”, v. 1.1, 172 pages, January 2008, https://www.ist-winner.org/.

[19] 3GPP TS 36.211; Physical Channels and Modulation (Release 8).

[20] 3GPP TS 36.211; Medium Access Control (MAC) protocol specification (Release 8).

[21] L. Schumacher, J. P. Kermoal, F. Frederiksen, K. I. Pedersen, A. Algans, P. E. Mogensen, “ MIMO Channel Characterisation”, D2, version 1.1, IST-1999-11729 METRA, February 2001, https:www.metra.org/

[22] 3GPP TR25.996 V6.1 (2003-09)”Spatial channel model for multiple input multiple output (MIMO) simulations” Release 6.

[23] L. Schumacher : Description of a MATLAB implementation note, version 3.2

[24] IST-4-027756 WINNER II D1.1.2 V1.2 WINNER II Channel Models Part I Channel Models, Part II Radio Channel Measurement and Analysis Results.

[25] S. Boyd and L. Vandenberghe, “Convex Optimization” Cambridge, U.K. Cambridge University Press, 2004.

[26] A. Akella, G. Judd, S. Seshan, P. Steenkiste, “Self-Management in Chaotic Wireless Deployments”, Mobicom ’05, Cologne, Germany.

[27] K. Leung and B. –Jo ”J” Kim ,”Frequency Assignment for IEEE802.11 Wireless Networks”, 2003.

[28] A. Mishra, S. Banevjee, W. Arbaugh, “Weighted Coloring based Channel Assignment for WLANs”.

[29] B. Kaufmann, F. Baccelli, A. Chaintreau, V. Mhatre, K. Papagiannaki, C. Diot, ”Measurement –Based Self Organization of Interfering 802.11 Wireless Access Networks” Infocom 2007.

[30] V. Mhatre, K. Papagiannaki, F. Baccelli “ Interference Mitigation through Power Control in High Density 802.11 WLANs“ Infocom 2007.

[31] C. He, F. Liu, H. Yang, C. Chen, Ji Zhang “Co-channel Interference Mitigation in MIMO-OFDM system”

[33] IEEE 802.11h std IEEE 802.11. Part II : Wireless LAN Medium Access Control (MAC) and Physical Layer (PHY) specifications. Amendment 5 : Spectrum and Transmit Power Management.

Extentions in the 5 GHz Band in Europe, 2003

[34] J. B. Andersen “Array Gain and Capacity for Known Random Channels with Multiple Element Arrays at Both Ends”, IEEE journal on selected area in communications, vol. 18 No 11, November 2000, pp 2172-2178.

[35] E. Karipidis, N. D. Sidiropoulos and Z. –Q Luo, “ Transmit Beamforming to multiple co-channel multicast groups”, in Proc. IEEE CAMSAP 2005, Dec 12-14, Puerto Vallarta, Mexico.

[36] N. D. Sidiropoulos, T. N. Davidson, and Z.-Q Luo, “Transmit beamforming for physical layer Multicasting”IEEE Trans. On Signal Processing, vol 54, no 6, pp 2239-2251,June 2006.

[37] M. Bengtsson and B. Ottersten ,”Optimal and suboptimal transmit beamforming” in Handbook of Antennas in Wireless Communications, L.C.Godora, Ed. Boca Raton, FL:CRC 2002.

[38] J.F. Sturm, “Using SeDuMi 1.02 , a MATLAB Toolbox for optimization over symmetric cones “, Optimization Methods and Software, vol 11-12, pp 625-653,1999

[39] Z. Q-Luo,Lecture 13 in Lecture Notes for EE 8950 :Engineering Optimization, University of Minnesota, Minneapolis, Spring 2004, available upon request to luozq@ece.umn.edu.

[40] I. Koutsopoulos, L. Tassiulas, “ Carrier assignment algorithms for OFDM – based and other multi-carrier wireless networks with channel adaptation”, accepted under minor revision, IEEE Transactions on Communications, February 2007

[41] D. Kivanc and Hui Liu,”Subcarrier allocation and Power Control for OFDMAth” ,Signals, Systems and Computers 2000.Conference Record of the Thirty-Four Asilomar Conference on,volume 1, pp.147-151.

[42] Xiaoxin Qiu, Kapil Chawla, “ On the performance of Adaptive Modulation in Cellular Systems” IEEE Transactions on Communications, vol. 47, NO. 6, JUNE 1999

[43] A. T .Hoang,Y.-C. Liang and Md H. Islam,“Maximizing Throughput of Cognitive Radio Networks with Limited Primary Users’ Cooperation”,Institute for Infocomm Research, Technical Report.

[44] J. A. Mc Hugh , “Algorithmic Graph theory “Prentice Hall 1990.

[45] IEEE 802.11 WG,”IEEE 802.11n draft 2.0” Jan. 2007.

[46] L. Schumacher :,”WLAN MIMO Channel Matlab program” , download information:www.info.fundp.ac.be/~lsc/Research/IEEE_802.11_HTSG_CMSC/

distrbution_terms.htm

[47] M.-T. Sun, L. Huang, A. Arora,T.-H. Lai,”Reliable MAC layer multicast in IEEE 802.11 wireless networks”, in Proc. of Int. Conf. on Parallel Processing(ICPP’02), Vancouver, Canada, 18.-21. Aug. 2002.

[48] J. Tourrilbes, “Robust broadcast: Improving the reliability of broadcast transmission on CSMA/CA,” in Proc. of PIMRC’98,1998.

[49] Giuseppe Bianchi,"Performance Analysis of the IEEE 802.11 Distributed Coordination Function", JSAC vol. 18,no 3,March 2000.

[50] WiMAX Forum, "A Comparative Analysis of Mobile WiMAX™ Deployment Alternatives in the AccessNetwork", May 2007

[51] IEEE 802.16 Broadband Wireless Access Working Group, ' IEEE 802.16m System Requirements',2007-10-19.

[52] P. Viswanath, D. Tse, R. Larroia, "Oportunistic Beamforming Using Dump Antennas", IEEE Transactions on Information Theory, Vol. 48,No 6, June 2002.

[53] Man-on Pun, V. Koivunen, H. Poor, "Opportunistic scheduling and beamforming for MIMO-SDMA Downlink systems with Linear Combining", PIMRC '07

[54] P. Svedman, S. K. Wilson, J. Cimimi, B. Ottersten, " A simplified Opportunistic Feedback and Scheduling Scheme for OFDM", Proceeding IEEE VTC spring, May 2004.

[55] Butler, J. and R. Lowe, "Beam Forming Matrix simplifies Design of Electronically Scanned Antennas," Electronic Design, 1961.

[56] E. Y. Kim, J. Chun, "Random Beamforming in MIMO systems Exploiting Efficient Multiuser Diversity ", VTC 2005,spring

[57] E.Y. Kim, J. Chun, "A random Beamforming Technique in MIMO systems Exploiting Multiuser Diversity", IEEE Journal on selected areas in communications, Vol 21, No 5, June 2003

[58] R. Bosisio, U. Spagnolini, "On the Sum-Rate of Opportunistic Beamforming schemes with Multiple Antennas at the Receiver", ICC 07.

[59] M. Sharif, B. Hassibi, "On the Capacity of MIMO broadcast Channel with partial side information", IEEE Transactions on information Theory, vol. 51, No 2, February 2005.

[60] Jafar, S.A.; Goldsmith, A,"Transmitter Optimization and Optimality of Beam forming for Multiple Antenna Systems". Wireless Communications, IEEE Transactionson Volume 3, Issue 4, July 2004.

[61] Jorswieck E.A, Boche, H, "Channel Capacity and Capacity-Range of Beam forming in MIMO wireless systems under Correlated Fading with Covariance Feedback". Wireless Communications, IEEE Transactions onVolume 3, Issue 5, Sept. 2004

[62] Hung-Ta Pai, "Limited feedback for Antenna selection in MIMO-OFDM system", Consumer Communications and Networking Conference, 2006. CCNC 2006.

3rd IEEE,Volume 2, Issue , 8-10 Jan. 2006.

[63] Cimini, L.J., Jr.; Babak Daneshrad; Sollenberger, N.R.,"Clustered OFDM with transmitter diversity and coding", Global Telecommunications Conference, 1996.

[64] Shad,F. Todd,T.D. Kezys,V. Litva,J. Commun. Res. Lab., McMaster Univ., Hamilton, Ont. " Indoor SDMA capacity using a smart antenna base station", in IEEE ICUPC'97 San Diego, oct 1997.

[65] J.G. Proakis, "Digital Communications", 3rd ed.,New York, Mc-Graw-Hill 1995

[66] Derryberry, R.T. Gray, S.D. Ionescu, D.M. Mandyam, G. Raghothaman, B. "Transmit diversity in 3G CDMA systems"IEEE communications. Magazine ,Apr 2002.

[67] V Raghavan, RW Heath, AM Sayeed " Systematic codebook designs for quantized beamforming in correlated MIMO channels" IEEE Journal on selected areas in communications, 2007.

[68] Xiaoming She, Jingxiu Liu, Lan Chen, Hidekazu Toaka, Kenichi Higuchi, "Multi-Codebook Based Beamforming and Scheduling for MIMO-OFDM Systems with Limited Feedback.", IEICE Transactions.,November 2008.

[69] David Love , Wiroonsak Santipach , Michael L. Honig " What is the Value of Limited Feedback for MIMO Channels", IEEE communications magazine, October 2004.

[70] "Feedback for long term beamforming", C802.16m-09/1427r1, 2009-07-08.

[71] Kai-Kit Wong,Jia Chen , "Time-division multiuser MIMO with statistical feedback", EURASIP Journal on Advances in Signal Processing,Volume 8 , Issue 1 January 2008.

[72] Lucatti, D. Pattarina, A. Trecordi, "Bounds and performance of reuse partitioning in cellular networks" INFOCOM'96.

[73] A Goldsmith, SA Jafar, N Jindal, S Vishwanath . "Capacity limits of MIMO channels" IEEE Journal on selected areas in Communications, 2003 .

[74] J. Zhang, R. Chen, J. G. Andrews and Robert W. Heath Jr. "Coordinated Multi-cell MIMO systems with Cellular Block Diagonalization"Proc. of Asilomar Conference on Signals, Systems, and Computers, Pacific Grove, CA, Nov. 4-7, 2007

[75] Wan Choi and Jeffrey G. Adrews, "Inter-cell scheduling in a cellular MIMO system" , www.ece.rice.edu/ctw2006/posters/ctw-choi.pdf

[76] Hongyuan Zhang Mehta, N.B. Molisch, A.F. Jin Zhang Huaiyu Dai "On the Fundamentally Asynchronous Nature of Interference in Cooperative Base Station Systems" ICC 2007.

[77] Erik Dahlman, Stefan Parkvall, Johan Skold and Per Beming "3G Evolution: HSPA and LTE for Mobile Broadband ", Second edition, Academic Press 2008.

[78] Technical Specification Group Radio Access Network, ARIB TR-T12-36.913 V8.0.1" Requirements for further

[79] M. C. Necker, " Towards frequency reuse 1 cellular FDM/TDM systems" in Proc. Of the ACM International Symposium on Modeling, Analysis and Simulation of Wireless and Mobile Systems, Oct. 2006.

[80] Forenza, A. McKay, M.R. Collings, I.B. Heath, R.W. “Switching between OSTBC and Spatial Multiplexing with Linear Receivers in Spatially Correlated MIMO Channels”, Proc. IEEE VTC Melbourne, May 2006.

[81] Francisca Martínez, Jaime Campos, Antonio Ramírez,Valentín Polo, Alejandro Martínez, David Zorrilla, Javier Martí, “Transmission of IEEE 802.16d WiMAX signals over radio-over-fibre IMDD links”, WWIC 2007 5th International Conference on Wired / Wireless Internet Communications May 23-25 2007, Coimbra, Portugal

[82] W. Choi and J. G. Andrews, “ Downlink Performance and Capacity of Distributed Antenna Systems in a Multicell environment”, IEEE Trans. Wireless Commun. , Jan 2007.

[83] Duk-Kyung KIM and Tae-Heon KIM, “Enhancing the performance of an OFDMA-Based Cellular System Using Distributed Antennas”, IEICE trans. Commun. April 2006.

[84] Chen LIUand Wen-bo WANG, “Performance Analysis of a Sectorized Distributed Antenna System with Reduced Co-Channel Interference”, 2006 The Journal of China Universities of Posts and Telecommunications Published by Elsevier B.V.

[85] Charles. H. Cox, “Analog Optical Links: Theory and Practice”, Cambride University Press, 2004.

[86] I. Harjula, A. Ramirez, F. Martinez, D. Zorrilla, M. Katz and V. Polo, “Practical Issues in the Combining of MIMO Techniques and RoF in OFDM/A Systems,” Proc. of the 7th WSEAS International Conference on ELECTRONICS, HARDWARE, WIRELESS and OPTICAL COMMUNICATIONS (EHAC’08), pp.244-248 (2008)

[87] Shidong Zhou Ming Zhao Xibin Xu Jing Wang Yan Yao “Distributed Wireless Communication System : A New Architecture for Future Public Wireless Access.”, IEEE Communications Magazine, Mar 2003.

[88] Simon Haukin, “Adaptive filter Theory” third edition.

[89] M. Marques, J. Ambrosio, C. Reis, D. Gouveia, J. Riscado, D. Robalo, F. J. Velez, R. Costa, “ DESIGN AND PLANNING OF IEEE 802.16 NETWORKS”, PIMRC’07.

[90] B. Upase, M. Hunukumbure, S. Vadgama, “ Radio Network Dimensioning and Planning for WiMAX Networks”, FUJITSU Sci. Tech. J. October 2007, www.fujitsu.com/downloads/MAG/vol43-4/paper09.pdf

[91] IEEE802.16 Broadband Wireless Access working group, Text and Table for Draft 802.16m Evaluation Methodology: Link Budget Template

Publications

[92] C. Papathanasiou, L. Tassiulas, 'Multicast Transmission over IEEE 802.11n WLAN' , IEEE International Conference on Communications (ICC), May 2008 Beijing China

[93] C. Papathanasiou, L. Tassiulas, "Joint Beamforming and Channel Selection for Multicast IEEE 802.11n WLANs", ICST Intl. Symposium on Modeling and Optimization in Mobile, Ad Hoc and Wireless Networks (WiOpt), March 2008 Berlin Germany.

[94] C. Papathanasiou, I. Koutsopoulos, L. Tassiulas, “Space Division Multiple Access (SDMA) in an IEEE 802.11N WLAN”, NEWCOM++ - ACoRN Joint Workshop, March 2009 Barcelona Spain.

[95] C. Papathanasiou, I. Koutsopoulos, L. Tassiulas, 'Interference Mitigation in Co-Working IEEE 802.11n WLANs', IEEE Wireless Telecommunications Symposium (WTS), April 2009 Prague Czech Republic.

[96] C. Papathanasiou, N. Dimitriou, L. Tassiulas, 'Downlink Multi-user Transmission for Higher User Speeds in IEEE 802.16m', ICST Intl. Symposium on Modeling and Optimization in Mobile, Ad Hoc and Wireless Networks (WiOpt), June 2009 Seoul Korea

[97] C. Papathanasiou, I. Koutsopoulos, L. Tassiulas, “Low-Complexity Beamforming Techniques for IEEE 802.11n WLANs” IEEE Vehicular Technology Conference 2009-Fall (VTC) , September 2009, Anchorage Alaska.

[98] C. Papathanasiou, N. Dimitriou, L. Tassiulas, 'Downlink Transmission Optimization and Statistical Feedback Strategies in a Multi-User IEEE 802.16m System', IEEE Global Communications Conference (Globecom), November 2009, Hawaii, USA

[99] S. Stefanatos, C. Papathanasiou, N. Dimitriou, “Downlink Mobile OFDMA Resource Allocation With Minimum User Rate Requests”, IEEE Global Communications Conference 2009, November (Globecom), Hawaii, USA

[100] C.Edemen, A.Akan, S.Tan, E.Arikan, N.Dimitriou, C.Papathanasiou and M.Assaad , "Impact Of Multi-Antenna Schemes And Fequency Reuse On Broadband OFDM System Level Performance", WiMAGIC workshop, Brussels, 28 September 2009.

[101] C. Papathanasiou, N. Dimitriou, L. Tassiulas, “ Spatial Multiplexing based on Distributed Antenna Arrays for Mobile WiMAX Networks”, PIMRC 2010

[102] C. Papathanasiou, N. Dimitriou, L. Tassiulas “ Adaptive Radio Resource Management in a Sectored Cell for Broadband Wireless Access Systems”, Towards IMT Advanced and Beyond, PIMRC 2010 Workshop.

Book Chapter

[103] Book: “ Cross Layer Designs in WLAN systems”, ISBN: 9781848762275 by Troubador Publishing, Ltd, Leicester, UK, 01 September 2010. Chapter 7: C. Papathanasiou, N. Dimitriou, L. Tassiulas, “ Radio Resource Allocations for Interference Management in 802.11n WLANs”

Submissions

[104] C. Papathanasiou, N. Dimitriou, L. Tassiulas, “On the applicability of steerable Base Station Antenna Beams in IEEE 802.16m Networks with high user mobility”, COMPUTER NETWORKS journal,elsevier, major revision.

[105] C. Papathanasiou, N. Dimitriou, L. Tassiulas,, “ On the use of Distributed Directive Antenna Arrays in mobile OFDMA Networks”, VTC spring 2011